

THESIS FOR THE DEGREE OF DOCTOR OF PHILOSOPHY

# Engineering Yeast Metabolism for Production of Sesquiterpenes

STEFAN TIPPMANN



Department of Biology and Biological Engineering  
CHALMERS UNIVERSITY OF TECHNOLOGY  
Gothenburg, Sweden 2016

Engineering Yeast Metabolism for Production of Sesquiterpenes  
Stefan Tippmann  
ISBN 978-91-7597-459-0

© STEFAN TIPPMANN, 2016.

Doktorsavhandlingarnar vid Chalmers Tekniska Högskola  
Ny serie nr 4140  
ISSN 0346-718X

Department of Biology and Biological Engineering  
Chalmers University of Technology  
SE-412 96 Gothenburg, Sweden

Telephone +46 (0)31 772 1000

The cover illustrates production of sesquiterpenes by fermentation of  
the yeast *Saccharomyces cerevisiae*.

Printed by Chalmers Reproservice  
Gothenburg, Sweden 2016

## **Engineering Yeast Metabolism for Production of Sesquiterpenes**

Stefan Tippmann

Department of Biology and Biological Engineering

Chalmers University of Technology

## **Abstract**

Sesquiterpenes belong to the large and diverse group of isoprenoids, which are ubiquitous in the plant kingdom and have various applications in the chemical industry as fragrances, pharmaceuticals and as substitutes for petroleum-based gasoline, diesel and jet fuels. In this project, production of sesquiterpenes was studied in *Saccharomyces cerevisiae* using farnesene as an example with the objective to gain new insights into the synthesis of these compounds and to evaluate different metabolic engineering strategies.

Farnesyl diphosphate (FPP) represents the universal precursor for all sesquiterpenes and different strategies were addressed to increase production of this intermediate and to allow for its efficient conversion to farnesene. As FPP is provided by the mevalonate pathway, we aimed at increasing the flux through the pathway by incorporation of malonyl-CoA using a recently identified acetoacetyl-CoA synthase from *Streptomyces* sp. strain CL190. While the enzyme had detrimental effects on growth as well as on product formation, it was able to compensate for the loss of the essential, endogenous acetoacetyl-CoA thiolase. Additionally, a homologous enzyme with superior efficiency could be identified. Secondly, as FPP is required as substrate for different pathways and represents a metabolic branch point, a novel tool for enzyme co-localization was developed to divert more flux towards farnesene. The system utilizes scaffolds based on affibodies and could improve product yields by more than twofold. Furthermore, the role of terpene synthases on the production of farnesene was elucidated by comparing farnesene synthases with different plant origins, i.e. *Malus domestica*, *Citrus junos* and *Artemisia annua*. While the selected candidates produced similar amounts of farnesene (up to 170 mg/L), these enzymes appeared to be superior in comparison to other sesquiterpene synthases, i.e. santalene synthase. Lastly, the response to increased product formation was investigated using transcriptome and metabolome analysis, which highlighted changes across various metabolic pathways and identified pantothenic acid as a potential target for future engineering strategies.

In conclusion, the study evaluates different metabolic engineering strategies for production of sesquiterpenes in *S. cerevisiae* and provides new insights into the cellular response during their production. Additionally, utilization of affibodies as a novel tool in metabolic engineering to increase chemical production in *S. cerevisiae* was highlighted.

**Keywords:** *Saccharomyces cerevisiae*, metabolic engineering, sesquiterpenes, isoprenoids, affibodies, metabolomics, transcriptomics



# Acknowledgements

I would like to acknowledge all the people who contributed directly or indirectly to the work presented in this thesis. First and foremost, I would like to thank my supervisors Jens Nielsen and Verena Siewers for all their contributions, support and patience as well as for always taking time to help and discuss. It was a great experience to work with you. Besides, I am particularly grateful to Sakda Khoomrung, with whom I have been working on several different projects and who has contributed to this work in many different ways.

I also gratefully acknowledge Yun Chen and Raphael Ferreira, who have been working with on the acetoacetyl-CoA synthase expression in yeast as well as Intawat Nookaew and Partho Sarathi Sen for analyzing transcriptome and metabolome data with me. In this respect, I would also like to thank Francesco Gatto for his support and for helping me to understand the “basic bioinformatics”, as he would phrase it. Moreover, I gratefully acknowledge Josefina Anfelt and Paul Hudson from KTH in Stockholm, with whom I have been working on affibody scaffolds for several years. Thank you for all the efforts to finish the project successfully! Likewise, I thank Florian David and Jacqueline Rand for their help and valuable discussions of the project. Furthermore, I would like to thank António Roldão for the perpetual troubleshooting and assistance during numerous yeast fermentations.

The Systems & Synthetic Biology Division has been a great work environment and I am very grateful to all the people in the group for the daily discussions, advice and support. In addition, I wish to thank Rahul Kumar for his encouragements and very valuable advice regarding the directions of my project as well as Andreas Hellström for all the good discussions and help in the lab.

Lastly, I wish to thank my family for their continuous support. Thanks to you I was able to take on this challenge in the first place. Throughout the last years you kept telling me, you don’t really understand what all of this is about and I hope this thesis will provide some answers. At the end, a very special thanks to my greatest supporter, “min sambo”, Melanie. The past years have been very adventurous: by the time I started, Paul was born, Emil was only 4 years old and we had just moved to Sweden. Organization became a crucial skill to live up to the standards for PhD students in the group and to keep up the family life simultaneously. It often felt impossible to manage both and I know I missed out on some end. Thank you for all your support!



# List of Publications

The thesis is based on the following publications and manuscripts:

- I Tippmann S, Chen Y, Siewers V and Nielsen J (2013) From fragrances and pharmaceuticals to advanced biofuels: Production of isoprenoids in *Saccharomyces cerevisiae*. *Biotechnology Journal* 8(12):1435-1444
- II Tippmann S, Scalcinati G, Siewers V and Nielsen J (2016) Production of farnesene and santalene by *Saccharomyces cerevisiae* using fed-batch cultivations with RQ-controlled feed. *Biotechnology and Bioengineering* 113(1):72-81
- III Tippmann S, Khoomrung S, Sarathi Sen P, Nookae I and Nielsen J Metabolic and transcriptomic response to production of farnesene in *Saccharomyces cerevisiae*. Manuscript in preparation.
- IV Tippmann S\*, Anfelt J\*, David F, Rand JM, Siewers V, Uhlén M, Nielsen J and Hudson EP Affibody scaffolds improve production of sesquiterpenes in *Saccharomyces cerevisiae*. Accepted for Publication in ACS Synthetic Biology  
doi:10.1021/acssynbio.6b00109. \*equal contribution
- V Tippmann S, Ferreira R, Siewers V, Nielsen J and Chen Y Effects of acetoacetyl-CoA synthase expression on production of sesquiterpenes in *Saccharomyces cerevisiae*. Under review.
- VI Tippmann S, Nielsen J and Khoomrung S (2016) Improved quantification of farnesene during microbial production from *Saccharomyces cerevisiae* in two-liquid-phase fermentations. *Talanta* 146:100-106

Additional publications not included in the thesis:

- VII Khoomrung S, Martinez JL, Tippmann S, Jansa-Ard S, Buffing MF, Nicastro R and Nielsen J (2015) Expanded metabolite coverage of *Saccharomyces cerevisiae* extract through improved chloroform/methanol extraction and tert-butyl-dimethylsilyl derivatization. *Analytical Chemistry Research* 6:9-16
- VIII Khoomrung S, Tippmann S, Martinez JL, Nookae I, Moritz T, and Nielsen J Comprehensive analysis of industrial yeast metabolome by high-resolution mass spectrometry. Manuscript in Preparation.

# Contribution Summary

- I Performed the literature study and wrote the manuscript.
- II Designed the study, performed all experiments on farnesene production and wrote the manuscript.
- III Designed the study, performed the experiments, processed and analyzed the metabolome data, analyzed the transcriptome data and wrote the manuscript.
- IV Assisted in designing the study, performed all experiments in *Saccharomyces cerevisiae* and wrote the manuscript.
- V Designed the study, performed all experiments and wrote the manuscript.
- VI Designed the study, performed all experiments and wrote the manuscript.

# Preface

This dissertation is submitted for the partial fulfillment of the degree of doctor of philosophy. It is based on work carried out between December 2011 and June 2016 in the Division for Systems and Synthetic Biology at the Department of Biology and Biological Engineering, Chalmers University of Technology under the supervision of Professor Jens Nielsen. The research was funded by the Knut and Alice Wallenberg Foundation, FORMAS and the Chalmers Foundation.

Stefan Tippmann

October 2016



# Contents

<b>Abstract</b> . . . . .	iii
<b>Acknowledgements</b> . . . . .	v
<b>List of Publications</b> . . . . .	vii
<b>1 Introduction</b> . . . . .	1
1.1 Chemistry, Origin and Industrial Applications . . . . .	1
1.2 Biosynthesis of Sesquiterpenes . . . . .	4
1.3 Metabolic Engineering for Sesquiterpene Production . . . . .	8
1.4 Outline and Objectives of the Thesis . . . . .	14
<b>2 Comparison of Farnesene Synthases</b> . . . . .	17
<b>3 Metabolic and Transcriptomic Response to Production of Farnesene</b> . . . . .	25
<b>4 Engineering the FPP Branch Point using Affibody Scaffolds</b> . . . . .	35
<b>5 Incorporation of Malonyl-CoA using Acetoacetyl-CoA Synthase</b> . . . . .	43
<b>6 Analysis of Organic Overlays for Quantification of Farnesene</b> . . . . .	51
<b>7 Conclusions</b> . . . . .	57
<b>References</b> . . . . .	61
 I From fragrances and pharmaceuticals to advanced biofuels: Production of isoprenoids in <i>Saccharomyces cerevisiae</i> . . . . .	79
II Production of farnesene and santalene by <i>Saccharomyces cerevisiae</i> us- ing fed-batch cultivations with RQ-controlled feed . . . . .	91
III Metabolic and transcriptomic response to production of farnesene in <i>Saccharomyces cerevisiae</i> . . . . .	103
IV Affibody scaffolds improve production of sesquiterpenes in <i>Saccharomyces cerevisiae</i> . . . . .	129

---

V Effects of acetoacetyl-CoA synthase expression on production of sesquiterpenes in <i>Saccharomyces cerevisiae</i> . . . . .	153
VI Improved quantification of farnesene during microbial production from <i>Saccharomyces cerevisiae</i> in two-liquid-phase fermentations . . . . .	187

*To Emil and Paul*



# Chapter 1

## Introduction

### 1.1 Chemistry, Origin and Industrial Applications

Sesquiterpenes belong to the large and chemically diverse group of isoprenoids, which exist in all living organisms, but are mainly produced by plants. As such, isoprenoids occur in plant leaves, resins and oils. One of the pioneers in analyzing and extracting these compounds from oils was Otto Wallach, who was awarded the Nobel Prize in Chemistry for his work in 1910. Until today, more than 40,000 different isoprenoids have been identified (Heldt and Piechulla, 2011). Isoprenoids, which are also called terpenoids, contain isoprene with the chemical formula  $C_5H_8$  as the main constituent and are classified according to number of these entities, which are linked linearly or in ring structures to form the molecule. This is also referred to as the “isoprene rule” (Ruzicka, 1953). For identification of this building block, which is shared by all isoprenoids, Leopold Ruzicka was awarded the Nobel Prize in Chemistry in 1939. While isoprenoids containing only one unit of isoprene are termed hemiterpenoids, mono-, sesqui-, di-, sester-, tri-, sesquar- and tetraterpenoids contain 2-8 isoprene units. Lastly, polyterpenoids group all isoprenoids with more than 8 units of isoprene. Some of these are relatively rare, as for instance sesquarterpenes, of which only 27 were known until 2013 (Sato, 2013). Additionally, a further classification is made in connection to their chemical modifications. While isoprenoids exclusively consisting of isoprene units are designated terpenes, molecules functionalized by other elements, i.e. oxygen, classify as terpenoids. The chemical structures of some terpenes and terpenoids are presented in Figure 1.1.

Isoprenoids adopt various biochemical functions, e.g. as pigments ( $\beta$ -carotene), vitamins (retinol) or photoprotective agents (astaxanthin). Besides, ubiquinone, which plays an important role in the electron transport chain is also partially derived from isoprenoids. In plants, isoprenoids are important for interactions with the environment and serve as defensive agents via different mechanisms (Cheng et al., 2007).

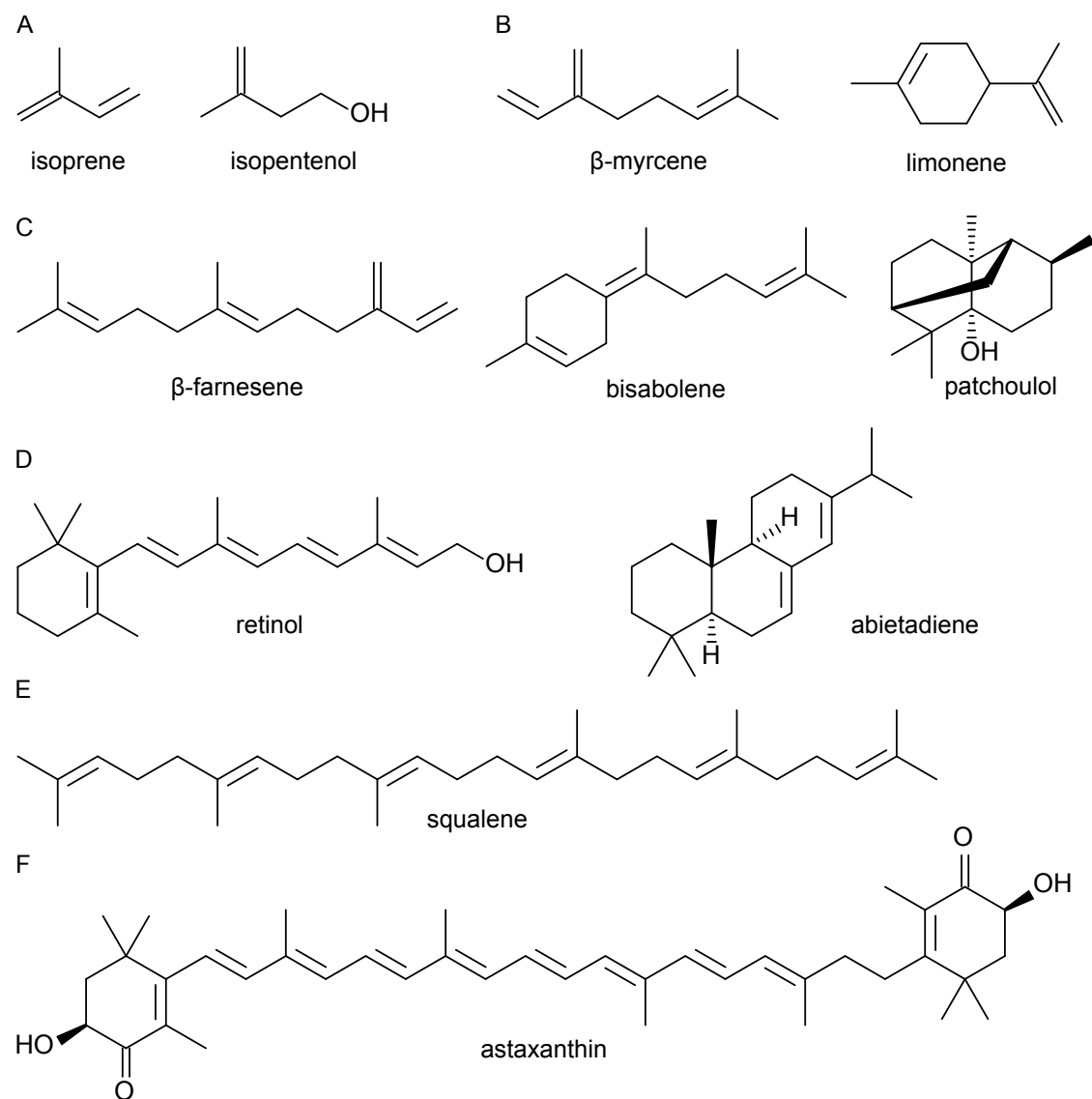


**Figure 1.1:** Chemical structures of different terpenes/terpenoids classified according to the number of isoprene units ( $\text{C}_5\text{H}_8)_n$ . (A) Hemiterpenes ( $n=1$ ), (B) Monoterpene ( $n=2$ ), (C) Sesquiterpenes ( $n=3$ ), (D) Diterpenes ( $n=4$ ), (E) Triterpenes ( $n=6$ ) and (F) Tetraterpenes ( $n=8$ ).

On one side, plants emit mixtures of isoprenoids to attract natural enemies of herbivores. As an example, among other sesquiterpenes, farnesene was identified to be released by maize in response to herbivore attack to attract natural enemies (Schnee et al., 2006). Likewise, elevated amounts of farnesene have been detected in the leaves of cucumbers upon attack by the spider mite *Tetranychus urticae* (Takabayashi et al., 1994) and similarly in apples, corn, potatoes and tobacco (Pare and Tumlinson, 1999). On the other hand, since many terpenoids have antimicrobial or antioxidant properties, they act as phytoalexins and are produced by plants in response to fungal infections (Prisic et al., 2004). Furthermore, together with other volatile organic compounds (VOCs), isoprenoids also serve the purpose of communicating with plants and

thereby to initiate defense mechanisms of their surrounding neighbors (Baldwin et al., 2006). Due to these characteristic properties, isoprenoids are mostly recognized as fragrances and pharmaceuticals. The sesquiterpene alcohol patchoulol, which is the main constituent of patchouli oil and responsible for its characteristic odor (Nikiforov et al., 1986), represents a valuable ingredient in the perfume industry (Frister and Beutel, 2015). In addition to patchoulol, there are several other mono- and sesquiterpenes that are used as fragrances (Ansari and Curtis, 1974; Davis and Croteau, 2000). On the other hand, astaxanthin is recognized for its antioxidant activity and has been attributed potential health benefits, for the immune system in general and for prevention of cardiovascular diseases (Higuera-Ciapara et al., 2006). Much focus has also been directed to the sesquiterpene lactone artemisinin, which is efficiently used in the treatment of malaria. The compound occurs naturally in the sweet wormwood *Artemisia annua* and has a long history in Chinese medicine as it has already been extracted and applied to treat parasitic infections during the Jin Dynasty (Miller and Su, 2011; Tu, 2011). For the discovery of artemisinin, Youyou Tu was awarded the Nobel Prize in Medicine in 2015. Yet isoprenoids generally offer a broad range of applications in various branches of the chemical industry. Natural rubber, which is harvested in large quantities by rubber tapping from the bark of the rubber tree *Hevea brasiliensis*, consists of poly(*cis*-1,4-isoprene) up to 94 % (Ohya and Koyama, 2005). With numerous products including tires and footwear, the demand for natural rubber exceeded 10 million tons in 2010 (Gronover et al., 2011; Ohya and Koyama, 2005). Squalane, the fully reduced form of the triterpene squalene, which used to be extracted from shark liver oil and olive oil for many years (McPhee et al., 2014), is used as a moisturizer in the cosmetic industry (Kim and Karadeniz, 2012). The sesquiterpene farnesene, which occurs naturally in ginger and lavender oil (Ansari and Curtis, 1974), but also in other numerous plants (Crock et al., 1997), finds diverse applications in the chemical industry as a feedstock for production of lubricants, surfactants and polymers (Benjamin et al., 2016). As an example, farnesene has become a valuable building block for production of synthetic squalene (McPhee et al., 2014).

However, much of the attention addressed to terpenes within recent years originates from their applications as fuel additives or as direct substitutes for petroleum-based gasoline, diesel and jet fuels. This applies particularly to hemi-, mono- and sesquiterpenes, which have been assigned high densities and similar combustion properties (e.g. heat of combustion, cetane number). Examples include the hemiterpene isopen-tenol, the monoterpenes limonene, camphene, myrcene and pinene (Harvey et al., 2010; Meylemans, 2012; Ryder, 2009; Tracy et al., 2009) as well as the sesquiterpenes farnesene, bisabolene and caryophyllene (Harvey et al., 2015; Peralta-Yahya et al., 2011; Renninger and McPhee, 2010). Due to the double bonds and the resulting instability, these molecules are usually used in their hydrogenated form. Recently, Millo et al. (2014) thoroughly compared the performance of a conventional diesel (Ultra-low-sulfur diesel, ULSD) with a diesel-farnesane mixture (diesel blended with 30 % farnesane) and pure farnesane, where farnesane indicates the fully reduced form of farnesene obtained via hydrogenation. Both fuels had heating values and

cetane numbers similar to the conventional diesel. Considering the environmental burden, emissions of nitrogen oxide and CO<sub>2</sub> from the farnesane blended fuel were comparable. On the other hand, significant reductions were observed for carbon monoxide and hydrocarbon emissions. Furthermore, due to the absence of sulfur and aromatics, there are potential benefits with respect to the emission of sulfur oxides and the production of soot. Apart from this, with a significantly reduced cloud point, farnesane-based fuel possesses improved cold weather properties over conventional diesel (George et al., 2015; Millo et al., 2014; Renninger and McPhee, 2010).

## 1.2 Biosynthesis of Sesquiterpenes

There are two forms of activated isoprene, which eventually give rise to the incredible diversity of isoprenoids, namely isopentenyl diphosphate (IPP) and its isomer dimethylallyl diphosphate (DMAPP). These building blocks were identified by Feodor Lynen, one of the Nobel Laureates in Medicine in 1964 (Lynen et al., 1958) and are either provided by the mevalonate (MVA) pathway or alternatively, by the methylerythritol phosphate (MEP) pathway, which is also sometimes referred to as deoxyxylulose phosphate (DXP) pathway. In general terms, the MVA pathway is utilized by eukarya and archaea, while the MEP pathway is used by bacteria. However, there are exceptions to the rule and the two pathways are partly shared among the three domains of life. Whole genome sequencing has revealed that there are bacteria that express the MVA pathway, e.g. *Staphylococcus aureus* (Eisenreich et al., 2004). On the other hand, studies on the biosynthesis of menaquinone and naphpterpin using <sup>13</sup>C labeling showed that *Streptomyces aeriuovifer* operates both pathways simultaneously (Seto et al., 1996). Similarly, plants produce IPP and DMAPP from the MVA pathway in the cytosol, but utilize the MEP pathway in plastids (Tholl, 2015). Hence, a clear classification regarding which of the two pathways is used is difficult to make. However, utilization of the MEP pathway can be more accurately limited to bacteria and plastid bearing organisms. Furthermore, it is noteworthy that the MVA pathways from eukarya and archaea differ, as archaea lack the last three eukaryal MVA pathway enzymes (Lombard and Moreira, 2011; Matsumi et al., 2011). Until today, only two of these are known, one of which was surprisingly first identified in *Streptomyces* sp. strain CL190, i.e. Idi2 (Kaneda et al., 2001), and subsequently found to be present in archaea as well (Barkley et al., 2004). Likewise, the MVA pathways of bacteria and eukarya are not identical, i.e. some bacteria have been reported to produce acetoacetyl-CoA, the first intermediate, by condensation of malonyl-CoA and acetyl-CoA (Takagi et al., 2000), which is different from eukarya as described later. As one of the key mechanisms, horizontal gene transfer has been used as an explanation for this diversity. While the evolution of the two pathways is still being investigated (Lange et al., 2000; Lombard et al., 2012), it has also been speculated that the MVA pathway existed in a common ancestor of the three domains, but was lost and substituted by the MEP pathway in bacteria (Lombard and Moreira, 2011). Since the

yeast *S. cerevisiae* produces IPP and DMAPP via the MVA pathway, the main focus of this section is set on the MVA pathway. The identification of the MEP pathway can be accredited to Rohmer et al. (1993), while an extensive elucidation of the pathway has been presented by Eisenreich et al. (2004). An overview of the MVA pathway and the subsequent reactions for production of sesquiterpenes are presented in Figure 1.2.

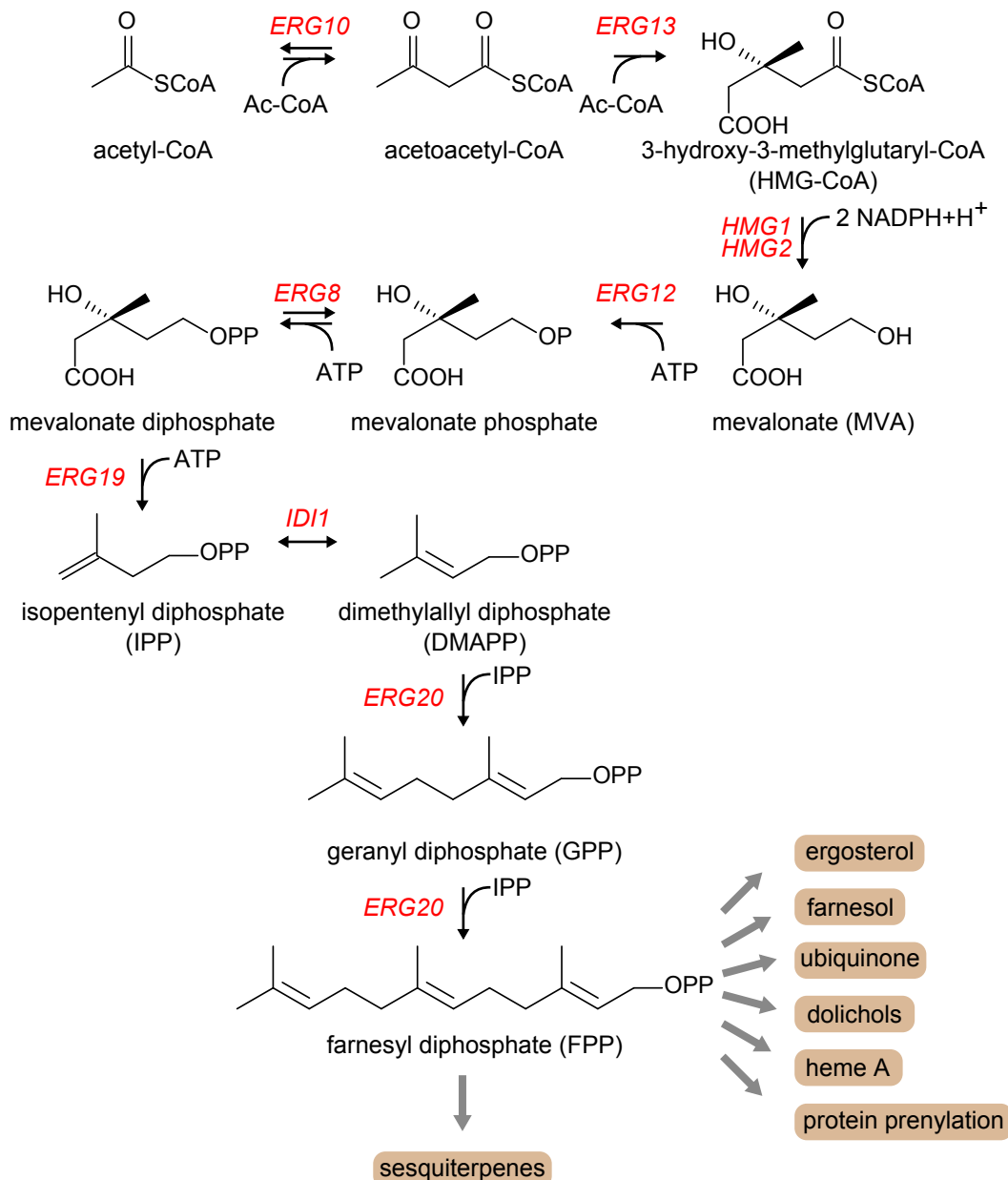


**Figure 1.2:** Production of sesquiterpenes using the mevalonate pathway of *S. cerevisiae*. Sesquiterpenes are synthesized from FPP, which is also a precursor for several other products such as ergosterol. Gene names are written as red italics. *ERG10* - acetoacetyl-CoA thiolase, *ERG13* - HMG-CoA synthase, *HMG1/2* - HMG-CoA reductase, *ERG12* - mevalonate kinase, *ERG8* - phosphomevalonate kinase, *ERG19* - mevalonate diphosphatase, *IDI1* - isopentenyl diphosphate isomerase, *ERG20* - farnesyl diphosphate synthase.

Similar to the MEP pathway, several detailed descriptions of the MVA pathway are

available in the literature (Heldt and Piechulla, 2011; McGarvey and Croteau, 1995; Miziorko, 2011). Much of the exploration of the MVA pathway can be accredited to Konrad Bloch and Feodor Lynen, who were particularly interested in the synthesis of cholesterol and eventually awarded the Nobel Prize in Medicine in 1964 (Bloch, 1992; Goldfine and Vance, 2001; Lynen et al., 1958). Their discoveries significantly contributed to the development of statins to treat high cholesterol levels in humans, e.g. by the competitive inhibitor mevilonin/lovastatin (Alberts et al., 1980). In the initial step of the pathway, two molecules of acetyl-CoA are converted to acetoacetyl-CoA in a reversible Claisen condensation, which is catalyzed by acetoacetyl-CoA thiolase (Erg10). The following condensation of acetoacetyl-CoA with another acetyl-CoA yields 3-hydroxy-3-methylglutaryl-CoA (HMG-CoA), produced by HMG-CoA synthase (Erg13). Subsequently, the thioester of HMG-CoA is converted into the alcohol by HMG-CoA reductase to produce mevalonate. This step was first described in yeast in 1960 and consists of two consecutive reductions, which both require one molecule of NADPH+H<sup>+</sup>: first, for conversion of the thioesterified carboxyl group to an aldehyde and second, for conversion of the aldehyde to an alcohol (Durr and Rudney, 1960; Friesen and Rodwell, 2004). Two variants of the reductase are known in *S. cerevisiae*, i.e. Hmg1 and Hmg2 (Basson et al., 1986), both of which are located in the membrane of the endoplasmic reticulum. While their COOH-terminal catalytic domains are almost identical (93 %), their NH<sub>2</sub>-terminal membrane anchoring domains are only 50 % identical (Hampton et al., 1996). Much attention has been addressed to this enzyme, since it represents the flux controlling step in sterol synthesis (Chappell et al., 1995; Ohto et al., 2009; Siperstein and Fagan, 1966) and is targeted by statins to manipulate sterol levels (Friesen and Rodwell, 2004). Besides, the enzyme plays a central role in the regulation of the pathway as it will be described later on. In the following two reactions, mevalonate is then phosphorylated by mevalonate kinase and phosphomevalonate kinase, Erg12 and Erg8, respectively, to produce mevalonate phosphate and mevalonate diphosphate. The second of these consecutive phosphorylations is reversible. The next step represents the ATP-dependent decarboxylation of mevalonate diphosphate to isopentenyl diphosphate, which is catalyzed by mevalonate diphosphate decarboxylase (Erg19). Finally, dimethylallyl diphosphate (DMAPP) is produced in an isomerization reaction of isopentenyl diphosphate (IPP) by isopentenyl diphosphate isomerase (Idi1). The second part in the synthesis of sesquiterpenes requires production of farnesyl diphosphate (FPP), which is achieved by two successive prenylations. For this purpose, a carbocation is generated from DMAPP, which is subsequently extended by IPP in an electrophilic alkylation and eventually deprotonated to form geranyl diphosphate (GPP) (Dewick, 2001). Monoterpenes are directly derived from GPP, while the extension of the carbon chain with an additional molecule of IPP generates FPP. Both of these prenylation reactions are catalyzed by farnesyl diphosphate synthase (Erg20).

Ultimately, FPP represents the universal precursor of all sesquiterpenes. However, as indicated in Figure 1.2, it is also a crucial intermediate for production of several important metabolites or adopts different functions inside the cell by itself. For instance, FPP and geranylgeranyl diphosphate (GGPP) are used to prenylate proteins,

an important posttranslational modification to allow for membrane trafficking (Wang and Casey, 2016). Similarly, dolichols are based on FPP and represent another important posttranslational modification (Grabinska and Palamarczyk, 2002). Dimster-Denk et al. (1999) nicely summarized the synthesis of the different compounds that are derived from FPP. Additionally, the pathway is used for synthesis of ergosterol, which is the main sterol in *S. cerevisiae* and an important component of the membrane (van der Rest et al., 1995). The first step of ergosterol synthesis represents the dimerization of two molecules of FPP to squalene, which is catalyzed by squalene synthase (Erg9). Subsequently, squalene is converted in a multitude of reactions to ergosterol via the main intermediates lanosterol, zymosterol, fecosterol and episterol. In order to ensure the supply of ergosterol, *S. cerevisiae* responds to low sterol levels by upregulating the transcription of several of the involved genes (Dimster-Denk et al., 1999). This feedback mechanism utilizes conserved elements within the promoter regions, which are called sterol regulatory elements (SRE) (Goldstein and Brown, 1990) and function as binding motifs for a class of corresponding transcription factors, i.e. SRE binding proteins (SREBPs). At low sterol concentrations, SREBPs translocate to the nucleus to initiate expression of genes involved in ergosterol synthesis. Two of these transcription factors are Upc2 and Ecm22, which have been identified to bind among others to the SREs of *ERG2* and *ERG3* (Vik and Rine, 2001). Besides, other finely tuned mechanisms come into play to regulate the flux through the MVA pathway. One of the primary targets is the HMG-CoA reductase (Hmg1/Hmg2), catalyzing the rate limiting reaction of the pathway to produce mevalonate, but some of these mechanisms also apply to other pathway enzymes such as the acetoacetyl-CoA thiolase (Erg10) and squalene synthase (Erg9) (Dimster-Denk and Rine, 1996; Kennedy et al., 1999).

HMG-CoA reductase is subject to feedback and cross regulation, which function in reversed direction for each of the two isozymes (Hampton et al., 1996), indicating that these enzymes are expressed specifically under certain conditions. First of all, HMG-CoA reductase is regulated by feedback inhibition. In particular, accumulation of early pathway intermediates (intermediates before squalene) inhibits translation of Hmg1 (Dimster-Denk et al., 1994). Besides, mevalonate and farnesol have been reported to reduce HMG-CoA reductase activity (Brown and Goldstein, 1980) and to promote its degradation (Meigs et al., 1996), respectively. In contrast, Hmg2 is inhibited by late pathway intermediates. In addition to this, the two enzymes vary significantly regarding their stability, which has been shown to be dependent on the pathway flux. While Hmg1 is highly stable, Hmg2 is unstable and degraded at high pathway fluxes (Hampton and Rine, 1994). The second regulation mechanism is triggered by the availability of oxygen. It is noteworthy that until the production of squalene, the pathway for ergosterol synthesis is completely independent of oxygen. Starting with the following reaction, the epoxidation of squalene, however, several steps require the presence of molecular oxygen, which hence determines if ergosterol can be synthesized or not. The response towards varying levels of oxygen is mediated by heme, which has been identified as a positive regulator of *HMG1*, i.e. by activation of the transcription factor Hap1, which in turn stimulates expression of *HMG1* and as

a negative regulator of *HMG2* (Thorsness et al., 1989).

In conclusion, Hampton et al. (1996) suggested the interplay of the two mechanisms to regulate sterol synthesis via HMG-CoA reductase in *S. cerevisiae* as follows. Under aerobic conditions, the presence of oxygen allows for production of ergosterol by providing the co-substrate for the late pathway reactions to occur. Additionally, expression of *HMG1* is stimulated via the activated transcription factor Hap1. This in turn results in low abundance of early mevalonate pathway intermediates and thereby unlocks the inhibition of Hmg1 translation. With regard to Hmg2, high pathway fluxes promote instability of the enzyme, while the late pathway intermediates and the activated Hap1 inhibit its expression. However, once oxygen becomes a scarce resource, ergosterol cannot be synthesized anymore due to the lack of oxygen. The highly stable Hmg1 causes accumulation of early pathway intermediates and in consequence inhibits further translation of Hmg1. Furthermore, activation of *HMG1* expression via Hap1 is omitted as well. Vice versa, expression of *HMG2* is stimulated due to the loss of the heme mediated repression and the stability of the enzyme is enhanced in connection to the reduced pathway flux. In this situation, the MVA pathway still provides essential metabolites. However, while early pathway intermediates such as FPP are potentially toxic, they also promote degradation of Hmg2 through a posttranslational mechanism (Gardner and Hampton, 1999). Ultimately, this allows *S. cerevisiae* to respond to changes in the environmental conditions (i.e. sustained anaerobic conditions or return to aerobic conditions) in a more flexible manner and prevents accumulation of toxic intermediates.

### 1.3 Metabolic Engineering for Sesquiterpene Production

To exploit the versatile applications of terpenes within the chemical industry, there is a strong need for efficient production processes to meet the demand for these compounds. Chemical synthesis is widely used for this purpose. For instance, the monoterpene citral, which not only serves as a lemon scent, but also as a building block for the production of ionone and carotenoids, can be produced efficiently from isobutene and formaldehyde. Chemical synthesis is often based on petroleum derived chemicals and requires extreme pH and temperatures. Nonetheless, chemical synthesis provides 75 % of all raw materials in the perfume industry. In case of citral, BASF's annual production exceeds 40,000 tonnes (Schaefer, 2014). On the other hand, extraction from plants, their natural origin, represents the most obvious way for the production of isoprenoids. However, although these compounds are considered to be ubiquitous in plants, they are often synthesized in small amounts. As an example, artemisinin can be efficiently extracted from *Artemisia annua* by liquid solvent extraction (Liu et al., 2011), but the amount of artemisinin per dry weight only reaches up to 0.44 % (Mannan et al., 2010). Generation of transgenic plants has improved

the yield up to 1.5 %, which could recently be increased ninefold upon further engineering (Dilshad et al., 2015). Nonetheless, the yield remains liable to seasonal and geographical conditions (Wallaart et al., 2000). Besides, commercial extraction processes make use of hazardous solvents such as petroleum ether, hexane or similar, which show highest extraction yields (Lapkin et al., 2006). Most importantly, plant-based production of artemisinin suffers from the long cultivation time and the production cycle can take up to one year and a half in total (Peplow, 2013).

In an alternative approach, sesquiterpenes can be produced by microbial fermentation, which circumvents several of the described problems of the conventional production processes. The yeast *S. cerevisiae* can be engineered to efficiently convert simple carbon sources in a number of consecutive reactions into specific products, e.g. artemisinic acid (Keasling, 2008). For this purpose, the necessary reactions have to be implemented into the host in addition to the mevalonate pathway. In contrast to the agricultural artemisinin supply, production of semi-synthetic artemisinin using *S. cerevisiae* and its subsequent conversion into artemisinin-based combination therapies (ACTs) requires less than three months (Peplow, 2013). This concept has been applied to different compounds and metabolic engineering has enabled production of various chemicals (Nielsen, 2015; Nielsen and Keasling, 2016). As an example, *S. cerevisiae* was recently engineered for production of reticuline, a precursor of morphine (De-Loache et al., 2015). Despite its potential, development of these bioprocesses remains challenging with respect to development time and costs. Process development for production of artemisinin by *S. cerevisiae* required 10 years and US \$50 million (Nielsen and Keasling, 2016). Yet the tools to engineer yeast metabolism for chemical production are steadily advancing, which will eventually shorten the time to develop sustainable bioprocesses (David and Siewers, 2015; Jensen and Keasling, 2015). In this respect, especially CRISPR/Cas9 is becoming a powerful tool for the construction of microbial cell factories (Jakočiūnas et al., 2016).

Production of terpenes has been studied extensively in *S. cerevisiae* and *Escherichia coli*. Nowadays, several terpenes can already be produced for commercialization from microbial fermentation processes including the sesquiterpenes artemisinin, farnesene, valencene, nootkatone and elemene as well as the hemiterpene isoprene (Leavell et al., 2016). Based on the degree of reduction (Dugar and Stephanopoulos, 2011; Villadsen et al., 2011), farnesene can be produced from glucose at a maximum theoretical yield of 0.32 g/g. With respect to the native pathway used for product formation in *S. cerevisiae*, i.e. glucose conversion to pyruvate during glycolysis, conversion of pyruvate to acetyl-CoA and the subsequent MVA pathway to produce IPP, the pathway yield for farnesene and all sesquiterpenes with the general formula C<sub>15</sub>H<sub>24</sub> amounts to 0.25 g/(g glucose). In consequence, according to the definition from Dugar and Stephanopoulos (2011), production of farnesene from the MVA pathway is characterized by a pathway efficiency of approximately 78 % (ratio of pathway yield to maximum theoretical yield). Besides, production of one mole of farnesene from the MVA pathway requires 9 moles of acetyl-CoA, 9 moles of ATP and 6 moles of NADPH+H<sup>+</sup>. With a yield of 0.30 g/(g glucose), the MEP pathway is more efficient

from this perspective as it requires 14 % less carbon for production of farnesene from glucose (Ajikumar et al., 2010, Supplementary Material). This is partly due to the decarboxylation reactions involved in the production by *S. cerevisiae*, firstly to convert pyruvate to acetaldehyde and secondly to convert mevalonate to IPP. In both reactions CO<sub>2</sub> is being produced and carbon for product formation is lost. In order to allow for efficient production of terpenes, various metabolic engineering strategies have been pursued, which mainly include, but are not limited to: engineering of the MVA pathway, engineering of the FPP branch point, expression of the heterologous MVA/MEP pathway, reducing product toxicity, engineering acetyl-CoA metabolism and utilization of alternative pathways/product formation strategies. One of the prerequisites for terpene production is the expression of the involved terpene synthase, which has not been listed here as it will be discussed separately using the example of farnesene. While these concepts have been applied for different products, the main focus is set to sesquiterpenes. A comparable overview of metabolic engineering approaches used for production of sesquiterpenes has also been presented by Rodriguez et al. (2014).

**Engineering of the MVA pathway.** The main objective of this strategy is to increase the flux carried by the MVA pathway and thereby to provide more FPP for production of sesquiterpenes. To a large extent, this can be achieved by increasing the transcript levels of the pathway genes. For instance, overexpression of every gene involved in the MVA pathway has been used for the production of the artemisinin precursor artemisinic acid in *S. cerevisiae* (Paddon et al., 2013; Westfall et al., 2012). However, the reduction of HMG-CoA to mevalonate plays a crucial role in this respect, which has previously been identified as the flux controlling reaction of the pathway. Consistent with this observation, overexpression of *HMG1* was shown to have the most significant impact on production of prenyl alcohols in *S. cerevisiae* among the MVA pathway genes (Ohto et al., 2009). As described earlier, HMG-CoA reductase also plays an important role in the regulation of sterol synthesis. In order to reduce the regulatory effects on the enzyme and to maintain high pathway fluxes, a truncated variant (tHmg1) lacking the NH<sub>2</sub>-terminal ER-anchoring domain was constructed, which could significantly improve production of squalene (Donald et al., 1997; Polakowski et al., 1998). Several studies have made use of this truncated version, occasionally in combination with integrating several copies of the gene to assure high expression levels (Asadollahi et al., 2010; Scalcinati et al., 2012b; Westfall et al., 2012). Additionally, Ma et al. (2011) compared five variants of the enzyme for production of amorphadiene from the heterologously expressed MVA pathway in *E. coli* and found HMG-CoA reductase from *Delftia acidovorans* to be significantly more efficient than tHmg1 from *S. cerevisiae*. The same study also highlights the potential impact of co-factor requirements on the pathway efficiency. In contrast to the yeast tHmg1, which uses NADPH as co-factor, the enzyme from *D. acidovorans* is NADH-dependent. This is advantageous, because NADH accumulates during glycolysis, while NADPH is consumed during the MVA pathway. Additional expression of an NAD<sup>+</sup>-dependent formate dehydrogenase in combination with supplementation of 50 mM formate improved co-factor balance and further increased production substantially. Modifying co-factor requirements has also been addressed in *S. cerevisiae* to improve production

of farnesene and santalene. As such, Meadows et al. (2016) utilized a HMG-CoA reductase from *Silicibacter pomeroyi* for production of farnesene, which is specific to NADH. In contrast, Scalcinati et al. (2012b) improved co-factor balance by deleting the gene of the NADPH-dependent glutamate dehydrogenase (*GDH1*) and overexpressing the NADH-dependent isozyme (*GDH2*). Another approach to increase the flux through the pathway is by targeting the regulation of sterol synthesis, which has been utilized for production of santalene, bisabolene and artemisinic acid (Peralta-Yahya et al., 2011; Ro et al., 2006; Scalcinati et al., 2012b; Westfall et al., 2012). This strategy aims at upregulating the entire MVA pathway by overexpressing a mutant of the transcription factor Upc2, which has previously been reported to increase its transcriptional activation (Davies et al., 2005).

**Engineering of the FPP branch point.** Increasing the pool of FPP by overexpression of MVA pathway genes is likely to increase the flux of FPP into other pathways. Therefore, a strategy particularly applied for production of sesquiterpenes constitutes engineering of the FPP branch point. As an example, the two phosphatases Lpp1 and Dpp1 have been shown to hydrolyze prenyl diphosphates, possibly to prevent accumulation of these intermediates to toxic levels (Faulkner et al., 1999). Deletion of these enzymes has been used successfully to reduce formation of farnesol from FPP during the production of santalene in *S. cerevisiae* (Scalcinati et al., 2012a,b). However, several other studies reported no, or even a negative effect upon deletion of these phosphatases (Farhi et al., 2011; Ignea et al., 2014; Takahashi et al., 2007). In contrast, deletion of *ERG9* encoding squalene synthase would result in auxotrophy for ergosterol and require supplementation of the medium. In order to circumvent this problem and downregulate sterol synthesis, different promoters have been used to reduce the expression of squalene synthase. Replacing the endogenous promoter of *ERG9* by the *MET3* promoter ( $P_{MET3}$ ), which is repressed by addition of methionine, has been shown to efficiently reduce ergosterol levels and to improve production of amorphadiene, patchoulol and cubebol (Asadollahi et al., 2008; Paradise et al., 2008). A variation of this approach was presented by Paddon et al. (2013), who used the  $P_{CTR3}$ , which can be downregulated by addition of CuSO<sub>4</sub>. In addition, *ERG9* expression has also been downregulated to improve production of santalene (Scalcinati et al., 2012a). Here, the promoter of the hexose transporter Hxt1 ( $P_{HXT1}$ ) was used, which is mainly induced at high glucose concentrations in *S. cerevisiae* ( $\geq 1\%$ ) (Ozcan and Johnston, 1995; Reifenberger et al., 1995). Since expression responds to the glucose concentration, there is no requirement for medium supplements. Recently, downregulation of *ERG9* was also enabled by expression from ergosterol responsive promoters, i.e. *ERG1*, *2*, *3* and *11* (Yuan and Ching, 2015). Thereby, a sufficient supply of ergosterol could be maintained while titers of amorphadiene increased significantly. Besides deleting and downregulating competing side reactions to increase the availability of FPP for sesquiterpene production, construction of fusion proteins between the FPP synthase (Erg20) and the terpene synthase has promoted production of mono- and sesquiterpenes, such as pinene (Sarria et al., 2014), patchoulol (Albertsen et al., 2011) and farnesene (Wang et al., 2011). These constructs are generated by expression of the fusion partners from the same reading frame and are believed

to channel the substrate from one enzyme to the other by increasing the proximity between the enzymes (Elleuche, 2014). In all of the listed studies, titers could be improved by 50 % or more.

**Expression of the heterologous MVA/MEP pathway.** As there are two distinct pathways to provide the essential building blocks IPP and DMAPP, additional expression of the heterologous pathway has been used as a tool to increase their supply. An additional benefit of this strategy concerns the regulation of the heterologous pathway, which is assumed to be omitted. In one of the earlier studies, Takagi et al. (2000) showed that expression of the MVA pathway from *Streptomyces* sp. strain CL190 in *E. coli* is sufficient to complement for the loss of the endogenous MEP pathway. Soon after, this strategy was utilized for production of amorphadiene in *E. coli* (Martin et al., 2003). Since then, partial or complete expression of the MVA pathway in *E. coli* has been used frequently for production of terpenes (Sarria et al., 2014; Wang et al., 2011). However, expression of the heterologous pathway represents a metabolic burden to the cell, resulting in accumulation of toxic intermediates (e.g. HMG-CoA) and imbalances in gene expression (Kizer et al., 2008; Martin et al., 2003; Pitera et al., 2007). In order to allow for its optimal application for sesquiterpene production, several studies have addressed fine tuning of the heterologous MVA pathway expression (Anthony et al., 2009; Dahl et al., 2013; Pfleger et al., 2006; Pitera et al., 2007). *Vice versa*, functional expression of the MEP pathway in *S. cerevisiae* has been investigated, but not fully achieved yet. For instance, the pathway has been expressed from episomal plasmids in the presence of the MVA pathway and after addition of lovastatin to inhibit HMG-CoA reductase, the strain was still able to sustain growth (Maury et al., 2008). However, Partow et al. (2012) pursued an alternative strategy and integrated the MEP pathway into the genome. In addition to inhibiting the HMG-CoA reductase using lovastatin, *ERG13* was deleted to generate an auxotrophy for mevalonate and to exclude the possibility that HMG-CoA reductase is not completely inhibited by lovastatin. The resulting strain was unable to sustain growth, indicating that the heterologous pathway was not functional. This was mainly assigned to the requirement for iron-sulfur clusters of the last two enzymes of the pathway, IspG and IspH, which could not be functionally expressed in *S. cerevisiae*, neither under aerobic nor anaerobic conditions. At about the same time, a similar study was conducted by Carlsen et al. (2013), who came to the same conclusion.

**Reducing product toxicity.** Toxicity does not only arise from accumulation of pathway intermediates, but also from the product itself, which represents a major obstacle to terpene production. Particularly monoterpenes have been reported to affect both, *E. coli* and *S. cerevisiae* (Brennan et al., 2012; Dunlop et al., 2011; Sarria et al., 2014), whereas sesquiterpenes like bisabolene did not affect cell viability (Peralta-Yahya et al., 2011). One of the most toxic monoterpenes is limonene, which reduces growth of *S. cerevisiae* by 50 % at 0.44 mM (Brennan et al., 2012). Addition of an organic overlay proved to be a simple strategy to substantially increase the tolerance by sequestering the toxic compound (Brennan et al., 2012). Besides, the focus has been set to the transport mechanisms in order to improve tolerance to these compounds.

Expression of the efflux pumps TtgB from *Pseudomonas putida* and AcrB from *E. coli* significantly improved the tolerance of *E. coli* towards pinene and limonene (Dunlop et al., 2011). Additionally, the ATP-binding cassette (ABC) transporter MdlB was shown to be upregulated during exposure of *E. coli* to isopentenol and could improve its production by 12 % (Foo et al., 2014). Similarly, several ABC transporters were shown to be upregulated in *S. cerevisiae* upon exposure to limonene, i.e. Pdr5, Pdr15 and Yor1. However, overexpression of these proteins failed to improve the viability towards limonene (Hu et al., 2012). The mode of action is not fully resolved, but significant changes in gene expression were observed regarding cell wall biogenesis (Brennan et al., 2013). However, significant advances have been made recently as a truncated variant of the tricalbin protein Tcb3 has been identified to improve tolerance towards the monoterpenes limonene, pinene and myrcene by 9, 11 and 8-fold respectively, upon evolutionary engineering of *S. cerevisiae* (Brennan et al., 2015).

**Engineering acetyl-CoA metabolism.** The pool of cytosolic acetyl-CoA plays an important role for the production of terpenes and several novel approaches have been presented within the last years to increase it. For example, expression of the pyruvate dehydrogenase complex (Pdh) from *Enterococcus faecalis* in the cytosol of *S. cerevisiae* could be used to directly convert pyruvate to acetyl-CoA, which abolishes the ATP cost for cytosolic acteyl-CoA supply in comparison to the endogenous pathway (Kozak et al., 2014). In fact, the yield of farnesene on glucose was calculated to reach up to 91 % of the theoretical maximum by providing acetyl-CoA from the pentose-phosphate-pathway using the phosphoketolase (PK) and phosphotransacetylase (PTA) in combination with ATP-independent acetyl-CoA supply from pyruvate using the Pdh (van Rossum et al., 2016). This strategy has been implemented in part for the production of farnesene in *S. cerevisiae* by utilization of the phosphoketolase pathway (PK/PTA) (Meadows et al., 2016). In addition, expression of ATP citrate lyase (Acl) from *Aspergillus nidulans* to produce acetyl-CoA from citrate was shown to promote synthesis of MVA pathway intermediates (Rodriguez et al., 2016). Apart from this, acetyl-CoA synthesis has also been utilized as a metabolic switch for production of farnesene in an industrial setup. As such, reducing the concentration of pantothenate in the medium, which is essential for acetyl-CoA synthesis, was shown to decrease production of farnesene while improving the genetic stability and fitness of the highly engineered strain. After reaching peak cell density, addition of pantothenate could then be used to initiate production of farnesene at improved yields (Sandoval et al., 2014).

**Alternative pathways/product formation strategies.** Novel pathways have been recently proposed for production of isopentenol in *E. coli* with the main objective to improve energy efficiency and prevent accumulation of the toxic intermediate IPP (Kang et al., 2016). The first alternative involved direct decarboxylation of mevalonate to isopentenol using the mevalonate diphosphate decarboxylase from *S. cerevisiae*. This approach only showed limited success, since binding of the diphosphate group was shown to be important. However, clear improvements were observed in the second approach where mevalonate phosphate was decarboxylated to isopentenyl

phosphate and subsequently converted to isopentenol via additional overexpression of the endogenous phosphatase AphA. Lastly, metabolic engineering has realized efficient production of taxadiene in *E. coli* with final titers of up to 1 g/L (Ajikumar et al., 2010). Taxadiene constitutes the first intermediate in the synthesis of the anticancer drug paclitaxel and is directly produced from GGPP. In comparison, production of taxadiene in *S. cerevisiae* did not exceed 72 mg/L hitherto (Ding et al., 2014). However, to circumvent problems regarding the expression of cytochrome P450 enzymes in *E. coli*, which catalyze the oxygenations required for the synthesis of paclitaxel and can be expressed in *S. cerevisiae*, production of oxygenated taxanes has been enabled by distributing the pathway for their production to both organisms. As such, in a co-culture with xylose as the main carbon source, *E. coli* was able to provide acetate and taxadiene to *S. cerevisiae* for growth and product formation, which in return relieved acetate toxicity on *E. coli* and ultimately allowed for production of taxanes from a cheap and abundant feedstock (Zhou et al., 2015).

## 1.4 Outline and Objectives of the Thesis

The mevalonate pathway is of crucial importance for the yeast *S. cerevisiae* as it is utilized to produce sterols, ubiquinone and dolichols. Besides, the pathway intermediate farnesyl diphosphate (FPP) is an important substrate for protein farnesylation and heme A synthesis. Over many years research efforts have focused on engineering of the mevalonate pathway to allow for the efficient and sustainable production of sesquiterpenes, which are of great commercial interest due to their diverse applications in the fuel, food, cosmetic and pharmaceutical industry. Among others, *S. cerevisiae* has been engineered for production of a number of sesquiterpenes such as the precursors of the antimalarial drug artemisinin, amorpha-4,11-diene and artemisinic acid (Paddon et al., 2013; Ro et al., 2006; Westfall et al., 2012) and the fragrances patchoulol, cubebol and santalene (Asadollahi et al., 2010; Scalcinati et al., 2012a). This project aimed at investigating synthesis of sesquiterpenes in *S. cerevisiae* with the objective to gain new insights into the underlying metabolic pathways and to identify novel metabolic engineering strategies. To provide a brief overview of the thesis, the following aspects were addressed in this project to study farnesene production in *S. cerevisiae*.

In the first part, the main objective was to study the relevance of terpene synthases for sesquiterpene production. These enzymes are responsible for catalyzing the terminal conversion of FPP to the desired sesquiterpene and are not endogenous to yeast. Santalene synthase from *Clausena lansium* led to final titers of 163 mg/L in engineered *S. cerevisiae* (Scalcinati, 2012) and the question arose whether this result is comparable to production of farnesene, which requires a different terpene synthase. In addition, since various farnesene synthases have been identified in plants (e.g. apple, maize, orange, etc.), the question of how different isozymes compare to each other when

expressed in *S. cerevisiae* was addressed to determine if differences can be assigned to the origin of these enzymes.

Production of santalene was enabled by combining several metabolic engineering strategies (Scalcanati, 2012). As a consequence of the engineering, the resulting strain displayed several physiological alterations in chemostat cultivations, such as reduction of the biomass yield. These observations initiated efforts to thoroughly investigate the effects of the different genetic modifications, to identify flux controlling reactions and ultimately, to derive potential metabolic engineering targets. For this purpose, transcriptome and metabolome analysis were used to characterize the strain during the production of farnesene, which allows for a comparison of three distinct metabolic conditions.

Efficient production of sesquiterpenes depends on diverting flux at the FPP branch point, which is achieved by deleting or downregulating competing reactions. Additionally, FPP can be utilized more efficiently by construction of fusion proteins, which increase the accessibility of FPP to the terpene synthase (Albertsen et al., 2011). In this project, affinity proteins called affibodies were used to construct enzyme scaffolds to increase the proximity between the FPP and farnesene synthase and thereby to increase production of farnesene. Several parameters that potentially affect the functionality of the system were addressed. Eventually, the concept was also extended to three enzymes for a different pathway.

Acetyl-CoA is the main substrate of the mevalonate pathway. Overall, 9 moles of acetyl-CoA are required for production of 1 mole of farnesene. However, the first reaction of the mevalonate pathway catalyzed by acetoacetyl-CoA thiolase (Erg10) is thermodynamically unfavorable. In order to overcome this limitation and to improve utilization of acetyl-CoA for the mevalonate pathway, a recently identified acetoacetyl-CoA synthase was expressed to incorporate malonyl-CoA as a substrate and thereby to increase production of farnesene. The impact of the enzyme was evaluated by studying growth and product formation. Additionally, different homologous enzymes were compared to identify an enzyme with superior efficiency.

Quantification of sesquiterpenes plays an important role during the metabolic engineering process. Because of their low volatility and hydrophobicity, sesquiterpenes are sequestered in extractive organic overlays to reduce product loss due to gas stripping effects. High product capacity and compatibility with the producing strain are key criteria for the selection of these solvents. However, since the solvents used as overlay often have detrimental effects on analytical techniques, we examined the existing procedures for the analysis of organic overlays in order to provide solutions for efficient and reliable sample analysis.



## Chapter 2

# Comparison of Farnesene Synthases

Terpene synthases and cyclases catalyze the synthesis of cyclic and acyclic terpenes from prenyl diphosphates and hence their functional expression in *S. cerevisiae* represents a prerequisite for the production of these compounds. A large variety of these enzymes exists in plants, which possess terpene synthase gene families containing up to 150 genes (Chen et al., 2011). As a result of this, novel terpene synthases are still being discovered in plants, such as the recently identified santalene synthase from *Santalum album* (Srivastava et al., 2015). Additionally, genome sequencing and phylogenetic analysis have recently revealed the existence of these enzymes in various bacteria (Yamada et al., 2015). Conversion of prenyl diphosphates to terpenes is achieved via Wagner-Meerwein rearrangements. The reaction mechanism involves ionization of the prenyl diphosphate to form a reactive carbocation, which is followed by hydride and alkyl shifts to increase the stability and allow for cyclization, and eventually terminated by deprotonation (Davis and Croteau, 2000; Degenhardt et al., 2009; Dewick, 2001). The active site of the enzyme is located at the COOH-terminus and contains a conserved aspartate-rich motif (DDXXD), which is involved in the metal-dependent ionization of the prenyl diphosphate (Bohlmann et al., 1998; Chen et al., 2011; Starks et al., 1997). Through the production of multiple products by the same enzyme, terpene synthases are to a large extent responsible for the chemical diversity of terpenes (Degenhardt et al., 2009). Nonetheless, single product terpene synthases have been reported to exist as well (Davis and Croteau, 2000). However, several factors influence the product portfolio such as the availability of co-factors. As an example, the specificity of a farnesene synthase from peppermint for (*E*)- $\beta$ -farnesene varied between 85 and 98 % depending on utilization of Mg<sup>2+</sup> or Mn<sup>2+</sup> as co-factor (Crock et al., 1997). Besides, a modified product profile was obtained by a sesquiterpene synthase from *Sorghum bicolor* as a result of a single amino acid mutation, which was responsible for a change of the deprotonation site within the active center (Garms et al., 2012).

Terpene synthases with various plant origins have been used for production of sesquiter-

penes in *S. cerevisiae*. While production of santalene has been realized by expression of santalene synthase from *Clausena lansium* (Scalcanati et al., 2012a), the terpene synthases from *Citrus paradisi* and *Pogostemon cablin* have been utilized for production of valencene, cubebol and patchoulol (Albertsen et al., 2011; Asadollahi et al., 2008). Farnesene is produced from FPP in a single enzymatic reaction by farnesene synthase using a mechanism, which is illustrated in Figure 2.1.

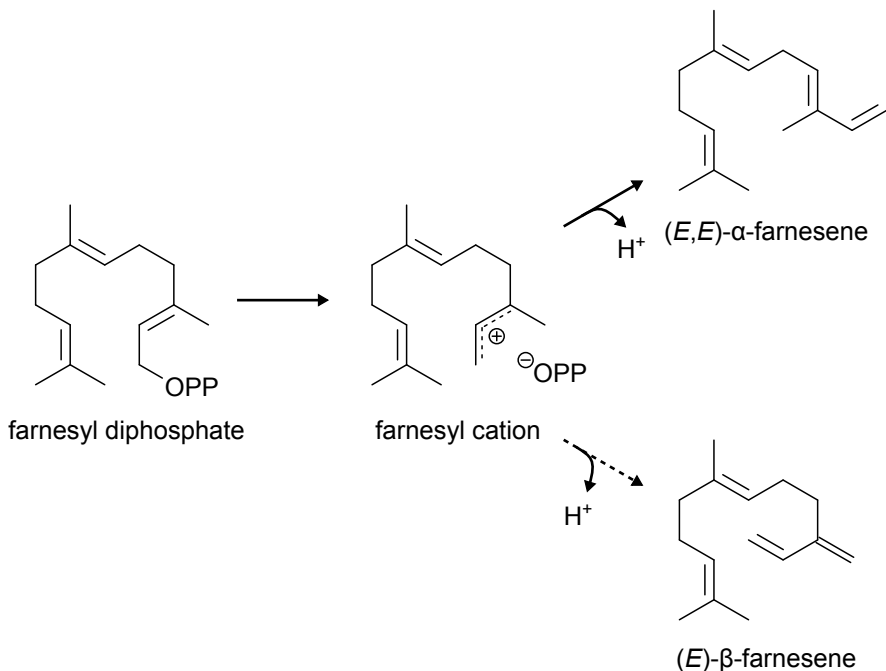


**Figure 2.1:** Simplified reaction mechanism catalyzed by farnesene synthase for conversion of farnesyl diphosphate (FPP) to either  $\alpha$ - or  $\beta$ -farnesene. OPP represents the diphosphate group and dashed arrows indicate that the reaction proceeds via several intermediates. The scheme has been adopted from Davis and Croteau (2000) and Tholl (2015).

The reaction is initiated by ionization of FPP to produce the reactive farnesyl cation, which is subsequently deprotonated to  $(E,E)\text{-}\alpha\text{-farnesene}$ . In case of  $(E)\text{-}\beta\text{-farnesene}$ , the reaction proceeds via the intermediates nerolidyl diphosphate and nerolidyl cation and is similarly terminated by deprotonation (Davis and Croteau, 2000; Tholl, 2015). Overall there are six farnesene isomers in total.

The selection of enzymes has been shown to be of crucial importance for the efficient production of sesquiterpenes from the MVA pathway (Ma et al., 2011). Since farnesene synthase catalyzes the final reaction of the pathway to produce farnesene, it potentially imposes limitations on the overall productivity. Similarly, production of bisabolene was suggested to be limited by the bisabolene synthase (Kirby et al., 2014). For this reason, the main question of this study was to investigate if farnesene synthases from distinct plant origins also produce distinct amounts of farnesene when expressed in *S. cerevisiae*. Therefore, three different farnesene synthases were compared regarding their ability to produce farnesene. Similar studies have been conducted for production of sesquiterpenes in *E. coli* and *S. cerevisiae* (Martin et al.,

2001; Peralta-Yahya et al., 2011; Xie et al., 2012). As an example, bisabolene synthase from *Picea abies* produced 23 mg/L bisabolene, while the corresponding synthase from *Pseudotsuga menziesii* reached final titers of 69 mg/L (Peralta-Yahya et al., 2011). Similarly, Xie et al. (2012) identified clear variations concerning the production of sesquiterpenes using different terpene synthases from *Ricinus communis*. Moreover, a remarkable variation of the production was observed in this study when comparing expression in *E. coli* and *S. cerevisiae*. Several farnesene synthases have been isolated and characterized, e.g. from *Zea mays* (Schnee et al., 2002) and *Mentha piperita* (Crock et al., 1997). Besides, the coding sequences for several of these enzymes are available at the National Center for Biotechnology Information (NCBI, [www.ncbi.nlm.nih.gov](http://www.ncbi.nlm.nih.gov)). In this study, we selected one  $\alpha$ -farnesene synthase from *Malus domestica* (Green et al., 2007) and two  $\beta$ -farnesene synthases from *Citrus junos* (Maruyama et al., 2001) and *Artemisia annua* (Picaud et al., 2005). The selection of the synthases was motivated by the fact that these had been studied *in vitro* before and hence had a confirmed ability to produce farnesene. Besides, BLAST analysis using the amino acid sequences suggested potential differences between the candidates, as farnesene synthase from *Citrus junos* and *Artemisia annua* shared the highest level of identity among the three enzymes with 41 %. On the other hand,  $K_m$ -values of the farnesene synthase from *M. domestica* and *A. annua* for FPP were reported to be relatively similar with 3 and 2.1  $\mu\text{M}$ , respectively (Green et al., 2007; Picaud et al., 2005). All three genes were codon optimized for expression in *S. cerevisiae*. As illustrated by the example of bisabolene synthase, codon optimization caused the most significant improvement in production (Peralta-Yahya et al., 2011).

In the first experiment, the three synthases were expressed from a high-copy 2-micron plasmid in the reference *S. cerevisiae* strain CEN.PK113-5D (*MATa MAL2-8c SUC2 ura3-52*). Although final farnesene titers after 48 h of cultivation in shake flasks were low with around 4 mg/L<sub>aq</sub>, the results presented in Figure 2.2 show that strains expressing farnesene synthase from *M. domestica* produced approximately 20 and 47 % more compared to strains expressing farnesene synthase from *C. junos* and *A. annua*, respectively. In this genetic background, intracellular concentrations of FPP can be considered to limit the production of farnesene. Consistent with the literature, additional expression of *tHMG1* to increase the flux through the pathway improved production by 30 % on average for each of the three synthases.

In order to further investigate differences between the selected candidates at high FPP concentrations, the enzymes were then expressed in strain SCIGS22, which was engineered to overproduce sesquiterpenes by combining several metabolic engineering approaches (Scalcanati et al., 2012b). Apart from this, the rationale for utilizing this strain was to assess how much the final titers of farnesene could be improved in comparison to the results obtained from the shake flask cultivation and also to compare production of farnesene and santalene with respect to the terpene synthases. Figure 2.3 provides an overview of the engineering strategies pursued for construction of strain SCIGS22, which have already been described in more detail in the introduction (section 1.3).

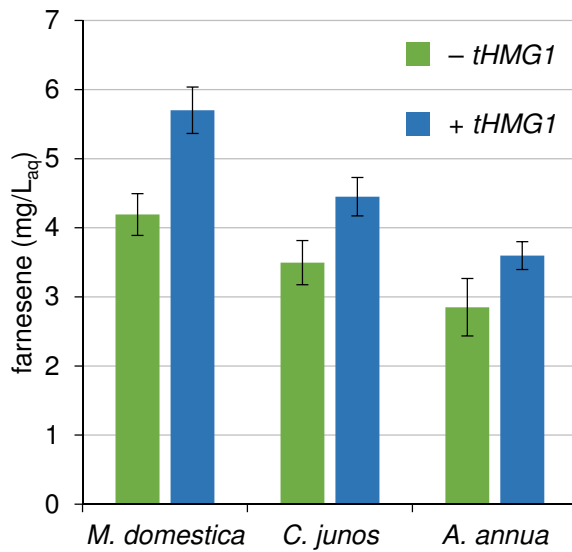


**Figure 2.2:** Comparison of farnesene synthase from *Malus domestica*, *Citrus junos* and *Artemisia annua* for production of farnesene in *S. cerevisiae* strain CEN.PK113-5D. Production was compared in combination with overexpression of *tHMG1* encoding a truncated version of the HMG-CoA reductase. Data represents average concentrations of three independent shake flask cultivations based on the volume of aqueous medium with standard deviation after 48 h of cultivation.

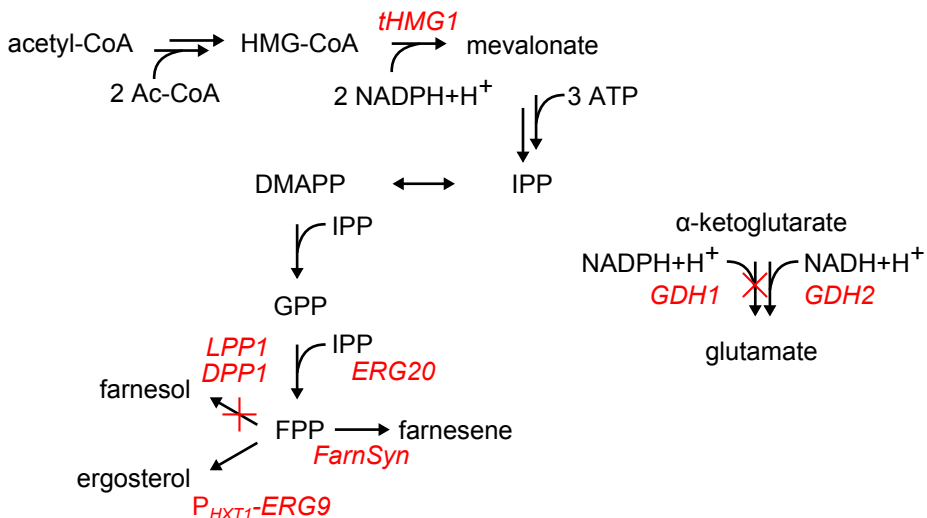


**Figure 2.3:** Simplified illustration of the MVA pathway and ammonium assimilation to highlight the modifications used for increased production of sesquiterpenes in *S. cerevisiae* strain SCIGS22. Gene names are written as red italics. The truncated HMG-CoA reductase (*tHMG1*) and the farnesene synthase from *C. junos* (*FarnSyn*) were expressed from a multi-copy plasmid. Further details are provided in the text.

In summary, *ERG20* encoding FPP synthase was overexpressed for increased flux through the MVA pathway and by-product formation was reduced by deletion of the two phosphatases *Lpp1* and *Dpp1*. Additionally, sterol synthesis was downregulated

by expression of squalene synthase (*ERG9*) using  $P_{HXT1}$ . Lastly, the NADPH-dependent glutamate dehydrogenase (Gdh1) was deleted and the NADH-dependent isozyme (Gdh2) was overexpressed to improve co-factor balance. Lastly, one of the three selected farnesene synthases (*FarnSyn*) was expressed from a multi-copy plasmid together with the truncated variant of the HMG-CoA reductase (*tHMG1*). In order to compare production of farnesene in this strain to the reference CEN.PK113-5D, cultivations were performed in fed-batch mode, which is widely used in industrial fermentations to attain high cell densities by reducing ethanol formation under aerobic conditions. This phenomenon has been observed in *S. cerevisiae* at glucose concentration above 90-100 mg/L (Woehrer and Roehr, 1981) and 150 mg/L (Verduyn et al., 1984). More importantly, downregulating the expression of *ERG9* using  $P_{HXT1}$  requires low glucose concentrations, which can be achieved with this experimental setup. Thereby, biomass can be accumulated during the batch phase with excess amounts of glucose, while reduction of the glucose concentration initiates the production phase by hindering sterol synthesis. Accurate design of the feed profile based on the strain physiology (i.e.  $Y_{SX}$ ) is essential to attain optimal performance. While overfeeding results in ethanol formation, underfeeding would likewise reduce the productivity during the fed-batch phase. For this purpose, the respiratory quotient (*RQ*) was additionally used as a feedback parameter to trigger the feed with the objective to indirectly control the glucose concentration in the medium and to maintain fully respiratory conditions. The *RQ* has been proposed as a suitable parameter to control and optimize fermentation processes, because of its fast response time upon changes regarding the feed and because its value specifically represents different metabolic states (Woehrer and Roehr, 1981). Hence, the main rationale for using this approach was to optimize the production of farnesene, particularly because downregulation of an essential gene could potentially hamper growth and affect the physiology of the strain, which could likewise lead to the production of ethanol. Calculated online from the exhaust gas analysis as the ratio of the carbon dioxide transfer rate (*CTR*) to the oxygen transfer rate (*OTR*), the set point of the *RQ* was 1, which indicates complete oxidation of glucose (Villadsen et al., 2011; Woehrer and Roehr, 1981). Similarly, an *RQ* feedback control has also been used to improve production of glutathione by *S. cerevisiae* (Xiong et al., 2010) and more recently, to improve large scale production of erythromycin by *Saccharopolyspora erythraea* (Chen et al., 2015). Besides, comparable strategies have also been developed using the pH to reduce acetate formation by *E. coli* (Kim et al., 2004).

Typical profiles of the *RQ*, vessel volume and feed rate using this control scheme are depicted in Figure 2.4 A. In the beginning of the fed-batch phase, the feeding rate increased exponentially to account for exponential growth. Once the *RQ* exceeded a value of 1, indicating a transition from respiration to aerobic fermentation, the feed was deactivated. Using this feed profile, *S. cerevisiae* strain CEN.PK113-5D reached final biomass concentrations of up to 25 gDCW/L and produced approximately 50 mg/L<sub>aq</sub> of farnesene within 32 h (Figure 2.4 B, top row). Apart from this, concentrations of ethanol remained close to 0. Similar to the results obtained from the experiment performed in shake flasks, CEN.PK113-5D expressing farnesene syn-

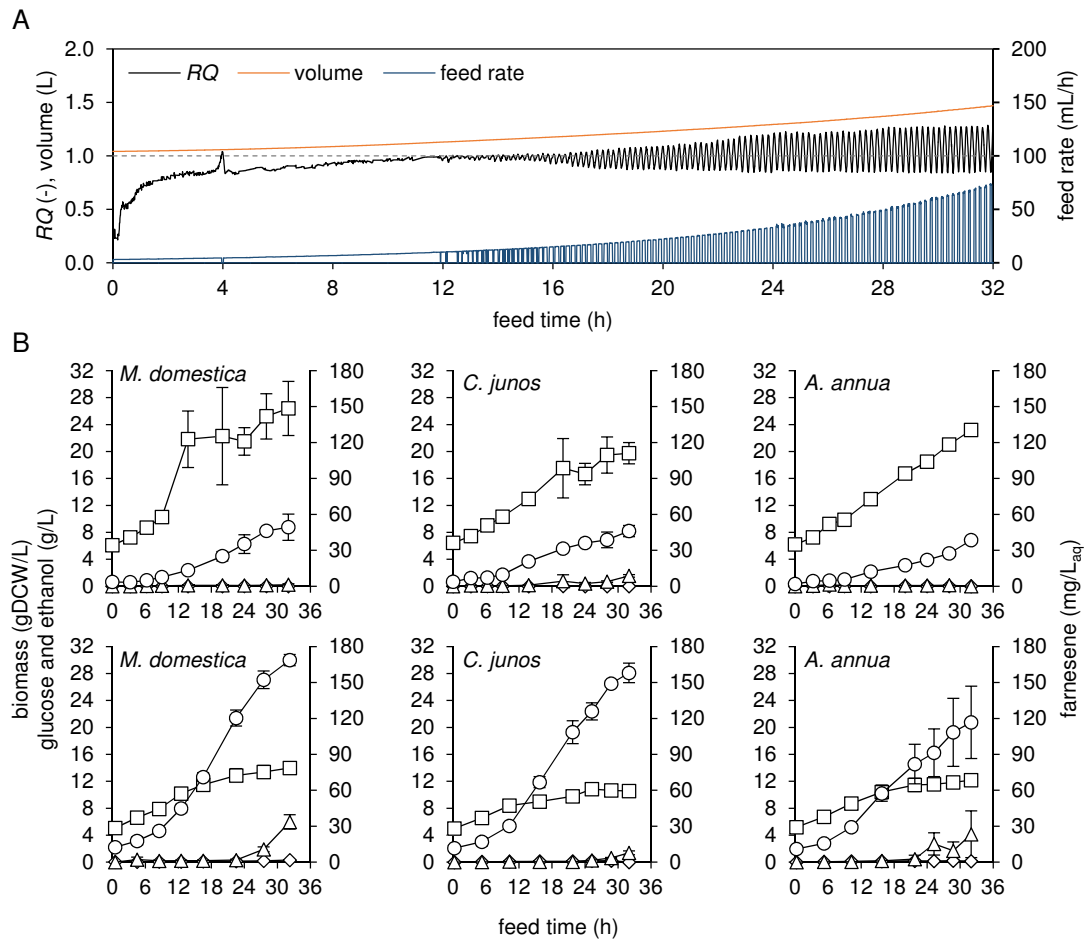


**Figure 2.4:** Comparison of three plant terpene synthases from *Malus domestica*, *Citrus junos* and *Artemisia annua* for production of farnesene in *S. cerevisiae* using fed-batch cultivations with respiratory quotient (RQ)-controlled exponential feeding. (A) Representative profiles of the RQ, volume and feed rate during the feed phase. (B) Profiles for concentrations of biomass (□), glucose (◇), ethanol (△) and farnesene (○). Top row shows results for the reference strain CEN.PK113-5D, while the bottom row shows results for the engineered strain SCIGS22. In all experiments, the farnesene synthase was expressed from a high-copy plasmid together with the truncated version of HMG-CoA reductase (*tHMG1*). Data represents average concentrations of two or three biological replicates with standard deviation. Farnesene concentrations were expressed based on volume of aqueous medium.

thase from *M. domestica* reached highest final titers with 49 mg/L<sub>aq</sub>, which were 7 and 28 % higher compared to the farnesene synthase from *C. junos* and *A. annua*, respectively. However, the difference was not significant due to the large standard deviation obtained for farnesene synthase from *M. domestica* (Table 3, publication II appended to the thesis). The yield of farnesene per glucose on the other hand was identical for all three synthases with  $Y_{S\text{Far}}=0.001 \text{ g}/(\text{g glucose})$ , showing no significant difference between the enzymes. In comparison, highest farnesene titers for strain SCIGS22 were again obtained by expressing farnesene synthase from *M. domestica* with 169 mg/L<sub>aq</sub> and an increase of 7 and 45 % over the enzymes from *C. junos* and *A. annua*, respectively (Figure 2.4 B, bottom row). In contrast, biomass

concentrations were significantly reduced and did not exceed 15 gDCW/L. Similar to strain CEN.PK113-5D, there was no indication for superior efficiency for any of the enzymes based on the farnesene yield on glucose  $Y_{S\text{Far}}$ , which were almost identical and amounted to 0.003 g/(g glucose) for *M. domestica* and *C. junos*, and 0.002 g/(g glucose) for *A. annua*. However, significant variations of the biomass yield were observed, most likely as a result of the ethanol formation observed for strain SCIGS22 expressing farnesene synthase from *M. domestica* and *A. annua*. Taking this into consideration, farnesene synthase from *C. junos* expressed in strain SCIGS22 resulted in the highest yield with  $Y_{X\text{Far}}=0.022$  g/gDCW. Several reasons could explain the formation of ethanol during the cultivation of strain SCIGS22 such as limitations in the mass transfer (Villadsen and Patil, 2007). Most importantly, however, deactivation of *ERG9* expression could have led to insufficient supply of ergosterol to sustain growth, eventually resulting in production of ethanol. Besides, *RQ* values were usually oscillating around 1, where ethanol formation could have occurred at  $RQ>1$ . In this scenario, consumption of ethanol could potentially be beneficial as the highest titers for production of sesquiterpenes have been observed using a pure ethanol or a mixed glucose-ethanol feed medium (Paddon et al., 2013). Concluding, the results obtained from the shake flask cultivations as well as the fed-batch cultivations consistently indicated beneficial properties of the synthase from *M. domestica* based on the final farnesene titers. However, consideration of the farnesene yield per gram biomass ( $Y_{X\text{Far}}$ ), which compensates for the variation of the biomass yield, a farnesene synthase with superior efficiency could not be clearly identified. Nonetheless, production of farnesene was significantly improved as a result of the modifications made for construction of strain SCIGS22. Although the selected enzymes showed considerable differences regarding their amino acid sequences, facilitating the expression of their genes by codon optimization could have diminished the differences between them regarding their catalytic efficiency. Surprisingly, cultivation of strain SCIGS22 expressing  $\alpha$ -santalene synthase from *C. lansium* resulted in almost identical final titers with 163 mg/L<sub>aq</sub> of  $\alpha$ -santalene (Scalcinati, 2012). However, the reduction of the yield per gram biomass  $Y_{X\text{San}}$ , which amounted to 0.006 g/gDCW and thereby represents a decrease of at least 50 % compared to the yields obtained for the farnesene synthases, indicates considerable differences regarding the efficiency of distinct terpene synthases. Based on this, these results emphasize the importance of the terpene synthase selection for production of sesquiterpenes. To avoid extensive screening, engineering of the terpene synthase has emerged as an alternative strategy to improve the efficiency of these enzymes (Yu et al., 2012; Zhao et al., 2012). For instance, mutagenesis of the catalytic domain of an  $\alpha$ -pinene synthase using error-prone PCR led to the identification of a variant, which showed increased consumption of GPP and significantly improved production of pinene in *E. coli* (Tashiro et al., 2016).



## Chapter 3

# Metabolic and Transcriptomic Response to Production of Farnesene

In the first study of this project, three farnesene synthases with distinct plant origin were compared for production of farnesene in *S. cerevisiae*. Although no significant differences were observed between the three selected enzymes, a clear increase in the production of farnesene was observed when these enzymes were expressed in a genetic background engineered for sesquiterpene production. As described in the introduction, numerous metabolic engineering strategies have been reported to increase production of sesquiterpenes in *S. cerevisiae*. Limitations on the production of farnesene upon enhanced pathway activity may for example arise from the accumulation of toxic intermediates such as IPP/DMAPP and FPP (Rodriguez et al., 2014; Yuan and Ching, 2015). Similarly, increased levels of HMG-CoA during the heterologous expression of the MVA pathway in *E. coli* were shown to inhibit growth (Pitera et al., 2007). Limitations could likewise be connected with the toxicity of the product itself or an inefficient secretion machinery, which has been mainly shown for monoterpenes. For instance, transcriptome analysis showed that exposure to limonene impaired cell wall biogenesis in *S. cerevisiae* (Brennan et al., 2013). Furthermore, downregulation of sterol synthesis could affect the regulation of the MVA pathway and hence the overall productivity at increased pathway fluxes. Likewise, the modified assimilation of nitrogen to improve co-factor balance was expected to lead to an altered amino acid metabolism. In this respect, it is important to understand the effect of these perturbations before further modifications are made. As a result, with the objective to derive novel metabolic engineering targets to further improve production of sesquiterpenes in *S. cerevisiae*, the response of the engineered strain SCIGS22 to the genetic modifications was thoroughly investigated during the production of farnesene. For this purpose, strain CEN.PK113-5D and SCIGS22, both expressing the truncated HMG-CoA reductase (*tHMG1*) and farnesene synthase from *C. junos* from a multi-copy plasmid, were cultivated in fed-batch mode, which allows to compare the two strains in three distinct metabolic states. Initially, the cultivation was started as a batch. In this condi-

tion, high glucose concentrations in the medium lead to fermentative metabolism and much of the glucose is converted to ethanol by *S. cerevisiae* (Fiechter and Seghezzi, 1992; Sonnleitner and Kaepeli, 1986). Subsequent to the depletion of glucose, *S. cerevisiae* switches from fermentative metabolism to oxidation of ethanol, which involves activation of the glyoxylate cycle and gluconeogenesis (De Jong-Gubbels et al., 1995). Lastly, the fed-batch phase was designed to avoid fermentative metabolism and to attain complete oxidation of glucose as well as to activate downregulation of *ERG9* using P<sub>HXT1</sub>.

In the first part, physiological differences were determined based on the fermentation data. To study perturbations affecting specific pathways, metabolite profiling is often used, which aims to quantify changes of a predefined set of metabolites. Among other results, this technique has aided the discovery that efflux of methylerythritol cyclodiphosphate reduces terpenoid production from the MEP pathway in *E. coli* (Zhou et al., 2012). Similarly, metabolite profiling in combination with microarray analysis has been used to study the mechanism behind HMG-CoA toxicity originating from the heterologous expression of the MVA pathway in *E. coli* (Kizer et al., 2008). In this study, metabolome analysis was employed to characterize the phenotype of the engineered strain, which aims at measuring the relative changes in the abundance levels of all low-molecular weight compounds inside the cell. In this respect, metabolomics has become a powerful technology (Merlo et al., 2011) and its potential for synthetic biology has been highlighted by Ellis and Goodacre (2012) and Nguyen et al. (2012). For instance, metabolome analysis has been recently used to study the response of *S. cerevisiae* towards different stress conditions i.e. increased temperatures and concentrations of copper (Farrés et al., 2014, 2016). With respect to the production of farnesene, metabolome analysis could promote the identification of changes in other pathways and hence help to identify future engineering targets. Recently, several knockouts were predicted *in silico* and confirmed to increase production of amorphadiene without direct connection to the pathway used for product formation, such as hexokinase of the Embden-Meyerhof-Parnas pathway, isocitrate dehydrogenase of the TCA cycle and phosphoserine aminotransferase involved amino acid metabolism (Sun et al., 2014). However, despite the potential of metabolomics, several challenges were taken into consideration. Most importantly, the high turnover rate of various metabolites inside the cell could potentially result in large variations in the data set and ultimately hamper the deduction of a clear conclusion. Secondly, precise identification of the elemental composition based on accurate mass measurements using LC-qTOF remains challenging (Kind and Fiehn, 2006). Lastly, although a highly efficient methanol-based extraction method was used (A et al., 2005), the extraction method as well as the selection of the solvent, were shown to significantly affect the outcome of metabolome studies (Duportet et al., 2012). For these reasons, transcriptome analysis based on RNAseq, which has been used extensively to study *S. cerevisiae* (Fletcher et al., 2015; Nookaew et al., 2012; Papini et al., 2012), was applied to complement the results from the metabolome analysis and to identify correlations between the two data sets. This approach, i.e. the integration of these data sets, has been recently described to highlight active metabolic pathways in *Rhodospirillum*

*ruberum* and *Bacillus subtilis* (Cho et al., 2015).

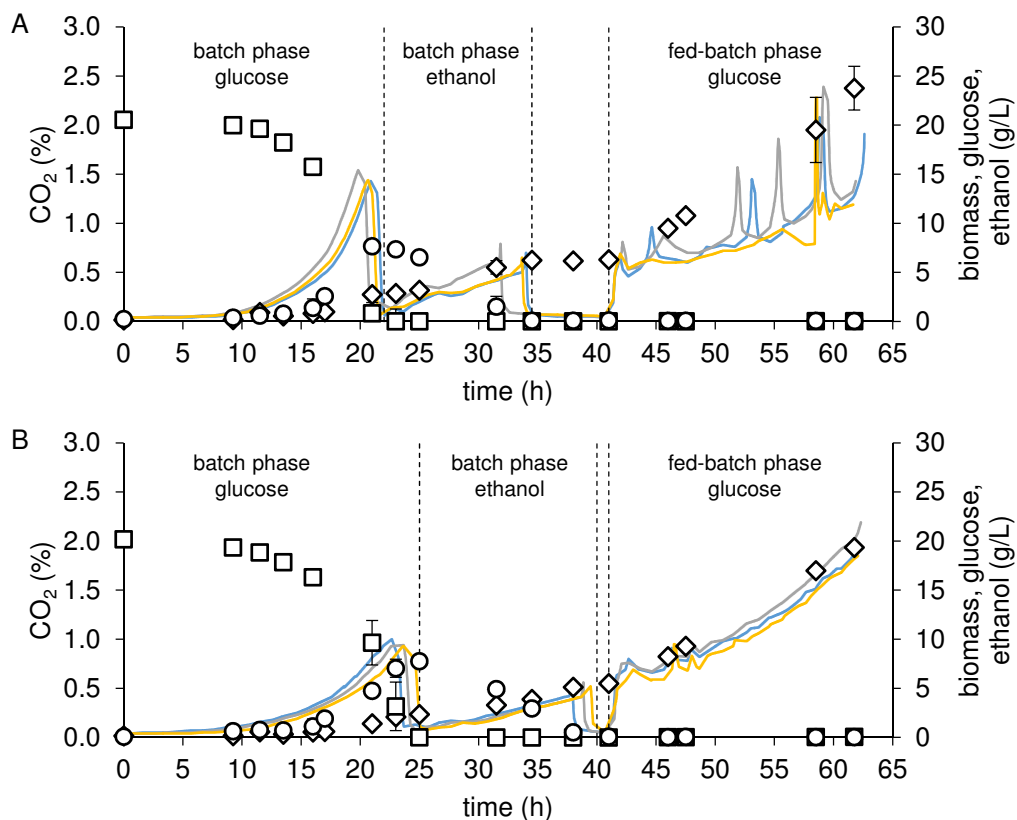


**Figure 3.1:** Fed-batch cultivation of *S. cerevisiae* strain CEN.PK113-5D (A) and SCIGS22 (B) for physiological comparison. Both strains expressed farnesene synthase from *C. juncos* and the truncated HMG-CoA reductase (*tHMG1*) from plasmid. Cultivations were started as batch and the feed was initiated after depletion of the carbon sources (i.e. glucose and ethanol). Data represents average concentrations of three biological replicates with standard deviation for biomass ( $\diamond$ ), glucose ( $\square$ ), ethanol ( $\circ$ ). Solid lines represent percentage of  $\text{CO}_2$  in the exhaust gas for each replicate.

**Physiology.** First of all, physiological changes arising from the genetic modifications were addressed. Figure 3.1 shows the concentrations of biomass, glucose and ethanol at discrete time points and the continuous analysis of the  $\text{CO}_2$  content in the exhaust gas during each of the three conditions, i.e. batch phase on glucose (B-Glu), batch phase on ethanol (B-Eth) and finally, fed-batch on glucose (FB-Glu). The consumption of glucose during the batch phase was slightly prolonged for strain SCIGS22, while the maximum  $\text{CO}_2$  content was reduced from approximately 1.5 to 1.0 %. Additionally the specific growth rate  $\mu$  and the specific biomass yield were reduced while the ethanol yield slightly increased (Table 3.1). These alterations are potentially connected to ergosterol synthesis as expression of *ERG9* is hindered at low glucose concentrations, which presumably results in increased ethanol formation and reduced production of  $\text{CO}_2$ . Besides, a decrease in the growth rate was also observed upon deletion of *GDH1*, which could, however, be restored by overexpression of *GDH2*.

(Moreira Dos Santos et al., 2003). On the other hand, decreased growth capabilities of the strain could also indicate toxicity of the product. Similar observations were also made during the consumption of ethanol where the expression of *ERG9* from  $P_{HXT1}$  was expected to be significantly reduced. During the fed-batch phase, both strains grew at an almost identical growth rate and again the biomass yield was reduced on average for strain SCIGS22. However, in contrast to the results of the batch phase, which indicate delayed consumption of substrates for the engineered strain SCISG22, particularly ethanol, the engineered strain showed a 30 % increase of the glucose consumption rate from 0.103 to 0.134 g/(gDCW · h).

**Table 3.1:** Physiological parameters for strains CEN.PK113-5D (WT) and SCIGS22 (ENG) obtained during the fed-batch cultivations with exponential feeding. Both strains express the truncated HMG-CoA reductase (*tHMG1*) and a farnesene synthase from *C. junos* from a multi-copy plasmid. Data represents average values of three biological replicates  $\pm$  standard deviation.  $\mu$ -specific growth rate,  $Y_{SX}/Y_{SE}$ -biomass/ethanol yield,  $r_S$ -specific substrate consumption rate.

		batch		fed-batch
		glucose	ethanol	glucose
$\mu$ (1/h)	WT	0.220 $\pm$ 0.005	0.074 $\pm$ 0.003	0.073 $\pm$ 0.005
	ENG	0.189 $\pm$ 0.020	0.058 $\pm$ 0.004	0.069 $\pm$ 0.002
$Y_{SX}$ (gDCW/g)	WT	0.131 $\pm$ 0.002	0.457 $\pm$ 0.026	0.651 $\pm$ 0.076
	ENG	0.118 $\pm$ 0.009	0.375 $\pm$ 0.038	0.516 $\pm$ 0.021
$Y_{SE}$ (g/g)	WT	0.378 $\pm$ 0.014	-	-
	ENG	0.397 $\pm$ 0.004	-	-
$r_S$ (g/(gDCW · h))	WT	1.673 $\pm$ 0.015	0.163 $\pm$ 0.006	0.103 $\pm$ 0.007
	ENG	1.604 $\pm$ 0.221	0.156 $\pm$ 0.005	0.134 $\pm$ 0.003

**Metabolome.** For the analysis of the metabolome and the transcriptome, samples for metabolite extraction and RNA sequencing were collected during each of the three distinct phases based on the CO<sub>2</sub> content in exhaust gas. Untargeted metabolome analysis was performed using LC-qTOF. As a result, a total of 3,590 unique metabolic features could be extracted from positive and negative ion mode for all three conditions. Pairwise comparison of the two strains in each condition was performed using SIMCA (Umetrics AB, Sweden) with the objective to determine the statistical significance of the changes in the abundance levels of the metabolic features. Based on this, the clearest response of the engineered strain was observed during FB-Glu as 675 features changed abundance ( $p<0.01$ ) (Figure 3.2 A). Already from the PCA plot (Figure 2A of manuscript III appended to the thesis) it can be seen, that strain SCIGS22 clearly separated from the reference in this condition. In comparison, only 144 and 137 features changed uniquely during B-Glu and B-Eth, respectively, while only 20 features were significantly changing independent of the condition. Two strategies were then pursued to analyze changes in the metabolome of the strains in the

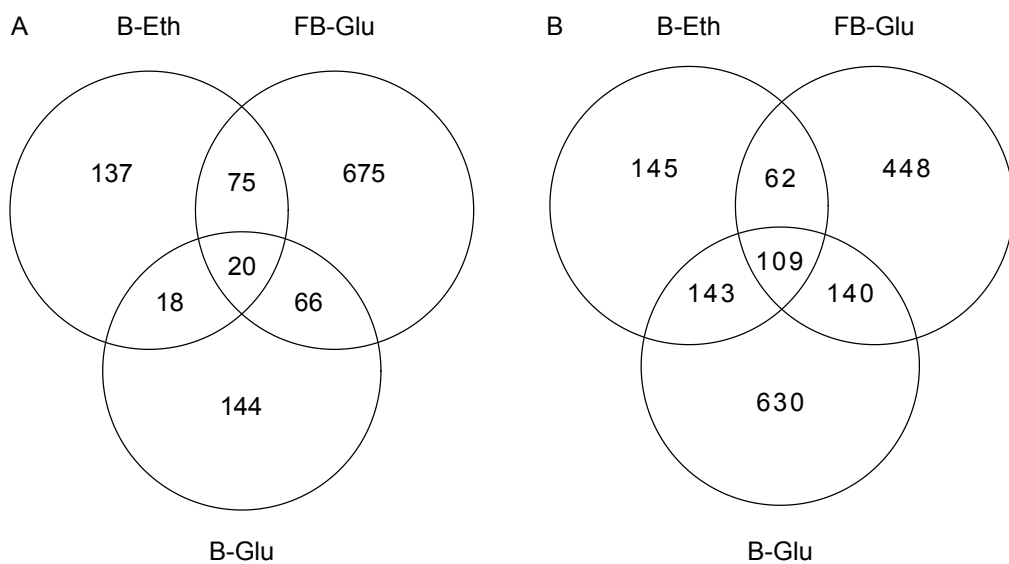


**Figure 3.2:** Venn diagrams illustrating the significant changes ( $p<0.01$ ) in the metabolome (A) and transcriptome (B) of the engineered strain SCIGS22 in three distinct growth conditions during the production of farnesene, i.e. glucose fermentation during the batch phase (B-Glu), ethanol respiration during the batch phase (B-Eth) and glucose respiration during the fed-batch phase (FB-Glu).

different conditions. First, the features were ranked according to strongest change between the strains, where 52 metabolites had at least a twofold increase or decrease during B-Glu ( $\log_2 |\text{FC}|>1$  and  $p<0.01$ ). Out of these, 17 increased abundance, while the abundance for the residual 35 features was reduced. Accordingly, statistically significant changes in the abundance levels were observed for 39 (26 up/13 down) and 291 (62 up/229 down) features during B-Eth and FB-Glu, respectively. The METLIN library (<http://metlin.scripps.edu/>), which contains over 25,000 compounds (Baker, 2011), was then used for the identification of these features as metabolites based on the accurate mass measurements. For this purpose, a 5 ppm range was adopted for the relative mass accuracy of each metabolite. However, unambiguous identification from the library was complicated due to the fact that several hits were usually returned within the specified accuracy range, often reflecting metabolites with extremely similar chemical formula and structures (e.g. phospholipids with different saturation). In total, all 3,590 features were mapped to 16,388 metabolites. Nonetheless, particularly phospholipids, i.e. phosphatidylcholine and phosphatidylethanolamine were unambiguously observed to change in the engineered strain during B-Glu, which corresponds to an exact match in the library with the experimentally determined mass measurement. Similar metabolites were also found to change during B-Eth, together with several amino acids like lysine and leucine (0-2 ppm). As for the last condition, FB-Glu, the identified changes encompassed a diverse range of metabolic pathways, including not only phospholipids and amino acids, but also several intermediates of the MVA pathway such as IPP/DMAPP and mevalonic acid. Additionally, pantothenic acid was identified as an exact match, which is required for coenzyme A (CoA) synthesis and increased abundance by a  $\log_2(\text{FC})$  of 5.0. To understand which pathways

were mostly affected by the changes of the metabolite abundance, an enrichment analysis was performed using the online tool Metabolites Biological Role (MBRole) (Chagoyen and Pazos, 2011). For this purpose, the KEGG IDs that mapped to changed metabolic features in each condition were retrieved from the METLIN library and enriched in each KEGG metabolic pathway, taking into account that the universe of KEGG IDs is reduced to the set of IDs that matched the whole metabolome (background set). Only very few pathways were shown to be overrepresented based on this analysis in the different conditions ( $p < 0.01$ , Table 3.2). As already suggested by previous results for B-Glu, amino acid and phospholipid metabolism were among them. In addition to this, the pentose phosphate pathway, which generates NADPH and is used for production of amino acids, was found to be overrepresented in this condition. Lastly, no enrichments were found for the FB-Glu. This confirms the observation that the changes in the abundance level of the metabolites were widely distributed across numerous pathways, which ultimately resulted in no enrichment of a specific pathway.

**Table 3.2:** Overview of the results from the enrichment analysis performed using MBRole, based on KEGG IDs retrieved from the METLIN library.

label	<i>p</i> -value	adjusted <i>p</i> -value	# of metabolites	
			in background	in set
<i>B-Glu</i>				
Arginine and proline metabolism	$1.49 \cdot 10^{-4}$	$5.45 \cdot 10^{-3}$	30	13
Glycerophospholipid metabolism	$2.49 \cdot 10^{-4}$	$5.48 \cdot 10^{-3}$	8	6
Pentose phosphate pathway	$6.80 \cdot 10^{-4}$	$9.98 \cdot 10^{-3}$	12	7
Nitrogen metabolism	$3.58 \cdot 10^{-3}$	$3.94 \cdot 10^{-2}$	3	3
Metabolic pathways	$6.50 \cdot 10^{-3}$	$5.72 \cdot 10^{-2}$	268	52
<i>B-Eth</i>				
Histidine metabolism	$1.57 \cdot 10^{-3}$	$6.18 \cdot 10^{-2}$	12	7
Arginine and proline metabolism	$2.43 \cdot 10^{-3}$	$6.18 \cdot 10^{-2}$	30	12
Nitrogen metabolism	$5.31 \cdot 10^{-3}$	$9.03 \cdot 10^{-2}$	3	3

**Transcriptome.** With regard to the alterations of the transcriptome, particularly the ethanol consumption phase of the batch phase and the fed-batch phase were of interest as an impaired supply of ergosterol caused by the downregulation of *ERG9* in these conditions was expected to result in most changes. However, the highest number of differentially expressed genes were identified in B-Glu with 630 genes, followed by 145 and 448 genes for B-Eth and FB-Glu, respectively ( $p < 0.01$ ). Additionally, 109 genes were found to change expression independent of the condition (Figure 3.2 B).

Similar to the metabolome analysis, pairwise comparison of the two strains was performed in each of the three conditions. The focus was set to the most significantly differentially expressed genes and specifically, to changes associated to the MVA pathway and the assimilation of nitrogen (Figure 3.3 and Tables 3-5 in manuscript III appended to the thesis). Considering conditions B-Glu and B-Eth, the strongest increase in expression was observed for the transporter Opt2, which was reported to localize in the peroxisomal membrane and to be crucial for glutathione homeostasis (Elbaz-Alon et al., 2014). Besides, a clear upregulation of *HES1* was detected, the product of which has been described to be involved in the regulation of ergosterol synthesis (Beh et al., 2001; Jiang et al., 1994). This response was observed across all conditions, but particularly in B-Eth and FB-Glu with a  $\log_2(\text{FC})$  of 1.5 and 3.1, respectively, presumably due to downregulation of *ERG9*. With respect to the MVA pathway, expression of all genes targeted to improve production of sesquiterpenes strongly changed in each condition. In particular, transcript levels were significantly reduced for *LPP1*, *DPP1* and *GDH1*, while transcript levels of *GDH2* and *ERG20* were significantly increased in the engineered strain. In contrast, the transcript levels of the residual MVA pathway genes remained nearly unchanged and only a minor upregulation of the upper MVA pathway genes, i.e. *ERG10*, *ERG13*, *ERG12*, *ERG8* and *ERG19* was observed during the fed-batch phase (Figure 3.3 A). Expression of *ERG9* was not affected during B-Glu, while its repression during B-Eth was stronger than in FB-Glu ( $\log_2(\text{FC})$  of -4.41 and -3.49, respectively).

Apart from this, due to the deletion of *GDH1* and the overexpression of *GDH2*, changes regarding the amino acid metabolism were anticipated. While Gdh1 converts  $\alpha$ -ketoglutarate to glutamate using NADPH as co-factor, Gdh2 catalyzes the same reaction using NADH. However, the activity of Gdh2 is significantly reduced compared to Gdh1 and the reaction is mostly proceeding in the reversed direction (Miller and Magasanik, 1990; Nissen et al., 2000). These modifications have been studied extensively in *S. cerevisiae*, mainly with the objective to reduce glycerol formation (Bro et al., 2004; Moreira Dos Santos et al., 2003; Nissen et al., 2000; Patil and Nielsen, 2005). In connection with this,  $\alpha$ -ketoglutarate dehydrogenase (*KGD1*) was observed to be downregulated, presumably to favor the conversion of  $\alpha$ -ketoglutarate to glutamate catalyzed by Gdh2 (Bro et al., 2004). Besides, ammonium and several sugar phosphates were identified as reporter metabolites in the *gdh1* $\Delta$  background, which connect the Embden-Meyerhof-Parnas pathway and the pentose phosphate pathway as the main source of NADPH (Patil and Nielsen, 2005). With respect to the present study, several genes involved in nitrogen metabolism were upregulated such as the ammonium transporters encoded by *MEP1*, 2 and 3 as well as genes of the allantoin degradation pathway, i.e. *DAL1*, 2, 3 and *DUR1*, 2, which convert urea to ammonium (Figure 3.3 B). As these reactions increase the concentration of ammonium, which is required for the production of glutamate and glutamine (Magasanik and Kaiser, 2002), these results indicate impaired synthesis of amino acids. Likewise transcript levels increased for *GLN1*, whose gene product, i.e. glutamine synthase, converts glutamate to glutamine. This hypothesis is further supported by the fact that *PUT1* or 4, whose gene products convert proline to glutamate, were upregulated indepen-

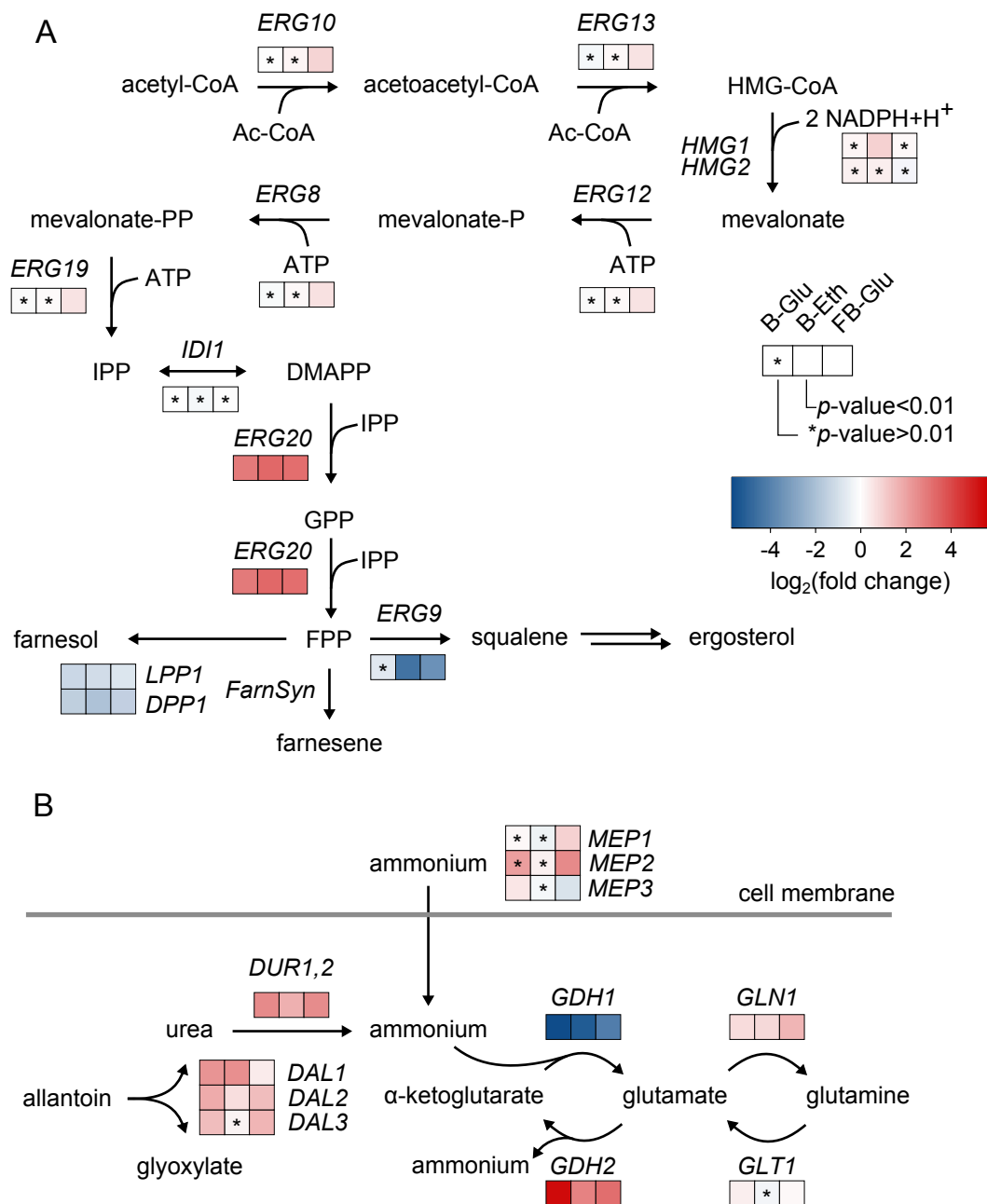


**Figure 3.3:** Changes of the expression level for genes involved in (A) the MVA pathway and (B) nitrogen metabolism. The color code indicates the  $\log_2$  of the fold change in each of the three conditions, i.e. glucose fermentation and ethanol respiration during the batch phase (B-Glu/B-Eth) as well as glucose oxidation during the fed-batch phase (FB-Glu).

dent of the condition. However, *DAL80*, which was among the genes with the highest fold change and has been reported to function as a negative regulator of genes involved in nitrogen degradation pathways, including *PUT1* and *4*, was surprisingly found to be upregulated simultaneously (Daugherty et al., 1993). Notably, these results are consistent with the metabolome data, which likewise suggested changes in proline and arginine metabolism. To identify pathways mostly affected by changes

in gene expression, gene set analysis was performed. Numerous pathways were significantly affected (Figure 6, manuscript III,  $p<0.0001$ ). In particular, expression changes mainly affected allantoin and nitrogen catabolism and peptide transport, which were overrepresented across all conditions. Likewise, steroid and ergosterol biosynthesis were significantly enriched during FB-Glu. On the other hand, ribosome biosynthesis, translation and arginine biosynthesis were significantly downregulated in all conditions, presumably in relation to the reduced growth rate of the strain. In addition, thiamine (vitamin B1) biosynthesis was significantly downregulated. In fact, several genes of the biosynthetic pathway were among the most significantly changing genes during FB-Glu such as *THI4*, *THI5* and *THI13*. Thiamine diphosphate represents an important co-factor for decarboxylations, among others required for conversion  $\alpha$ -ketoglutarate to succinyl-CoA by  $\alpha$ -ketoglutarate dehydrogenase (Li et al., 2010). As such, downregulation of its synthesis could potentially increase the pool of  $\alpha$ -ketoglutarate for synthesis of glutamate and glutamine.

In summary, these results highlight that modifying *S. cerevisiae* for improved production of sesquiterpenes caused a clearly altered response of the strain in all conditions tested, i.e. B-Glu, B-Eth and FB-Glu, with changes spread over several metabolic pathways. Changes were not only observed for the MVA pathway, but also with regard to nitrogen, amino acid and redox metabolism. Remarkably, clear consistency was observed between the metabolome and transcriptome data in this respect. Increased abundance of pantothenic acid could indicate an elevated demand for cytosolic acetyl-CoA. Recently, this metabolite has been used as a metabolic switch to improve strain stability and initiate production of farnesene (Sandoval et al., 2014). Besides, pathway regulation in relation to *HES1* could potentially represent a target to include in future studies. However, further analysis is required at this point to derive a clear conclusion that could aid the metabolic engineering process and ultimately improve the efficiency of *S. cerevisiae* to produce sesquiterpenes.



## Chapter 4

# Engineering the FPP Branch Point using Affibody Scaffolds

As described in the introduction, one of the most important modifications to increase production of sesquiterpenes in *S. cerevisiae* includes redirecting flux at the FPP branch point, which can be achieved by downregulating or deleting competing side reactions such as the synthesis of ergosterol and the dephosphorylation of FPP to farnesol. However, many of these reactions are essential and deletion would severely impair the physiology of the strain or require medium supplementation. Apart from this, enzyme fusions have been used to efficiently channel intermediates from one enzyme to another and thereby to increase the availability of FPP for production of sesquiterpenes. These fusions are constructed by expression of the FPP synthase and the terpene synthase from the same reading frame while a linker is usually inserted in between to allow for sufficient flexibility and correct folding. As such, production of patchoulol in *S. cerevisiae* increased twofold using a fusion of the FPP synthase and the terpene synthase (Albertsen et al., 2011). A similar fusion was also used to increase the efficiency of the heterologously expressed MVA pathway in *E. coli*, improving production of pinene and farnesene by 52 and 51 %, respectively (Sarria et al., 2014; Wang et al., 2011). Alternatively, channeling of pathway intermediates can be achieved by assembling enzymes on synthetic scaffolds. For example, proteins can be spatially organized on RNA scaffolds (Delebecque et al., 2011), which has been used successfully to increase production of succinate in *E. coli* by 88 % (Sachdeva et al., 2014). In addition, protein-protein interaction domains from metazoans have been employed to construct enzyme complexes of the first three reactions of the MVA pathway, which ultimately led to a 77-fold increase in the production of mevalonate (Dueber et al., 2009).

In this study we developed a scaffold system based on affibodies and investigated its potential to redirect flux at the FPP branch point to improve production of sesquiterpenes. Affibodies represent a class of affinity proteins, which consist of the engineered

IgG binding domain of protein A from *Staphylococcus aureus* (Z domain) (Nilsson et al., 1987). Phage-display has aided the generation and selection of affibodies for versatile applications against various target proteins including insulin, HER2 ( $Z_{HER2}$ ), Taq polymerase ( $Z_{Taq}$ ), and IgA ( $Z_{IgA}$ ) (Löfblom et al., 2010; Nygren, 2008). Additionally, specific anti-idiotypic binders have been raised against  $Z_{Taq}$  and  $Z_{IgA}$  for potential applications in affinity chromatography based protein recovery (Eklund et al., 2002). These affibodies bind their targets with dissociation constants ( $K_D$ ) of 0.7 (anti- $Z_{Taq}$ ) and 0.9  $\mu\text{M}$  (anti- $Z_{IgA}$ ), respectively. In a different study, a dissociation constant as low as 0.1  $\mu\text{M}$  has been reported for the  $Z_{Taq}$ -anti- $Z_{Taq}$  complex (Lendel et al., 2006). We hypothesized that *in vivo* assembly of these two affibody complexes could keep the FPP synthase and the farnesene synthase in close proximity and thereby enhance the effective concentration of FPP as precursor for production of farnesene (Figure 4.1).

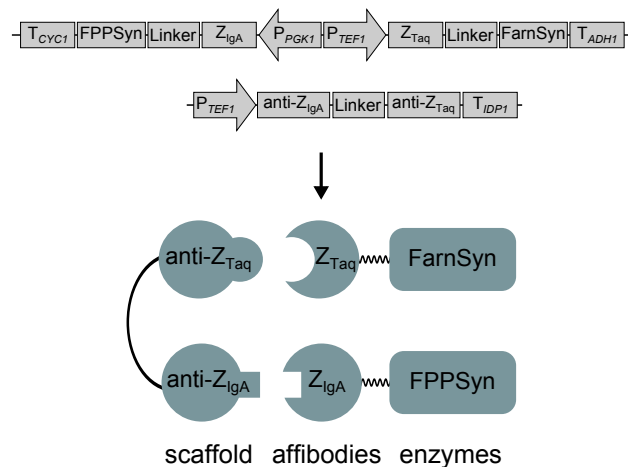


**Figure 4.1:** Construction of an affibody scaffold in *S. cerevisiae* for increased production of sesquiterpenes. *ERG20* encoding farnesyl diphosphate synthase (FPPSyn) was expressed from the same reading frame with affibody  $Z_{IgA}$ . Likewise, farnesene synthase from *C. juncos* (FarnSyn) was fused to affibody  $Z_{Taq}$ . The scaffold, a fusion of the anti-idiotypic affibodies anti- $Z_{Taq}$ -anti- $Z_{IgA}$ , was constructed in a similar fashion and expressed separately. All fusions utilize a 20-amino acid linker of the form (SSSSG)<sub>4</sub>.

In order to test this hypothesis, two distinct strategies were pursued for the construction of the affibody scaffolds. First, the fusions of the enzymes to their affibody partners (Z-fusions), i.e.  $Z_{IgA}$ -FPPSyn and  $Z_{Taq}$ -FarnSyn, were expressed from a 2 micron multi-copy plasmid. Additionally, the same plasmid was also used for expression of the affibody scaffold, anti- $Z_{Taq}$ -anti- $Z_{IgA}$ . Importantly, strong promoters were used for the expression of all parts, i.e.  $P_{TEF1}$  and  $P_{PGK1}$  (Partow et al., 2010). After 72 h of cultivation in shake flasks, the control strains expressing only the two enzymes with or without Z-fusion produced around 9 mg/L<sub>aq</sub> of farnesene (Figure 4.2 A). Although final titers increased slightly on average, additional expression of the scaffold from  $P_{TEF1}$  did not improve production of farnesene significantly. Subsequently, expression of the scaffold was also tested using  $P_{ADH1}$  and  $P_{KEX2}$ , which are significantly weaker than  $P_{TEF1}$  (Nacken et al., 1996; Partow et al., 2010), mainly because the enzyme-

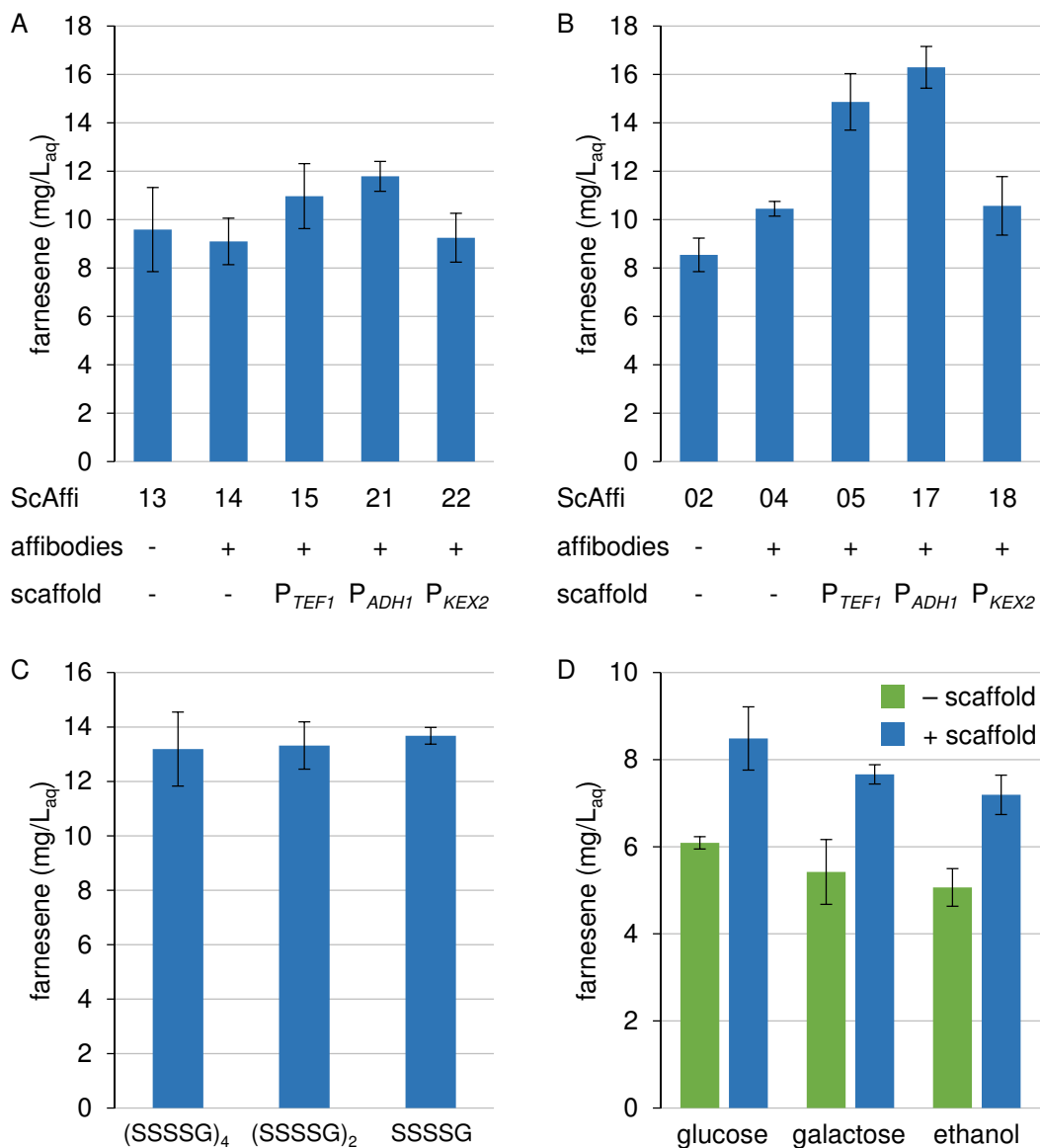


**Figure 4.2:** Construction of affibody scaffolds for increased sesquiterpene production in *S. cerevisiae*. (A) The affibody-enzyme fusions,  $Z_{IgA}$ -FPPSyn and  $Z_{Taq}$ -FarnSyn, were expressed together with the affibody scaffold, anti- $Z_{Taq}$ -anti- $Z_{IgA}$ , from the same multi-copy plasmid. (B) Chromosomal integration of the affibody-enzyme fusions and expression of the scaffold from a low-copy plasmid. In both scenarios, different promoters were compared for expression of the scaffold. (C) Reduction of the linker length for the affibody scaffold, anti- $Z_{Taq}$ -anti- $Z_{IgA}$ , from 20 ((SSSSG)<sub>4</sub>) to 10 ((SSSSG)<sub>2</sub>) and 5 (SSSSG) amino acids. In all cases, the affibody scaffold was expressed from a low-copy plasmid and the affibody-enzyme fusion was integrated into the chromosome. (D) Impact of different carbon sources on the effect of the affibody-mediated enzyme scaffolding in strain ScAffi05. Data represents average farnesene concentrations with respect to volume of aqueous medium of three biological replicates with standard deviations after 72 h of cultivation in shake flasks.

to-scaffold ratio has been identified as a key parameter for the optimization of the scaffold effect (Dueber et al., 2009). In particular, the scaffold may only mediate an effect within a narrow concentration range, which is also called the “pro-zone” effect, as scaffold concentrations exceeding the optimum increase the abundance of non-functional complexes consisting of only one of the enzymes (Bray and Lay, 1997; Levchenko et al., 2000). However, scaffold expression from these promoters did not significantly improve final farnesene titers, reaching almost 12 mg/L<sub>aq</sub>. However, as final OD600 values were notably reduced for strain ScAffi21 expressing the scaffold from P<sub>ADH1</sub>, specific farnesene production based on biomass concentration increased evidently. Lastly, expression of the scaffold from P<sub>KEX2</sub> in strain ScAffi22 led to almost identical farnesene titers as strain ScAffi14, expressing no scaffold. Based on the result that production of farnesene could not be improved following this approach, we concluded that further adjustment of the enzyme-to-scaffold ratio is required to obtain a visible effect of the scaffold.

To vary the expression level of the two parts, the scaffold was expressed from a centromeric, low-copy plasmid (with 2-8 plasmids per cell (Karim et al., 2013)), while the genes of the Z-fused enzymes were integrated into the chromosome. In this scenario, a clear increase in the final titers of farnesene was already observed in the absence of the scaffold (ScAffi04, Figure 4.2 B). As the selected affibodies were raised against different targets, unspecific cross-binding between the two fusions, i.e. Z<sub>IgA</sub> and Z<sub>Taq</sub>, could not be detected in previous studies and was thus excluded as an explanation (Eklund et al., 2002). Instead, we hypothesized that the affibodies could potentially improve the folding and stability of the proteins as previously observed for other Z-fusions (Samuelsson et al., 1994). Besides, a 42 % increase in final farnesene titers was observed when the scaffold was expressed in addition from P<sub>TEF1</sub> (ScAffi05), reaching approximately 14 mg/L<sub>aq</sub>. In comparison, scaffold expression from P<sub>ADH1</sub> resulted in slightly higher concentrations with 16 mg/L<sub>aq</sub>. Lastly, similar to the result obtained for strain ScAffi22, scaffold expression from P<sub>KEX2</sub> led to approximately 10 mg/L<sub>aq</sub> of farnesene and was hence almost identical to no scaffold expression, suggesting that the concentration of the scaffold was too low to exert an effect (ScAffi18).

Based on these results, two distinct parameters were investigated as a means for further improving the Z-based scaffolding of the FPP and farnesene synthase, the first one being the linker used for the different fusions. Several studies have discussed the importance of the linker length and composition and highlighted its potential to improve protein folding and activity (George and Heringa, 2002; Huang et al., 2016; Robinson and Sauer, 1998; Sarria et al., 2014; van Leeuwen et al., 1997). Considering the two strategies pursued to construct affibody scaffolds in *S. cerevisiae*, a 20 amino acid linker of the form (SSSSG)<sub>4</sub> was used for the Z-fusions as well as for the fusion of the anti-idiotypic affibodies. More efficient channeling of the intermediates could potentially be enabled by reducing the length of the linker used for the scaffold to 10 and 5 amino acids. In all three scenarios, plasmid-based expression was used for the scaffold while the two Z-fusions were integrated into the chromosome (ScAffi05).

However, clearly no effect was visible as final titers were nearly identical (Figure 4.2 C), illustrating that the distance between the FPP synthase and the farnesene synthase is not a crucial parameter within the range tested. Secondly, strain ScAffi05 was used to investigate the effect of different carbon sources, i.e. glucose, galactose and ethanol, which are metabolized via different pathways and were expected to provide different flux through the MVA pathway. As an example, intracellular concentrations of HMG-CoA clearly varied between growth on glucose and galactose (Seker et al., 2005). For this experiment, all carbon sources were used at an initial concentration of 1 % w/v in order to facilitate growth in ethanol. As anticipated, final titers of farnesene were slightly reduced on galactose and ethanol. The effect of the scaffold, however, was nearly identical for all carbon sources and improved production by approximately 40 % on average (Figure 4.2 D).

Lastly, the effect of the scaffolding approach was tested in *S. cerevisiae* strain SCICK16, which was engineered for improved production of sesquiterpenes by downregulation of *ERG9* using *P<sub>HXT1</sub>* and by deletion of *LPP1* and *DPP1* (Scalcanati et al., 2012a). In addition, *tHMG1* and the genes of the Z-fusions of the FPP and farnesene synthase were integrated into the strain and the scaffold was expressed from *P<sub>ADH1</sub>* using a centromeric, low-copy plasmid. The strain was cultivated in fed-batch mode with exponential feeding to maintain low glucose concentrations and to benefit from the downregulation of *ERG9*. As it can be seen from Figure 4.3, expression of the scaffold increased the yield of farnesene by 135 % and the final concentrations by 120 %. In comparison, the overall yield and final farnesene titer increased by 65 and 40 %, respectively, when the scaffold was expressed from *P<sub>TEF1</sub>* (Supplementary Figure 4, paper IV).

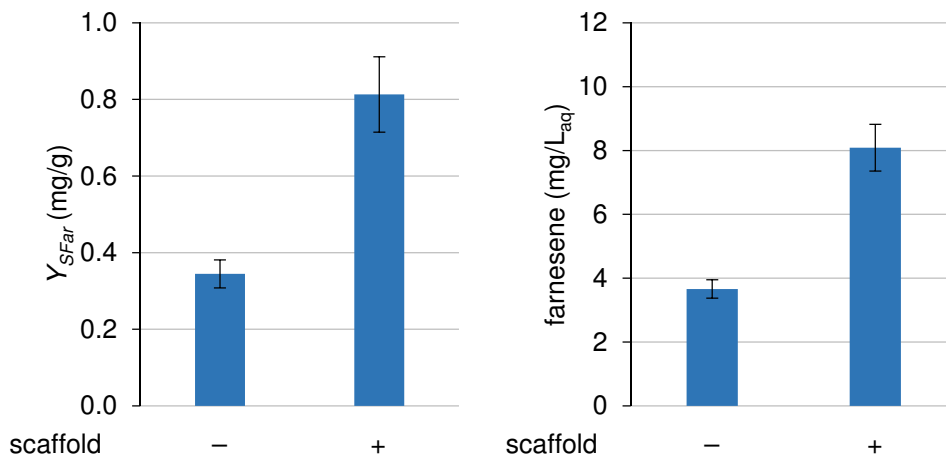


**Figure 4.3:** Expression of the affibody-mediated enzyme fusion between the FPP synthase and the farnesene synthase during fed-batch cultivations with exponential feeding. Data represents average values of three biological replicates with standard deviation for the overall product yield on glucose ( $Y_{SFar}$ ) and the final concentration of farnesene with respect to aqueous medium after 6 h of feeding.

In conclusion, affibody scaffolds were implemented as a novel metabolic engineering tool to improve production of sesquiterpenes in *S. cerevisiae*. With the objective to channel intermediates from one enzyme to the other, the FPP synthase and the farnesene synthase have been assembled on a scaffold utilizing the specific recognition between affibodies. Different parameters were investigated to optimize the functionality of the system and consistent with the literature, the enzyme-to-scaffold ratio was identified as a key parameter (Dueber et al., 2009; Levchenko et al., 2000). In both studies it has been shown that the scaffold concentration should not exceed a certain maximum to avoid presence of unsaturated scaffold. With respect to the presented results, no direct conclusion about the enzyme-to-scaffold ratio could be derived and it can only be speculated, which ratios are required to mediate an effect of the scaffold. In future studies, this questions could be investigated by coupling fluorescent proteins such as GFP and YFP to the scaffold and the enzymes to quantify their expression levels. Alternatively, qPCR could be applied for this purpose. However, the structure of the enzymes could explain the effect of the scaffold and should be taken into consideration. The farnesene synthase has been reported to function as a monomer and as an oligomer (Green et al., 2007; Rupasinghe et al., 2000). On the other hand, the FPP synthase has been described as a dimer (Eberhardt and Rilling, 1975). Hence, at least one of the enzymes would be able to bind more than one scaffold, thereby leading to the formation of an enzyme cluster. Two hypothetical constellations have been illustrated in Figure 4.4. Based on this, the effect observed by assembling enzymes onto an affibody scaffold arises presumably from co-localization of the enzymes, as it has also been suggested by previous studies (Castellana et al., 2014; Dueber et al., 2009). In fact, efficient channeling of intermediates only functions in a narrow range of distances between the enzymes and also depends on the orientation of the active sites (Bauler et al., 2010). Using DNA nanostructures to precisely adjust the distance between a glucose oxidase and a horseradish peroxidase, Fu et al. (2012) observed the strongest activity enhancement of these enzymes for an inter-enzyme distance of 10 nm. The activity was substantially lower for all other distances tested. Reconsidering the results obtained from the presented scaffolding approach, strategies to further optimize the effect of the scaffold could for example aim at increasing the binding stability of the partners by selecting affibodies with higher affinity. In addition, the effect could potentially be improved by COOH-terminal fusion of the affibodies to the enzymes, which could have a stronger influence on the folding or catalytic activity of the FPP and farnesene synthase. Likewise, although the linker between the two anti-idiotypic affibodies could not be used to optimize the functionality of the system, the linker of the two Z-fusions represents a future target as it potentially influences the activity of the enzymes. Hence, varying its length or composition could be used to improve the scaffolding effect. Moreover, there are several experiments to complement the current results and to further investigate the applicability of the scaffolding approach for this pathway. As such, construction of a conventional fusion between the FPP synthase and farnesene synthase by expression of both enzymes from the same reading frame would be an interesting addition to the current results. Besides, construction of a fusion using a single pair of affibodies, i.e. by expression of  $Z_{IgA}$ -FPPSyn and anti- $Z_{IgA}$ -FarnSyn, represents an alternative strategy for co-localizing only two en-

zymes. Nonetheless, farnesene was used here as an example to establish the concept and due to the availability of several different affibody pairs, affibody scaffolds could allow to assemble several pathway enzymes on a scaffold in future metabolic engineering studies. With the objective to demonstrate that affibody scaffolds can be used for other pathways, the concept has been transferred for production of polyhydroxybutyrate (PHB) in *E. coli* from the heterologous pathway of *Synechocystis* sp. PCC 6803. In this case, three enzymes were assembled on a scaffold and consistent with the results for production of farnesene in *S. cerevisiae*, a positive effect of the scaffold was observed for a narrow enzyme-to-scaffold ratio.

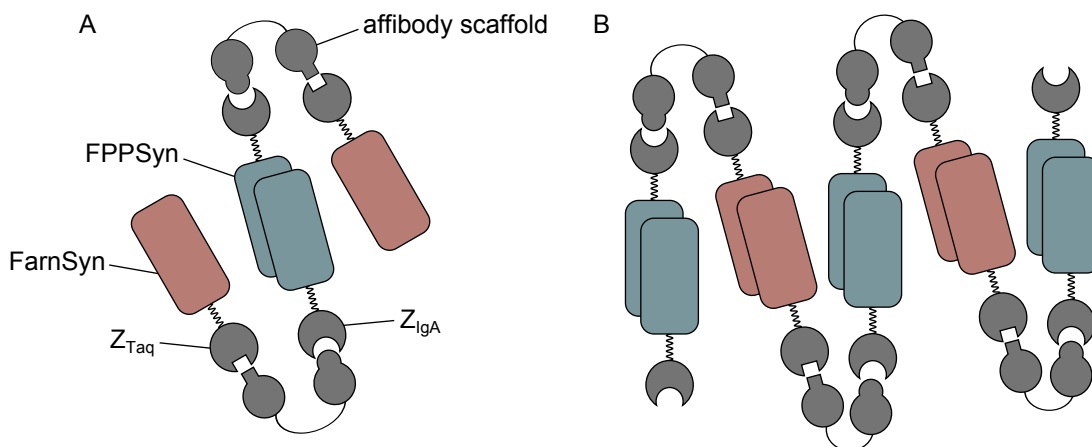


**Figure 4.4:** Schematic illustration of the putative co-localization mechanism of the farnesyl diphosphate (FPP) and farnesene synthase mediated by affibody scaffolds. Based on the literature, it was assumed that FPP synthase (FPPSyn) forms a dimer inside the cell, while the farnesene synthase (FarnSyn) is either present as monomer (A) or dimer (B).



# Chapter 5

## Incorporation of Malonyl-CoA using Acetoacetyl-CoA Synthase

Acetyl-CoA is the key substrate of the MVA pathway and consequently its supply is of crucial importance for the production of sesquiterpenes in *S. cerevisiae*. In fact, production of one mole of farnesene requires 9 moles of acetyl-CoA. As described in the introduction, maximum theoretical yields for production of sesquiterpenes from the MVA pathway can be approached by increasing the pool of acetyl-CoA (van Rossum et al., 2016). In addition, cytosolic acetyl-CoA needs to be converted efficiently by acetoacetyl-CoA thiolase (*Erg10*) in the first reaction of the MVA pathway. However, the reaction is reversible and with  $\Delta G^{\circ} \approx 7$  kcal/mol, acetoacetyl-CoA thiolytic is thermodynamically more favored (Lan and Liao, 2012; Weber, 1991). In consequence, high concentrations of acetyl-CoA are required to drive the forward reaction. This limitation has also been demonstrated for the production of butanol in *Synechocystis* sp. PCC 6803 as overexpression of the corresponding  $\beta$ -ketothiolase (*phaA*) did not improve production of butanol, but instead resulted in increased acetate formation (Anfelt et al., 2015). In addition, several studies, which use the heterologous expression of the MVA pathway for terpene production in *E. coli*, often do not include *ERG10*, but rely on the endogenous thiolase (AtoB) (Martin et al., 2003; Sarria et al., 2014). Within the MVA pathway gene cluster of *Streptomyces* sp. strain CL190, *nphT7* has been identified to encode an acetoacetyl-CoA synthase, which catalyzes the non-decarboxylative condensation of acetyl-CoA and malonyl-CoA to acetoacetyl-CoA (Figure 5.1) (Okamura et al., 2010). This reaction is thermodynamically more favorable (estimated  $\Delta G^{\circ} = -0.9$  kcal/mol) and most importantly, it has been shown to be irreversible (Okamura et al., 2010; Weber, 1991). Several studies have used the enzyme to promote production of acetoacetyl-CoA-derived chemicals, such as production of butanol in cyanobacteria, *E. coli* and *S. cerevisiae* as well as production of polyhydroxybutyrate in plants (Lan and Liao, 2012; McQualter et al., 2015; Menon et al., 2015; Schadeweg and Boles, 2016). This study aimed at investigating if acetoacetyl-CoA synthase from *Streptomyces* sp. strain CL190 can improve sesquiter-

pene production in *S. cerevisiae* by utilization of malonyl-CoA for the MVA pathway.

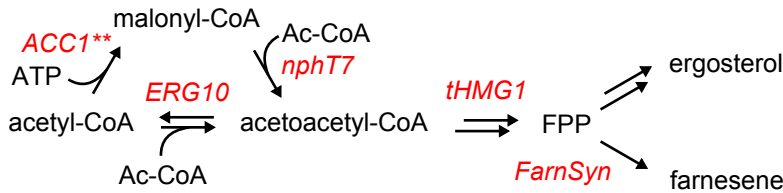


**Figure 5.1:** Expression of acetoacetyl-CoA synthase (*nphT7*) from *Streptomyces* sp. strain CL190 for incorporation of malonyl-CoA into the MVA pathway. Gene names are written as red italics. *ACC1\*\** encodes the engineered variant of acetyl-CoA carboxylase (Shi et al., 2014).

For this purpose, *nphT7* from *Streptomyces* sp. strain CL190 (*nphT7<sub>SCL</sub>*) was expressed from a multi-copy plasmid together with the truncated variant of the HMG-CoA reductase (*tHMG1*) and the farnesene synthase from *C. juncos*. Furthermore, four different *nphT7* homologs were selected, which could affect the efficiency of this bypass, i.e. from *Streptomyces glaucescens*, *Streptomyces afghaniensis*, *Streptomyces lactacystinaeus* and *Nocardia brasiliensis*. The latter two belong to the group of β-ketoacyl-acyl carrier protein (ACP) synthase III (KASIII), which accept malonyl-ACP as substrate to produce acetoacetyl-ACP. However, as they share a motif with NphT7 from *Streptomyces* sp. strain CL190, which is putatively involved in CoA recognition, these enzymes could catalyze the same reaction (Okamura et al., 2010). More details regarding the selection of these enzymes are provided in manuscript V. After 72 h of cultivation in shake flasks, surprisingly none of the selected enzymes improved production of farnesene (Figure 5.2 A). Instead, final titers were slightly reduced on average. The efficiency of the bypass was assumed to be strongly dependent on the availability of malonyl-CoA, which is produced from acetyl-CoA by acetyl-CoA carboxylase (Acc1) and represents the essential precursor for lipids and fatty acids. Construction of the variant Acc1\*\* by site-directed mutagenesis was shown to omit posttranscriptional regulation, resulting in a substantial increase in the production of fatty acids (Shi et al., 2014). For this reason, chromosomal integration of *ACC1\*\** was used to secure high concentrations of malonyl-CoA and thereby to promote the conversion to acetoacetyl-CoA by NphT7. However, *ACC1\*\** integration appeared to be disadvantageous for farnesene production as final titers slightly decreased (Figure 5.2 B). Likewise, NphT7 failed to improve farnesene production under this condition.

As increased production of acetoacetyl-CoA could promote thiolysis activity of the endogenous Erg10, expression of *nphT7* may lead to the generation of a futile cycle involving acetyl, malonyl and acetoacetyl-CoA (Figure 5.1). In consequence, the effect of the acetoacetyl-CoA synthase would be diminished. For this reason, the endogenous *ERG10* was substituted by *nphT7<sub>SCL</sub>* as an alternative strategy to investigate if this enzyme can support production of farnesene. In this scenario, acetoacetyl-CoA is exclusively produced from malonyl-CoA, which allows for a comparison of the bypass to the native pathway regarding its efficiency. Although the flux through this pathway was expected to be sufficient to complement for the loss of *ERG10*, since malonyl-CoA

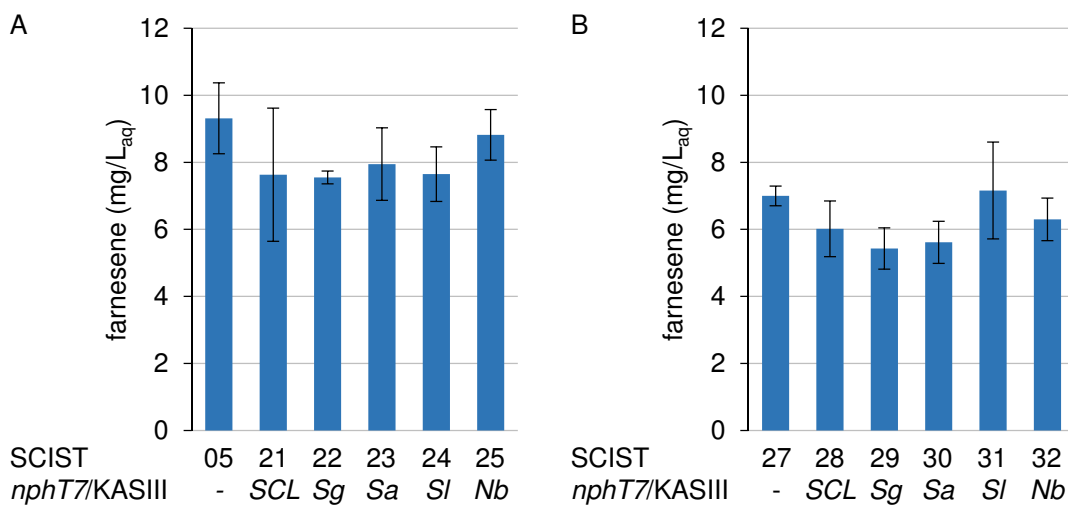


**Figure 5.2:** Comparison of different acetoacetyl-CoA synthase homologs for incorporation of malonyl-CoA into the MVA pathway with and without integration of *ACC1\*\** (A and B). All strains express *tHMG1*, farnesene synthase from *C. juncos* and one of the selected *nphT7* homologs from plasmid. *SCL* - *Streptomyces* sp. strain CL190, *Sg* - *S. glaucescens*, *Sa* - *S. afghaniensis*, *Sl* - *S. lactacystinaeus*, *Nb* - *N. brasiliensis*. Bars represent average farnesene concentrations of three biological replicates with standard deviation after 72 h of cultivation in shake flasks.

represents an essential intermediate in fatty acid synthesis, overexpression of *ACC1\*\** was again used as a means to increase its supply. Notably, the pathway for farnesene production changes significantly due to this modification as the pathway is extended by an additional reaction and the requirement for ATP increases likewise. However, although energy conservation plays a crucial role in metabolic engineering (De Kok et al., 2012), ATP has been used to drive production of butanol in *Synechococcus elongatus* PCC 7942 (Lan and Liao, 2012). With respect to the results presented in Figure 5.3 A, *ACC1\*\** expression was again observed to be detrimental for production of farnesene (strain SCIST16). Most importantly, however, substitution of *ERG10* by *nphT7<sub>SCL</sub>* caused a substantial drop in the production of farnesene from almost 10 to approximately 0.8 mg/L<sub>aq</sub> on average, which could not be restored by increasing the flux towards malonyl-CoA using *ACC1\*\** expression (SCIST20, Figure 5.3 A). As these results suggest poor efficiency of the enzyme, two strategies were pursued to enhance expression of the gene and thereby to improve the phenotype of the strain. First, as strains SCIST18 and 20 utilize the endogenous promoter of *ERG10*, expression of *nphT7<sub>SCL</sub>* using *P<sub>TEF1</sub>* was used as a way to improve pathway efficiency, which eventually caused an almost 4-fold improvement in the production of farnesene (SCIST39 vs. SCIST18, Figure 5.3 A). Secondly, pathway efficiency could also be improved by expression of *nphT7<sub>SCL</sub>* from a multi-copy plasmid together with the farnesene synthase and the truncated HMG-CoA reductase in the *erg10Δ::nphT7<sub>SCL</sub>* background, leading to a 2.5-fold increase (SCIST33 vs. 20, Figure 5.3 B). Similarly, the four additional homologs selected for comparison against *nphT7<sub>SCL</sub>* showed clear differences when expressed in the same genetic background, with *nphT7* from *S. glaucescens* increasing

production more than 4-fold (SCIST34 vs. 20, Figure 5.3 B). Apart from this, it is noteworthy that while acetoacetyl-CoA synthase from *Streptomyces* sp. strain CL190 was able to complement the loss of Erg10, a reduction of the final optical density and an impaired consumption of ethanol was clearly indicative of an altered strain physiology (Supplementary Figure 2, manuscript V).

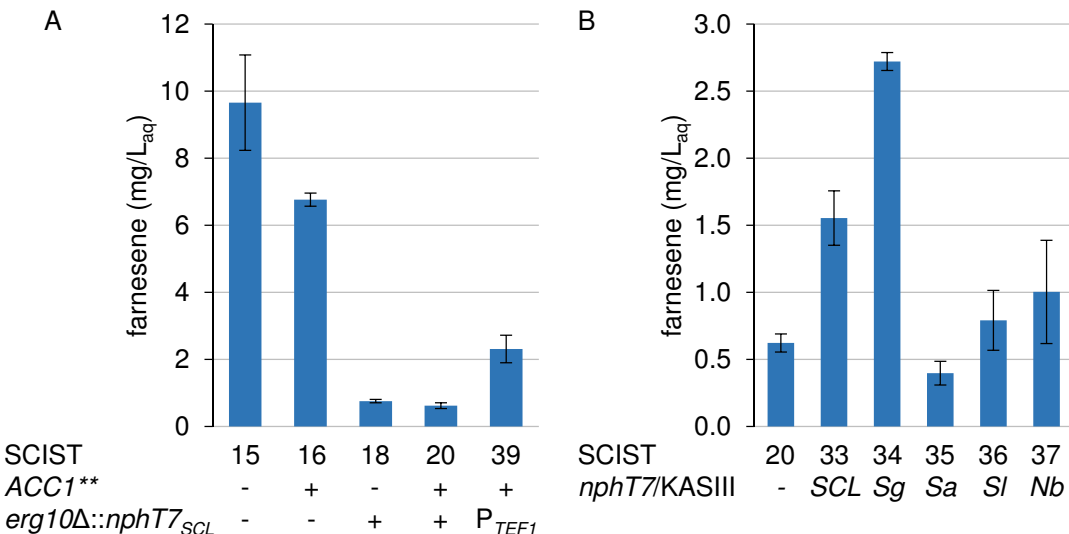


**Figure 5.3:** Replacing *ERG10* by *nphT7* from *Streptomyces* sp. strain CL190 (*nphT7<sub>SCL</sub>*). (A) All strains express *tHMG1* and farnesene synthase from *C. junos* from a multi-copy plasmid. Additionally integration of *ACC1\*\** was used to increase flux towards malonyl-CoA. (B) Improved production of acetoacetyl-CoA from malonyl-CoA by expression of an additional copy of one of the selected acetoacetyl-CoA synthases in the *erg10Δ::nphT7<sub>SCL</sub>* background. Bars represent average farnesene concentrations of three biological replicates with standard deviation after 72 h of cultivation in shake flasks.

To assess the impact of the bypass via malonyl-CoA on the physiology of *S. cerevisiae*, cultivations were performed in a microbioreactor (Biolector, m2p-labs, Germany), which allows for online measurements of the optical density. A clear variation in the growth profile was observed for all strains harboring the *erg10Δ::nphT7<sub>SCL</sub>* background (Figure 5.4). This includes prolongation of the lag phase, but particularly of the ethanol consumption phase (30-80 h after inoculation), which was slightly enhanced upon *ACC1\*\** expression. As a result, stationary phase was not reached before 80 h of cultivation in comparison to approximately 30 h for the control strain (SCIST05). Moreover, a decrease of the specific growth rate  $\mu$  was calculated (Supplementary Figure 3, manuscript V). Nonetheless, the growth profile could be partially restored by expression of *nphT7<sub>SCL</sub>* from  $P_{TEF1}$ , which is in accordance with the results obtained for farnesene production (SCIST39, Figure 5.3 A). Besides, similar observations were also made for *nphT7* from *S. glaucescens*, which had a stronger effect on growth in comparison to the expression of the other homologs (Supplementary Figure 4, manuscript V).

Replacing the endogenous *ERG10* by *nphT7<sub>SCL</sub>* failed to improve production of far-

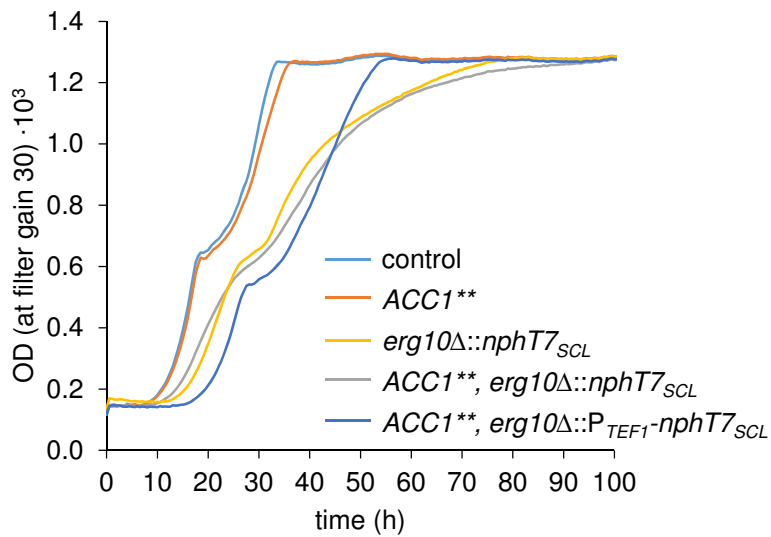


**Figure 5.4:** Effect of replacing *ERG10* by *nphT7* from *Streptomyces* sp. strain CL190 on growth of *S. cerevisiae*. Online measurements of the optical density (OD) in 30 min intervals. The descriptions indicate relevant genotypes of strain SCIST16, 18, 20 and 39. Strain SCIST15 was used as control. In all strains, the truncated HMG-CoA reductase (*tHMG1*) and the farnesene synthase from *C. junos* were expressed from a multi-copy plasmid. Data represents average values of four biological replicates.

nesene and severely impaired growth of *S. cerevisiae* (Figure 5.3 and 5.4), indicating poor efficiency of the enzyme in comparison to the endogenous acetoacetyl-CoA thiolase. Overexpression of *ACC1\*\**, which has been shown to increase the pool of malonyl-CoA (Shi et al., 2014), could not improve the efficiency of this bypass. Likewise, increasing the copy number or the expression level of *nphT7* only showed limited success. To minimize the loss of malonyl-CoA for fatty acid synthesis, expression of *FAS1* encoding the β-subunit of fatty acid synthase was subsequently downregulated using *P<sub>HXT1</sub>*. In addition to *tHMG1* and the farnesene synthase from *C. junos*, *nphT7* from *S. glaucescens* was expressed from the plasmid, which showed advanced efficiency in previous experiments (Figure 5.3 B). As downregulation requires low glucose concentrations, strain SCIST43 (*erg10Δ::P<sub>TEF1</sub>-nphT7<sub>SCL</sub>*, *P<sub>FAS1</sub>Δ::P<sub>HXT1</sub>*) was again cultivated in fed-batch mode with a biomass propagation phase during the batch and a subsequent fed-batch phase with reduced growth and increased sesquiterpene production. To optimize the productivity and minimize accumulation of ethanol in connection to the downregulation, the feeding was controlled using the respiratory quotient (*RQ*). Strain SCIST40 (*erg10Δ::P<sub>TEF1</sub>-nphT7<sub>SCL</sub>*), which was used as a reference and is identical except for the downregulation of *FAS1*, reached around 8.5 gDCW/L after 18 h of feeding. With a final farnesene titer of approximately 15 mg/L<sub>aq</sub> at the end of the fed-batch and an overall product yield on glucose *Y<sub>SFar</sub>* of 0.571 mg/(g glucose) on average, production of farnesene was still significantly reduced in comparison to CEN.PK113-5D expressing farnesene synthase from *C. junos* and *tHMG1* from plasmid, for which *Y<sub>SFar</sub>* amounted 0.843 mg/(g glucose) on average (see chapter 2). In contrast, strain SCIST43 displayed a clearly altered growth

profile during the batch phase (Supplementary Figure 5, manuscript V), presumably due to insufficient expression of *FAS1*. In fact, the strength of the *FAS1* promoter has been reported to be significantly higher than the *HXT1* promoter even at a glucose concentrations of 2 % (Keren et al., 2013). However, the strain was surprisingly unable to sustain growth during the fed-batch phase, even at high concentrations of glucose, which increased up to 16 g/L and should have relieved the suppression of *FAS1* expression. In accordance with these results, the biomass concentration remained at approximately 2 gDCW/L, while production of farnesene was almost abolished (Figure 5.5 D). Several changes were also observed regarding the lipid profile at the end of the experiment, confirming efficient downregulation of *FAS1*. Most importantly, the content of triacylglycerols (TAGs) was substantially decreased (Table 3, manuscript V). The viability of the strain was not investigated. However, the slightly decreasing content of CO<sub>2</sub> in the exhaust gas is indicative of severe stress under this condition. Accumulation of malonyl-CoA to toxic levels could explain this phenotype as coenzyme A has been described as a potential mediator of toxicity by increasing the reactivity of carboxylic acids (Brass, 1994). Similar observations have also been reported for other thioesters of coenzyme A. As an example, HMG-CoA was shown to disrupt the regulation of fatty acid synthesis in *E. coli*, indicated by significantly increased levels of malonyl-CoA (Kizer et al., 2008). Besides, malonyl-CoA has been suggested to induce apoptosis in human cancer cells (Pizer et al., 2000).

In conclusion, none of the selected acetoacetyl-CoA synthases was able to improve production of farnesene in *S. cerevisiae*. In comparison with the literature, several metabolic engineering studies have used NphT7, whereas its effect has been described differently. For instance, butanol production in *S. cerevisiae* was slightly increased by expression of *nphT7* from *Streptomyces* sp. strain CL190 (Schadeweg and Boles, 2016). On the other hand, butanol production in *E. coli* was approximately 6-fold higher when acetoacetyl-CoA was supplied by AtoB instead of NphT7 (Menon et al., 2015). With regard to the presented results, we assume the effect of the enzyme was most likely diminished when expressed in addition to *ERG10* due to the generation of a futile cycle. In this respect, a more efficient conversion of the elevated acetoacetyl-CoA concentrations to HMG-CoA by HMG-CoA synthase may be crucial. However, as indicated by the acetoacetyl-CoA analog, 3-oxobutylsulfoxy-CoA, acetoacetyl-CoA reduces HMG-CoA synthase activity (Charlier et al., 1997). Hence, the potential of utilization of malonyl-CoA for the MVA pathway might be limited as increased levels of acetoacetyl-CoA could affect downstream reactions. On the other hand, substitution of *ERG10* by *nphT7<sub>SCL</sub>* to evaluate the efficiency of the bypass via malonyl-CoA resulted in detrimental effects on growth and farnesene production. Expression of the gene from P<sub>TEF1</sub> showed clear improvement, indicating that the effect might be connected to the poor efficiency of the enzyme. This hypothesis was supported by the observation that increased levels of malonyl-CoA in combination with a reduction of *FAS1* expression did not lead to increased production, but to zero growth. In addition, these results potentially highlight the importance of acetoacetyl-CoA thiolysis as a means to control cytosolic levels of acetyl-CoA. Nonetheless, it could be shown that acetoacetyl-CoA synthase is able to complement the loss of *ERG10*, while NphT7

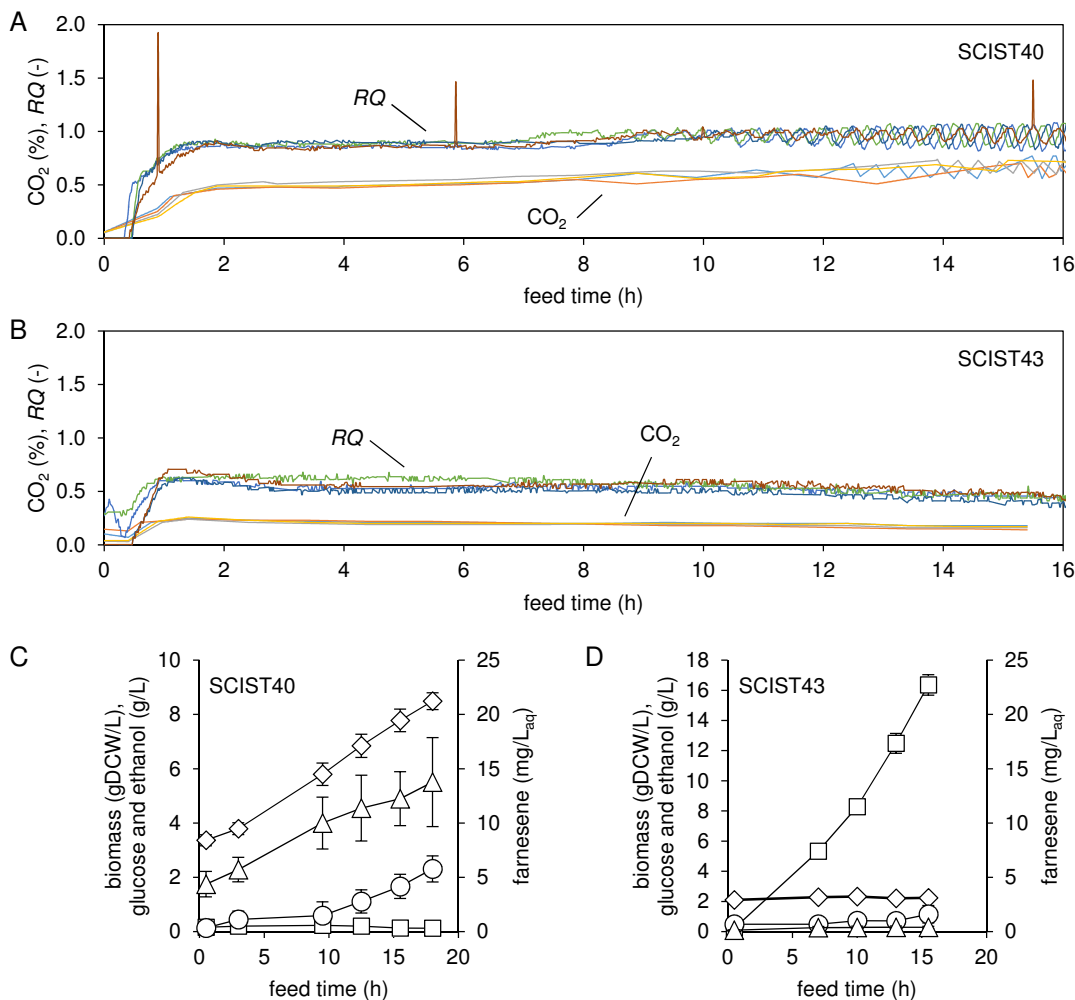


**Figure 5.5:** Downregulation of *FAS1* using  $P_{HXT1}$  for improved utilization of malonyl-CoA for the MVA pathway. Fed-batch cultivation with RQ-controlled feed of strain SCIST40 ( $erg10\Delta::P_{TEF1}\text{-}nphT7_{SCL}$ ) and SCIST43 ( $erg10\Delta::P_{TEF1}\text{-}nphT7_{SCL}$ ,  $P_{FAS1}\Delta::P_{HXT1}$ ). (A and B) Online measurements of the respiratory quotient (RQ) and the  $\text{CO}_2$  content of the exhaust gas. (C and D) Concentrations of biomass (◊), glucose (□), ethanol (○) and farnesene (△). Data represents average values of four biological replicates with standard deviation.

from *S. glaucescens* showed superior efficiency in comparison to the other candidates. Finally, engineering the supply of acetyl-CoA, potentially combined with overexpression of a thiolase from another organism, might be more suitable for the purpose of driving the conversion towards acetoacetyl-CoA. For instance, previous studies on the production of farnesene have used the corresponding thiolase from *Clostridium acetobutylicum* (Sandoval et al., 2014). In fact, *in vitro* assays showed an approximately 40-fold increase of the thiolase activity from *C. acetobutylicum* over acetoacetyl-CoA synthase from *Streptomyces* sp. strain CL190, when expressed from a low-copy plasmid in *S. cerevisiae* (Schadeweg and Boles, 2016).



# Chapter 6

## Analysis of Organic Overlays for Quantification of Farnesene

Different challenges arise regarding the production of terpenes, which are associated with the chemical and antimicrobial properties of these compounds. First and foremost, terpenes are prone to be removed from the medium by gas stripping due to their low water solubility (Schuhfried et al., 2015). Among other examples, this effect has been reported for production of amorphadiene and taxadiene in *E. coli* (Ajikumar et al., 2010; Martin et al., 2003) as well as for production of bisabolene in *S. cerevisiae* (Kirby et al., 2014). Secondly, particularly monoterpenes have been shown to be severely toxic (Brennan et al., 2012; Dunlop et al., 2011). To minimize product loss and toxicity, terpenes are commonly recovered from the medium during the fermentation using an extractive overlay, which is added as a second liquid phase. This approach is often referred to as “*in situ* product removal” (ISPR), which has been used as an efficient tool to increase productivity of diverse fermentation processes (Freeman et al., 1993; Malinowski, 2001). By growing *S. cerevisiae* in the presence of dibutyl phthalate, the tolerance towards limonene increased 702-fold (Brennan et al., 2012), highlighting the potential of this cultivation setup. Different solvents have been used as extractive overlays for production of terpenes in lab scale, such as decane (Wang et al., 2011), dodecane Scalcinati et al. (2012b), methyl oleate (Westfall et al., 2012) and isopropyl myristate (IPM) (Paddon et al., 2013; Westfall et al., 2012). However, other solvents such as diisononyl phthalate and oleyl alcohol have also been investigated regarding their compatibility with *S. cerevisiae* (Asadolahi et al., 2008). Some of the primary selection criteria for solvents to be used for this application include compatibility with the host, i.e. it needs to be non-toxic, high product capacity and immiscibility with the medium (Bruce and Daugulis, 1991). In this respect, the partition coefficient  $\log(P_{\text{OW}})$ , which is a measure of the hydrophobicity of a solute by describing its distribution between octanol and water, represents an important indicator of the suitability of a solvent (Bruce and Daugulis, 1991). As such, for compatibility with *S. cerevisiae* solvents require a  $\log(P_{\text{OW}}) > 5$  (Bruce

and Daugulis, 1991). With a  $\log(P_{\text{OW}})$  of 6.1 (ChemIDplus Database, National Institutes of Health, <https://chem.sis.nlm.nih.gov/chemidplus/chemidlite.jsp>), dodecane has been used in a number of studies including all experiments reporting concentrations of farnesene in this project. However, while dodecane is compatible with *S. cerevisiae* and suitable to capture hydrophobic products, several challenges have to be taken into consideration regarding the analysis of this organic overlay. While method development mostly focuses on the analysis of intracellular metabolites (Khoomrung et al., 2013; Rodriguez et al., 2014), quantification of sesquiterpenes in dodecane was investigated here with the objective to improve existing analytical procedures.

In the first part, the importance of dodecane was investigated with respect to reducing potential product toxicity and product loss due to gas stripping. Based on previous experiments regarding the toxicity of sesquiterpenes, farnesene was not expected to be toxic (Peralta-Yahya et al., 2011) and in fact, exposure of *S. cerevisiae* strain CEN.PK113-7D to farnesene did not affect growth even at concentrations of 500 mM (Figure 6.1 A). This observation could be related to the strong hydrophobicity of farnesene with a  $\log(P_{\text{OW}})$  of 7.1 (ChemIDplus), while the  $\log(P_{\text{OW}})$  values for many of the highly toxic monoterpenes have been reported to be <5 (Schmid et al., 1992). To quantify the loss of farnesene due to gas stripping, *S. cerevisiae* strain CEN.PK113-5D expressing the truncated HMG-CoA reductase (*tHMG1*) and the farnesene synthase from *C. junos* from a multi-copy plasmid was cultivated in aerated bioreactors in the presence and absence of an extractive dodecane overlay. In the first scenario, dodecane was used for the *in situ* extraction, which was added to a final concentration of 10 % v/v directly after inoculation. In the latter case, a sample was taken and farnesene was extracted from the medium using dodecane at the same concentration (*ex situ* recovery). In both cases, samples were taken at the end of the experiment and farnesene was eventually quantified in the dodecane overlay. Patchoulol was used as an internal standard to account for differences regarding the extraction yield. An alternative method for quantification of gas stripping effects has also been proposed by Cappaert and Larroche (2004). Notably, the concentration of farnesene was substantially reduced without *in situ* recovery using dodecane (~99 %), clearly highlighting the requirement of an extractive overlay to minimize product loss (Figure 6.1 B). Obviously, the low concentration of farnesene obtained in the *ex situ* extraction scenario is also representative of its low solubility. Farnesene that was possibly attached to the glass of the vessel if not removed by the gas flow, was not accounted for in this experiment. In addition, an approximately 30 % increase in the biomass concentration was observed in the presence of dodecane, potentially due to promoting the secretion of the product or reducing the contact with toxic by-products (e.g. farnesol). Similarly, beneficial effects on growth have also been reported for utilization of IPM (Paddon et al., 2013).

For detection of sesquiterpenes, the overlay is recovered from the medium by centrifugation and subsequently analyzed by gas chromatographic separation coupled with mass spectrometry detection (GC-MS). Due to its high sensitivity and the possibility for library-based identification of the product and other by-products, GC-MS

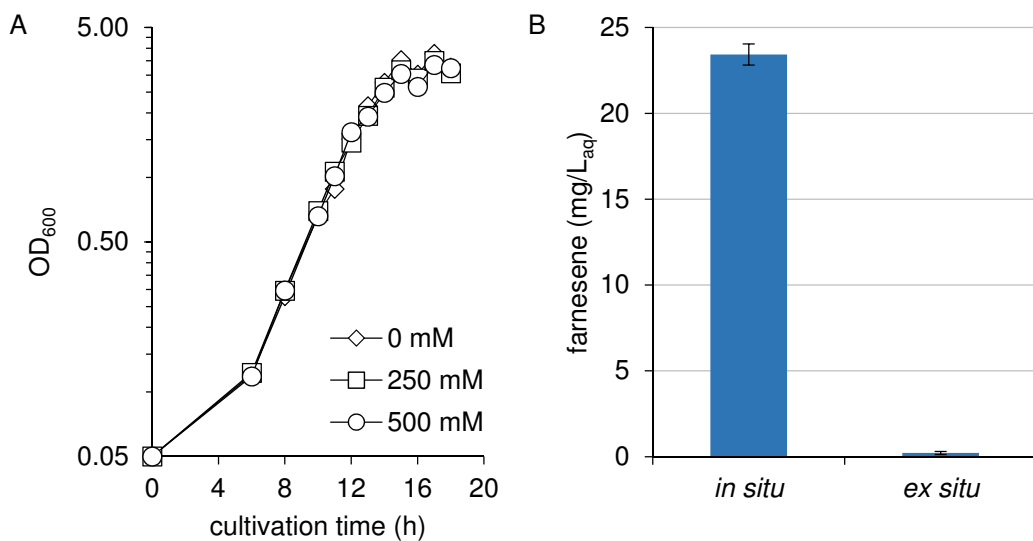


**Figure 6.1:** (A) Growth of *S. cerevisiae* CEN.PK113-7D (*MATA MAL2-8c SUC2*) exposed to different concentrations of farnesene, which was added 10 h after inoculation. (B) Aerobic batch cultivation of *S. cerevisiae* CEN.PK113-5D expressing truncated HMG-CoA reductase (*tHMG1*) and farnesene synthase from *C. junos*. The cultivation was performed in the presence (*in situ*) and in the absence (*ex situ*) of an extractive dodecane overlay. Bars represent average concentrations of farnesene with respect to aqueous medium of three biological replicates after 48 h of cultivation time.

represents the preferred technique for analysis. In connection with this, analysis is often performed on non-polar columns with the stationary phase consisting of 5 % phenyl-arylene, 95 % dimethylsiloxane (ZB-5MS) or similar such as DB-5MS (Rodriguez et al., 2014; Wang et al., 2010; Zhou et al., 2015), SLB-5MS (Asadollahi et al., 2008) and TR-5MS (Peralta-Yahya et al., 2011). Based on our experiments, utilization of ZB-5MS showed low sensitivity for farnesene and very high background noise arising from dodecane. In addition, the interaction of dodecane with the stationary phase was very strong, leading to carry-over of the solvent to the following injections. In a comparison of different alternatives, utilization of a ZB-50 column with higher polarity of the stationary phase (50 %-phenyl-50 %-dimethylsiloxane) not only increased sensitivity for farnesene in dodecane, but also reduced the carry-over of dodecane from one injection to the other (Figure 2 and 3, paper VI). Using the ZB-50 column, construction of a five-point calibration curve for quantification of farnesene in dodecane using 5 consecutive injections of each standard showed sufficient linearity and reproducibility ( $R^2=0.9872$ , intraday; <3 % residual standard deviation (RSD), Figure 6.2 A). A slight decrease in the intensity at the highest concentration of farnesene possibly indicates that the linearity cannot be extended above 50 mg/L.

For investigation of the stability of the method, two sets of standards were analyzed with 50 injections of pure dodecane samples in between (Figure 6.2 B). As a result, a substantial drop in the sensitivity was observed due to the dodecane, which amounted to approximately 50 % in each concentration. These results indicate that dodecane

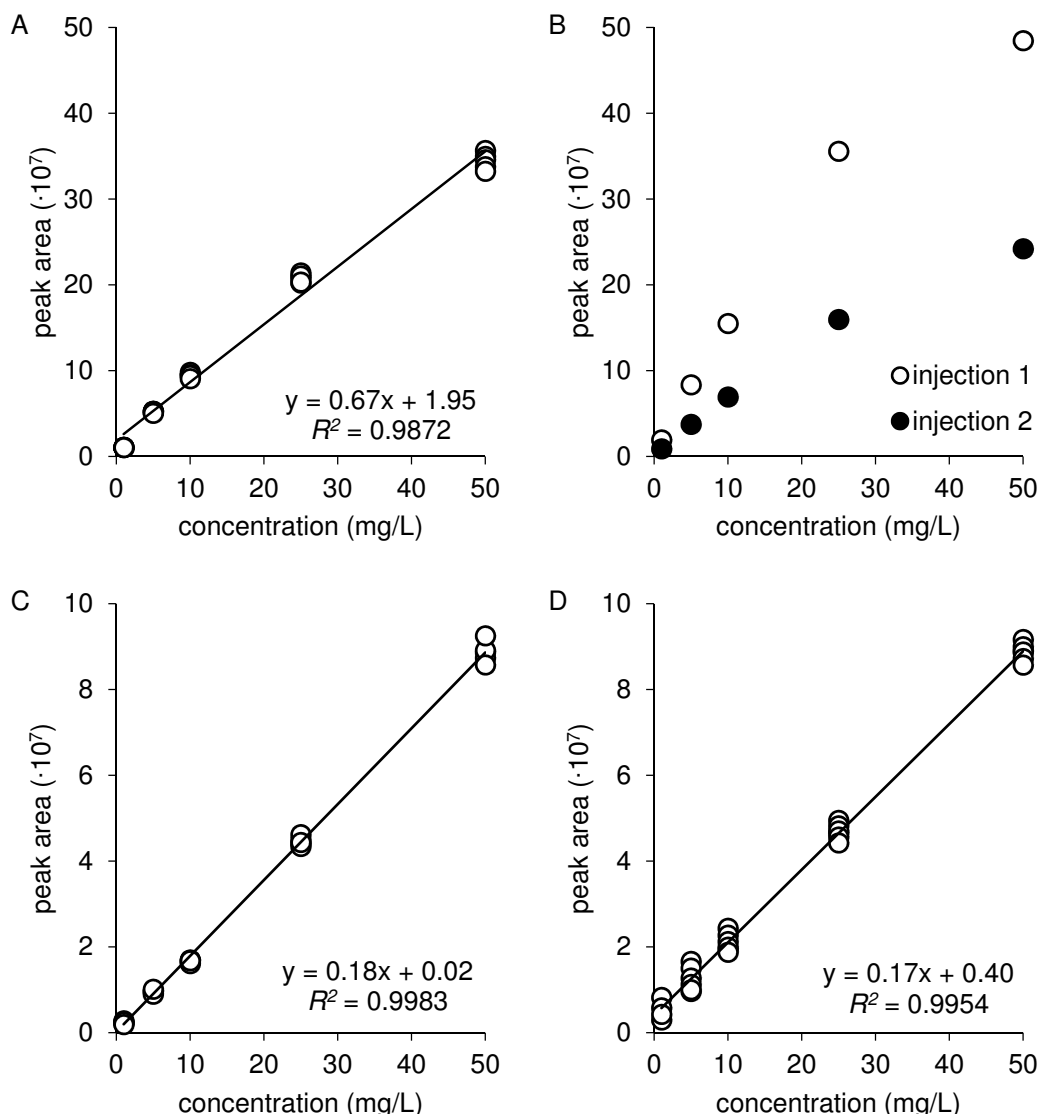


**Figure 6.2:** Comparison of two different techniques for quantification of farnesene in dodecane. (A) Method calibration from 5 injections at each concentration for quantification of farnesene using GC-MS ( $n=5$ ). (B) Calibration of the method using two sets of farnesene standards with 50 dodecane samples injected in between. (C) Method calibration for quantification of farnesene using GC-FID ( $n=5$ ). (D) Calibration of the method using six sets of repeatedly injected farnesene standards, with 50 undiluted dodecane samples injected in between each set.

severely impaired the ionization efficiency of the MS, not allowing for quantification of farnesene. As evaporation of dodecane to switch the solvent for sample analysis by GC-MS was significantly increasing the time for sample preparation (Supplementary Table 1, paper VI), two alternative approaches were investigated to reduce the effects of dodecane on the MS. First, the drift was shown to be minimized by introduction of a co-solvent such as hexane, which interacts less with the stationary phase and elutes at the void volume. In fact, dilutions of dodecane in hexane significantly

reduced the contamination of the MS (Figure 6, paper VI). However, this approach not only reduces the contaminations from the dodecane, but also the sensitivity of the method. Furthermore, high dilutions were required before an improvement was observed (Supplementary Figure 3, paper VI). With respect to the literature, 100x dilutions of the dodecane overlay were recommended by a previous study (Rodriguez et al., 2014). Secondly, the effect of dodecane was also investigated on the flame ionization detector (FID), which generates ions using a hydrogen flame and is widely applied due to its predictable response and broad range of linearity (Holm, 1999). As anticipated, calibration of the method using GC-FID displayed clear linearity for the selected concentration range with lower sensitivity compared to MS detection ( $R^2=0.9983$ , intraday; <10 % RSD, Figure 6.2 C). The stability of the FID, however, was clearly superior as injection of 250 dodecane samples showed almost no effect on the sensitivity of the detector, which indicates that the contaminations from the dodecane are very efficiently decomposed by the flame (Figure 6.2 D).

In summary, production of farnesene does not require an extractive overlay for the purpose of reducing product toxicity, but rather for minimizing product loss due to gas stripping. In addition, dodecane could also exert other beneficial effects such as sequestering toxic by-products or promoting the secretion of farnesene. While this requirement refers to lab scale fermentations, which are performed during the metabolic engineering process and often yield low product quantities, industrial scale production of farnesene with volume fractions exceeding 15 %, obviously represents a completely different scenario (Meadows et al., 2016). Despite the simplicity of the experimental setup, dodecane was shown to have detrimental effects on analytical procedures involving GC-MS, which have to be considered for reliable product quantification. These challenges were illustrated and solutions to potentially reduce the associated effects were presented and evaluated.



*I have not failed. I have just found  
10,000 ways that don't work.*

---

Thomas Alva Edison

# Chapter 7

## Conclusions

Within the last 15 years, engineering metabolism for production of sesquiterpenes has been investigated intensively, leading among others to the efficient production of farnesene and the precursor of the anti-malarial drug artemisinic acid, which highlight the potential of *S. cerevisiae* as a cell factory for sustainable production of chemicals from renewable carbon sources (Meadows et al., 2016; Paddon et al., 2013). An important milestone along the way represents the efficient production of amorphadiene to high titers (~40 g/L) by Westfall et al. (2012), which was published in January that year, right after I started. Hence the objective of this project was not to enable large scale production of sesquiterpenes in *S. cerevisiae* as this had been clearly demonstrated. Instead, using farnesene as an example for industrially relevant sesquiterpenes, the objective was to investigate the impact of different metabolic engineering strategies as well as to support the design of new ones. This involved studying the transcriptome and metabolome of an existing platform strain for sesquiterpene production to generate a clear image of the engineered metabolism. Although final concentrations were low in comparison to the results reported from a large commercial effort (Meadows et al., 2016), several changes were identified with respect to the MVA pathway, amino acid synthesis, acetyl-CoA metabolism and MVA pathway regulation, which could potentially be limiting to the synthesis of these compounds. Hence, these investigations will hopefully improve the understanding of the response of the strain during the production of farnesene and potentially aid the identification of new targets. In this respect, further analysis will include confirmation of the most significant changes by targeted metabolite analysis. For this purpose, we recently developed a GC-MS-based method for efficient amino acid analysis (Khoomrung et al., 2015).

In addition, three different reactions of the MVA pathway were addressed and their potential to support production of sesquiterpenes was examined. As such, expression of acetoacetyl-CoA synthase from *Streptomyces* sp. strain CL190 served as a potential strategy to utilize malonyl-CoA for the MVA pathway and thereby to alleviate limita-

tions on the pathway flux imposed by the thermodynamically unfavorable conversion of acetyl-CoA to acetoacetyl-CoA in the first reaction. Although this approach failed to improve production of farnesene, presumably due to the poor efficiency of the acetoacetyl-CoA synthase, expression of the heterologous enzyme could replace the endogenous thiolase, whereas the homolog from *S. glaucescens* demonstrated clear superiority among the selected candidates. Considering the participation of FPP as a substrate in numerous metabolic reactions, the specific recognition between affibodies has been shown to be a useful tool for co-localizing pathway enzymes and to efficiently redirect substrate towards a specific product. In this respect, the MVA pathway with the FPP branch point represented a suitable scenario to demonstrate the concept, which could ultimately be transferred to the production of PHB in *E. coli*. Nonetheless, the requirement for case-dependent optimization of the enzyme-to-scaffold ratio was evident. Following the pathway for product formation, the final conversion of FPP to farnesene was addressed and the impact of the terpene synthase selection was evaluated. While the three selected farnesene synthases did not show significant differences, the results suggested advanced efficiency of these enzymes compared to the terpene synthase used for production of santalene. Lastly, focus was also set to problems concerning the analysis of sesquiterpenes in dodecane. Despite the large number of available studies, few reports discuss analytical challenges in connection with the utilization of an extractive overlay. These problems were clearly illustrated and available solutions were evaluated.

In conclusion, the results described in this project not only provide a contribution to production of sesquiterpenes, but are also potentially useful for other metabolic engineering studies in *S. cerevisiae*. This applies particularly to the scaffolding approach using affibodies and the evaluation of different acetoacetyl-CoA synthases, which are transferable to other pathways and acetoacetyl-CoA derived products, respectively. With regard to the future of terpene production by *S. cerevisiae*, it is likely that existing platform strains will be transferred for production of other industrial relevant isoprenoids (Nielsen, 2015). As an example, significant progress has been recently made to overcome monoterpene toxicity and metabolic engineering could eventually allow for the efficient production of these compounds (Brennan et al., 2015). Besides, advances made in genome editing using CRISPR/Cas9 will facilitate the construction of novel cell factories. One of the key elements for the construction of cell factories constitutes redirecting metabolism towards the desired product or the introduction of a heterologous pathway. Although functional expression of the iron-sulfur cluster enzymes required for the bacterial MEP pathway in *S. cerevisiae* has not been achieved yet, introduction of the MEP pathway or the MVA pathway from plants could represent engineering approaches to support production of terpenes. Additionally, screening of enzymes from other organisms with higher efficiency or different co-factor requirements, remains an essential part of metabolic engineering, as illustrated by the example of farnesene (Meadows et al., 2016). In addition, enzyme mutagenesis for increased productivity, which has been recently illustrated for pinene synthase, represents an approach to overcome limitations imposed by expression of heterologous enzymes, which could play a more pronounced role in the future (Tashiro et al.,

2016). Apart from this, despite the complexity of the MVA pathway regulation, future engineering strategies could likely be more directed towards the transcription machinery of *S. cerevisiae* as the expression level of numerous genes can be influenced by modification of transcription factors. While only limited improvements on the production of sesquiterpenes were observed after expression of the mutant allele of the transcription factor *UPC2* (*upc2-1*) (Ro et al., 2006), global transcription machinery engineering (gTME) has been successfully used to increase tolerance towards high concentrations of glucose/ethanol, a desirable trait for industrial scale fermentations of *S. cerevisiae* (Alper et al., 2006). Similarly, targeting transcription has also been used for increased uptake of galactose. Disruption of the regulatory network for galactose uptake by overexpression of *tTUP1*, encoding a truncated variant of the repressor Tup1, led to increased expression of genes involved in galactose metabolism (*GAL1*, *GAL4* and *GAL80*) and ultimately improved galactose fermentation by 250 % (Lee et al., 2011). With respect to the production of terpenes in *S. cerevisiae*, the construction of transcription factor mutant libraries by random mutagenesis could also aid the identification of new targets, which induce enhanced pathway activity. While the efficient screening of mutants is of key importance for this approach, different methods specific to isoprenoid production are already available (Emmerstorfer-Augustin et al., 2016). As illustrated by the example of bisabolene, non-ionic surfactants such as Tween 20 can be used to screen for improved producers, as the surfactant-mediated toxicity is relieved by increased sesquiterpene production (Kirby et al., 2014). In conclusion, due to the advances in the field of metabolic engineering, novel opportunities are emerging to allow for the efficient production of chemicals from the MVA pathway, which will expand the product portfolio of *S. cerevisiae* and support the transition towards a more bio-based economy. In this respect, this project represents a useful contribution for future studies by investigating different aspects that influence the production of these compounds.



# References

- A, J., Trygg, J., Gullberg, J., Johansson, A. I., Jonsson, P., Antti, H., Marklund, S. L., and Moritz, T. (2005). Extraction and GC/MS analysis of the human blood plasma metabolome. *Analytical Chemistry*, 77(24):8086–8094.
- Ajikumar, P. K., Xiao, W. H., Tyo, K. E. J., Wang, Y., Simeon, F., Leonard, E., Mucha, O., Phon, T. H., Pfeifer, B., and Stephanopoulos, G. (2010). Isoprenoid pathway optimization for taxol precursor overproduction in *Escherichia coli*. *Science*, 330(6000):70–74.
- Alberts, A. W., Chen, J., Kuron, G., Hunt, V., Huff, J., Hoffman, C., Rothrock, J., Lopez, M., Joshua, H., Harris, E., Patchett, A., Monaghan, R., Currie, S., Stapley, E., Albers-Schonberg, G., Hensens, O., Hirshfield, J., Hoogsteen, K., Liesch, J., and Springer, J. (1980). Mevinolin: a highly potent competitive inhibitor of hydroxymethylglutaryl-coenzyme A reductase and a cholesterol-lowering agent. *Proceedings of the National Academy of Sciences of the United States of America*, 77(7):3957–3961.
- Albertsen, L., Chen, Y., Bach, L. S., Rattleff, S., Maury, J., Brix, S., Nielsen, J., and Mortensen, U. H. (2011). Diversion of flux toward sesquiterpene production in *Saccharomyces cerevisiae* by fusion of host and heterologous enzymes. *Applied and Environmental Microbiology*, 77(3):1033–1040.
- Alper, H., Moxley, J., Nevoigt, E., Fink, G. R., and Stephanopoulos, G. (2006). Engineering yeast transcription machinery for improved ethanol tolerance and production. *Science*, 314(5805):1565–1568.
- Anfelt, J., Kaczmarzyk, D., Shabestary, K., Renberg, B., Rockberg, J., Nielsen, J., Uhllén, M., and Hudson, E. P. (2015). Genetic and nutrient modulation of acetyl-CoA levels in *Synechocystis* for n-butanol production. *Microbial Cell Factories*, 14(1):1–12.
- Ansari, H. R. and Curtis, A. J. (1974). Sesquiterpenes in the perfumery industry. *Journal of the Society of Cosmetic Chemists of Japan*, 25(4):203–231.
- Anthony, J. R., Anthony, L. C., Nowroozi, F., Kwon, G., Newman, J. D., and Keasling, J. D. (2009). Optimization of the mevalonate-based isoprenoid biosynthetic pathway in *Escherichia coli* for production of the anti-malarial drug precursor amorph-4,11-diene. *Metabolic Engineering*, 11(1):13–19.
- Asadollahi, M. A., Maury, J., Møller, K., Nielsen, K. F., Schalk, M., Clark, A., and Nielsen, J. (2008). Production of plant sesquiterpenes in *Saccharomyces cerevisiae*: Effect of *ERG9* repression on sesquiterpene biosynthesis. *Biotechnology and Bioengineering*, 99(3):666–677.

- Asadollahi, M. A., Maury, J., Schalk, M., Clark, A., and Nielsen, J. (2010). Enhancement of farnesyl diphosphate pool as direct precursor of sesquiterpenes through metabolic engineering of the mevalonate pathway in *Saccharomyces cerevisiae*. *Biotechnology and Bioengineering*, 106(1):86–96.
- Baker, M. (2011). Metabolomics: from small molecules to big ideas. *Nature Methods*, 8(2):117–121.
- Baldwin, I. T., Halitschke, R., Paschold, A., von Dahl, C. C., and Preston, C. A. (2006). Volatile signaling in plant-plant interactions: "talking trees" in the genomics era. *Science*, 311(5762):812–815.
- Barkley, S. J., Cornish, R. M., and Poulter, C. D. (2004). Identification of an archaeal type II isopentenyl diphosphate isomerase in methanothermobacter thermotrophicus. *Journal of Bacteriology*, 186(6):1811–1817.
- Basson, M. E., Thorsness, M., and Rine, J. (1986). *Saccharomyces cerevisiae* contains two functional genes encoding 3-hydroxy-3-methylglutaryl-coenzyme A reductase. *Proceedings of the National Academy of Sciences of the United States of America*, 83(15):5563–5567.
- Bauler, P., Huber, G., Leyh, T., and McCammon, J. A. (2010). Channeling by proximity: The catalytic advantages of active site colocalization using brownian dynamics. *The Journal of Physical Chemistry Letters*, 1(9):1332–1335.
- Beh, C. T., Cool, L., Phillips, J., and Rine, J. (2001). Overlapping functions of the yeast oxysterol-binding protein homologues. *Genetics*, 157(3):1117–1140.
- Benjamin, K. R., Silva, I. R., Cherubim, J. P., McPhee, D., and Paddon, C. J. (2016). Developing commercial production of semi-synthetic artemisinin, and of β-farnesene, an isoprenoid produced by fermentation of brazilian sugar. *Journal of the Brazilian Chemical Society*, 27(8):1339–1345.
- Bloch, K. (1992). Sterol molecule: structure, biosynthesis, and function. *Steroids*, 57(8):378–383.
- Bohlmann, J., Meyer-Gauen, G., and Croteau, R. (1998). Plant terpenoid synthases: Molecular biology and phylogenetic analysis. *Proceedings of the National Academy of Sciences*, 95(8):4126–4133.
- Brass, E. P. (1994). Overview of coenzyme A metabolism and its role in cellular toxicity. *Chemico-Biological Interactions*, 90(3):203–214.
- Bray, D. and Lay, S. (1997). Computer-based analysis of the binding steps in protein complex formation. *Proceedings of the National Academy of Sciences*, 94(25):13493–13498.
- Brennan, T. C., Turner, C. D., Krömer, J. O., and Nielsen, L. K. (2012). Alleviating monoterpene toxicity using a two-phase extractive fermentation for the bioproduction of jet fuel mixtures in *Saccharomyces cerevisiae*. *Biotechnology and Bioengineering*, 109(10):2513–2522.
- Brennan, T. C. R., Krömer, J. O., and Nielsen, L. K. (2013). Physiological and transcriptional responses of *Saccharomyces cerevisiae* to D-limonene show changes to the cell wall but not to the plasma membrane. *Applied and Environmental Microbiology*, 79(12):3590–3600.
- Brennan, T. C. R., Williams, T. C., Schulz, B. L., Palfreyman, R. W., Krömer, J. O., and Nielsen, L. K. (2015). Evolutionary engineering improves tolerance for replace-

- ment jet fuels in *Saccharomyces cerevisiae*. *Applied and Environmental Microbiology*, 81(10):3316–3325.
- Bro, C., Regenberg, B., and Nielsen, J. (2004). Genome-wide transcriptional response of a *Saccharomyces cerevisiae* strain with an altered redox metabolism. *Biotechnology and Bioengineering*, 85(3):269–276.
- Brown, M. S. and Goldstein, J. L. (1980). Multivalent feedback regulation of HMG-CoA reductase, a control mechanism coordinating isoprenoid synthesis and cell growth. *Journal of Lipid Research*, 21(5):505–517.
- Bruce, L. J. and Daugulis, A. J. (1991). Solvent selection strategies for extractive bioeatalysis. *Biotechnology Progress*, 7(2):116–124.
- Cappaert, L. and Larroche, C. (2004). Simple calculation for compounds lost by gas stripping in a two-phase liquid system involving dilute substances. *Biotechnology Letters*, 26(2):137–141.
- Carlsen, S., Ajikumar, P. K., Formenti, L. R., Zhou, K., Phon, T. H., Nielsen, M. L., Lantz, A. E., Kielland-Brandt, M. C., and Stephanopoulos, G. (2013). Heterologous expression and characterization of bacterial 2-C-methyl-D-erythritol-4-phosphate pathway in *Saccharomyces cerevisiae*. *Applied Microbiology and Biotechnology*, 97(13):5753–5769.
- Castellana, M., Wilson, M. Z., Xu, Y., Joshi, P., Cristea, I. M., Rabinowitz, J. D., Gitai, Z., and Wingreen, N. S. (2014). Enzyme clustering accelerates processing of intermediates through metabolic channeling. *Nature Biotechnology*, 32(10):1011–1018.
- Chagoyen, M. and Pazos, F. (2011). MBRole: enrichment analysis of metabolomic data. *Bioinformatics*, 27(5):730–731.
- Chappell, J., Wolf, F., Proulx, J., Cuellar, R., and Saunders, C. (1995). Is the reaction catalyzed by 3-hydroxy-3-methylglutaryl coenzyme A reductase a rate-limiting step for isoprenoid biosynthesis in plants? *Plant Physiology*, 109(4):1337–1343.
- Charlier, H. A., Narasimhan, C., and Miziorko, H. M. (1997). Inactivation of 3-hydroxy-3-methylglutaryl-CoA synthase and other acyl-coa-utilizing enzymes by 3-oxobutylsulfoxyl-CoA. *Biochemistry*, 36(6):1551–1558.
- Chen, F., Tholl, D., Bohlmann, J., and Pichersky, E. (2011). The family of terpene synthases in plants: A mid-size family of genes for specialized metabolism that is highly diversified throughout the kingdom. *Plant Journal*, 66(1):212–229.
- Chen, Y., Wang, Z., Chu, J., Xi, B., and Zhuang, Y. (2015). The glucose RQ-feedback control leading to improved erythromycin production by a recombinant strain *Saccharopolyspora erythraea* ZL1004 and its scale-up to 372-m<sup>3</sup> fermenter. *Bioprocess and Biosystems Engineering*, 38(1):105–112.
- Cheng, A.-X., Lou, Y.-G., Mao, Y.-B., Lu, S., Wang, L.-J., and Chen, X.-Y. (2007). Plant terpenoids: Biosynthesis and ecological functions. *Journal of Integrative Plant Biology*, 49(2):179–186.
- Cho, K., Evans, B. S., Wood, B. M. K., Kumar, R., Erb, T. J., Warlick, B. P., Gerlt, J. A., and Sweedler, J. V. (2015). Integration of untargeted metabolomics with transcriptomics reveals active metabolic pathways. *Metabolomics*, 11(3):503–517.
- Crock, J., Wildung, M., and Croteau, R. (1997). Isolation and bacterial expression of a sesquiterpene synthase cDNA clone from peppermint (*Mentha x piperita*, l.) that produces the aphid alarm pheromone(E)-β-farnesene. *Proceedings of the National*

- Academy of Sciences, 94(24):12833–12838.
- Dahl, R. H., Zhang, F., Alonso-Gutierrez, J., Baidoo, E., Batth, T. S., Redding-Johanson, A. M., Petzold, C. J., Mukhopadhyay, A., Lee, T. S., Adams, P. D., and Keasling, J. D. (2013). Engineering dynamic pathway regulation using stress-response promoters. *Nature Biotechnology*, 31(11):1039–1046.
- Daugherty, J. R., Rai, R., el Berry, H. M., and Cooper, T. G. (1993). Regulatory circuit for responses of nitrogen catabolic gene expression to the *GLN3* and *DAL80* proteins and nitrogen catabolite repression in *Saccharomyces cerevisiae*. *Journal of Bacteriology*, 175(1):64–73.
- David, F. and Siewers, V. (2015). Advances in yeast genome engineering. *FEMS Yeast Research*, 15(1):1–14.
- Davies, B. S. J., Wang, H. S., and Rine, J. (2005). Dual activators of the sterol biosynthetic pathway of *Saccharomyces cerevisiae*: Similar activation/regulatory domains but different response mechanisms. *Molecular and Cellular Biology*, 25(16):7375–7385.
- Davis, E. M. and Croteau, R. (2000). Cyclization enzymes in the biosynthesis of monoterpenes, sesquiterpenes, and diterpenes. In *Biosynthesis: Aromatic Polyketides, Isoprenoids, Alkaloids*, pages 53–95. Springer Berlin Heidelberg.
- De Jong-Gubbels, P., Vanrolleghem, P., Heijnen, S., Van Dijken, J. P., and Pronk, J. T. (1995). Regulation of carbon metabolism in chemostat cultures of *Saccharomyces cerevisiae* grown on mixtures of glucose and ethanol. *Yeast*, 11(5):407–418.
- De Kok, S., Kozak, B. U., Pronk, J. T., and Van Maris, A. J. A. (2012). Energy coupling in *Saccharomyces cerevisiae*: Selected opportunities for metabolic engineering. *FEMS Yeast Research*, 12(4):387–397.
- Degenhardt, J., Köllner, T. G., and Gershenzon, J. (2009). Monoterpene and sesquiterpene synthases and the origin of terpene skeletal diversity in plants. *Phytochemistry*, 70(15–16):1621–1637.
- Delebecque, C. J., Lindner, A. B., Silver, P. A., and Aldaye, F. A. (2011). Organization of intracellular reactions with rationally designed RNA assemblies. *Science*, 333(6041):470–474.
- DeLoache, W. C., Russ, Z. N., Narcross, L., Gonzales, A. M., Martin, V. J. J., and Dueber, J. E. (2015). An enzyme-coupled biosensor enables (S)-reticuline production in yeast from glucose. *Nature Chemical Biology*, 11(7):465–471.
- Dewick, P. M. (2001). Secondary metabolism: The building blocks and construction mechanisms. In *Medicinal Natural Products*, pages 7–34. John Wiley & Sons, Ltd.
- Dilshad, E., Cusido, R. M., Palazon, J., Estrada, K. R., Bonfill, M., and Mirza, B. (2015). Enhanced artemisinin yield by expression of *rol* genes in *Artemisia annua*. *Malaria Journal*, 14(1):424.
- Dimster-Denk, D. and Rine, J. (1996). Transcriptional regulation of a sterol-biosynthetic enzyme by sterol levels in *Saccharomyces cerevisiae*. *Molecular and Cellular Biology*, 16(8):3981–3989.
- Dimster-Denk, D., Rine, J., Phillips, J., Scherer, S., Cundiff, P., DeBord, K., Gilliland, D., Hickman, S., Jarvis, A., Tong, L., and Ashby, M. (1999). Comprehensive evaluation of isoprenoid biosynthesis regulation in *Saccharomyces cerevisiae* utilizing the genome reporter matrix. *Journal of Lipid Research*, 40(5):850–860.

- Dimster-Denk, D., Thorsness, M. K., and Rine, J. (1994). Feedback regulation of 3-hydroxy-3-methylglutaryl coenzyme A reductase in *Saccharomyces cerevisiae*. *Molecular Biology of the Cell*, 5(6):655–665.
- Ding, M. Z., Yan, H. F., Li, L. F., Zhai, F., Shang, L. Q., Yin, Z., and Yuan, Y. J. (2014). Biosynthesis of taxadiene in *Saccharomyces cerevisiae*: Selection of geranylgeranyl diphosphate synthase directed by a computer-aided docking strategy. *PLoS ONE*, 9(10):1–9.
- Donald, K. A., Hampton, R. Y., and Fritz, I. B. (1997). Effects of overproduction of the catalytic domain of 3-hydroxy-3-methylglutaryl coenzyme A reductase on squalene synthesis in *Saccharomyces cerevisiae*. *Applied and Environmental Microbiology*, 63(9):3341–3344.
- Dueber, J. E., Wu, G. C., Malmirchegini, G. R., Moon, T. S., Petzold, C. J., Ullal, A. V., Prather, K. L. J., and Keasling, J. D. (2009). Synthetic protein scaffolds provide modular control over metabolic flux. *Nature Biotechnology*, 27(8):753–759.
- Dugar, D. and Stephanopoulos, G. (2011). Relative potential of biosynthetic pathways for biofuels and bio-based products. *Nature Biotechnology*, 29(12):1074–1078.
- Dunlop, M. J., Dossani, Z. Y., Szmidt, H. L., Chu, H. C., Lee, T. S., Keasling, J. D., Hadi, M. Z., and Mukhopadhyay, A. (2011). Engineering microbial biofuel tolerance and export using efflux pumps. *Molecular Systems Biology*, 7(1):487.
- Duportet, X., Aggio, R. B. M., Carneiro, S., and Villas-Bôas, S. G. (2012). The biological interpretation of metabolomic data can be misled by the extraction method used. *Metabolomics*, 8(3):410–421.
- Durr, I. F. and Rudney, H. (1960). The reduction of  $\beta$ -hydroxy- $\beta$ -methylglutaryl coenzyme A to mevalonic acid. *Journal of Biological Chemistry*, 235(9):2572–2578.
- Eberhardt, N. L. and Rilling, H. C. (1975). Prenyltransferase from *Saccharomyces cerevisiae*. purification to homogeneity and molecular properties. *Journal of Biological Chemistry*, 250(3):863–866.
- Eisenreich, W., Bacher, A., Arigoni, D., and Rohdich, F. (2004). Biosynthesis of isoprenoids via the non-mevalonate pathway. *Cellular and Molecular Life Sciences CMSL*, 61(12):1401–1426.
- Eklund, M., Axelsson, L., Uhlén, M., and Nygren, P. (2002). Anti-idiotypic protein domains selected from protein A-based affibody libraries. *Proteins: Structure, Function and Genetics*, 48(3):454–462.
- Elbaz-Alon, Y., Morgan, B., Clancy, A., Amoako, T. N. E., Zalckvar, E., Dick, T. P., Schwappach, B., and Schuldiner, M. (2014). The yeast oligopeptide transporter Opt2 is localized to peroxisomes and affects glutathione redox homeostasis. *FEMS Yeast Research*, 14(7):1055.
- Elleuche, S. (2014). Bringing functions together with fusion enzymes—from nature's inventions to biotechnological applications. *Applied Microbiology and Biotechnology*, 99(4):1545–1556.
- Ellis, D. I. and Goodacre, R. (2012). Metabolomics-assisted synthetic biology. *Current Opinion in Biotechnology*, 23(1):22–28.
- Emmerstorfer-Augustin, A., Moser, S., and Pichler, H. (2016). Screening for improved isoprenoid biosynthesis in microorganisms. *Journal of Biotechnology*, 235:112–120.
- Farhi, M., Marhevka, E., Masci, T., Marcos, E., Eyal, Y., Ovadis, M., Abeliovich, H., and

- Vainstein, A. (2011). Harnessing yeast subcellular compartments for the production of plant terpenoids. *Metabolic Engineering*, 13(5):474–481.
- Farrés, M., Piña, B., and Tauler, R. (2014). Chemometric evaluation of *Saccharomyces cerevisiae* metabolic profiles using LC-MS. *Metabolomics*, 11(1):210–224.
- Farrés, M., Piña, B., and Tauler, R. (2016). LC-MS based metabolomics and chemometrics study of the toxic effects of copper on *Saccharomyces cerevisiae*. *Metallomics*, 8:790–798.
- Faulkner, A., Chen, X., Rush, J., Horazdovsky, B., Waechter, C. J., Carman, G. M., and Sternweis, P. C. (1999). The *LPP1* and *DPP1* gene products account for most of the isoprenoid phosphate phosphatase activities in *Saccharomyces cerevisiae*. *Journal of Biological Chemistry*, 274(21):14831–14837.
- Fiechter, A. and Seghezzi, W. (1992). Regulation of glucose metabolism in growing yeast cells. *Journal of Biotechnology*, 27(1):27–45.
- Fletcher, E., Feizi, A., Kim, S., Siewers, V., and Nielsen, J. (2015). RNA-seq analysis of *Pichia anomala* reveals important mechanisms required for survival at low pH. *Microbial Cell Factories*, 14(1):1–11.
- Foo, J. L., Jensen, H. M., Dahl, R. H., George, K., Keasling, J. D., Lee, T. S., Leong, S., and Mukhopadhyay, A. (2014). Improving microbial biogasoline production in *Escherichia coli* using tolerance engineering. *mBio*, 5(6).
- Freeman, A., Woodley, J. M., and Lilly, M. D. (1993). *In situ* product removal as a tool for bioprocessing. *Nature Biotechnology*, 11(9):1007–1012.
- Friesen, J. A. and Rodwell, V. W. (2004). The 3-hydroxy-3-methylglutaryl coenzyme-A (HMG-CoA) reductases. *Genome Biology*, 5(11):248–248.
- Frister, T. and Beutel, S. (2015). Moschusduft und patchouliöl. *Chemie in unserer Zeit*, 49(5):294–301.
- Fu, J., Liu, M., Liu, Y., Woodbury, N. W., and Yan, H. (2012). Interenzyme substrate diffusion for an enzyme cascade organized on spatially addressable DNA nanostructures. *Journal of the American Chemical Society*, 134(12):5516–5519.
- Gardner, R. G. and Hampton, R. Y. (1999). A highly conserved signal controls degradation of 3-hydroxy-3- methylglutaryl-coenzyme A (HMG-CoA) reductase in eukaryotes. *Journal of Biological Chemistry*, 274(44):31671–31678.
- Garms, S., Chen, F., Boland, W., Gershenson, J., and Köllner, T. G. (2012). A single amino acid determines the site of deprotonation in the active center of sesquiterpene synthases SbTPS1 and SbTPS2 from *Sorghum bicolor*. *Phytochemistry*, 75:6–13.
- George, K. W., Alonso-Gutierrez, J., Keasling, J. D., and Lee, T. S. (2015). Isoprenoid drugs, biofuels, and chemicals-artemisinin, farnesene, and beyond. In *Biotechnology of Isoprenoids*, pages 355–389. Springer International Publishing.
- George, R. A. and Heringa, J. (2002). An analysis of protein domain linkers: Their classification and role in protein folding. *Protein Engineering*, 15(11):871–879.
- Goldfine, H. and Vance, D. E. (2001). Obituary: Konrad E. Bloch (1912-2000). *Nature*, 409(6822):779–779.
- Goldstein, J. L. and Brown, M. S. (1990). Regulation of the mevalonate pathway. *Nature*, 343(6257):425–430.
- Grabinska, K. and Palamarczyk, G. (2002). Dolichol biosynthesis in the yeast *Sac-*

- charomyces cerevisiae*: an insight into the regulatory role of farnesyl diphosphate synthase. *FEMS Yeast Research*, 2(3):259–265.
- Green, S., Friel, E. N., Matich, A., Beuning, L. L., Cooney, J. M., Rowan, D. D., and MacRae, E. (2007). Unusual features of a recombinant apple  $\alpha$ -farnesene synthase. *Phytochemistry*, 68(2):176–188.
- Gronover, C., Wahler, D., and Prüfer, D. (2011). Natural rubber biosynthesis and physic-chemical studies on plant derived latex. In *Biotechnology of Biopolymers*, pages 75–88. InTech.
- Hampton, R., Dimster-Denk, D., and Rine, J. (1996). The biology of HMG-CoA reductase: The pros of contra-regulation. *Trends in Biochemical Sciences*, 21(4):140–145.
- Hampton, R. Y. and Rine, J. (1994). Regulated degradation of HMG-CoA reductase, an integral membrane protein of the endoplasmic reticulum, in yeast. *Journal of Cell Biology*, 125(2):299–312.
- Harvey, B. G., Merriman, W. W., and Koontz, T. A. (2015). High-density renewable diesel and jet fuels prepared from multicyclic sesquiterpanes and a 1-hexene-derived synthetic paraffinic kerosene. *Energy & Fuels*, 29(4):2431–2436.
- Harvey, B. G., Wright, M. E., and Quintana, R. L. (2010). High-density renewable fuels based on the selective dimerization of pinenes. *Energy and Fuels*, 24(1):267–273.
- Heldt, H.-W. and Piechulla, B. (2011). A large diversity of isoprenoids has multiple functions in plant metabolism. In *Plant Biochemistry (Fourth Edition)*, pages 409–429. Academic Press.
- Higuera-Ciapara, I., Felix-Valenzuela, L., and Goycoolea, F. M. (2006). Astaxanthin: A review of its chemistry and applications. *Critical Reviews in Food Science and Nutrition*, 46(2):185–196.
- Holm, T. (1999). Aspects of the mechanism of the flame ionization detector. *Journal of Chromatography A*, 842(1-2):221–227.
- Hu, F., Liu, J., Du, G., Hua, Z., Zhou, J., and Chen, J. (2012). Key cytomembrane ABC transporters of *Saccharomyces cerevisiae* fail to improve the tolerance to D-limonene. *Biotechnology Letters*, 34(8):1505–1509.
- Huang, Z., Li, G., Zhang, C., and Xing, X. H. (2016). A study on the effects of linker flexibility on acid phosphatase PhoC-GFP fusion protein using a novel linker library. *Enzyme and Microbial Technology*, 83:1–6.
- Ignea, C., Pontini, M., Maffei, M. E., Makris, A. M., and Kampranis, S. C. (2014). Engineering monoterpene production in yeast using a synthetic dominant negative geranyl diphosphate synthase. *ACS Synthetic Biology*, 3(5):298–306.
- Jakočiūnas, T., Jensen, M. K., and Keasling, J. D. (2016). CRISPR/Cas9 advances engineering of microbial cell factories. *Metabolic Engineering*, 34:44–59.
- Jensen, M. K. and Keasling, J. D. (2015). Recent applications of synthetic biology tools for yeast metabolic engineering. *FEMS Yeast Research*, 15(1):1–10.
- Jiang, B., Brown, J. L., Sheraton, J., Fortin, N., and Bussey, H. (1994). A new family of yeast genes implicated in ergosterol synthesis is related to the human oxysterol binding protein. *Yeast*, 10(3):341–353.
- Kaneda, K., Kuzuyama, T., Takagi, M., Hayakawa, Y., and Seto, H. (2001). An unusual isopentenyl diphosphate isomerase found in the mevalonate pathway gene cluster from *Streptomyces* sp. strain CL190. *Proceedings of the National Academy of Sciences*,

- 98(3):932–937.
- Kang, A., George, K. W., Wang, G., Baidoo, E., Keasling, J. D., and Lee, T. S. (2016). Isopentenyl diphosphate (IPP)-bypass mevalonate pathways for isopentenol production. *Metabolic Engineering*, 34:25–35.
- Karim, A. S., Curran, K. A., and Alper, H. S. (2013). Characterization of plasmid burden and copy number in *Saccharomyces cerevisiae* for optimization of metabolic engineering applications. *FEMS Yeast Research*, 13(1):107–116.
- Keasling, J. D. (2008). Synthetic biology for synthetic chemistry. *ACS Chemical Biology*, 3(1):64–76.
- Kennedy, M. A., Barbuch, R., and Bard, M. (1999). Transcriptional regulation of the squalene synthase gene (*ERG9*) in the yeast *Saccharomyces cerevisiae*. *Biochimica et Biophysica Acta - Gene Structure and Expression*, 1445(1):110–122.
- Keren, L., Zackay, O., Lotan-Pompan, M., Barenholz, U., Dekel, E., Sasson, V., Aidenberg, G., Bren, A., Zeevi, D., Weinberger, A., Alon, U., Milo, R., and Segal, E. (2013). Promoters maintain their relative activity levels under different growth conditions. *Molecular Systems Biology*, 9(1):701.
- Khoomrung, S., Chumnanpuen, P., Jansa-Ard, S., Ståhlman, M., Nookaew, I., Borén, J., and Nielsen, J. (2013). Rapid quantification of yeast lipid using microwave-assisted total lipid extraction and HPLC-CAD. *Analytical Chemistry*, 85(10):4912–4919.
- Khoomrung, S., Martinez, J. L., Tippmann, S., Jansa-Ard, S., Buffing, M. F., Nicastro, R., and Nielsen, J. (2015). Expanded metabolite coverage of *Saccharomyces cerevisiae* extract through improved chloroform/methanol extraction and tert-butyldimethylsilyl derivatization. *Analytical Chemistry Research*, 6:9–16.
- Kim, B. S., Lee, S. C., Lee, S. Y., Chang, Y. K., and Chang, H. N. (2004). High cell density fed-batch cultivation of *Escherichia coli* using exponential feeding combined with pH-stat. *Bioprocess and Biosystems Engineering*, 26(3):147–150.
- Kim, S.-K. and Karadeniz, F. (2012). Biological importance and applications of squalene and squalane. In *Advances in Food and Nutrition Research*, volume 65, pages 223–233. Academic Press.
- Kind, T. and Fiehn, O. (2006). Metabolomic database annotations via query of elemental compositions: Mass accuracy is insufficient even at less than 1 ppm. *BMC Bioinformatics*, 7(1):1–10.
- Kirby, J., Nishimoto, M., Chow, R. W. N., Pasumarthi, V. N., Chan, R., Chan, L. J. G., Petzold, C. J., and Keasling, J. D. (2014). Use of nonionic surfactants for improvement of terpene production in *Saccharomyces cerevisiae*. *Applied and Environmental Microbiology*, 80(21):6685–6693.
- Kizer, L., Pitera, D. J., Pfleger, B. F., and Keasling, J. D. (2008). Application of functional genomics to pathway optimization for increased isoprenoid production. *Applied and Environmental Microbiology*, 74(10):3229–3241.
- Kozak, B. U., van Rossum, H. M., Luttik, M. A. H., Akeroyd, M., Benjamin, K. R., Wu, L., de Vries, S., Daran, J. M., Pronk, J. T., and van Maris, A. J. A. (2014). Engineering acetyl coenzyme A supply: Functional expression of a bacterial pyruvate dehydrogenase complex in the cytosol of *Saccharomyces cerevisiae*. *mBio*, 5(5).
- Lan, E. I. and Liao, J. C. (2012). ATP drives direct photosynthetic production of 1-

- butanol in cyanobacteria. *Proceedings of the National Academy of Sciences of the United States of America*, 109(16):6018–6023.
- Lange, B. M., Rujan, T., Martin, W., and Croteau, R. (2000). Isoprenoid biosynthesis: The evolution of two ancient and distinct pathways across genomes. *Proceedings of the National Academy of Sciences*, 97(24):13172–13177.
- Lapkin, A. A., Plucinski, P. K., and Cutler, M. (2006). Comparative assessment of technologies for extraction of artemisinin. *Journal of Natural Products*, 69(11):1653–1664.
- Leavell, M. D., McPhee, D. J., and Paddon, C. J. (2016). Developing fermentative terpenoid production for commercial usage. *Current Opinion in Biotechnology*, 37:114–119.
- Lee, K. S., Hong, M. E., Jung, S. C., Ha, S. J., Yu, B. J., Koo, H. M., Park, S. M., Seo, J. H., Kweon, D. H., Park, J. C., and Jin, Y. S. (2011). Improved galactose fermentation of *Saccharomyces cerevisiae* through inverse metabolic engineering. *Biotechnology and Bioengineering*, 108(3):621–631.
- Lendel, C., Dogan, J., and Härd, T. (2006). Structural basis for molecular recognition in an affibody:affibody complex. *Journal of Molecular Biology*, 359(5):1293–1304.
- Levchenko, A., Bruck, J., and Sternberg, P. W. (2000). Scaffold proteins may biphasically affect the levels of mitogen-activated protein kinase signaling and reduce its threshold properties. *Proceedings of the National Academy of Sciences of the United States of America*, 97(11):5818–5823.
- Li, M., Petteys, B. J., McClure, J. M., Valsakumar, V., Bekiranov, S., Frank, E. L., and Smith, J. S. (2010). Thiamine biosynthesis in *Saccharomyces cerevisiae* is regulated by the NAD<sup>+</sup>-dependent histone deacetylase Hst1. *Molecular and Cellular Biology*, 30(13):3329–3341.
- Liu, N. Q., Schuehly, W., von Freyhold, M., and Van der Kooy, F. (2011). A novel purification method of artemisinin from *Artemisia annua*. *Industrial Crops and Products*, 34(1):1084–1088.
- Löfblom, J., Feldwisch, J., Tolmachev, V., Carlsson, J., Ståhl, S., and Frejd, F. Y. (2010). Affibody molecules: Engineered proteins for therapeutic, diagnostic and biotechnological applications. *FEBS Letters*, 584(12):2670–2680.
- Lombard, J., López-García, P., and Moreira, D. (2012). The early evolution of lipid membranes and the three domains of life. *Nature Reviews Microbiology*, 10(7):507–515.
- Lombard, J. and Moreira, D. (2011). Origins and early evolution of the mevalonate pathway of isoprenoid biosynthesis in the three domains of life. *Molecular Biology and Evolution*, 28(1):87–99.
- Lynen, F., Eggerer, H., Henning, U., and Kessel, I. (1958). Farnesyl-pyrophosphat und 3-methyl- $\Delta^3$ -butenyl-1-pyrophosphat, die biologischen vorstufen des squalens. zur biosynthese der terpene, III. *Angewandte Chemie*, 70(24):738–742.
- Ma, S. M., Garcia, D. E., Redding-Johanson, A. M., Friedland, G. D., Chan, R., Batth, T. S., Haliburton, J. R., Chivian, D., Keasling, J. D., Petzold, C. J., Soon Lee, T., and Chhabra, S. R. (2011). Optimization of a heterologous mevalonate pathway through the use of variant HMG-CoA reductases. *Metabolic Engineering*, 13(5):588–597.

- Malinowski, J. J. (2001). Two-phase partitioning bioreactors in fermentation technology. *Biotechnology Advances*, 19(7):525–538.
- Mannan, A., Ahmed, I., Arshad, W., Asim, M. F., Qureshi, R. A., Hussain, I., and Mirza, B. (2010). Survey of artemisinin production by diverse *Artemisia* species in northern pakistan. *Malaria Journal*, 9(1):310.
- Martin, V. J. J., Piteral, D. J., Withers, S. T., Newman, J. D., and Keasling, J. D. (2003). Engineering a mevalonate pathway in *Escherichia coli* for production of terpenoids. *Nature Biotechnology*, 21(7):796–802.
- Martin, V. J. J., Yoshikuni, Y., and Keasling, J. D. (2001). The *in vivo* synthesis of plant sesquiterpenes by *Escherichia coli*. *Biotechnology and Bioengineering*, 75(5):497–503.
- Maruyama, T., Ito, M., and Honda, G. (2001). Molecular cloning, functional expression and characterization of (*E*)- $\beta$ -farnesene synthase from *Citrus junos*. *Biological and Pharmaceutical Bulletin*, 24(10):1171–1175.
- Matsumi, R., Atomi, H., Driessen, A. J. M., and van der Oost, J. (2011). Isoprenoid biosynthesis in archaea-biochemical and evolutionary implications. *Research in Microbiology*, 162(1):39–52.
- Maury, J., Asadollahi, M. A., Möller, K., Schalk, M., Clark, A., Formenti, L. R., and Nielsen, J. (2008). Reconstruction of a bacterial isoprenoid biosynthetic pathway in *Saccharomyces cerevisiae*. *FEBS Letters*, 582(29):4032–4038.
- McGarvey, D. J. and Croteau, R. (1995). Terpenoid metabolism. *The Plant Cell*, 7(7):1015–1026.
- McPhee, D., Pin, A., Kizer, L., and Perelman, L. (2014). Deriving renewable-squalane from sugarcane. *Cosmetics & Toiletries Magazine*, 129(6):20–26.
- McQualter, R. B., Petrasovits, L. A., Gebbie, L. K., Schweitzer, D., Blackman, D. M., Chrysanthopoulos, P., Hodson, M. P., Plan, M. R., Riches, J. D., Snell, K. D., Brumbley, S. M., and Nielsen, L. K. (2015). The use of an acetoacetyl-CoA synthase in place of a  $\beta$ -ketothiolase enhances poly-3-hydroxybutyrate production in sugarcane mesophyll cells. *Plant Biotechnology Journal*, 13(5):700–707.
- Meadows, A. L., Hawkins, K. M., Tsegaye, Y., Antipov, E., Kim, Y., Raetz, L., Dahl, R. H., Tai, A., Mahatdejkul-Meadows, T., Xu, L., Zhao, L., Dasika, M. S., Murarka, A., Lenihan, J., Eng, D., Leng, J. S., Liu, C.-L., Wenger, J. W., Jiang, H., Chao, L., Westfall, P., Lai, J., Ganesan, S., Jackson, P., Mans, R., Platt, D., Reeves, C. D., Saija, P. R., Wichmann, G., Holmes, V. F., Benjamin, K., Hill, P. W., Gardner, T. S., and Tsong, A. E. (2016). Rewriting yeast central carbon metabolism for industrial isoprenoid production. *Nature*, 537(7622):694–697.
- Meigs, T. E., Roseman, D. S., and Simoni, R. D. (1996). Regulation of 3-hydroxy-3-methylglutaryl-coenzyme A reductase degradation by the nonsterol mevalonate metabolite farnesol *in vivo*. *Journal of Biological Chemistry*, 271(14):7916–7922.
- Menon, N., Pásztor, A., Menon, B. R. K., Kallio, P., Fisher, K., Akhtar, M. K., Leys, D., Jones, P. R., and Scrutton, N. S. (2015). A microbial platform for renewable propane synthesis based on a fermentative butanol pathway. *Biotechnology for Biofuels*, 8(1).
- Merlo, M., Jankevics, A., Takano, E., and Breitling, R. (2011). Exploring the metabolic state of microorganisms using metabolomics. *Bioanalysis*, 3(21):2443–2458.
- Meylemans, H.A., Q. R. H. B. (2012). Efficient conversion of pure and mixed terpene

- feedstocks to high density fuels. *Fuel*, 97:560–568.
- Miller, L. H. and Su, X. (2011). Artemisinin: Discovery from the Chinese herbal garden. *Cell*, 146(6):855–858.
- Miller, S. M. and Magasanik, B. (1990). Role of NAD-linked glutamate dehydrogenase in nitrogen metabolism in *Saccharomyces cerevisiae*. *Journal of Bacteriology*, 172(9):4927–4935.
- Millo, F., Bensaïd, S., Fino, D., Marcano, S. J. C., Vlachos, T., and Debnath, B. K. (2014). Influence on the performance and emissions of an automotive euro 5 diesel engine fueled with F30 from farnesane. *Fuel*, 138:134–142.
- Miziorko, H. M. (2011). Enzymes of the mevalonate pathway of isoprenoid biosynthesis. *Archives of Biochemistry and Biophysics*, 505(2):131–143.
- Moreira Dos Santos, M., Thygesen, G., Kötter, P., Olsson, L., and Nielsen, J. (2003). Aerobic physiology of redox-engineered *Saccharomyces cerevisiae* strains modified in the ammonium assimilation for increased NADPH availability. *FEMS Yeast Research*, 4(1):59–68.
- Nacken, V., Achstetter, T., and Degryse, E. (1996). Probing the limits of expression levels by varying promoter strength and plasmid copy number in *Saccharomyces cerevisiae*. *Gene*, 175(1-2):253–260.
- Nguyen, Q. T., Merlo, M. E., Medema, M. H., Jankevics, A., Breitling, R., and Takano, E. (2012). Metabolomics methods for the synthetic biology of secondary metabolism. *FEBS Letters*, 586(15):2177–2183.
- Nielsen, J. (2015). Yeast cell factories on the horizon: Metabolic engineering in yeast gets increasingly more versatile. *Science*, 349(6252):1050–1051.
- Nielsen, J. and Keasling, J. D. (2016). Engineering cellular metabolism. *Cell*, 164(6):1185–1197.
- Nikiforov, A., Jirovetz, L., and Buchbauer, G. (1986). ( $\pm$ )-patchouli-alcohol, the dominant odor component of the patchouli-oil (singapor.). *Monatshefte für Chemie/Chemical Monthly*, 117(8):1095–1098.
- Nilsson, B., Moks, T., Jansson, B., Abrahmsén, L., Elmblad, A., Holmgren, E., Henrichson, C., Jones, T. A., and Uhlén, M. (1987). A synthetic IgG-binding domain based on staphylococcal protein A. *Protein Engineering, Design and Selection*, 1(2):107–113.
- Nissen, T. L., Kielland-Brandt, M. C., Nielsen, J., and Villadsen, J. (2000). Optimization of ethanol production in *Saccharomyces cerevisiae* by metabolic engineering of the ammonium assimilation. *Metabolic Engineering*, 2(1):69–77.
- Nookae, I., Papini, M., Pornputtapong, N., Scalcinati, G., Fagerberg, L., Uhlén, M., and Nielsen, J. (2012). A comprehensive comparison of RNA-seq-based transcriptome analysis from reads to differential gene expression and cross-comparison with microarrays: a case study in *Saccharomyces cerevisiae*. *Nucleic Acids Research*, 40(20):10084–10097.
- Nygren, P. (2008). Alternative binding proteins: Affibody binding proteins developed from a small three-helix bundle scaffold. *FEBS Journal*, 275(11):2668–2676.
- Ohto, C., Muramatsu, M., Obata, S., Sakuradani, E., and Shimizu, S. (2009). Overexpression of the gene encoding HMG-CoA reductase in *Saccharomyces cerevisiae* for production of prenyl alcohols. *Applied Microbiology and Biotechnology*, 82(5):837–

- 845.
- Ohya, N. and Koyama, T. (2005). Biosynthesis of natural rubber and other natural polyisoprenoids. In *Biopolymers*. Wiley-VCH Verlag GmbH & Co. KGaA.
- Okamura, E., Tomita, T., Sawa, R., Nishiyama, M., and Kuzuyama, T. (2010). Unprecedented acetoacetyl-coenzyme A synthesizing enzyme of the thiolase superfamily involved in the mevalonate pathway. *Proceedings of the National Academy of Sciences of the United States of America*, 107(25):11265–11270.
- Ozcan, S. and Johnston, M. (1995). Three different regulatory mechanisms enable yeast hexose transporter (*HXT*) genes to be induced by different levels of glucose. *Molecular and Cellular Biology*, 15(3):1564–1572.
- Paddon, C. J., Westfall, P. J., Pitera, D. J., Benjamin, K., Fisher, K., McPhee, D., Leavell, M. D., Tai, A., Main, A., Eng, D., Polichuk, D. R., Teoh, K. H., Reed, D. W., Treynor, T., Lenihan, J., Jiang, H., Fleck, M., Bajad, S., Dang, G., Dengrove, D., Diola, D., Dorin, G., Ellens, K. W., Fickes, S., Galazzo, J., Gaucher, S. P., Geistlinger, T., Henry, R., Hepp, M., Horning, T., Iqbal, T., Kizer, L., Lieu, B., Melis, D., Moss, N., Regentin, R., Secrest, S., Tsuruta, H., Vazquez, R., Westblade, L. F., Xu, L., Yu, M., Zhang, Y., Zhao, L., Lievense, J., Covello, P. S., Keasling, J. D., Reiling, K. K., Renninger, N. S., and Newman, J. D. (2013). High-level semi-synthetic production of the potent antimalarial artemisinin. *Nature*, 496(7446):528–532.
- Papini, M., Nookae, I., Uhlén, M., and Nielsen, J. (2012). *Scheffersomyces stipitis*: a comparative systems biology study with the crabtree positive yeast *Saccharomyces cerevisiae*. *Microbial Cell Factories*, 11(1):1–16.
- Paradise, E. M., Kirby, J., Chan, R., and Keasling, J. D. (2008). Redirection of flux through the FPP branch-point in *Saccharomyces cerevisiae* by down-regulating squalene synthase. *Biotechnology and Bioengineering*, 100(2):371–378.
- Pare, P. W. and Tumlinson, J. H. (1999). Plant volatiles as a defense against insect herbivores. *Plant Physiology*, 121(2):325–332.
- Partow, S., Siewers, V., Bjørn, S., Nielsen, J., and Maury, J. (2010). Characterization of different promoters for designing a new expression vector in *Saccharomyces cerevisiae*. *Yeast*, 27(11):955–964.
- Partow, S., Siewers, V., Daviet, L., Schalk, M., and Nielsen, J. (2012). Reconstruction and evaluation of the synthetic bacterial MEP pathway in *Saccharomyces cerevisiae*. *PLoS ONE*, 7(12):1–12.
- Patil, K. R. and Nielsen, J. (2005). Uncovering transcriptional regulation of metabolism by using metabolic network topology. *Proceedings of the National Academy of Sciences of the United States of America*, 102(8):2685–2689.
- Peplow, M. (2013). Malaria drug made in yeast causes market ferment. *Nature*, 494:160–161.
- Peralta-Yahya, P. P., Ouellet, M., Chan, R., Mukhopadhyay, A., Keasling, J. D., and Lee, T. S. (2011). Identification and microbial production of a terpene-based advanced biofuel. *Nature Communications*, 2:483.
- Pfleger, B. F., Pitera, D. J., Smolke, C. D., and Keasling, J. D. (2006). Combinatorial engineering of intergenic regions in operons tunes expression of multiple genes. *Nature Biotechnology*, 24(8):1027–1032.
- Picaud, S., Brodelius, M., and Brodelius, P. E. (2005). Expression, purification and

- characterization of recombinant (*E*)- $\beta$ -farnesene synthase from *Artemisia annua*. *Phytochemistry*, 66(9):961–967.
- Pitera, D. J., Paddon, C. J., Newman, J. D., and Keasling, J. D. (2007). Balancing a heterologous mevalonate pathway for improved isoprenoid production in *Escherichia coli*. *Metabolic Engineering*, 9(2):193–207.
- Pizer, E. S., Thupari, J., Han, W. F., Pinn, M. L., Chrest, F. J., Frehywot, G. L., Townsend, C. A., and Kuhajda, F. P. (2000). Malonyl-coenzyme-A is a potential mediator of cytotoxicity induced by fatty-acid synthase inhibition in human breast cancer cells and xenografts. *Cancer Research*, 60(2):213–218.
- Polakowski, T., Stahl, U., and Lang, C. (1998). Overexpression of a cytosolic hydroxymethylglutaryl-CoA reductase leads to squalene accumulation in yeast. *Applied Microbiology and Biotechnology*, 49(1):66–71.
- Prsic, S., Xu, M., Wilderman, P. R., and Peters, R. J. (2004). Rice contains two disparate ent-copalyl diphosphate synthases with distinct metabolic functions. *Plant Physiology*, 136(4):4228–4236.
- Reifenberger, E., Freidel, K., and Ciriacy, M. (1995). Identification of novel *HXT* genes in *Saccharomyces cerevisiae* reveals the impact of individual hexose transporters on glycolytic flux. *Molecular Microbiology*, 16(1):157–167.
- Renninger, N. and McPhee, D. (2010). Fuel compositions comprising farnesane and farnesane derivatives and method of making and using same. US Patent 7,846,222.
- Ro, D. K., Paradise, E. M., Quellet, M., Fisher, K. J., Newman, K. L., Ndungu, J. M., Ho, K. A., Eachus, R. A., Ham, T. S., Kirby, J., Chang, M. C. Y., Withers, S. T., Shiba, Y., Sarpong, R., and Keasling, J. D. (2006). Production of the antimalarial drug precursor artemisinic acid in engineered yeast. *Nature*, 440(7086):940–943.
- Robinson, C. R. and Sauer, R. T. (1998). Optimizing the stability of single-chain proteins by linker length and composition mutagenesis. *Proceedings of the National Academy of Sciences*, 95(11):5929–5934.
- Rodriguez, S., Denby, C. M., Vu, T., Baidoo, E. E. K., Wang, G., and Keasling, J. D. (2016). ATP citrate lyase mediated cytosolic acetyl-CoA biosynthesis increases mevalonate production in *Saccharomyces cerevisiae*. *Microbial Cell Factories*, 15(1):48.
- Rodriguez, S., Kirby, J., Denby, C. M., and Keasling, J. D. (2014). Production and quantification of sesquiterpenes in *Saccharomyces cerevisiae*, including extraction, detection and quantification of terpene products and key related metabolites. *Nature Protocols*, 9(8):1980–1996.
- Rohmer, M., Knani, M., Simonin, P., Sutter, B., and Sahm, H. (1993). Isoprenoid biosynthesis in bacteria: a novel pathway for the early steps leading to isopentenyl diphosphate. *Biochemical Journal*, 295(Pt 2):517–524.
- Rupasinghe, H. P. V., Paliyath, G., and Murr, D. P. (2000). Sesquiterpene  $\alpha$ -farnesene synthase: Partial purification, characterization, and activity in relation to superficial scald development in apples. *Journal of the American Society for Horticultural Science*, 125(1):111–119.
- Ruzicka, L. (1953). The isoprene rule and the biogenesis of terpenic compounds. *Experientia*, 9(10):357–367.
- Ryder, J. (2009). Jet fuel compositions. US Patent 7,589,243.

- Sachdeva, G., Garg, A., Godding, D., Way, J. C., and Silver, P. A. (2014). *In vivo* co-localization of enzymes on RNA scaffolds increases metabolic production in a geometrically dependent manner. *Nucleic Acids Research*, 42(14):9493–9503.
- Samuelsson, E., Moks, T., Uhlen, M., and Nilsson, B. (1994). Enhanced *in vitro* refolding of insulin-like growth factor I using a solubilizing fusion partner. *Biochemistry*, 33(14):4207–4211.
- Sandoval, C. M., Ayson, M., Moss, N., Lieu, B., Jackson, P., Gaucher, S. P., Horning, T., Dahl, R. H., Denery, J. R., Abbott, D. A., and Meadows, A. L. (2014). Use of pantothenate as a metabolic switch increases the genetic stability of farnesene producing *Saccharomyces cerevisiae*. *Metabolic Engineering*, 25:215–226.
- Sarria, S., Wong, B., Martín, H. G., Keasling, J. D., and Peralta-Yahya, P. (2014). Microbial synthesis of pinene. *ACS Synthetic Biology*, 3(7):466–475.
- Sato, T. (2013). Unique biosynthesis of sesquiterpenes ( $C_{35}$  terpenes). *Bioscience, Biotechnology, and Biochemistry*, 77(6):1155–1159.
- Scalcinati, G. (2012). Metabolic engineering of *Saccharomyces cerevisiae* for sesquiterpene production. *PhD Thesis*, Chalmers University of Technology.
- Scalcinati, G., Knuf, C., Partow, S., Chen, Y., Maury, J., Schalk, M., Daviet, L., Nielsen, J., and Siewers, V. (2012a). Dynamic control of gene expression in *Saccharomyces cerevisiae* engineered for the production of plant sesquiterpene  $\alpha$ -santalene in a fed-batch mode. *Metabolic Engineering*, 14(2):91–103.
- Scalcinati, G., Partow, S., Siewers, V., Schalk, M., Daviet, L., and Nielsen, J. (2012b). Combined metabolic engineering of precursor and co-factor supply to increase  $\alpha$ -santalene production by *Saccharomyces cerevisiae*. *Microbial Cell Factories*, 11(1):117.
- Schadeweg, V. and Boles, E. (2016). n-butanol production in *Saccharomyces cerevisiae* is limited by the availability of coenzyme A and cytosolic acetyl-CoA. *Biotechnology for Biofuels*, 9(1):44.
- Schaefer, B. (2014). Flavours and fragrances. In *Natural Products in the Chemical Industry*, pages 45–168. Springer Berlin Heidelberg.
- Schmid, C., Steinbrecher, R., and Ziegler, H. (1992). Partition coefficients of plant cuticles for monoterpenes. *Trees*, 6(1):32–36.
- Schnee, C., Köllner, T. G., Gershenzon, J., and Degenhardt, J. (2002). The maize gene terpene synthase 1 encodes a sesquiterpene synthase catalyzing the formation of (*E*)- $\beta$ -farnesene, (*E*)-nerolidol, and (*E,E*)-farnesol after herbivore damage. *Plant Physiology*, 130(4):2049–2060.
- Schnee, C., Köllner, T. G., Held, M., Turlings, T. C. J., Gershenzon, J., and Degenhardt, J. (2006). The products of a single maize sesquiterpene synthase form a volatile defense signal that attracts natural enemies of maize herbivores. *Proceedings of the National Academy of Sciences of the United States of America*, 103(4):1129–1134.
- Schuhfried, E., Aprea, E., Mäk, T. D., and Biasioli, F. (2015). Refined measurements of Henry's law constant of terpenes with inert gas stripping coupled with PTR-MS. *Water, Air, & Soil Pollution*, 226(4):1–13.
- Seker, T., Møller, K., and Nielsen, J. (2005). Analysis of acyl CoA ester intermediates of the mevalonate pathway in *Saccharomyces cerevisiae*. *Applied Microbiology and Biotechnology*, 67(1):119–124.

- Seto, H., Watanabe, H., and Furihata, K. (1996). Simultaneous operation of the mevalonate and non-mevalonate pathways in the biosynthesis of isopentenyl diphosphate in *Streptomyces aerius*. *Tetrahedron Letters*, 37(44):7979–7982.
- Shi, S., Chen, Y., Siewers, V., and Nielsen, J. (2014). Improving production of malonyl coenzyme A-derived metabolites by abolishing Snf1-dependent regulation of Acc1. *mBio*, 5(3).
- Siperstein, M. D. and Fagan, V. M. (1966). Feedback control of mevalonate synthesis by dietary cholesterol. *Journal of Biological Chemistry*, 241(3):602–609.
- Sonnleitner, B. and Kaeppler, O. (1986). Growth of *Saccharomyces cerevisiae* is controlled by its limited respiratory capacity: Formulation and verification of a hypothesis. *Biotechnology and Bioengineering*, 28(6):927–937.
- Srivastava, P. L., Daramwar, P. P., Krithika, R., Pandreka, A., Shankar, S. S., and Thulasiram, H. V. (2015). Functional characterization of novel sesquiterpene synthases from Indian sandalwood, *Santalum album*. *Scientific Reports*, 5:10095.
- Starks, C. M., Back, K., Chappell, J., and Noel, J. P. (1997). Structural basis for cyclic terpene biosynthesis by tobacco 5-epi-aristolochene synthase. *Science*, 277(5333):1815.
- Sun, Z., Meng, H., Li, J., Wang, J., Li, Q., Wang, Y., and Zhang, Y. (2014). Identification of novel knockout targets for improving terpenoids biosynthesis in *Saccharomyces cerevisiae*. *PLoS ONE*, 9(11):1–6.
- Takabayashi, J., Dicke, M., and Posthumus, M. A. (1994). Volatile herbivore-induced terpenoids in plant-mite interactions: Variation caused by biotic and abiotic factors. *Journal of Chemical Ecology*, 20(6):1329–1354.
- Takagi, M., Kuzuyama, T., Takahashi, S., and Seto, H. (2000). A gene cluster for the mevalonate pathway from *Streptomyces* sp. strain CL190. *Journal of Bacteriology*, 182(15):4153–4157.
- Takahashi, S., Yeo, Y., Greenhagen, B. T., McMullin, T., Song, L., Maurina-Bunker, J., Rosson, R., Noel, J. P., and Chappell, J. (2007). Metabolic engineering of sesquiterpene metabolism in yeast. *Biotechnology and Bioengineering*, 97(1):170–181.
- Tashiro, M., Kiyota, H., Kawai-Noma, S., Saito, K., Ikeuchi, M., Iijima, Y., and Umeno, D. (2016). Bacterial production of pinene by a laboratory-evolved pinene-synthase. *ACS Synthetic Biology*, 5(9):1011–1020.
- Tholl, D. (2015). Biosynthesis and biological functions of terpenoids in plants. In *Biotechnology of Isoprenoids*, pages 63–106. Springer International Publishing.
- Thorsness, M., Schafer, W., D'Ari, L., and Rine, J. (1989). Positive and negative transcriptional control by heme of genes encoding 3-hydroxy-3-methylglutaryl coenzyme A reductase in *Saccharomyces cerevisiae*. *Molecular and Cellular Biology*, 9(12):5702–5712.
- Tracy, N. I., Chen, D., Crunkleton, D. W., and Price, G. L. (2009). Hydrogenated monoterpenes as diesel fuel additives. *Fuel*, 88(11):2238 – 2240.
- Tu, Y. (2011). The discovery of artemisinin (qinghaosu) and gifts from Chinese medicine. *Nature Medicine*, 17(10):1217–1220.
- van der Rest, M. E., Kamminga, A. H., Nakano, A., Anraku, Y., Poolman, B., and Konings, W. N. (1995). The plasma membrane of *Saccharomyces cerevisiae*: Structure, function, and biogenesis. *Microbiological Reviews*, 59(2):304–322.

- van Leeuwen, H. C., Strating, M. J., Rensen, M., de Laat, W., and van der Vliet, P. C. (1997). Linker length and composition influence the flexibility of Oct-1 DNA binding. *The EMBO Journal*, 16(8):2043–2053.
- van Rossum, H. M., Kozak, B. U., Pronk, J. T., and van Maris, A. J. A. (2016). Engineering cytosolic acetyl-coenzyme A supply in *Saccharomyces cerevisiae*: Pathway stoichiometry, free-energy conservation and redox-cofactor balancing. *Metabolic Engineering*, 36:99–115.
- Verduyn, C., Zomerdijk, T. P. L., van Dijken, J. P., and Scheffers, W. A. (1984). Continuous measurement of ethanol production by aerobic yeast suspensions with an enzyme electrode. *Applied Microbiology and Biotechnology*, 19(3):181–185.
- Vik, Å. and Rine, J. (2001). Upc2p and Ecm22p, dual regulators of sterol biosynthesis in *Saccharomyces cerevisiae*. *Molecular and Cellular Biology*, 21(19):6395–6405.
- Villadsen, J., Nielsen, J., and Lidén, G. (2011). Elemental and redox balances. In *Bioreaction Engineering Principles*, pages 63–118. Springer US.
- Villadsen, J. and Patil, K. R. (2007). Optimal fed-batch cultivation when mass transfer becomes limiting. *Biotechnology and Bioengineering*, 98(3):706–710.
- Wallaart, T. E., Pras, N., Beekman and, A. C., and Quax, W. J. (2000). Seasonal variation of artemisinin and its biosynthetic precursors in plants of *Artemisia annua* of different geographical origin: Proof for the existence of chemotypes. *Planta Med*, 66(01):57–62.
- Wang, C., Yoon, S. H., Jang, H. J., Chung, Y. R., Kim, J. Y., Choi, E. S., and Kim, S. W. (2011). Metabolic engineering of *Escherichia coli* for α-farnesene production. *Metabolic Engineering*, 13(6):648–655.
- Wang, C., Yoon, S. H., Shah, A. A., Chung, Y. R., Kim, J. Y., Choi, E. S., Keasling, J. D., and Kim, S. W. (2010). Farnesol production from *Escherichia coli* by harnessing the exogenous mevalonate pathway. *Biotechnology and Bioengineering*, 107(3):421–9.
- Wang, M. and Casey, P. J. (2016). Protein prenylation: unique fats make their mark on biology. *Nature Reviews Molecular Cell Biology*, 17(2):110–122.
- Weber, A. L. (1991). Origin of fatty acid synthesis: Thermodynamics and kinetics of reaction pathways. *Journal of Molecular Evolution*, 32(2):93–100.
- Westfall, P. J., Pitera, D. J., Lenihan, J. R., Eng, D., Woolard, F. X., Regentin, R., Horning, T., Tsuruta, H., Melis, D. J., Owens, A., Fickes, S., Diola, D., Benjamin, K. R., Keasling, J. D., Leavell, M. D., McPhee, D. J., Renninger, N. S., Newman, J. D., and Paddon, C. J. (2012). Production of amorphadiene in yeast, and its conversion to dihydroartemisinic acid, precursor to the antimalarial agent artemisinin. *Proceedings of the National Academy of Sciences of the United States of America*, 109(3):E111–E118.
- Woehrer, W. and Roehr, M. (1981). Regulatory aspects of bakers' yeast metabolism in aerobic fed-batch cultures. *Biotechnology and Bioengineering*, 23(3):567–581.
- Xie, X., Kirby, J., and Keasling, J. D. (2012). Functional characterization of four sesquiterpene synthases from *Ricinus communis* (castor bean). *Phytochemistry*, 78:20–28.
- Xiong, Z. Q., Guo, M. J., Guo, Y. X., Chu, J., Zhuang, Y. P., Wang, N. S., and Zhang, S. L. (2010). RQ feedback control for simultaneous improvement of GSH yield and gsh content in *Saccharomyces cerevisiae* T65. *Enzyme and Microbial Technology*,

- 46(7):598–602.
- Yamada, Y., Kuzuyama, T., Komatsu, M., Shin-ya, K., Omura, S., Cane, D. E., and Ikeda, H. (2015). Terpene synthases are widely distributed in bacteria. *Proceedings of the National Academy of Sciences*, 112(3):857–862.
- Yu, X. D., Pickett, J., Ma, Y. Z., Bruce, T., Napier, J., Jones, H. D., and Xia, L. Q. (2012). Metabolic engineering of plant-derived (*E*)- $\beta$ -farnesene synthase genes for a novel type of aphid-resistant genetically modified crop plants. *Journal of Integrative Plant Biology*, 54(5):282–299.
- Yuan, J. and Ching, C. B. (2015). Dynamic control of *ERG9* expression for improved amorpho-4,11-diene production in *Saccharomyces cerevisiae*. *Microbial Cell Factories*, 14(1).
- Zhao, L., Xu, L., Westfall, P., and Main, A. (2012). Methods of developing terpene synthase variants. US Patent Application 13/363,588.
- Zhou, K., Qiao, K., Edgar, S., and Stephanopoulos, G. (2015). Distributing a metabolic pathway among a microbial consortium enhances production of natural products. *Nature Biotechnology*, 33(4):377–383.
- Zhou, K., Zou, R., Stephanopoulos, G., and Too, H. P. (2012). Metabolite profiling identified methylerythritol cyclodiphosphate efflux as a limiting step in microbial isoprenoid production. *PLoS ONE*, 7(11).



# **From fragrances and pharmaceuticals to advanced biofuels: Production of isoprenoids in *Saccharomyces cerevisiae***

Stefan Tippmann, Yun Chen, Verena Siewers and Jens Nielsen

*Biotechnology Journal* 8(12):1435-1444, 2013



## Mini-Review

# From flavors and pharmaceuticals to advanced biofuels: Production of isoprenoids in *Saccharomyces cerevisiae*

Stefan Tippmann<sup>1</sup>, Yun Chen<sup>1</sup>, Verena Siewers<sup>1,2</sup> and Jens Nielsen<sup>1,2</sup>

<sup>1</sup> Systems & Synthetic Biology, Department of Chemical and Biological Engineering, Chalmers University of Technology, Gothenburg, Sweden

<sup>2</sup> Novo Nordisk Foundation Center for Biosustainability, Technical University of Denmark, Hørsholm, Denmark

Isoprenoids denote the largest group of chemicals in the plant kingdom and are employed for a wide range of applications in the food and pharmaceutical industry. In recent years, isoprenoids have additionally been recognized as suitable replacements for petroleum-derived fuels and could thus promote the transition towards a more sustainable society. To realize the biofuel potential of isoprenoids, a very efficient production system is required. While complex chemical structures as well as the low abundance in nature demonstrate the shortcomings of chemical synthesis and plant extraction, isoprenoids can be produced by genetically engineered microorganisms from renewable carbon sources. In this article, we summarize the development of isoprenoid applications from flavors and pharmaceuticals to advanced biofuels and review the strategies to design microbial cell factories, focusing on *Saccharomyces cerevisiae* for the production of these compounds. While the high complexity of biosynthetic pathways and the toxicity of certain isoprenoids still denote challenges that need to be addressed, metabolic engineering has enabled large-scale production of several terpenoids and thus, the utilization of these compounds is likely to expand in the future.

Received 22 APR 2013  
Revised 14 AUG 2013  
Accepted 11 SEP 2013

**Keywords:** Biofuels · Isoprenoids · Metabolic engineering · Microbial cell factories · *Saccharomyces cerevisiae*

## 1 Introduction

Isoprenoids are known as secondary metabolites, which provide plant oils and resins with characteristic smells. In addition, they comprise crucial photosynthetic pigments such as carotenoids, are assumed to be involved in fruit ripening processes and serve plants as defense against herbivores [1–3]. Isoprenoids also include metabolites important for cellular function such as dolichols, ubiqui-

nones, growth regulators, and sterols [4]. For instance, the triterpene squalene is converted in a sequence of consecutive reactions into ergosterol, which is vital for membrane integrity in fungi.

Isoprenoids have received great attention in research owing to several reasons. First and foremost, isoprenoids have a considerable societal relevance due to a broad spectrum of applications ranging from food products, pharmaceuticals, and cosmetics to fuels. Second, with more than 40 000 compounds [5], isoprenoids are not only the largest, but also one of the structurally and functionally most diverse group of chemicals in the plant kingdom.

This review attempts to forge a bridge over the diverse applications of isoprenoids with a main focus on those considered to be advanced biofuel precursors. For this purpose, some of the most eminent examples from each field will be presented as well as the strategies for commercial production of isoprenoids in the microbial host *Saccharomyces cerevisiae*. Therefore, isoprenoids' underlying biosynthetic pathway will be elucidated to illustrate

**Correspondence:** Prof. Jens Nielsen, Systems & Synthetic Biology, Department of Chemical and Biological Engineering, Chalmers University of Technology, Kemivägen 10, SE-412 96 Gothenburg, Sweden  
**E-mail:** nielsenj@chalmers.se

**Abbreviations:** **CVS**, citrus valencene synthase; **DMAPP**, dimethylallyl pyrophosphate; **FPP**, farnesyl pyrophosphate; **GGPP**, geranylgeranyl pyrophosphate; **GPP**, geranyl pyrophosphate; **HMG-CoA**, hydroxymethylglutaryl-CoA; **IPP**, isopentenyl pyrophosphate; **MEP**, 2-C-methyl-D-erythritol-4-phosphate; **MVA**, mevalonate

the complexity and challenges of developing microbial cell factories.

## 2 Production of isoprenoids

The production of isoprenoids can be realized by several different means. Considering their natural occurrence in plants, the most obvious method is isolation. Hereby, parts of the plant such as the peel or tree bark are collected and the target isoprenoid is extracted by mincing and subsequent hydro- or steam distillation. However, even though isoprenoids are ubiquitous in nature, many of them are present in low quantities in the plant source. The leaves of *Artemisia annua* were reported to contain the largest amounts of the antimalarial drug artemisinin with 0.44% per dry weight [6]. Considering over 200 million infections of malaria in 2010 [7], plant extraction is not sustainable as it cannot be employed for large-scale production. Furthermore, slow plant growth and yield dependency on seasonal changes as well as geographical conditions highlight further shortcomings of the extraction from plant material.

Likewise plant extraction, chemical synthesis is characterized by a number of drawbacks. First and foremost, the stereochemistry of pharmaceuticals and flavors, which is essential for their functionality, often complicates enantioselective synthesis and reduces the overall yield. As an example, for the efficient synthesis of the complex diterpenoid taxol, which possesses 11 stereogenic centers, 37 steps are required, while yields of 0.4% are attained [8]. Furthermore, hazardous solvents, which are often required for chemical synthesis, as for the allylic oxidation of (+)-valencene for the production of nootkatone, pose health risks, and raise environmental concerns [9].

Besides plant extraction and chemical synthesis, biotechnology offers alternative production strategies for

isoprenoids. Most promising is the application of engineered microbes, which has several advantages over the previous strategies. Microorganisms feature fast growth, can be cultivated easily and production by microorganisms is easy to scale. Most importantly, microbes are able to couple a sequence of enzymatic reactions to specifically produce a desired chemical from inexpensive and renewable carbon sources such as glucose [10]. In addition, biological systems can be altered, redesigned, and even completely new pathways can be established using synthetic biology tools, which allows for the production of a wide range of chemicals [11].

The development of microbial cell factories is a complex task, which not only requires extensive knowledge about cellular metabolism and recombinant DNA technologies, but also the integration of other engineering disciplines. However, first and foremost, an appropriate host organism has to be selected with regard to the desired chemical. For production of functional isoprenoids, mainly *S. cerevisiae* and *Escherichia coli* are employed, since they are amenable to genetic manipulations with extensive molecular resources. The comparison of isoprenoid production presented in Table 1 shows that the titers achieved by metabolic engineering of *E. coli* are in most cases superior. Besides, slower growth of *S. cerevisiae* and its lacking ability to utilize alternative carbon sources such as xylose, which is abundant in plant biomass, denote economical disadvantages, and obstacles regarding its use in prospective industrial applications [12]. On the other hand, it allows for a facilitated expression of functional cytochrome P450 enzymes, which are essential for the modification of many isoprenoids and thereby responsible for their structural diversity. In addition, *S. cerevisiae* is more robust in large-scale fermentations compared to *E. coli*. It is relatively tolerant to low pH and high concentrations of sugars, as well as fairly resistant to inhibitors [13, 14]. Furthermore, a number of advanced molecular biology tools have been developed for precision

**Table 1.** Examples of isoprenoids produced in *S. cerevisiae* and *E. coli*

Isoprenoid	<i>S. cerevisiae</i>		<i>E. coli</i>	
	Titer	References	Titer	References
<b>Monoterpenes</b>				
Limonene	–	–	~60 mg/L	[68]
<b>Sesquiterpenes</b>				
Farnesol	4.63 g/L	[83]	135.5 mg/L	[76]
α-Farnesene	9.8 mg/L	[57]	400 mg/L	[57]
β-Farnesene	762 mg/L	[57]	1100 mg/L	[57]
Bisabolene	>900 mg/L	[77]	>900 mg/L	[77]
Amorphadiene	40 g/L	[47]	25 g/L	[48]
Artemisinic Acid	25 g/L	[46]	–	–
Valencene	1.5 mg/L	[35]	–	–
<b>Diterpenes</b>				
Taxadiene	8.7 mg/L	[51]	1 g/L	[52]

engineering of yeast [15, 16] as well as much information about regulation of its metabolism is available [17–19]. It is therefore the preferred cell factory for industrial production and in this review, we therefore focus on the production of isoprenoids in *S. cerevisiae*.

### 3 Biosynthesis of isoprenoids

Isoprenoids are all assembled from activated forms of isoprene, namely isopentenyl pyrophosphate (IPP) and its isomer dimethylallyl pyrophosphate (DMAPP). These two precursors are made via two different pathways: the mevalonate (MVA) and the 2-C-methyl-D-erythritol-4-phosphate (MEP) pathway. The MVA pathway was first

discovered in the 1960s [20, 21] and was assumed to be the only pathway leading to IPP in all living organisms for almost 40 years. However, in the 1990s, the MEP pathway was found in bacteria, green algae, and higher plants as an alternative pathway [22]. With some exceptions, the MVA pathway is utilized by most eukaryotes as well as archaea, whereas the MEP pathway is typically found in prokaryotes and the plastids of photosynthetic organisms [23].

DMAPP is a reactive primer which undergoes elongation by head-to-tail condensation with one or more IPP molecules, to form geranyl pyrophosphate (GPP), farnesyl pyrophosphate (FPP), or geranylgeranyl pyrophosphate (GGPP) (Fig. 1). By terpene synthases, the precursors GPP, FPP, and GGPP can be cyclized and/or rearranged to form

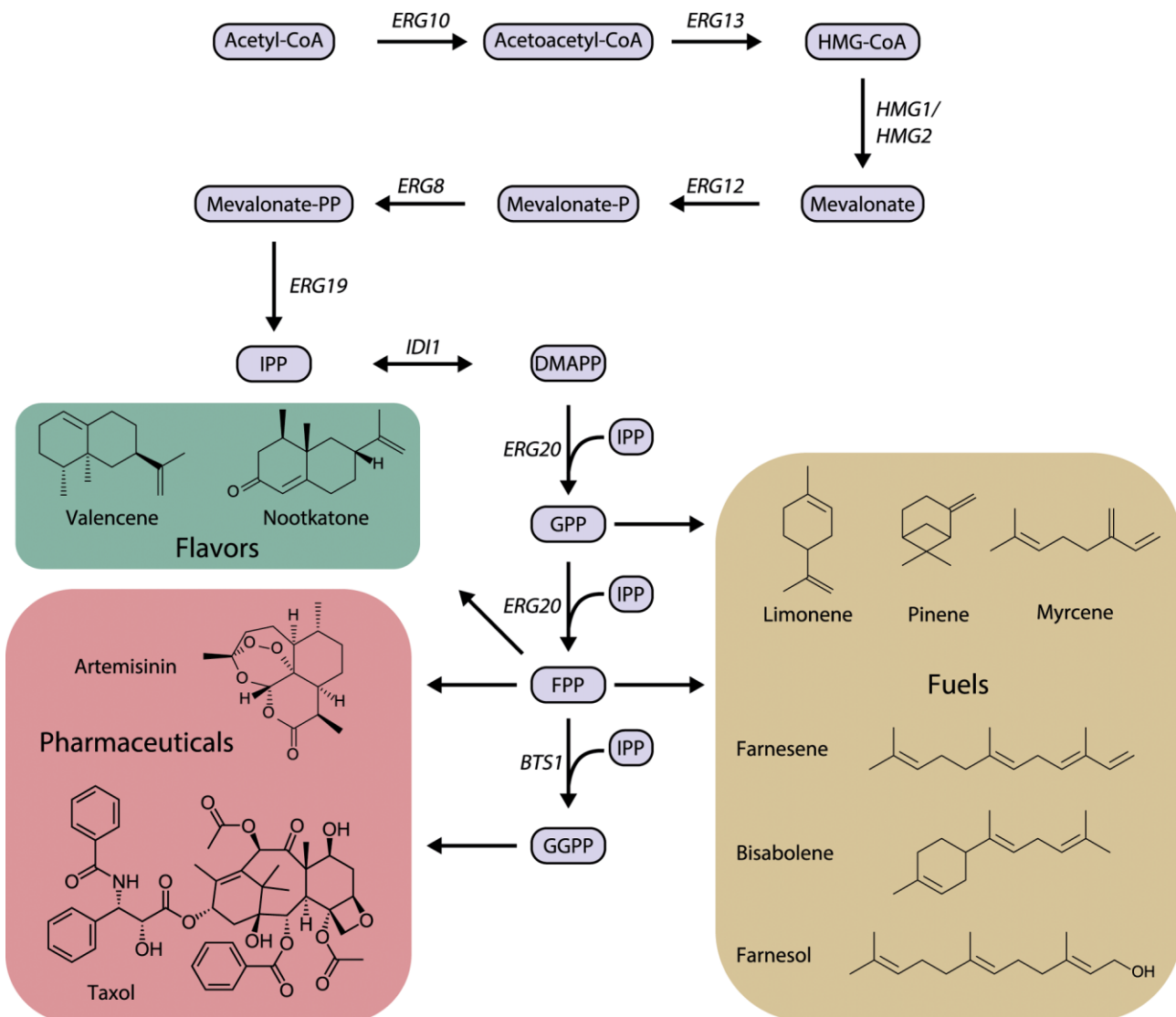


**Figure 1.** Production of isoprenoids in *Saccharomyces cerevisiae*: Overview of the mevalonate pathway and products that can be derived from it. Gene names are in italics. *ERG10*, acetoacetyl-CoA thiolase; *ERG13*, HMG-CoA synthase; *HMG1/HMG2*, HMG-CoA reductases; *ERG12*, mevalonate kinase; *ERG8*, phosphomevalonate kinase; *ERG19*, mevalonate pyrophosphate decarboxylase; *IDI1*, IPP:DMAPP isomerase; *ERG20*, FPP synthase; *BTS1*, GGPP synthase.

monoterpenes, sesquiterpenes, and diterpenes, respectively. Once the basic skeletons are formed, they are often further modified by terpene modifying enzymes, particularly cytochrome P450 monooxygenases, to generate functional products constituting the enormous diversity of isoprenoid families.

### 3.1 The MVA pathway

The yeast *S. cerevisiae* uses the MVA pathway to generate the precursors IPP and DMAPP from acetyl-CoA through seven enzymatic reactions (Fig. 1). This involves the conversion of three molecules of acetyl-CoA to MVA via acetoacetyl-CoA and hydroxymethylglutaryl-CoA (HMG-CoA). MVA subsequently undergoes phosphorylation and decarboxylation to form IPP. A stereospecific isomerization reaction converts IPP to its isomer DMAPP.

Several enzymes, especially HMG-CoA reductase, IPP isomerase, and FPP synthase, have been elucidated as key enzymes for engineering isoprenoid biosynthesis in *S. cerevisiae*. Two isozymes, Hmg1p and Hmg2p, both possess HMG-CoA reductase function, Hmg1p being responsible for about 83% of the enzyme activity in wild type yeasts, depending on the cultivation conditions [24]. On the post-translational level, Hmg2p was shown to undergo endoplasmic reticulum-associated degradation (ERAD) depending on ubiquitination [25], while Hmg1p was found to be relatively stable. *ERG20* encodes GPP synthase/FPP synthase, which combines IPP and DMAPP to GPP and catalyzes the subsequent addition of another IPP to yield FPP. A study in which Erg20p was overexpressed revealed an increased ergosterol production which indicates that FPP synthase may be a flux controlling enzyme [26].

Furthermore, FPP is situated at an important intersection building the connection to numerous compounds and primary metabolism. It is further condensed to squalene and subsequently undergoes nineteen conversion steps to form ergosterol, which is essential for cell growth and has a great impact on the regulation of membrane permeability and fluidity. FPP is also an important precursor for biosynthesis of many primary metabolites, such as dolichols, ubiquinone, carotenoids, and prenylated proteins [27].

### 3.2 The MEP pathway

The MEP pathway generates IPP and DMAPP in eight reactions based on pyruvate and glyceraldehyde 3-phosphate. In the first part, which requires the enzymes Dxs and Dxr, the two precursors are condensed to 1-deoxy-D-xylulose 5-phosphate, which is subsequently reduced to MEP. In a sequence of further reactions catalyzed by enzymes specified as IspD, IspE, and IspF, MEP is converted to 2-C-methyl-D-erythritol-2,4-cyclopyrophosphate. The following reduction to 1-hydroxy-2-methyl-2-(*E*)-

butenyl 4-pyrophosphate and final conversion to IPP/DMAPP are catalyzed by IspG and IspH.

A comparative study of the two distinct biosynthetic pathways has shown that the MEP pathway is stoichiometrically more efficient than the MVA pathway [28]. For this reason and in order to bypass endogenous regulation, recent efforts have addressed the heterologous expression of the MEP pathway in *S. cerevisiae* [29, 30]. However, the strains were unable to grow and could not compensate for the loss of the endogenous MVA pathway, which was inhibited using lovastatin or by deletion of *ERG13*. Labeling experiments revealed that the heterologous pathway was only active until 2-C-methyl-D-erythritol-2,4-cyclopyrophosphate, since *S. cerevisiae* failed to functionally express the iron sulfur cluster proteins that catalyze the last two reactions [29].

## 4 From flavors and pharmaceuticals to biofuels

### 4.1 Flavors

Two major families of isoprenoids, monoterpenoids (10 carbons) and sesquiterpenoids (15 carbons) are traditionally valued as fragrances and flavors, as they are the primary constituents of essential oils from flowers. They have been commercialized for ages but depend on plant extractions which are considered expensive and unreliable. Recently, two sesquiterpenoids, named nootkatone and valencene have been made available in commercial quantities by Allylix using a microbial fermentation process [31]. Nootkatone is a high-value flavorant used in perfumery and the flavor industry. It is a natural constituent of citrus oils, and stands out as a distinguished flavor and aroma of grapefruit. Valencene is also a characteristic fruit flavor and aroma component, which is currently used in beverage and chewing gum flavors, as well as in the production of nootkatone.

Valencene is commonly identified in nature but the corresponding synthase gene had not been cloned until Sharon-Asa et al. [32], Greenhagen [33], and Lücker et al. [34] isolated and characterized different *Citrus* valencene synthase (CVS) genes, the product of which catalyzes the cyclization of FPP to valencene. Since then, some efforts have specifically addressed valencene biosynthesis, but also other fragrances and flavors. All strategies described are clustered into four.

- (1) *Enhancing flux through the MVA pathway.* Co-expression of a heterologous *Arabidopsis* or human FPP synthase (AsFPPS or HsFPPS) with truncated Hmg1p lacking the N-terminal regulatory domain (tHmg1) improved valencene production four-fold [35]. In a recent study, a multi-step engineering approach was taken to increase the flux through the MVA pathway in order to enhance the production of the sesquiterpene santal-

ene [36]. This involved overexpression of *tHMG1* as well as *ERG20* (encoding FPP synthase) and *GDH2* (NADH dependent glutamate dehydrogenase). Additionally, a point-mutated version of the transcription factor Upc2p was introduced to upregulate the expression of MVA pathway genes.

- (2) *Limiting the use of the FPP pool.* Down-regulation of squalene synthase in yeast by replacing the native *ERG9* promoter with the tunable *MET3* promoter increased valencene production by 50% [37], and this strategy was further pursued for production of santalene [38]. In another study, by introducing a knockout mutation of the squalene synthase gene (*erg9Δ*) and simultaneously obtaining a mutant capable of efficient aerobic uptake of ergosterol from the culture media, accumulation of farnesol (the dephosphorylated form of FPP) was significantly increased, indicating an enhancement in the FPP pool [39]. Similarly, the use of a defective squalene synthase (dErg9) allowing more FPP to be available for isoprenoid production while still producing sufficient squalene to allow cell growth is beneficial, especially as this does not require the addition of nutrients such as ergosterol or methionine [40]. On the other hand, Farhi et al. [35] found that neither eliminating geranylgeranyl diphosphate synthase (Bts1p) nor two endogenous lipid phosphatases (diacylglycerol diphosphate phosphatase [Dpp1p] and lipid phosphate phosphatase [Lpp1p], both involved in dephosphorylation of FPP) could enhance valencene biosynthesis, which was similar to the finding that a single *DPP1* knock-out did not exhibit improved valencene production [39].
- (3) *Spatial subcellular arrangement of metabolic enzymes.* Mitochondrial targeting of a valencene synthase led to a three-fold rise in valencene titers compared to the ones generated by the corresponding cytosolic forms of the synthase. Combination of this approach with mitochondrial targeting of FPP synthase led to an additional 40% improvement [35].
- (4) *Synthase engineering.* Greenhagen elucidated the catalytic mechanism of terpene synthases leading to formation of valencene and other compounds [33, 41]. A transition between valencene and germacrene A production was found at approximately pH 8.2, which is close to the p*K<sub>a</sub>* value of cysteine (pH 8.4). This is consistent with the fact that germacrene A synthases only differ from CVS by the presence of C440 in the active site. Either the single mutant CVS-I516V or the double mutant CVS-C402S/V516I exhibited a significant increase in the proportion of germacrene A. Although there has been no report on improving the synthase activity so far, this structure-function analysis would facilitate engineering activities and specificities of terpene synthases.

## 4.2 Pharmaceuticals

The potential of isoprenoids in the treatment of diseases is widely acknowledged. Since ancient times plant oils and herbal medicines have been used as antifungal and antibacterial agents. Many of them contain monoterpenoids, which are known for their cytotoxicity [42]. In the following some of the large efforts that have been made to enable microbial production of artemisinin and taxol are presented, which were addressed among others in several reviews in the recent past [43, 44].

### 4.2.1 Artemisinin

The discovery of artemisinin denotes a landmark in the treatment of malaria and dates far back into Chinese history, as its ability to efficiently inhibit parasite growth was first identified during the Jin Dynasty [45]. Nowadays, this sesquiterpene lactone is still utilized as the first-line treatment against malaria in artemisinin-based combination therapies (ACTs). Following the biosynthetic pathway, FPP is converted to amorphadiene, which is subsequently oxidized via three reactions to artemisinic acid, the immediate precursor of artemisinin. As the final conversion is not yet fully understood, semi-synthetic production of artemisinin aims at providing its biochemical precursor artemisinic acid, which can subsequently be converted chemically to artemisinin via dihydroartemisinic acid at a yield between 40 and 45% [46]. Amorphadiene and artemisinic acid have both been successfully produced in *S. cerevisiae*. Overexpression of all MVA pathway genes to *ERG20* together with an amorphadiene synthase derived from *A. annua* led to final amorphadiene titers of 40 g/L in optimized fed-batch fermentations with pure ethanol feed [47]. In comparison, amorphadiene titers of 25 g/L were attained in a nitrogen and glucose limited fed-batch process with engineered *E. coli* [48]. Likewise, the authors reported successful conversion to artemisinic acid by overexpressing the involved cytochrome P450 oxidase (CYP71AV1) and its cognate reductase (CPR1), which was, however, manifold lower. The efficient conversion to artemisinic acid was recently achieved by introduction of the complete oxidation pathway from *A. annua* using the artemisinic alcohol and aldehyde dehydrogenase (ADH1/ALDH1) in combination with cytochrome b<sub>5</sub> (CYB5) together with CYP71AV1 and CPR1. Using this approach, final artemisinic acid titers of 25 g/L were attained in fed-batch fermentations demonstrating the crucial importance of the dehydrogenases [46].

### 4.2.2 Taxol

The complex diterpenoid Taxol is an effective antineoplastic drug in the treatment of different cancer types such as ovarian, breast, and colon cancer since it prevents microtubule depolymerization and thereby blocks the cell cycle [49].

**Table 2.** Comparison of conventional diesel and jet fuel with isoprenoid based biofuels<sup>a</sup>

Property	Unit	D2 diesel	Farnesane	Bisabolane (wt 50 %)	Limonane (wt 10 % in diesel)	Myrcane (wt 10 % in diesel)	Jet A	Limonene (dimers)
Density	g/mL	0.865	0.774	0.820	n.a.	n.a.	0.811	0.914
Cloud point	°C	-21	<-50	<-78	-11	-11	n.a.	n.a.
Flash point	°C	73	109	111	58.9	60	43	n.a.
Cetane number	-	41.6	58.6	41.9	42.8	44.7	n.a.	n.a.
Net heat of combustion	MJ/kg	42.4	44.2	n.a.	n.a.	n.a.	43.4	41.906
Viscosity	mm <sup>2</sup> /s (at °C)	2.440 (at 40°C)	2.325 (at 40°C)	2.91	2.311 (at 40°C)	3.899 (at 40°C)	4.1 (at 20°C)	n.a.
References	[57]	[57]	[77]	[63]	[63]	[59, 86]	[61]	

a) Farnesane, bisabolane, limonene, and myrcane refer to the hydrogenated forms of farnesene, bisabolene, limonene and myrcene, respectively. N.a., not available. Similar values were also presented in [64, 84, 85].

Taxol production is still strongly dependent on primary resources, but can be realized semi-synthetically from 10-deacetylbaicatin III and baicatin III, its biosynthetic precursors, which are extracted from the needles of various *Taxus* species. The biosynthetic production is equally complicated and not yet fully understood. In 19 enzymatic reactions, including 8 cytochrome P450-mediated oxygenations, taxol is derived from GGPP [50]. Approaches for microbial production of taxol have mostly focused on three aspects: the supply of GGPP for diterpene production, overexpression of taxadiene synthase for an increased conversion of GGPP to the committed intermediate taxa-4(5),11(12)-diene [51], and engineering of the cytochrome P450-mediated oxidation of taxadiene to taxa-4(20),11(12)-dien-5 $\alpha$ -ol [52]. Taxadiene titers of 8.7 mg/L were attained in *S. cerevisiae* by using a codon optimized taxadiene synthase from *Taxus chinensis*, *upc2-1*, a mutant allele of the transcriptional sterol regulator, and a GGPP synthase from *Sulfolobus acidocaldarius* in combination with a truncated HMG-CoA reductase (*tHmg1*) [51]. In comparison, taxadiene levels could already be raised up to 1 g/L in engineered *E. coli* [52], which is still over 100-fold higher. It is especially the high pathway complexity that demands for the integration of systems biology tools to promote microbial production of taxol and its precursors. Recently, a computational approach (a variation of the minimization of metabolic adjustment [MoMA] algorithm) was applied to enhance taxa-4(5),11(12)-diene production in *E. coli* [53]. As a result, four genetic engineering targets outside of the native isoprenoid precursor pathway were identified, which would improve cofactor availability and could thereby increase taxadiene accumulation.

### 4.3 Fuels

The ongoing search for alternative transportation fuels is complicated by demands for fuels that fit the current

infrastructure and that can be produced at low cost and at extremely high volumes. While the primary objective is to produce low cost and environmentally friendly fuels from renewable sources, they additionally have to fit narrow constraints in terms of density, chain length, combustion heat and efficiency, lubricity, and stability [54]. Within the past years, much research efforts have been dedicated to the use of terpenes for fuel applications [55, 56]. While monoterpenes have properties similar to conventional aviation fuels such as Jet A and Jet A-1, sesquiterpenes have potential applications as diesel. Table 2 lists properties of some terpene-derived fuels in comparison with conventional jet fuel and petroleum based diesel. The most promising examples include the monoterpane limonene, the sesquiterpenes farnesene and bisabolene and the sesquiterpene alcohol farnesol, which can either be used as fuel additives or directly as replacements for diesel and jet fuels in their hydrogenated form [57–59]. Other cyclized monoterpenes, which can be used as fuel precursors or additives are pinene, cymene, myrcene, camphene, and terpinene. Furthermore, valuable gasoline additives such as isopentanol and isoamylacetate can be produced from the isoprenoid pathway [56], and were shown to possess beneficial blend properties as they increase the octane number [60].

#### 4.3.1 Monoterpene fuels

Due to low densities, which limit the heating value, jet fuels produced from cellulosic butanol (Biojet) are considered to be deficient. On the other hand, limonene, pinene, and camphene are regarded as suitable raw material for high-density renewable fuels [61]. Pinene was reported to have a net heat of combustion comparable to JP-10 and dimerization of these isomers results in a higher density, which is beneficial for an additional increase of the combustion heat [62]. Since many liquid catalysts are hazardous, corrosive, and require large efforts for waste treatment and recycling, recent studies have focused on the

investigation of different catalysts to approach sustainable dimerization of pinenes and other monoterpenes [61, 62]. In addition, full hydrogenation of the reactive double bonds in the olefinic structures of limonene and myrcene was performed successfully using palladium and platinum catalysts, which increases their value as fuel [63].

The microbial production of monoterpenes is facing a fundamental challenge. Contrary to other isoprenoids, monoterpenes have been reported to be highly toxic, which makes them interesting antimicrobial agents. The mechanism of toxicity is not yet fully understood and it remains unclear if it is either derived directly from molecular interactions or from phase toxicity, which was recently discussed by Brennan et al. [64]. Based on their hydrophobicity, monoterpenes interact with cellular and mitochondrial membranes and dismantle membrane integrity. Microarray analysis of gene expression profiles of *S. cerevisiae* under  $\alpha$ -terpinene exposition revealed the up-regulation of genes associated with lipid and fatty acid metabolism, detoxification, and cell wall structure [65]. Based on these observations, the authors concluded that ergosterol synthesis is inhibited during the treatment with terpinene. Severe growth restrictions for *S. cerevisiae* were also observed under the impact of other monoterpenes.  $\beta$ -Pinene was shown to inhibit respiration and transport of H<sup>+</sup> and K<sup>+</sup>, which is essential for ATP generation [66]. Limonene was reported to inhibit growth completely at concentrations between 0.5 and 0.8 g/L [64, 67]. Under these circumstances, one possibility to realize microbial production of toxic biofuel precursors is to employ an extractive two-phase fermentation. By adding an immiscible organic layer onto the cultivation medium, the product can be harvested in situ and the harmful impact on the host organism can be reduced. Using dibutyl phthalate, the minimum inhibitory concentration (MIC) of limonene, an indicator of its toxicity, could be increased up to 42.1 g/L for *S. cerevisiae* [64]. However, the selection of an appropriate layer is elaborate, since organic solvents have to be adapted to product and host. On the other hand, efflux pumps are considered to be a promising opportunity to enhance biofuel tolerance. Recently, a computational approach was used to identify new efflux pumps, which improved resistance to toxic biofuels. For this purpose, a library of 43 efflux pumps from sequenced bacterial genomes was created and heterologously expressed in *E. coli*. As a result, strains expressing an efflux pump from *Alcanivorax borkumensis* revealed significantly increased limonene production [68]. Similarly, the pleiotropic drug resistance (PDR) network, a subgroup of ABC transporters, which serves the efflux of cytotoxic compounds and is therefore essential for detoxification, was expected to enhance limonene tolerance of *S. cerevisiae*. However, overexpression of several PDR transporters, which appeared to be upregulated under limonene stress, did not attain the desired effect [67].

#### 4.3.2 Sesquiterpene fuels

Since all sesquiterpenes originate from FPP, microbial production poses a challenge in terms of redirecting metabolic fluxes from this branch point. Regarding the production of the sesquiterpene alcohol farnesol in *S. cerevisiae*, deletion of squalene synthase and adjusting the pH to 7 elevated the final concentrations up to 102.8 mg/L, whereas ergosterol had to be added to the medium to maintain viability [69]. Besides, the abundance of the direct precursor FPP and the converting enzymes are considered to have the greatest impact on the production levels of this fuel compound. By overexpressing a modified Hmg1 reductase, a significant increase of farnesol production in *S. cerevisiae* was recorded at pH 7 with 145.7 mg/L [70]. Depyrophosphorylation of FPP can be realized by several enzymes. In *S. cerevisiae*, the native alkaline phosphatase Pho8p as well as the lipid phosphatases Dpp1p and Lpp1p were reported to hydrolyze FPP to farnesol in two reactions [71, 72]. On the other hand, pyrophosphatases are able to catalyze this reaction directly in one step and may denote a potential engineering target. However, no pyrophosphatase has been characterized with regard to farnesol formation until now [73]. Furthermore, the promiscuity of phosphatases in terms of their substrate specificity complicates the selection of an appropriate engineering target. Another possibility is the utilization of terpene synthases. Heterologous expression of the *OsTPS13* gene in *E. coli*, which encodes a farnesol synthase from *Oryza sativa*, showed that 84.2% of FPP could be converted to farnesol [74]. One last critical aspect for farnesol production in *S. cerevisiae* originates from its regulatory function. Farnesol causes degradation of HMG-CoA reductase and thereby inhibits its own production [75] – a fact that needs to be addressed in further engineering strategies.

In comparison, farnesol production in *E. coli* remains superior so far. Heterologous expression of the MVA pathway together with the overexpression of *ispA* led to final farnesol titers of 135.5 mg/L in only 48 h of cultivation time [76].

Further sesquiterpenes that can be used as fuel precursors comprise farnesene and bisabolene. The latter was recently identified as a biosynthetic precursor of D2 diesel, since its hydrogenated derivative bisabolane was presumed to be a potential fuel due to its chemical structure [77]. The authors, who used an existing microbial platform for amorphadiene production, were able to attain final titers above 900 mg/L of bisabolene in *E. coli* and *S. cerevisiae*, which imparted no toxic effects on the microbial hosts used in this study.

Farnesene was first identified in apple peel [78]. Besides its high energy density and low hygroscopicity, its hydrogenated form farnesane is characterized by a cetane number of 58, which is advantageous over conventional diesel [57, 79]. Stepwise optimization of  $\alpha$ -farnesene production has been performed successfully in *E. coli*. For this purpose, a codon optimized gene of the

plant synthase from *Malus domestica* was used and the rate limiting enzymes of the MEP pathway, Dxs and Idi, were overexpressed. In combination with the heterologously expressed MVA pathway and a fusion of the FPP synthase with the  $\alpha$ -farnesene synthase, this led to  $\alpha$ -farnesene accumulation up to 380 mg/L [79].

## 5 Future perspectives

The group of isoprenoids has been studied for many years and includes valuable products that are required in large quantities by the food and pharmaceutical industry. Additionally, several isoprenoids were assigned with fuel properties in the recent past, which has elevated the interest for these compounds. Even though chemical finishing is required, which increases the price of these fuels, they combine several advantageous properties and are beneficial over conventional biodiesel and jet fuel. Associated with the structural and functional diversity of this group of chemicals, the product range is likely to expand further in the future. However, the overall success will strongly depend on the production process, which is demanding in terms of productivity, cost efficiency and sustainability. While chemical synthesis and plant extraction suffer from numerous drawbacks, microbial cell factories have emerged as a platform technology for the supply of bulk and specialty chemicals. To this day, metabolic engineering has successfully enabled industrial production of for example valencene and farnesene in large-scale fermentation processes and there are bright prospects for further biobased isoprenoids. However, several challenges remain, one of them being engineering of the terpene synthases due to their often observed product promiscuity and low activities. While several studies succeeded in altering product specificity (e.g. [80, 81]) examples of increasing enzyme activity (e.g. [82]) remain scarce. As well-established cell factories, *S. cerevisiae* and *E. coli* have predominantly been employed. While the endogenous MEP pathway of *E. coli* is energetically more efficient than the MVA pathway, the expression of cytochrome P450 oxygenases is facilitated in yeast, which can be crucial for the production of active pharmaceutical ingredients such as taxol. Numerous strategies have been investigated ranging from overexpression of different plant synthases to heterologous expression of complete pathways. Yet the functional and regulatory complexity that is comprised by metabolic networks demands for the integration of other engineering disciplines in many cases. These may also be beneficial in establishing a functional MEP pathway in *S. cerevisiae*, an approach that is still to be demonstrated. It is especially the available tools from systems biology, which will progressively contribute to this field and have the potential to accelerate the design of future cell factories for isoprenoid production.



**Jens Nielsen** has an MSc degree in Chemical Engineering and a PhD degree (1989) in Biochemical Engineering from the Danish Technical University (DTU). He subsequently established his independent research group at DTU and was appointed full Professor in 1998. He was Fulbright visiting professor at MIT from 1995–1996. At DTU he founded and directed the Center for Microbial Biotechnology. In 2008 he was recruited as Professor and Director to Chalmers University of Technology, Sweden, where he is currently directing a research group of more than 50 people and the Life Science Area of Advance, which coordinates over 200 researchers from five departments. Jens Nielsen has published to date more than 380 research papers that have been cited more than 11 000 times (current H-index 53), co-authored more than 40 books and he is inventor of more than 50 patents.

We acknowledge financial support from the Swedish Research Council and the Novo Nordisk Foundation.

The authors declare no conflict of interest.

## 5 References

- [1] Lurie, S., Watkins, C. B., Superficial scald, its etiology and control. *Postharvest Biol. Technol.* 2012, **65**, 44–60.
- [2] Michereff, M. F. F., Laumann, R. A., Borges, M., Michereff-Filho, M. et al., Volatiles mediating a plant-herbivore-natural enemy interaction in resistant and susceptible soybean cultivars. *J. Chem. Ecol.* 2011, **37**, 273–285.
- [3] Pare, P. W., Tumlinson, J. H., Plant volatiles as a defense against insect herbivores. *Plant Physiol.* 1999, **121**, 325–331.
- [4] Chappell, J., The biochemistry and molecular biology of isoprenoid metabolism. *Plant Physiol.* 1995, **107**, 1–6.
- [5] Bohlmann, J., Keeling C. I., Terpenoid biomaterials. *Plant J.* 2008, **54**, 656–669.
- [6] Mannan, A., Ahmed, I., Arshad, W., Asim, M. F. et al., Survey of artemisinin production by diverse *Artemisia* species in northern Pakistan. *Malar. J.* 2010, doi: 10.1186/1475-2875-9-310.
- [7] WHO, World malaria report 2011. 2011.
- [8] Walji, A. M., MacMillan, D. W. C., Strategies to bypass the taxol problem. Enantioselective cascade catalysis, a new approach for the efficient construction of molecular complexity. *Synlett* 2007, **10**, 1477–1489.
- [9] Wilson, C. W., Shaw, P. E., Synthesis of nootkatone from valencene. *J. Agric. Food Chem.* 1978, **26**, 1430–1432.
- [10] Keasling, J. D., Synthetic biology for synthetic chemistry. *ACS Chem. Biol.* 2008, **3**, 64–76.
- [11] Collins, J., Synthetic Biology: Bits and pieces come to life. *Nature* 2012, **483**, S8–S10.
- [12] Kim, S. R., Park, Y. C., Jin, Y. S., Seo, J. H., Strain engineering of *Saccharomyces cerevisiae* for enhanced xylose metabolism. *Biotechnol. Adv.* 2013, **31**, 851–861.

- [13] Hong, K. K., Nielsen, J., Metabolic engineering of *Saccharomyces cerevisiae*: A key cell factory platform for future biorefineries. *Cell. Mol. Life Sci.* 2012, 69, 2671–2690.
- [14] Kim, I. K., Roldão, A., Siewers, V., Nielsen, J., A systems-level approach for metabolic engineering of yeast cell factories. *FEMS Yeast Res.* 2012, 12, 228–248.
- [15] Da Silva, N. A., Srikrishnan, S., Introduction and expression of genes for metabolic engineering applications in *Saccharomyces cerevisiae*. *FEMS Yeast Res.* 2012, 12, 197–214.
- [16] Krivoruchko, A., Siewers, V., Nielsen, J., Opportunities for yeast metabolic engineering: Lessons from synthetic biology. *Biotechnol. J.* 2011, 6, 262–276.
- [17] Nielsen, J., Jewett, M. C., Impact of systems biology on metabolic engineering of *Saccharomyces cerevisiae*. *FEMS Yeast Res.* 2008, 8, 122–131.
- [18] Oliveira, A. P., Sauer, U., The importance of post-translational modifications in regulating *Saccharomyces cerevisiae* metabolism. *FEMS Yeast Res.* 2012, 12, 104–117.
- [19] Oud, B., Van Maris, A. J. A., Daran, J. M., Pronk, J. T., Genome-wide analytical approaches for reverse metabolic engineering of industrially relevant phenotypes in yeast. *FEMS Yeast Res.* 2012, 12, 183–196.
- [20] Katsuki, H., Bloch, K., Studies on the biosynthesis of ergosterol in yeast. Formation of methylated intermediates. *J. Biol. Chem.* 1967, 242, 222–227.
- [21] Lynen, F., Biosynthetic pathways from acetate to natural products. *Pure Appl. Chem.* 1967, 14, 137–167.
- [22] Rohmer, M., Knani, M., Simonin, P., Sutter, B., Sahm, H., Isoprenoid biosynthesis in bacteria: A novel pathway for the early steps leading to isopentenyl diphosphate. *Biochem. J.* 1993, 295, 517–524.
- [23] Lange, B. M., Rujan, T., Martin, W., Croteau, R., Isoprenoid biosynthesis: The evolution of two ancient and distinct pathways across genomes. *Proc. Natl. Acad. Sci. USA* 2000, 97, 13172–13177.
- [24] Basson, M. E., Thorsness, M., Rine, J., *Saccharomyces cerevisiae* contains two functional genes encoding 3-hydroxy-3-methylglutaryl-coenzyme A reductase. *Proc. Natl. Acad. Sci. USA* 1986, 83, 5563–5567.
- [25] Shearer, A. G., Hampton, R. Y., Structural control of endoplasmic reticulum-associated degradation. Effect of chemical chaperones on 3-hydroxy-3-methylglutaryl-CoA reductase. *J. Biol. Chem.* 2004, 279, 188–196.
- [26] Daum, G., Lees, N. D., Bard, M., Dickson, R., Biochemistry, cell biology and molecular biology of lipids of *Saccharomyces cerevisiae*. *Yeast* 1998, 14, 1471–1510.
- [27] Lees, N. D., Bard, M., Kirsch, D. R., Biochemistry and molecular biology of sterol synthesis in *Saccharomyces cerevisiae*. *Crit. Rev. Biochem. Mol. Biol.* 1999, 34, 33–47.
- [28] Dugar, D., Stephanopoulos, G., Relative potential of biosynthetic pathways for biofuels and bio-based products. *Nat. Biotechnol.* 2011, 29, 1074–1078.
- [29] Carlsen, S., Ajikumar, P. K., Formenti, L. R., Zhou, K. et al., Heterologous expression and characterization of bacterial 2-C-methyl-D-erythritol-4-phosphate pathway in *Saccharomyces cerevisiae*. *Appl. Microbiol. Biotechnol.* 2013, 97, 5753–5769.
- [30] Partow, S., Siewers, V., Daviet, L., Schalk, M., Nielsen, J., Reconstruction and evaluation of the synthetic bacterial MEP pathway in *Saccharomyces cerevisiae*. *PLoS ONE* 2012, doi: 10.1371/journal.pone.0052498.
- [31] News – science & business developments. *Ind. Biotechnol.* 2011, 7, 309–321.
- [32] Sharon-Asa, L., Shalit, M., Frydman, A., Bar, E. et al., Citrus fruit flavor and aroma biosynthesis: Isolation, functional characterization, and developmental regulation of Cstps1, a key gene in the production of the sesquiterpene aroma compound valencene. *Plant J.* 2003, 36, 664–674.
- [33] Greenhagen, B. T., *Original of isoprenoid diversity: A study of structure–function relationships in sesquiterpene systems* (doctoral dissertation). University of Kentucky 2003.
- [34] Lücker, J., Bowen, P., Bohlmann, J., *Vitis vinifera terpenoid cyclases: Functional identification of two sesquiterpene synthase cDNAs encoding (+)-valencene synthase and (-)-germacrene D synthase and expression of mono- and sesquiterpene synthases in grapevine flowers and berries*. *Phytochemistry* 2004, 65, 2649–2659.
- [35] Farhi, M., Marhevka, E., Masci, T., Marcos, E. et al., Harnessing yeast subcellular compartments for the production of plant terpenoids. *Metab. Eng.* 2011, 13, 474–481.
- [36] Scalcinati, G., Partow, S., Siewers, V., Schalk, M. et al., Combined metabolic engineering of precursor and co-factor supply to increase a-santalene production by *Saccharomyces cerevisiae*. *Microb. Cell Fact.* 2012, doi: 10.1186/1475-2859-11-117.
- [37] Asadollahi, M. A., Maury, J., Möller, K., Nielsen, K. F. et al., Production of plant sesquiterpenes in *Saccharomyces cerevisiae*: Effect of erg9 repression on sesquiterpene biosynthesis. *Biotechnol. Bioeng.* 2008, 99, 666–677.
- [38] Scalcinati, G., Knuf, C., Partow, S., Chen, Y. et al., Dynamic control of gene expression in *Saccharomyces cerevisiae* engineered for the production of plant sesquiterpene a-santalene in a fed-batch mode. *Metab. Eng.* 2012, 14, 91–103.
- [39] Takahashi, S., Yeo, Y., Greenhagen, B. T., McMullin, T. et al., Metabolic engineering of sesquiterpene metabolism in yeast. *Biotechnol. Bioeng.* 2007, 97, 170–181.
- [40] Julien, B., Burlingame, R., *Method for production of isoprenoids*. US Patent US8481286 B2.
- [41] Greenhagen, B. T., O'Maille, P. E., Noel, J. P., Chappell, J., Identifying and manipulating structural determinants linking catalytic specificities in terpene synthases. *Proc. Natl. Acad. Sci. USA* 2006, 103, 9826–9831.
- [42] Naigre, R., Kalck, P., Roques, C., Roux, I., Michel, G., Comparison of antimicrobial properties of monoterpenes and their carbonylated products. *Planta Med.* 1996, 62, 275–277.
- [43] Chang, M. C. Y., Keasling J. D., Production of isoprenoid pharmaceuticals by engineered microbes. *Nat. Chem. Biol.* 2006, 2, 674–681.
- [44] Huang, B., Guo, J., Yi, B., Yu, X. et al., Heterologous production of secondary metabolites as pharmaceuticals in *Saccharomyces cerevisiae*. *Biotechnol. Lett.* 2008, 30, 1121–1137.
- [45] Tu, Y., The discovery of artemisinin (qinghaosu) and gifts from Chinese medicine. *Nat. Med.* 2011, 17, 1217–1220.
- [46] Paddon, C. J., Westfall, P. J., Pitera, D. J., Benjamin, K. et al., High-level semi-synthetic production of the potent antimalarial artemisinin. *Nature* 2013, 496, 528–532.
- [47] Westfall, P. J., Pitera, D. J., Lenihan, J. R., Eng, D. et al., Production of amorphadiene in yeast, and its conversion to dihydroartemisinic acid, precursor to the antimalarial agent artemisinin. *Proc. Natl. Acad. Sci. USA* 2012, 109, E111–E118.
- [48] Tsuruta, H., Paddon, C. J., Eng, D., Lenihan, J. R. et al., High-level production of amorpha-4, 11-diene, a precursor of the antimalarial agent artemisinin, in *Escherichia coli*. *PLoS ONE* 2009, doi: 10.1371/journal.pone.0004489.
- [49] Schiff, P. B., Fant, J., Horwitz, S. B., Promotion of microtubule assembly in vitro by taxol. *Nature* 1979, 277, 665–667.
- [50] Croteau, R., Ketchum, R. E. B., Long, R. M., Kaspera, R., Wildung, M. R., Taxol biosynthesis and molecular genetics. *Phytochem. Rev.* 2006, 5, 75–97.
- [51] Engels, B., Dahm, P., Jennewein, S., Metabolic engineering of taxadiene biosynthesis in yeast as a first step towards taxol (paclitaxel) production. *Metab. Eng.* 2008, 10, 201–206.
- [52] Ajikumar, P. K., Xiao, W. H., Tyo, K. E. J., Wang, Y. et al., Isoprenoid pathway optimization for taxol precursor overproduction in *Escherichia coli*. *Science* 2010, 330, 70–74.

- [53] Boghigian, B. A., Armando, J., Salas, D., Pfeifer, B. A., Computational identification of gene over-expression targets for metabolic engineering of taxadiene production. *Appl. Microbiol. Biotechnol.* 2012, 93, 2063–2073.
- [54] Buijs, N. A., Siewers, V., Nielsen, J., Advanced biofuel production by the yeast *Saccharomyces cerevisiae*. *Curr. Opin. Chem. Biol.* 2013, 17, 480–488.
- [55] Rude, M. A., Schirmer, A., New microbial fuels: A biotech perspective. *Curr. Opin. Microbiol.* 2009, 12, 274–281.
- [56] Zhang, F., Rodriguez, S., Keasling, J. D., Metabolic engineering of microbial pathways for advanced biofuels production. *Curr. Opin. Biotechnol.* 2011, 22, 775–783.
- [57] Renninger, N. S., McPhee, D. J., *Fuel compositions comprising farnesane and farnesane derivatives and method of making and using same*. US Patent 7399323 B2, 2008.
- [58] Renninger, N. S., Newman, J., Reiling, K. K., Regentin, R., Paddon, C. J., *Production of isoprenoids*. US Patent 7659097 B2, 2010.
- [59] Ryder, J. A., *Jet fuel compositions*. US Patent 7589243 B1, 2009.
- [60] Christensen, E., Yanowitz, J., Ratcliff, M., McCormick, R. L., Renewable oxygenate blending effects on gasoline properties. *Energy Fuels* 2011, 25, 4723–4733.
- [61] Meylmans, H. A., Quintana R. L. Harvey B. G., Efficient conversion of pure and mixed terpene feedstocks to high density fuels. *Fuel* 2012, 97, 560–568.
- [62] Harvey, B. G., Wright, M. E., Quintana, R. L., High-density renewable fuels based on the selective dimerization of pinenes. *Energy Fuels* 2010, 24, 267–273.
- [63] Tracy, N. I., Chen, D., Crunkleton, D. W., Price, G. L., Hydrogenated monoterpenes as diesel fuel additives. *Fuel* 2009, 88, 2238–2240.
- [64] Brennan, T. C., Turner, C. D., Krömer, J. O., Nielsen, L. K., Alleviating monoterpane toxicity using a two-phase extractive fermentation for the bioproduction of jet fuel mixtures in *Saccharomyces cerevisiae*. *Biotechnol. Bioeng.* 2012, 109, 2513–2522.
- [65] Parveen, M., Hasan, M. K., Takahashi, J., Murata, Y. et al., Response of *Saccharomyces cerevisiae* to a monoterpane: Evaluation of anti-fungal potential by DNA microarray analysis. *J. Antimicrob. Chemother.* 2004, 54, 46–55.
- [66] Uribe, S., Ramirez, J., Pena, A., Effects of  $\beta$ -pinene on yeast membrane functions. *J. Bacteriol.* 1985, 161, 1195–1200.
- [67] Hu, F., Liu, J., Du, G., Hua, Z. et al., Key cytomembrane ABC transporters of *Saccharomyces cerevisiae* fail to improve the tolerance to d-limonene. *Biotechnol. Lett.* 2012, 34, 1505–1509.
- [68] Dunlop, M. J., Dossani, Z. Y., Szmidt, H. L., Chu, H. C. et al., Engineering microbial biofuel tolerance and export using efflux pumps. *Mol. Syst. Biol.* 2011, doi: 10.1038/msb.2011.21.
- [69] Muramatsu, M., Ohto, C., Obata, S., Sakuradani, E., Shimizu, S., Alkaline pH enhances farnesol production by *Saccharomyces cerevisiae*. *J. Biosci. Bioeng.* 2009, 108, 52–55.
- [70] Ohto, C., Muramatsu, M., Obata, S., Sakuradani, E., Shimizu, S., Overexpression of the gene encoding HMG-CoA reductase in *Saccharomyces cerevisiae* for production of prenyl alcohols. *Appl. Microbiol. Biotechnol.* 2009, 82, 837–845.
- [71] Faulkner, A., Chen, X., Rush, J., Horazdovsky, B. et al., The lpp1 and dpp1 gene products account for most of the isoprenoid phosphate phosphatase activities in *Saccharomyces cerevisiae*. *J. Biol. Chem.* 1999, 274, 14831–14837.
- [72] Song, L., A soluble form of phosphatase in *Saccharomyces cerevisiae* capable of converting farnesyl diphosphate into E,E-farnesol. *Appl. Biochem. Biotechnol.* 2006, 128, 149–157.
- [73] Wang, C., Kim, J. Y., Choi, E. S., Kim, S. W., Microbial production of farnesol (FOH): Current states and beyond. *Process Biochem.* 2011, 46, 1221–1229.
- [74] Cheng, A. X., Xiang, C. Y., Li, J. X., Yang, C. Q. et al., The rice (E)- $\beta$ -caryophyllene synthase (OsTPS3) accounts for the major inducible volatile sesquiterpenes. *Phytochemistry* 2007, 68, 1632–1641.
- [75] Meigs, T. E., Roseman, D. S., Simoni, R. D., Regulation of 3-hydroxy-3-methylglutaryl-coenzyme A reductase degradation by the nonsterol mevalonate metabolite farnesol in vivo. *J. Biol. Chem.* 1996, 271, 7916–7922.
- [76] Wang, C., Yoon, S. H., Shah, A. A., Chung, Y. R. et al., Farnesol production from *Escherichia coli* by harnessing the exogenous mevalonate pathway. *Biotechnol. Bioeng.* 2010, 107, 421–429.
- [77] Peralta-Yahya, P. P., Ouellet, M., Chan, R., Mukhopadhyay, A. et al., Identification and microbial production of a terpene-based advanced biofuel. *Nat. Commun.* 2011, 2, 483.
- [78] Murray, K. E., Huelin, F. E., Davenport, J. B., Occurrence of farnesene in the natural coating of apples. *Nature* 1964, 204, 80.
- [79] Wang, C., Yoon, S. H., Jang, H. J., Chung, Y. R. et al., Metabolic engineering of *Escherichia coli* for a-farnesene production. *Metab. Eng.* 2011, 13, 648–655.
- [80] Yoshikuni, Y., Ferrin, T. E., Keasling, J. D., Designed divergent evolution of enzyme function. *Nature* 2006, 440, 1078–1082.
- [81] Kampranis, S. C., Ioannidis, D., Purvis, A., Mahrez, W. et al., Rational conversion of substrate and product specificity in a *Salvia* monoterpane synthase: Structural insights into the evolution of terpene synthase function. *Plant Cell* 2007, 19, 1994–2005.
- [82] Li, J. X., Fang, X., Zhao, Q., Ruan, J. X. et al., Rational engineering of plasticity residues of sesquiterpene synthases from *Artemisia annua*: Product specificity and catalytic efficiency. *Biochem. J.* 2013, 451, 417–426.
- [83] Millis, J. R., Maurina-Bunker, J., *Production of farnesol and geranylgeranol*. US Patent 6689593 B2, 2004.
- [84] Klettlinger, J., Rich, R., Yen, C., Surgenor, A., Thermal stability testing of Fischer-Tropsch fuel and various blends with Jet A, as well as aromatic blend additives. *IEEE Energytech* 2011, doi: 10.1109/EnergyTech.2011.5948544.
- [85] Murugesan, A., Umarani, C., Subramanian, R., Nedunchezhian, N., Bio-diesel as an alternative fuel for diesel engines – a review. *Renew. Sustain. Energy Rev.* 2009, 13, 653–662.
- [86] Hui, X., Kumar, K., Sung, C. J., Edwards, T., Gardner, D., Experimental studies on the combustion characteristics of alternative jet fuels. *Fuel* 2012, 98, 176–182.

# **Production of farnesene and santalene by *Saccharomyces cerevisiae* using fed-batch cultivations with RQ-controlled feed**

Stefan Tippmann, Gionata Scalcinati, Verena Siewers and Jens Nielsen

*Biotechnology and Bioengineering* 113(1):72-81, 2016



# Production of Farnesene and Santalene by *Saccharomyces cerevisiae* Using Fed-Batch Cultivations With RQ-Controlled Feed

Stefan Tippmann,<sup>1,2</sup> Gionata Scalcinati,<sup>1</sup> Verena Siewers,<sup>1,2</sup> Jens Nielsen<sup>1,2,3</sup>

<sup>1</sup>Department of Biology and Biological Engineering, Chalmers University of Technology, SE412 96, Gothenburg, Sweden; e-mail: nielsenj@chalmers.se telephone: +46-31772-38-04; fax: +46-31772-38-01

<sup>2</sup>Novo Nordisk Foundation Center for Biosustainability, Chalmers University of Technology, SE412 96, Gothenburg, Sweden

<sup>3</sup>Novo Nordisk Foundation Center for Biosustainability, Technical University of Denmark, DK2970, Hørsholm, Denmark

**ABSTRACT:** Terpenes have various applications as fragrances, cosmetics and fuels. One of the most prominent examples is the sesquiterpene farnesene, which can be used as diesel substitute in its hydrogenated form farnesane. Recent metabolic engineering efforts have enabled efficient production of several terpenes in *Saccharomyces cerevisiae* and *Escherichia coli*. Plant terpene synthases take on an essential function for sesquiterpene production as they catalyze the specific conversion of the universal precursor farnesyl diphosphate (FPP) to the sesquiterpene of interest and thereby impose limitations on the overall productivity. Using farnesene as a case study, we chose three terpene synthases with distinct plant origins and compared their applicability for farnesene production in the yeast *S. cerevisiae*. Differences regarding the efficiency of these enzymes were observed in shake flask cultivation with maximal final titers of 4 mg/L using  $\alpha$ -farnesene synthase from *Malus domestica*. By employing two existing platform strains optimized for sesquiterpene production, final titers could be raised up 170 mg/L in fed-batch fermentations with RQ-controlled exponential feeding. Based on these experiments, the difference between the selected synthases was not significant. Lastly, the same fermentation setup was used to compare these results to production of the fragrance sesquiterpene santalene, and almost equivalent titers were obtained with 163 mg/L, using the highest producing strain expressing a santalene synthase from *Clausena lansium*. However, a reduction of the product yield on biomass by 50% could indicate a higher catalytic efficiency of the farnesene synthase. *Biotechnol. Bioeng.* 2016;113: 72–81.

© 2015 Wiley Periodicals, Inc.

**KEYWORDS:** isoprenoids; terpene synthases; biofuels; yeast; metabolic engineering; fed-batch

Present address of Gionata Scalcinati is Genomatica Inc., 4757 Nexus Center Drive, San Diego, CA 92121.

Conflicts of interest: ST, GS, VN, and JN declare to have no competing interests.

Correspondence to: J. Nielsen

Received 19 March 2015; Accepted 15 June 2015

Accepted manuscript online 24 June 2015;

Article first published online 2 September 2015 in Wiley Online Library  
(<http://onlinelibrary.wiley.com/doi/10.1002/bit.25683/abstract>).

DOI 10.1002/bit.25683

## Introduction

Isoprenoids have attracted great interest in the recent past based on their applications in the food and pharmaceutical industry (Tippmann et al., 2013). In addition, particularly mono- and sesquiterpenes have been identified as suitable diesel and jet fuel substitutes (Meylemans et al., 2012; Millo et al., 2014). Production of these compounds by plant extraction mostly fails to meet industrial scale and is often not sustainable or dependent on seasonal and geographical changes. The design of microbial cell factories by metabolic engineering, however, offers an alternative production route by redirecting cellular metabolism towards a desired product, which has been successfully demonstrated for production of several sesquiterpenes in the yeast *Saccharomyces cerevisiae* (Asadollahi et al., 2008; Paddon et al., 2013; Peralta-Yahya et al., 2011; Scalcinati et al., 2012a). All isoprenoids are produced from the activated isoprene units isopentenyl diphosphate (IPP) and dimethylallyl diphosphate (DMAPP), which are both derived from the mevalonate pathway in *S. cerevisiae* (Fig. 1). The metabolic route to farnesene comprises nine enzymatic reactions from acetyl-CoA and is both highly energy and co-factor dependent, as the production of one mole of farnesene from three moles of acetyl-CoA requires nine moles of ATP and six moles of NADPH. Furthermore, the essential role of farnesyl diphosphate (FPP) for sterol synthesis limits the FPP availability for production of desired sesquiterpenes. Using a combination of different metabolic engineering strategies including engineering of the FPP branch point, increasing flux through the mevalonate pathway and improving co-factor balance, the production of the fragrance precursor  $\alpha$ -santalene was recently enabled in *S. cerevisiae* (Scalcinati et al., 2012b).

The terminal conversion of FPP to farnesene is catalyzed by farnesene synthase, which is not expressed by *S. cerevisiae* endogenously, but found in various plants (Chen et al., 2011). By removal of the diphosphate group, which results in a rearrangement of the double bonds in the molecule, two isomers are formed,  $\alpha$ - and  $\beta$ -farnesene, with six stereoisomers overall.

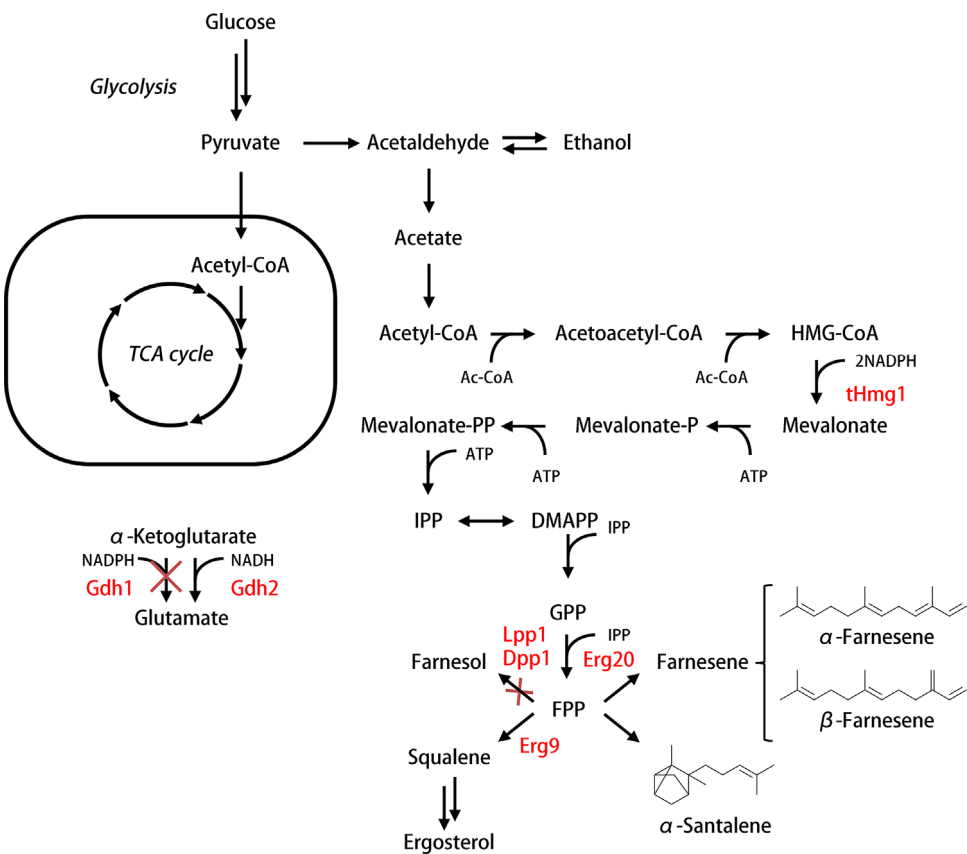


**Figure 1.** Production of farnesene and santalene from glucose in *S. cerevisiae*. Isoprenoids are synthesized via the mevalonate pathway from cytosolic acetyl-CoA, which is derived from pyruvate via the PDH bypass. The mevalonate pathway comprises seven steps and yields the isomers IPP and DMAPP. Condensations of the two isomers form the precursors for mono-, sesqui- or longer chain terpenoids. In the last step, FPP is converted by farnesene synthase to yield farnesene. Similarly, santalene is produced from FPP by santalene synthase. ATP and co-factor requirements are shown only for the mevalonate pathway. Enzymes in red denote engineering targets used in this study with tHmg1: truncated HMG-CoA reductase, Erg9: squalene synthase, Erg20: FPP synthase, Lpp1: lipid phosphate phosphatase, Dpp1: diacylglycerol diphosphate phosphatase, Gdh1/2: glutamate dehydrogenase. IPP: isopentenyl diphosphate, DMAPP: dimethylallyl diphosphate, GPP: geranyl diphosphate, FPP: farnesyl diphosphate, Ac-CoA: acetyl-coA.

Poor expression of these terpene synthases has been identified as a major constraint on production of sesquiterpenes (Martin et al., 2001). Moreover, substrate affinity and turnover of these enzymes are key parameters for an efficient production of farnesene from the FPP branch point, and have not been compared *in vivo* hitherto.

Farnesene synthases are widely spread in the plant kingdom and coding sequences are available for several organisms including *Zea mays*, *Cucumis melo*, *Pyrus communis* and *Mentha arvensis* (Nucleotide Database, National Center for Biotechnology Information). The objective of this study was to express three farnesene synthase genes from plants in *S. cerevisiae*, i.e., α-farnesene synthase from *Malus domestica* and β-farnesene synthase from *Citrus junos* and *Artemisia annua*, respectively, which have previously been characterized regarding their reaction conditions, co-factor requirements and product specificities (Crock et al., 1997; Green et al., 2007; Maruyama et al., 2001; Pechous and Whitaker, 2004; Picaud et al., 2005; Rupasinghe et al., 2000) and compare production of farnesene with production of another sesquiterpene. For this purpose, an existing platform for sesquiterpene production was used to investigate production capacity in comparison to α-santalene. Down-regulation

of sterol synthesis in this platform strain at low extracellular glucose concentrations (Scalcanati et al., 2012a) prompted us to investigate production of farnesene in glucose limited conditions. Fed-batch processes are widely used in industrial applications to attain high cell densities avoiding substrate inhibition and overflow metabolism, which is reported to occur in *S. cerevisiae* at glucose concentrations above 0.04 g/L and is known to reduce biomass yields (Geurts et al., 1980; Pham et al., 1998; Verduyn, 1991). We therefore chose an exponential feeding strategy to account for exponential growth of the host organism. Controlling the feed rate by the respiratory quotient (*RQ*) is an additional strategy to avoid overfeeding and carbon loss due to the Crabtree effect. Setting the *RQ* to a value of 1, which translates to the threshold for ethanol formation, aims at maintaining metabolism in a state optimized for growth.

## Materials and Methods

### Plasmid and Strain Construction

Synthetic, codon optimized genes for farnesene synthases from *M. domestica*, *C. junos*, and *A. annua* were purchased from GenScript

(GenScript, Piscataway, NJ) and cloned into plasmids pSP-G1 (Partow et al., 2010) and pICK01 (Scalcanati et al., 2012a) using restriction enzymes *NotI* and *PacI* (Thermo Fisher Scientific, Waltham, MA, USA) (Table I). Strains with auxotrophy for uracil were grown on YPD plates containing 20 g/L glucose, 10 g/L yeast extract, 20 g/L peptone from casein, and 20 g/L agar. Plasmid containing strains were grown on selective growth medium containing 6.9 g/L yeast nitrogen base w/o amino acids (Formedium, Hunstanton, UK), 0.77 g/L complete supplement mixture w/o uracil (Formedium), 20 g/L glucose, and 20 g/L agar.

## Growth Media

All batch cultivations in shake flasks and bioreactors were performed using minimal media as described by Verduyn et al. (1992) containing 20 g/L glucose, 5 g/L  $(\text{NH}_4)_2\text{SO}_4$ , 3 g/L  $\text{KH}_2\text{PO}_4$ , 0.5 g/L  $\text{MgSO}_4 \cdot 7\text{H}_2\text{O}$ , 1 mL/L trace element solution and 50  $\mu\text{L}/\text{L}$  antifoam. The medium was adjusted to pH 5 using 2 M KOH and 1 mL/L vitamin solution was added after sterilization. The feed medium for fed-batch cultivations was ten times concentrated and contained 200 g/L glucose.

## Shake Flask Cultivations

Strains were grown on plates containing selective growth medium at 30°C. A single colony was used to inoculate 5 mL of minimal medium, which was incubated overnight at 30°C and 200 rpm. Subsequently, 100 mL shake flasks without baffles containing 18 mL of liquid medium were inoculated at an OD600 of 0.1 and an extractive dodecane overlay ( $\geq 99\%$ , Sigma-Aldrich, St. Louis, MO) was added at 10% v/v to sequester farnesene. Shake flasks were incubated at 30°C and 160 rpm.

## Bioreactor Cultivations

Similar to the shake flask cultivations described above, a single colony from a fresh plate containing selective medium was used to inoculate 5 mL minimal medium and incubated overnight at 30°C and 200 rpm. Cells were then transferred to 50 mL of liquid medium in 500 mL shake flasks and cultivated overnight at 30°C and 160 rpm. Subsequently, the preculture was harvested by centrifugation at 4000 rpm for 5 min and resuspended in 10 mL of fresh medium. The OD600 was measured using a Genesis20 spectrophotometer (Thermo Fisher Scientific) to inoculate the

bioreactors at an OD600 of 0.1. All cultivations were performed in 2.5 L Applikon vessels (Applikon, Delft, The Netherlands) using the DasGip Microbiology PD system (DasGip, Jülich, Germany). Homogenous mixing was enabled using two six-blade Rushton turbines at 600 rpm. The temperature was controlled at 30°C and the pH was adjusted to 5 using 2 M KOH and 2 M HCl. The vessels were sparged with air at an initial rate of 60 L/h. To assure constant aeration at 1 vvm, the aeration rate was increased during the fed-batch phase according to the culture volume. The batch phase was started with an initial volume of 1 L. The feed was initiated after glucose and ethanol depletion, which was monitored by on-line  $\text{CO}_2$  measurements obtained from the exhaust gas analysis. Prior to feed start, 200 mL of dodecane were added to the vessels under aseptic conditions.

## RQ-Control and Feed Profile Development

Cultivations in bioreactors were conducted in fed-batch mode with RQ-controlled exponential feeding. The aerobic fed-batch process was performed in 2.5 L Applikon vessels (Applikon, Schiedam, The Netherlands) with an initial working volume of 1.0 L. Agitation at 800 rpm was maintained using an integrated stirrer (DasGip) and the temperature was monitored using a platinum RTD temperature sensor and kept at 30°C. The rate of aeration was set to 1 vvm by a mass flow controller. The pH of the medium was maintained at 5.0 by automatic addition of 2 M KOH and 2 M HCl. The temperature, agitation, gassing, pH and composition of the off-gas were monitored and controlled using the integrated DasGip monitoring and control system. Dissolved oxygen concentration was monitored with an autoclavable polarographic oxygen electrode (Mettler Toledo, Columbus, OH) and kept above 30% via stirrer speed and gas flow rate using the DasGip control system. The effluent gas from the fermentation was cooled, dried and analyzed for real-time determination of oxygen and  $\text{CO}_2$  concentration by DasGip fedbatch pro® gas analysis systems with the off gas analyzer GA4 based on zirconium dioxide and two-beam infrared sensor. The integrated mass flow sensor allowed for on-line monitoring and calculation of oxygen transfer rate (OTR) (mmol/h), carbon dioxide transfer rate (CTR) (mmol/h) and respiratory quotient (RQ) by dividing CTR by OTR. The seed cultures for the cultivations were grown at 30°C in 500 mL shake flasks containing 100 mL of culture with agitation in an orbital shaker at 100 rpm. Pre-cultures were used to inoculate the fermenters at a final dry weight of 1 mg/L. All cultivations were performed in duplicate or triplicate. The fed-batch cultures were

**Table I.** Overview of plasmids used in this study.

Plasmid	Gene(s)	Reference
pSP-G1	<i>URA3</i> based expression vector containing bidirectional $\text{P}_{TEFI}\text{-P}_{PGK1}$ promoter	(Partow et al., 2010)
pICK01	$\text{pSP-G1, P}_{PGK1}\text{-tHMG1, P}_{TEFI}\text{-SanSyn}$	(Scalcanati et al., 2012a)
pIST01	$\text{P}_{TEFI}\text{-FarnSyn}_M\text{d}$	This study
pIST02	$\text{P}_{TEFI}\text{-FarnSyn}_C\text{j}$	This study
pIST03	$\text{P}_{TEFI}\text{-FarnSyn}_A\text{a}$	This study
pIST04	$\text{P}_{TEFI}\text{-FarnSyn}_M\text{d, P}_{PGK1}\text{-tHMG1}$	This study
pIST05	$\text{P}_{TEFI}\text{-FarnSyn}_C\text{j, P}_{PGK1}\text{-tHMG1}$	This study
pIST06	$\text{P}_{TEFI}\text{-FarnSyn}_A\text{a, P}_{PGK1}\text{-tHMG1}$	This study

Md: *M. domestica*, Cj: *C. junos* and Aa: *A. annua*.

initiated as batch cultures using 20 g/L glucose. Feeding with fresh medium commenced only after residual ethanol produced from the glucose consumption phase was completely depleted. An exponential feed rate  $v(t)$  (L/h) was calculated as previously described by Scalcinati et al. (2012a). Assuming substrate concentration is at steady state ( $dS/dt = 0$ ), the exponential feed rate was calculated as

$$v(t) = \frac{\mu X_0 V_0 \exp(\mu t)}{Y_{SX}(S^{in} - S)} = v_0 \exp(\mu t) \quad (1)$$

with  $t$  as the feed time,  $\mu$  as the specific growth rate,  $X_0$  and  $V_0$  as the initial biomass concentration and reaction volume, respectively,  $Y_{SX}$  as the specific biomass yield and  $S$  as the substrate concentration in the feed medium (superscript in) and in the cultivation medium (Nielsen et al., 2002; pp. 411–416). A specific growth rate of 0.1 1/h was used, since overflow metabolism is reported to start at  $\mu > 0.25$  1/h (Nielsen et al., 2002). Glucose was assumed to be the rate limiting substrate to which *S. cerevisiae* responds following the Monod kinetics, where  $S \approx 0$  since  $S^{in} >> S$ . For calculation of the initial feed rate  $v_0$ , available chemostat data for strain SCIGS28, which differs from strains SCIST04-6 only by the terpene synthase on the plasmid, at a dilution rate of  $D = 0.1$  1/h were used.

To facilitate strain comparison, the same feeding strategy was applied in all experiments with  $v_0 = 0.003$  L/h, in order to keep the glucose concentration below the substrate consumption rate specified for these conditions (Scalcinati et al., 2012b). A correct feed rate was obtained using a modified single loop, set-point control method programming the fermenter fb-pro software (DasGip) and controlled using the DasGip control system. Additionally, the feed rate was controlled based on the respiratory culture response monitoring  $RQ$  values as indirect measure of the cell metabolic state. Online precise measurement of the exit gas composition allowed to adjust the feed rate through a proportional integral (PI) controller maintaining the  $RQ$  at the desired set point of 1.0 during feed phase, whereas pumps were started at  $RQ < 1$  and turned off at  $RQ > 1$  to avoid ethanol formation.

### Measurement of Cell Growth

Cell growth was determined by measuring optical density at 600 nm using a Genesis 20 spectrophotometer (Thermo Fisher Scientific). For cell dry weight measurement, a 5 mL sample was taken from the bioreactor and pipetted onto a pre-weighted filter with a pore size of 0.45  $\mu\text{m}$  (Sartorius, Göttingen, Germany). Subsequently, the filter was washed with 5 mL of water, dried in a microwave at 150 W for 15 min and stored in a desiccator until it was weighed again.

### Quantification of Extracellular Metabolites

In order to measure glucose, ethanol, glycerol, acetate and succinate during the fermentation, a sample was taken from the two-phase cultivation broth and centrifuged at 4000 rpm for 3 min. The organic overlay was removed and the cell suspension was filtered using a 0.45  $\mu\text{m}$  nylon filter (VWR International, Radnor, PA).

Subsequently, the sample was analyzed by HPLC using a Dionex Ultimate 3000 (Dionex, Sunnyvale, CA) equipped with an Aminex HPX-87H column (300 mm x 7.8 mm, Bio-Rad Laboratories, Hercules, CA) in connection with a variable wavelength detector (210 nm) and a refractive index detector (512  $\mu\text{RIU}$ ). The system was run at 45°C and a flow rate of 0.6 mL/min with 5 mM  $\text{H}_2\text{SO}_4$  as solvent. The analytes were detected by comparison with a known standard and quantified by external calibration.

### Quantification of Farnesene and Santalene

For quantification of farnesene, a sample was removed from the cultivation broth and separation of the two phases (aqueous and dodecane) was performed by centrifugation at 5000 rpm for 5 min. An aliquot was taken from the dodecane phase and either injected directly or diluted ten times in hexane. Farnesene isomers were detected on a Focus GC ISQ single quadrupole GC-MS and quantified on a Focus GC-FID (Thermo Fisher Scientific, USA) with identical analytical conditions as described by Tippmann et al. (2015). Since the signal intensity of the FID primarily depends on the number of carbon atoms (Holm, 1999), quantification of both isomers,  $\alpha$ - and  $\beta$ -farnesene, was performed by external calibration using trans- $\beta$ -farnesene analytical standards ( $\geq 90\%$ , Sigma-Aldrich) as presented by Wang et al. (2011). Santalene was quantified as described previously by Scalcinati et al. (2012b) with minor modifications. The organic overlay was collected by centrifugation at 5000 rpm for 5 min, diluted with an equal volume of 2-ethyl acetate (Sigma, St Luis, MO) containing  $\alpha$ -humulene ( $\geq 96\%$ , Sigma Aldrich) as internal standard and subsequently analyzed by GC-MS. Identification of santalene was performed comparing mass spectra and retention time with an authentic standard, while santalene concentrations were calculated using external calibration and corrected by recovery of the internal standard  $\alpha$ -humulene.

## Results

### Farnesene Production in Shake Flask Cultivations

In the first part of our study, three farnesene synthases were compared for farnesene production. For this purpose, *S. cerevisiae* CEN.PK113-5D strains harboring plasmids pIST01-03 were cultivated for 48 h in minimal medium overlayed with 10% v/v of dodecane to harvest the product. Farnesene titers are reported in Figure 2A. Highest farnesene titers were observed for  $\alpha$ -farnesene synthase from *M. domestica* with approximately 4 mg/L, whereas  $\beta$ -farnesene titers obtained with the synthases from *C. junos* and *A. annua* were slightly lower, i.e. approximately 3.5 and 3.0 mg/L, respectively. Furthermore, sesquiphellandrene, which is like farnesene directly derived from FPP, was detected as byproduct for farnesene synthase from *C. junos*, whereas the other two synthases showed high product specificity for farnesene in our experiments. In order to enhance farnesene production, the farnesene synthase genes were expressed from 2  $\mu\text{m}$  plasmids together with a truncated version of the 3-hydroxy-3-methylglutaryl-coenzyme A (HMG-CoA) reductase gene, *tHMG1*, which encodes a flux controlling enzyme of the mevalonate pathway

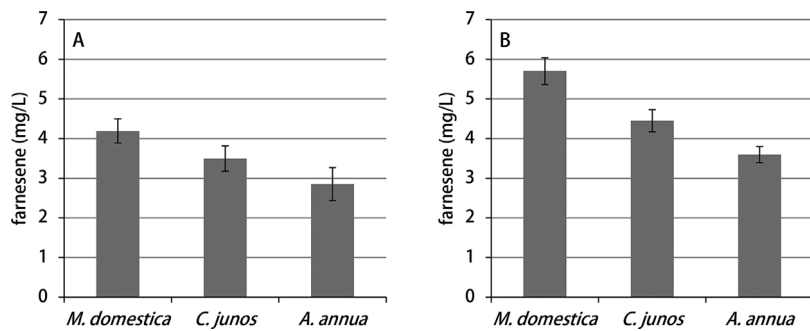


**Figure 2.** Comparison of yeast strains carrying three different farnesene synthase genes in shake flask cultivation. *S. cerevisiae* strain CEN.PK113-5D was transformed with plasmids pIST01-03 (Panel A) and pIST04-06 (Panel B) to compare farnesene synthase genes from different plant sources, i.e. *M. domestica*, *C. junos*, and *A. annua* and to study the effect of truncated HMG-CoA reductase tHmg1. Cells were cultivated for 48 h and farnesene was extracted using a dodecane overlay. Values represent average concentrations normalized to total culture volume of three biological replicates with standard deviation.

(Ohto et al., 2009). Opposed to native Hmg1, which is located in the ER membrane, tHmg1 represents the free cytosolic form of the enzyme as it misses the regulatory membrane binding domain (Polakowski et al., 1998). Evaluation of this plasmid set (pIST04-06) in shake flasks revealed an increase in titers by at least 25% after 48 h of cultivation time with farnesene synthase from *M. domestica* producing approximately 6 mg/L of  $\alpha$ -farnesene and farnesene synthases from *C. junos* and *A. annua* producing approximately 4.5 and 3.5 mg/L, respectively (Fig. 2B).

#### Production of Farnesene in Fed-Batch Cultivations With RQ-Controlled Exponential Feed

The comparison of three farnesene synthases in shake flasks revealed clear differences regarding their efficiency when tested in *S. cerevisiae* CEN.PK113-5D. In accordance with the literature, co-expression of *tHMG1* led to a significant improvement in

sesquiterpene titers. In order to further increase farnesene production, strains SCICK16 and SCIGS22, which were constructed for improved production of sesquiterpenes by engineering of the FPP branch point and increasing the flux through the mevalonate pathway (Scalcanati et al., 2012a; Scalcanati et al., 2012b), were transformed with plasmids pIST04-06 resulting in strains SCIST07-12 (Table II). Fed-batch cultivations were used for strain comparison as glucose limited conditions were necessary to benefit from down-regulation of *ERG9* encoding squalene synthase by the *HXT1* promoter (Ozcan and Johnston, 1995; Reifenberger et al., 1995). Additionally, the *RQ* was utilized in a feedback loop to indirectly control the glucose concentration and avoid ethanol formation. Typical fermentation profiles for volume, *RQ* and feed rate during the fed-batch phase are shown in Figure 3. As described earlier, feeding was initiated subsequent to glucose and ethanol depletion, where  $RQ < 1$ . With rising availability of glucose in the medium, the *RQ* approached the threshold of 1, where pumps were

**Table II.** Overview of *S. cerevisiae* strains used in this study.

Strain	Genotype	Plasmid	Reference
CEN.PK113-5D	<i>MATa</i> <i>MAL2-8c</i> <i>SUC2</i> <i>ura3-52</i>	None	P. Kötter, University of Frankfurt, Germany
SCICK16	<i>MATa</i> <i>MAL2-8c</i> <i>SUC2</i> <i>ura3-52</i> <i>lpp1Δ::loxP</i> <i>dpp1Δ::loxP</i> <i>P<sub>ERG9Δ::loxP-P<sub>HXT1</sub></sub></i>	None	(Scalcanati et al., 2012a)
SCIGS22	<i>MATa</i> <i>MAL2-8c</i> <i>SUC2</i> <i>ura3-52</i> <i>lpp1Δ::loxP</i> <i>dpp1Δ::loxP</i> <i>P<sub>ERG9Δ::loxP-P<sub>HXT1</sub></sub></i>	None	(Scalcanati et al., 2012b)
SCIGS24	<i>MATa</i> <i>MAL2-8c</i> <i>SUC2</i> <i>ura3-52</i> <i>lpp1Δ::loxP</i> <i>dpp1Δ::loxP</i> <i>P<sub>ERG9Δ::loxP-P<sub>HXT1</sub></sub></i>	pISP15	(Scalcanati et al., 2012b)
SCIST01	CEN.PK113-5D	pIST01	This study
SCIST02	CEN.PK113-5D	pIST02	This study
SCIST03	CEN.PK113-5D	pIST03	This study
SCIST04	CEN.PK113-5D	pIST04	This study
SCIST05	CEN.PK113-5D	pIST05	This study
SCIST06	CEN.PK113-5D	pIST06	This study
SCIST07	SCICK16	pIST04	This study
SCIST08	SCICK16	pIST05	This study
SCIST09	SCICK16	pIST06	This study
SCIST10	SCIGS22	pIST04	This study
SCIST11	SCIGS22	pIST05	This study
SCIST12	SCIGS22	pIST06	This study

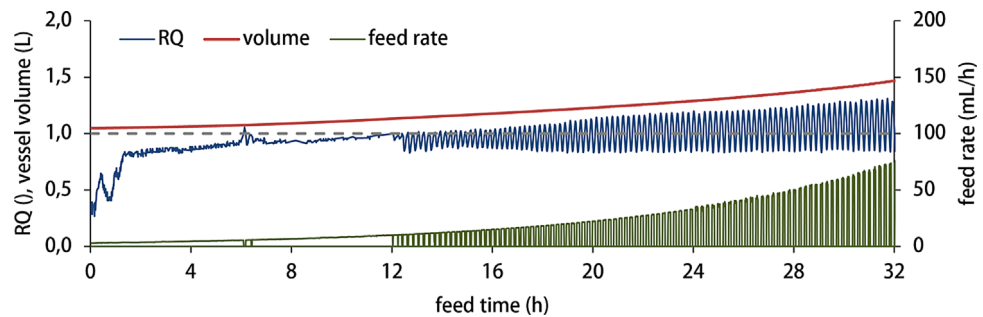


**Figure 3.** Time course of respiratory quotient (*RQ*), feed rate and volume during fed-batch phase with *RQ*-controlled exponential feeding. Data represent on-line measurements from cultivation of strain SCIST05.

turned off. The on/off switch of the feed at this value resulted in an oscillation of the *RQ* with slightly increasing amplitude over time. However, the *RQ* remained below 1.4 in all experiments.

Figure 4 illustrates the development of biomass, glucose, ethanol and farnesene concentration for all nine strains during the fed-batch phase, while Table III depicts physiological

parameters obtained from the data set. As it can be seen, *RQ* values were kept close to 1 on average throughout the fermentations, indicating successful functioning of the feedback control. This observation is also reflected by the ethanol concentration, which remained close to zero in all experiments. However, in some cases ethanol accumulation was observed at the

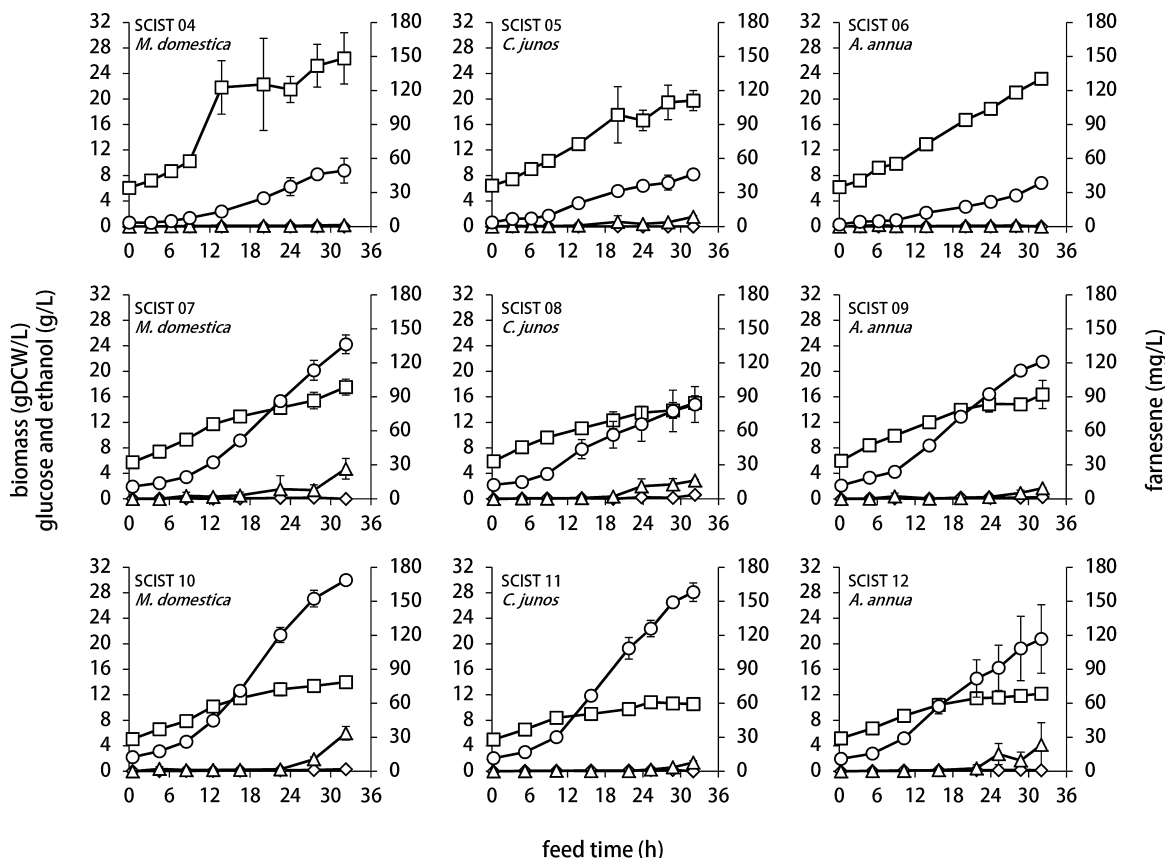


**Figure 4.** Production of farnesene in fed-batch cultivations with *RQ*-controlled exponential feeding. Background *S. cerevisiae* strains CEN.PK113-5D, SCICK16 and SCIGS22 were transformed with plasmids pIST04-06 carrying a farnesene synthase gene from *M. domestica*, *C. junos* or *A. annua* and HMG-CoA reductase gene tHMG1, resulting in strains SCIST04-12. The background strains carry the following modifications: PHXT1-*ERG9*, *dpp1* $\Delta$ , *lpp1* $\Delta$  (SCIST07-09) and PHXT1-*ERG9*, *dpp1* $\Delta$ , *lpp1* $\Delta$ , *ERG20* $\uparrow$ , *GDH2* $\uparrow$ , *gdh1* $\Delta$  (SCIST10-12). Data were obtained during the feed phase and represent average values of two or three independent biological replicates. Squares: biomass, diamonds: glucose, triangles: ethanol, circles: farnesene.

**Table III.** Physiological parameters of farnesene producing strains SCIST04-12 during fed-batch cultivations with *RQ*-controlled exponential feed.  $\mu$ : specific growth rate,  $r_s$ : specific substrate uptake rate,  $Y_{SX}$ : biomass yield,  $Y_{XFar}$ : farnesene yield and *RQ*: respiratory quotient.

Background strain	Farnesene synthase	$\mu \text{ h}^{-1}$	$r_s \text{ g}/(\text{gDCW} \cdot \text{h})$	$Y_{SX} \text{ gDCW/g}$	$Y_{XFar} \text{ g/gDCW}$	Final farnesene mg/L <sub>aqueous</sub>	<i>RQ</i> -
SCIST04	<i>M. domestica</i>	0.062 ± 0.004	0.149 ± 0.003	0.418 ± 0.017	0.002 ± 0.001	49.32 ± 10.95	0.96 ± 0.02
SCIST05	<i>C. junos</i>	0.048 ± 0.007	0.163 ± 0.016	0.297 ± 0.073	0.003 ± 0.000	46.03 ± 4.71	1.00 ± 0.02
SCIST06	<i>A. annua</i>	0.053 ± 0.002	0.170 ± 0.010	0.311 ± 0.007	0.002 ± 0.000	38.46 ± 0.28	1.00 ± 0.01
SCIST07	<i>M. domestica</i>	0.046 ± 0.004	0.172 ± 0.017	0.268 ± 0.002	0.009 ± 0.000	136.37 ± 8.23	0.97 ± 0.03
SCIST08	<i>C. junos</i>	0.035 ± 0.003	0.122 ± 0.007	0.288 ± 0.038	0.007 ± 0.001	83.30 ± 15.76	1.04 ± 0.02
SCIST09	<i>A. annua</i>	0.038 ± 0.005	0.146 ± 0.033	0.263 ± 0.025	0.010 ± 0.002	121.00 ± 1.91	1.02 ± 0.02
SCIST10	<i>M. domestica</i>	0.043 ± 0.001	0.193 ± 0.001	0.222 ± 0.007	0.015 ± 0.001	168.75 ± 4.68	0.98 ± 0.02
SCIST11	<i>C. junos</i>	0.032 ± 0.001	0.221 ± 0.003	0.146 ± 0.007	0.022 ± 0.002	158.09 ± 8.13	1.00 ± 0.01
SCIST12	<i>A. annua</i>	0.034 ± 0.000	0.199 ± 0.021	0.172 ± 0.017	0.013 ± 0.003	116.74 ± 30.26	1.01 ± 0.02

Values represent mean ± standard deviation of two or three biological replicates.

end of the fermentation for the heavily engineered strains SCIST07-12. Likewise, glucose concentration remained close to zero, which was the target condition to ensure down-regulation of *ERG9*. In consequence, production of ergosterol was limited, which led to reduced biomass formation as shown by the biomass yields in Table III. For strains SCIST07-12, final biomass concentrations did not exceed 15 gDCW/L, whereas up to 26 gDCW/L were obtained for strains SCIST04-06. However, while growth was impaired, farnesene production was increased substantially and reached final titers of up to ~170 mg/L. Similar to the results in shake flasks, highest titers were attained using  $\alpha$ -farnesene synthase from *M. domestica*, whereas expression of

$\beta$ -farnesene synthase from *C. junos* and *A. annua* resulted in final farnesene titers of approximately 160 and 120 mg/L, respectively. Surprisingly, while production could be significantly improved from background strain SCICK16 to SCIGS22 using farnesene synthases from *M. domestica* and *C. junos*, a similar increase was not observed with the farnesene synthase from *A. annua*. Ion chromatograms and mass spectra from GC-MS analysis of a dodecane sample from cultivation of strains SCIST04, SCIST06 and an authentic standard for  $\beta$ -farnesene are shown in Figure 5. While the retention time of  $\beta$ -farnesene from yeast was slightly shifted, most likely caused by dodecane, its mass spectrum revealed high resemblance to the analytical standard. In

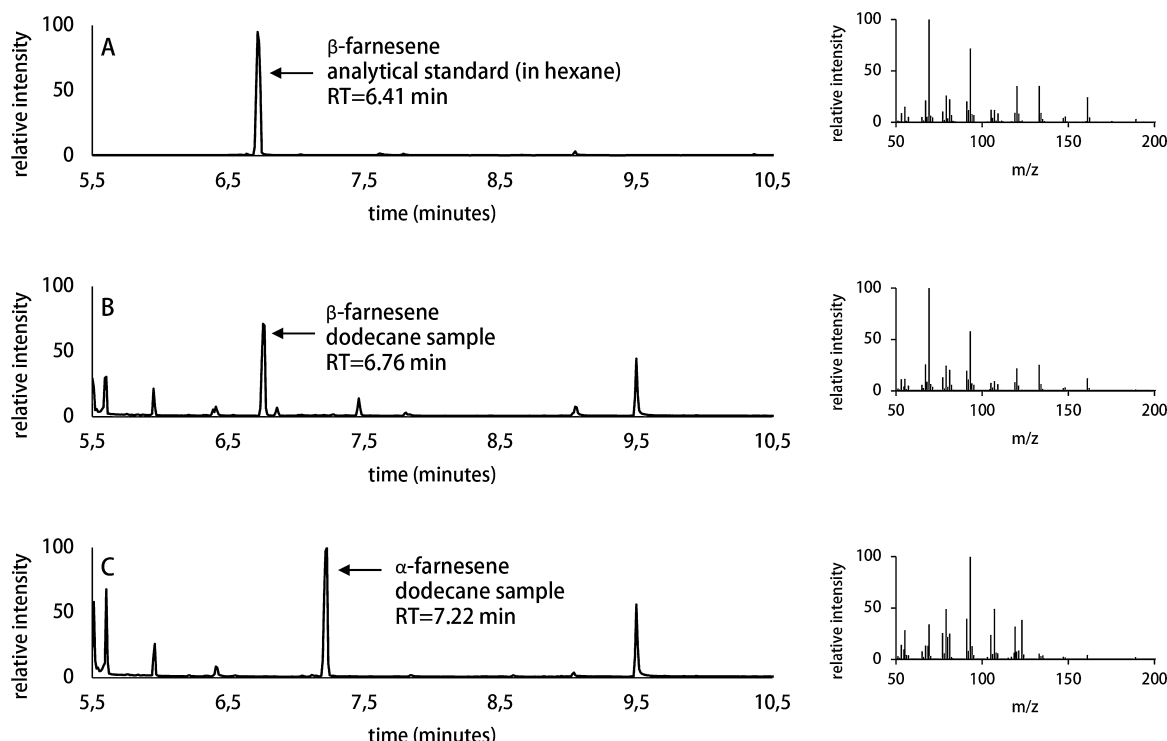


**Figure 5.** Total ion chromatograms (Left Panel) and mass spectra (Right Panel) obtained from GC-MS analysis of an authentic standard for  $\beta$ -farnesene (**A**) and dodecane samples from cultivation of strains SCIST06 (**B**) and SCIST04 (**C**) expressing the  $\beta$ -farnesene synthase gene from *A. annua* and the  $\alpha$ -farnesene synthase gene from *M. domestica*, respectively.

comparison,  $\alpha$ -farnesene had a longer retention time, but was identified by its mass spectrum.

### Production of Santalene in Fed-Batch Cultivations With RQ-Controlled Exponential Feed

Santalene is another commercially interesting sesquiterpene, which is directly produced from FPP by a specific plant terpene synthase. In order to evaluate the efficiency of the farnesene synthases in comparison to another sesquiterpene synthase, a similar RQ-controlled fed-batch fermentation with strain SCIGS24 was performed (Scalcnati et al., 2012b). This strain is identical to SCIST10-12 regarding its genetic background and only differs by carrying plasmid pISP15, which contains a codon optimized santalene synthase from *Clausena lansium* (see Table II). Similar to the fed-batch cultivations performed to investigate farnesene production, the feed was controlled using the RQ, which was maintained at 0.98 on average throughout the experiment. However, as the batch phase medium contained 30 g/L glucose, higher biomass concentrations were attained overall reaching up to 25 gDCW/L (Fig. 6). This is also indicated by the biomass yield of 0.281 gDCW/g, which was significantly higher. However, the product yield of 0.006 g/gDCW amounts only to half compared to the one observed for the farnesene synthases. Considering the production of santalene, with 163 mg/L of  $\alpha$ -santalene after approximately 30 h of feeding time, final titers were almost equivalent to cultivations using strains SCIST10-12.

## Discussion

The sesquiterpene farnesene fulfills various functions in plants and represents a biofuel precursor that can be obtained efficiently from yeast fermentation. Terpene production is strongly dependent on the availability of the precursors GPP, FPP and GGPP. Furthermore,

limitations to the overall productivity are added by terpene synthases, which catalyze the conversion of these precursors, but mostly originate from plant sources. The impact of these aspects was recently illustrated for mono-, sesqui- and diterpene production. Ding et al. (2014) selected suitable GGPP synthases by predicting their catalytic efficiency *in silico* and thereby raised production of the diterpene taxadiene up to 73 mg/L. Likewise, screening of different combinations of GPP and pinene synthases revealed to significantly improve production of pinene in *E. coli* (Sarria et al., 2014). Furthermore, Xie et al. (2012) isolated novel terpene synthases from *Ricinus communis*, which were tested for production of sesquiterpenes in *E. coli* and *S. cerevisiae*.

Recent studies have described production of farnesene in *E. coli* and characterization of several farnesene synthases *in vitro*. Yet a comparison of different farnesene synthases in an industrial process setup has not been reported. In this study we expressed three different farnesene synthase genes from plants in *S. cerevisiae* and successfully produced both,  $\alpha$ - and  $\beta$ -farnesene. All enzymes showed high product specificity in our experiments. Only in case of farnesene synthase from *C. juncos*, sesquiphellandrene was detected as byproduct. *S. cerevisiae* CEN.PK113-5D expressing  $\alpha$ -farnesene synthase from *M. domestica* produced 4 mg/L in shake flask cultivation, which was 17 and 32% higher in comparison to the corresponding synthases from *C. juncos* and *A. annua*, respectively. By using the same farnesene synthase in a *S. cerevisiae* strain optimized for sesquiterpene production (SCIST10), final titers of approximately 170 mg/L were attained in fed-batch cultivations using RQ-controlled exponential feeding. Similar to the results in shake flasks, farnesene synthase from *M. domestica* led to maximal titers in all strain backgrounds suggesting higher efficiency of this enzyme. However, when comparing the different synthases in the respective background strain (e.g. for SCIST07-09), the titer ratio clearly fluctuated, which could be explained by variations in the biomass yields  $Y_{SX}$ . Taking the product yields  $Y_{XFar}$  into consideration, a farnesene synthase with clearly superior efficiency could not be identified from these experiments. In general, performance of the fed-batch operation exerted a strong influence on the final product titers. As depicted in Table III, significant differences regarding the specific growth rates were observed between all strains, where a growth rate of 0.1 1/h was not attained. This was caused by the initial feed rate  $v_0$ , which was chosen too low and would require elevated biomass yields to compensate. However, based on these results, biomass yields of 0.3–0.4 gDCW/g were even slightly reduced compared to previous experiments, where  $Y_{SX}$  amounted for 0.5 gDCW/g (Scalcnati et al., 2012b).

As described above, feed control by RQ was used to maintain fully aerobic respiration as ethanol accumulation was anticipated to cease at an RQ of 1. However, ethanol formation was still observed at the end of the cultivations, mostly for strains SCIST07-12. Several aspects may have played a role for this effect. Most likely, higher fluctuations of the RQ, which occurred at the end of the fermentations in particular, could have led to overfeeding and thereby to ethanol formation. On the other hand, fed-batch cultivations with exponential feeding are normally only performed until mass transfer becomes limiting. At this point, the exponential feed phase is terminated and the feed is set to a constant value to avoid stress responses (Villadsen and Patil, 2007). Although the

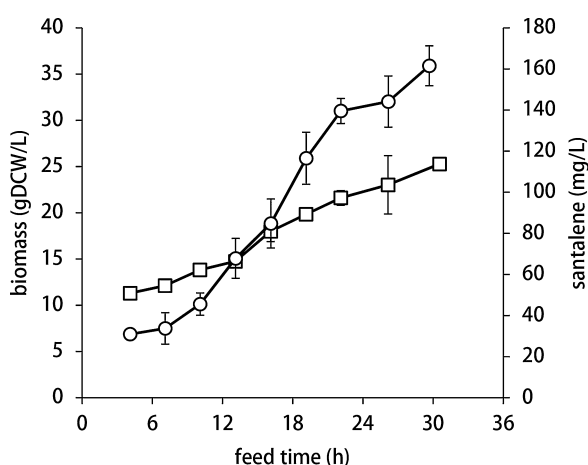


**Figure 6.** Production of santalene in fed-batch cultivations with RQ-controlled exponential feeding, using strain SCIGS24 expressing HMG-CoA reductase gene *tHMG1* and the  $\alpha$ -santalene synthase gene from *C. lansium* from plasmid pISP15. Data shown were obtained during the fed-batch phase and represent average values of three independent biological replicates. Squares: biomass, circles: santalene.

aeration rate was increased proportionally to the reaction volume, dissolved oxygen concentrations (*DO*) dropped below 20% in most experiments. As a result, partial limitation of oxygen may have contributed to ethanol formation as well. In addition, ethanol formation might have been directly related to down-regulation of *ERG9*, as insufficient feeding may have completely blocked ergosterol synthesis and thereby hindered growth. As a result, ethanol is produced for regeneration of NAD<sup>+</sup>. This can be seen particularly from the growth profiles of strains SCIST10-12. When biomass concentration almost reached steady state after 24 h, ethanol accumulation set in. On the other hand, ethanol accumulation in SCIST12 cultures also serves as a possible explanation why similar final farnesene titers were obtained for SCIST09 and 12 despite the additional genome modifications in SCIST12. For these reasons, farnesene titers would likely have been higher than reported in Table III, if ethanol formation had been cut off completely. Nonetheless, in an industrial scenario, the cultivation could be continued after the feed phase to allow for ethanol depletion by *S. cerevisiae*.

Reconsidering the impact of the selected plant terpene synthases, none of the three candidates revealed outstanding efficiency during the fed-batch evaluation. This, however, does not allow for a general conclusion in relation to farnesene synthases. Although alignment of the amino acid sequences of the selected candidates using the BLASTalgorithm did not score identities above 41%, greater genetic distances between the natural hosts may lead to identification of a synthase with superior efficiency. A different perspective on the efficiency of these enzymes might be obtained by comparing production of farnesene to other sesquiterpenes. We therefore used santalene as a second case study since it represents another sesquiterpene of great commercial interest, which requires a plant terpene synthase to catalyze the direct conversion of FPP to the desired product. By using  $\alpha$ -santalene synthase from *C. lansium*, 92 mg/L could be produced in fed-batch cultivations with exponential feeding at a fixed growth rate of 0.6 1/h (Scalcanati et al., 2012a). Cultivation of strain SCIGS24 carrying a plasmid for expression of *tHMG1* and a codon optimized santalene synthase in fed-batch with *RQ*-controlled feeding resulted in final titers of 163 mg/L. This observation indicates similar efficiencies of the santalene and farnesene synthase. However, as the biomass yield was significantly higher compared to strains SCIST10-12, the product yield on substrate during the fed-batch phase amounted to only 0.006 g/gDCW, which represents a more than 50% decrease compared to the results on farnesene in the same strain background. An explanation for this reduction may be the cyclization involved in santalene production, which adds complexity to the reaction and influences the kinetics of the corresponding enzyme.

To conclude on the experimental setup, *RQ*-controlled exponential feeding was successfully implemented to evaluate the three selected farnesene synthases in strains that are differently optimized for sesquiterpene production. However, instead of indirectly targeting a certain substrate concentration by controlling the *RQ*, feed control using a glucose sensor might be even more precise (Beom Soo et al., 1994). Nevertheless, high cell densities were attained and ethanol accumulation could be kept to a minimum. Furthermore, a clear improvement in farnesene

production was seen from strains SCIST04-06 to SCIST10-12. While similar titers were attained for santalene, the product yield on biomass was substantially lower in this case.

The authors wish to thank the Knut and Alice Wallenberg Foundation, FORMAS, the Swedish Research Council VR and the Novo Nordisk Foundation. We thank Dr. António Roldão for his assistance during the fed-batch experiments.

## References

- Asadollahi MA, Maury J, Møller K, Nielsen KF, Schalk M, Clark A, Nielsen J. 2008. Production of plant sesquiterpenes in *Saccharomyces cerevisiae*: Effect of *ERG9* repression on sesquiterpene biosynthesis. *Biotechnol Bioeng* 99(3):666–677.
- Beom Soo K, Seung Chul L, Sang Yup L, Ho Nam C, Yong Keun C, Seong Ihl W. 1994. Production of poly(3-hydroxybutyric acid) by fed-batch culture of *Alcaligenes eutrophus* with glucose concentration control. *Biotechnol Bioeng* 43(9): 892–898.
- Chen F, Tholl D, Bohlmann J, Pichersky E. 2011. The family of terpene synthases in plants: A mid-size family of genes for specialized metabolism that is highly diversified throughout the kingdom. *Plant J.* 66(1):212–229.
- Crock J, Wildung M, Croteau R. 1997. Isolation and bacterial expression of a sesquiterpene synthase cDNA clone from peppermint (*Mentha x piperita*, L.) that produces the aphid alarm pheromone (E)- $\beta$ -farnesene. *Proc Natl Acad Sci USA* 94(24):12833–12838.
- Ding MZ, Yan HF, Li LF, Zhai F, Shang LQ, Yin Z, Yuan YJ. 2014. Biosynthesis of taxadiene in *Saccharomyces cerevisiae*: Selection of geranylgeranyl diphosphate synthase directed by a computer-aided docking strategy. *PLoS ONE* 9(10):1–9.
- Geurts TGE, De Kok HE, Roels JA. 1980. A quantitative description of the growth of *Saccharomyces cerevisiae* CBS 426 on a mixed substrate of glucose and ethanol. *Biotechnol Bioeng* 22(10):2031–2043.
- Green S, Friel EN, Matich A, Beuning LL, Cooney JM, Rowan DD, MacRae E. 2007. Unusual features of a recombinant apple  $\alpha$ -farnesene synthase. *Phytochemistry* 68(2):176–188.
- Holm T. 1999. Aspects of the mechanism of the flame ionization detector. *J Chromatogr A* 842(1-2):221–227.
- Martin VJJ, Yoshikuni Y, Keasling JD. 2001. The *in vivo* synthesis of plant sesquiterpenes by *Escherichia coli*. *Biotechnol Bioeng* 75(5):497–503.
- Maruyama T, Ito M, Honda G. 2001. Molecular cloning, functional expression and characterization of (E)- $\beta$ -farnesene synthase from *Citrus junos*. *Biol Pharm Bull* 24(10):1171–1175.
- Meylemans HA, Quintana RL, Harvey BG. 2012. Efficient conversion of pure and mixed terpene feedstocks to high density fuels. *Fuel* 97:560–568.
- Millo F, Bensaid S, Fino D, Castillo Marcana SJ, Vlachos T, Debnath BK. 2014. Influence on the performance and emissions of an automotive Euro 5 diesel engine fueled with F30 from Farnesane. *Fuel* 138:134–142.
- Nielsen J, Villadsen J, Lidén G. 2002. Bioreaction engineering principles. Springer Verlag. p. 411–416.
- Ohto C, Muramatsu M, Obata S, Sakuradani E, Shimizu S. 2009. Overexpression of the gene encoding HMG-CoA reductase in *Saccharomyces cerevisiae* for production of prenyl alcohols. *Appl Microbiol Biotechnol* 82(5):837–845.
- Ozcan S, Johnston M. 1995. Three different regulatory mechanisms enable yeast hexose transporter (HXT) genes to be induced by different levels of glucose. *Mol Cell Biol* 15(3):1564–1572.
- Paddon CJ, Westfall PJ, Pitera DJ, Benjamin K, Fisher K, McPhee D, Leavell MD, Tai A, Main A, Eng D, Ellens KW, Fickes S, Galazzo J, Gaucher SP, Geistlinger T, Henry R, Hepp M, Horning T, Iqbal T, Kizer L, Lieu B, Melis D, Moss N, Regentin R, Secrest S, Tsuruta H, Vazquez R, Westblade LF, Xu L, Yu M, Zhang Y, Zhao L, Lievense J, Covello PS, Keasling JD, Reiling KK, Renninger NS, Newman JD. 2013. High-level semi-synthetic production of the potent antimalarial artemisinin. *Nature* 496(7446):528–532.
- Partow S, Siewers V, Björn S, Nielsen J, Maury J. 2010. Characterization of different promoters for designing a new expression vector in *Saccharomyces cerevisiae*. *Yeast* 27(11):955–964.

- Pechous SW, Whitaker BD. 2004. Cloning and functional expression of an (E,E)- $\alpha$ -farnesene synthase cDNA from peel tissue of apple fruit. *Planta* 219(1): 84–94.
- Peralta-Yahya PP, Ouellet M, Chan R, Mukhopadhyay A, Keasling JD, Lee TS. 2011. Identification and microbial production of a terpene-based advanced biofuel. *Nat Commun* 2:483.
- Pham HTB, Larsson G, Enfors SO. 1998. Growth and energy metabolism in aerobic fed-batch cultures of *Saccharomyces cerevisiae*: Simulation and model verification. *Biotechnol Bioeng* 60(4):474–482.
- Picaud S, Brodelius M, Brodelius PE. 2005. Expression, purification and characterization of recombinant (E)- $\beta$ -farnesene synthase from *Artemisia annua*. *Phytochemistry* 66(9):961–967.
- Polakowski T, Stahl U, Lang C. 1998. Overexpression of a cytosolic hydroxymethylglutaryl-CoA reductase leads to squalene accumulation in yeast. *Appl Microbiol Biotechnol* 49(1):66–71.
- Reifenberger E, Freidel K, Ciriacy M. 1995. Identification of novel HXT genes in *Saccharomyces cerevisiae* reveals the impact of individual hexose transporters on glycolytic flux. *Mol Microbiol* 16(1):157–167.
- Rupasinghe HPV, Paliyath G, Murr DP. 2000. Sesquiterpene  $\alpha$ -farnesene synthase: Partial purification, characterization, and activity in relation to superficial scald development in apples. *J Am Soc Hortic Sci* 125(1):111–119.
- Sarria S, Wong B, Martín HG, Keasling JD, Peralta-Yahya P. 2014. Microbial synthesis of pinene. *ACS Synth Biol* 3(7):466–475.
- Scalcanati G, Knuf C, Partow S, Chen Y, Maury J, Schalk M, Daviet L, Nielsen J, Siewers V. 2012a. Dynamic control of gene expression in *Saccharomyces cerevisiae* engineered for the production of plant sesquiterpene  $\alpha$ -santalene in a fed-batch mode. *Metab Eng* 14(2):91–103.
- Scalcanati G, Partow S, Siewers V, Schalk M, Daviet L, Nielsen J. 2012b. Combined metabolic engineering of precursor and co-factor supply to increase  $\alpha$ -santalene production by *Saccharomyces cerevisiae*. *Microb Cell Fact* 11:1–16.
- Tippmann S, Chen Y, Siewers V, Nielsen J. 2013. From flavors and pharmaceuticals to advanced biofuels: Production of isoprenoids in *Saccharomyces cerevisiae*. *Biotechnol J* 8(12):1435–1444.
- Tippmann S, Nielsen J, Khoomrung S. 2015. Improved quantification of farnesene during microbial production from *S. cerevisiae* in two-liquid-phase fermentations. Submitted.
- Verduyn C. 1991. Physiology of yeasts in relation to biomass yields. *Antonie Van Leeuwenhoek* 60(3-4):325–353.
- Verduyn C, Postma E, Scheffers WA, van Dijken JP. 1992. Effect of benzoic acid on metabolic fluxes in yeasts: A continuous-culture study on the regulation of respiration and alcoholic fermentation. *Yeast* 8(7):501–517.
- Villadsen J, Patil KR. 2007. Optimal fed-batch cultivation when mass transfer becomes limiting. *Biotechnol Bioeng* 98(3):706–710.
- Wang C, Yoon SH, Jang HJ, Chung YR, Kim JY, Choi ES, Kim SW. 2011. Metabolic engineering of *Escherichia coli* for  $\alpha$ -farnesene production. *Metab Eng* 13(6):648–655.
- Xie X, Kirby J, Keasling JD. 2012. Functional characterization of four sesquiterpene synthases from *Ricinus communis* (Castor bean). *Phytochemistry* 78:20–28.

# **Metabolic and transcriptomic response to production of farnesene in *Saccharomyces cerevisiae***

Stefan Tippmann, Sakda Khoomrung, Partho Sarathi Sen, Intawat Nookaew and Jens Nielsen

*Manuscript in Preparation*



Metabolic and transcriptomic response to production of farnesene in  
*Saccharomyces cerevisiae*

Stefan Tippmann<sup>1,2</sup>, Sakda Khoomrung<sup>1,2</sup>, Partho Sarathi Sen<sup>1,2</sup>, Intawat Nookaew<sup>1,2,3</sup> and Jens Nielsen<sup>1,2,4\*</sup>

<sup>1</sup>Department of Biology and Biological Engineering,  
Chalmers University of Technology, SE412 96 Gothenburg, Sweden

<sup>2</sup>Novo Nordisk Foundation Center for Biosustainability, Chalmers University of Technology, SE412 96  
Gothenburg, Sweden

<sup>3</sup>Department of Biomedical Informatics, University of Arkansas for Medical Sciences, Little Rock, AR  
72205, USA

<sup>4</sup>Novo Nordisk Foundation Center for Biosustainability, Technical University of Denmark, DK2970  
Hørsholm, Denmark

\*Corresponding Author: Jens Nielsen

Department of Biology and Biological Engineering,  
Chalmers University of Technology, Kemivägen 10, SE412 96, Gothenburg, Sweden.

E-mail: nielsenj@chalmers.se

Tel: +46 31772 38 04

Fax: +46 31 772 38 01

Keywords: isoprenoids, yeast, metabolome, transcriptome, metabolic engineering

## Abstract

Metabolic engineering has enabled sustainable production of several sesquiterpenes in *S. cerevisiae*, which have versatile applications within the chemical industry. While the effect of a genetic modification is mostly measured by its ability to improve product formation, modifications may exert effects away from the pathway used for product formation, which could provide insights on potential engineering targets. Systems biology provides tools to study and characterize microbial strains used for chemical production. In this study, production of farnesene in *S. cerevisiae* was investigated using metabolome and transcriptome analysis with the objective to study the global response of the strain to the modified metabolism. As expected, significant changes were observed regarding sterol synthesis for the strain engineered to produce farnesene. Additionally, pathways for nitrogen assimilation, amino acid and vitamin synthesis were mostly affected.

## Introduction

The yeast *Saccharomyces cerevisiae* has emerged to a suitable production host for a broad range of chemicals (Nielsen 2015). In our lab, *S. cerevisiae* was successfully engineered to produce the sesquiterpene and fragrance santalene (Scalcanati et al. 2012), a platform which could also be used for production of the diesel precursor farnesene (Tippmann et al. 2016). Several metabolic engineering strategies were combined to attain this phenotype. First, the flux through the mevalonate pathway was increased by overexpression of *tHMG1* and *ERG20*, encoding a truncated version of HMG-CoA reductase and farnesyl diphosphate synthase, respectively. Secondly, to increase the availability of the sesquiterpene precursor farnesyl diphosphate (FPP), *ERG9* encoding squalene synthase, was downregulated to reduce ergosterol formation and the two phosphatases Lpp1p and Dpp1p were deleted to minimize the production of farnesol. Lastly, ammonium assimilation was modified to improve co-factor balance of the pathway by deleting the NADPH-dependent glutamate dehydrogenase (*GDH1*) and overexpressing the NADH-dependent isozyme (*GDH2*). Downregulation of *ERG9* was enabled using the *HXT1* promoter, which shows reduced activity at low glucose concentrations (Ozcan and Johnston 1995; Reifenberger et al. 1995). By controlling the glucose concentration in fed-batch cultivations, this modification was activated and more flux could be diverted towards the desired product. As a result, increased production of sesquiterpenes was closely linked to the change of the environmental condition initiated during the fed-batch.

In the present study, we investigated the response of *S. cerevisiae* to these genetic modifications with the overall objective to identify flux controlling reactions during the production of sesquiterpenes and ultimately, to derive new metabolic engineering targets. As an example, tolerance towards farnesene or stress in connection to the overproduction of farnesene could potentially impose limitations to the product yield. Especially monoterpenes have been reported to exert toxic effects on *S. cerevisiae* (Brennan et al. 2013; Hu et al. 2012; Liu et al. 2013). Besides, accumulation of mevalonate pathway intermediates, such as prenyl diphosphates might as well be toxic to the cell, as it has been shown for *E. coli* (Martin et al. 2003; Withers et al. 2007). As an example, accumulation of HMG-CoA was identified to inhibit fatty acid synthesis (Kizer et al. 2008). Although these mechanisms have not been studied as extensively in yeast, similar observations have been reported (Yuan and Ching 2015). Apart from this, ergosterol synthesis represents a highly regulated pathway (Dimster-Denk and Rine 1996; Dimster-Denk et al. 1994; Hampton et al. 1996; Kennedy et al. 1999) and the response of the strain upon modification of the pathway is of key importance to increase its production capacity.

As first step, the physiology of the strain was investigated in fed-batch cultivations. Subsequently, the metabolome of the strain was studied, which has become a powerful technology to study the phenotype of both plants and microorganisms (Fiehn 2002; Merlo et al. 2011). Its potential to advance synthetic biology as a tool to investigate the response of microorganisms to changing environmental conditions and stresses or to identify limiting reactions in metabolic pathways has been highlighted by Ellis and Goodacre (2012) and Nguyen et al. (2012). In this respect, metabolomics has been recently used in *S. cerevisiae* to study copper toxicity (Farrés et al. 2016) and to optimize methionine production (Hayakawa et al. 2016). In *E. coli*, methylerythritol cyclodiphosphate efflux was identified to reduce production of isoprenoids from the methylerythritol 4-phosphate pathway using metabolite profiling (Zhou et al. 2012). We focused primarily on untargeted metabolomics as it cannot only be used to directly characterize the phenotype, but also to detect changes in other pathways. Recently, several *in silico* predicted gene deletions were experimentally confirmed to significantly improve amorphadiene production in *S. cerevisiae* (Sun et al. 2014). The identified genes were involved in versatile metabolic processes such glucose metabolism (i.e. glycolysis and TCA cycle), amino acid and redox metabolism; in several cases without apparent connection to the pathway used for product formation. Hence, untargeted analysis of the metabolome could provide further insights in comparison to solely quantifying mevalonate pathway intermediates. Due to the high turnover rate of low molecular weight compounds, however, which could potentially lead to high variations in the data and the fact that the unambiguous identification of all metabolites remains a challenging task, RNAseq-based transcriptomics was used to complement these results and to identify the origin of the phenotypic changes captured by the metabolome data. In conclusion, this study presents a profound analysis of the metabolic and transcriptomic changes in *S. cerevisiae* upon engineering of cellular metabolism for overproduction of sesquiterpenes.

## Materials and Methods

### *Reagents, solvents and standards*

#### Solvents

Methanol and acetonitrile, HPLC-grade, were obtained from Fischer Scientific (Waltham, MA, USA). Chloroform, Suprasolv for GC was obtained from Merck (Darmstadt, Germany). 2-Propanol, HPLC-grade was obtained from VWR (Radnor, PA, USA). H<sub>2</sub>O, Milli-Q.

### Reference and tuning standards

All reference and tuning standards were purchased from Agilent Technologies (Santa Clara, CA, USA), i.e. Purine (4 µM), HP-0921 (Hexakis(1H, 1H, 3H-tetrafluoropropoxy)phosphazine, 1 µM), Calibrant ESI-TOF, ESI-L Low Concentration Tuning Mix, HP-0321 (Hexamethoxyphosphazine, 0.1 mM).

### *Cultivation medium*

*S. cerevisiae* strains were grown on plates containing selective medium with 6.9 g/L yeast nitrogen base w/o amino acids (Formedium, Hunstanton, UK), 0.77 g/L complete supplement mixture w/o uracil (Formedium), 20 g/L glucose and 20 g/L agar. Shake flask cultivations were performed in minimal medium containing 30 g/L glucose, 7.5 g/L  $(\text{NH}_4)_2\text{SO}_4$ , 14.4 g/L  $\text{KH}_2\text{PO}_4$ , 0.5 g/L  $\text{MgSO}_4 \cdot 7\text{H}_2\text{O}$ , 2 mL/L trace element solution and 50 µL/L antifoam (Sigma-Aldrich, St. Louis, MO, USA). After sterilization, vitamin solution was added at a concentration of 1 mL/L. The batch phase medium during aerated bioreactor cultivations contained 20 g/L glucose, 5 g/L  $(\text{NH}_4)_2\text{SO}_4$ , 3 g/L  $\text{KH}_2\text{PO}_4$ , 0.5 g/L  $\text{MgSO}_4 \cdot 7\text{H}_2\text{O}$ , 1 mL/L trace element solution, 50 µL/L antifoam and 1 mL/L vitamin solution. The composition of the trace element and vitamin solution has been reported by Verduyn et al. (1992). The feed medium during the fed-batch phase was ten times concentrated and contained glucose to a concentration of 200 g/L.

### *Cultivation in bioreactors*

Prior to cultivations in bioreactors, a single colony from an agar plate containing selective medium was used to inoculate 5 mL of minimal medium. The culture was incubated at 200 rpm and 30 °C overnight. Subsequently, the culture was transferred to a baffled shake flask containing 50 mL of minimal medium and incubated at 200 rpm and 30 °C for 24 h. The optical density was measured at a wavelength of 600 nm using a spectrophotometer (Genesis20, Thermo Fisher Scientific, Waltham, MA, USA) and the batch phase medium was inoculated at an OD<sub>600</sub> of 0.1. Cultivations in bioreactors were performed using the DasGip Parallel Bioreactor Systems for Microbiology (Eppendorf, Hamburg, Germany). The vessels were flushed with air at an aeration rate of 1 vvm and homogenous mixing was enabled using a six-blade Rushton turbine at 600 rpm. The pH was controlled at 5 using 2 M KOH and 2 M HCl and the temperature was maintained at 30 °C. The feeding rate during the fed-batch phase was set to  $v(t)=0.003 \cdot \exp(0.08 \cdot t)$  with  $v$  as the feeding rate in L/h and  $t$  as time in h.

### *RNA and metabolite extraction*

Samples for RNA sequencing (RNAseq) and metabolome analysis were taken simultaneously during each of the three phases. While batch phase samples were taken towards the end of the glucose and ethanol phase, respectively, samples during the fed-batch phase were taken after one residence time (~22 h of feeding time). For RNA extraction, 2 mL samples were taken and instantly put on ice. The medium was

discarded after centrifugation at 0 °C and 8000 rpm for 2 min. Subsequently, the samples were frozen in liquid nitrogen and stored at -80 °C. RNA was extracted using the RNeasy Mini Kit (Qiagen, Hilden, Germany) and submitted to the National Genomics Infrastructure (NGI, Stockholm) for strand specific TruSeq RNA library preparation with poly-A selection and sequencing using an Illumina HiSeq 2500 (Illumina, San Diego, CA, USA). For metabolome analysis, quenching was performed as described previously (Khoomrung et al. 2015). Briefly, 20 mL of methanol were pre-cooled at -40 °C in an ethanol bath. A 5 mL culture sample was withdrawn from the vessel and directly added to the pre-cooled methanol. Subsequent to centrifugation of the sample at -20 °C and 4000 rpm for 5 min, the medium was discarded and the biomass was re-suspended in 20 mL ice-cold methanol. Lastly, the sample was centrifuged at -20 °C and 4000 rpm for 5 min again and the methanol phase was discarded. Metabolite extraction was performed according the known protocol described previously (A et al. 2005) using methanol-water (90:10 v/v) where the stable isotope of D4-Cholic acid, obtained from Sigma (St. Louis, MO, USA), was added used an internal standard.

#### *Metabolome analysis by LC-qTOF*

The chromatographic separation was performed on an Agilent 1290 Infinity UHPLC-system (Agilent Technologies). A 2 µL aliquot of re-suspended yeast extract was injected onto an Acquity UPLC HSS T3, 2.1 x 50 mm, 1.8 µm C<sub>18</sub> column in combination with a 2.1 mm x 5 mm, 1.8 µm VanGuard precolumn at 40 °C (Waters Corporation, Milford, MA, USA). The elution buffers were A (H<sub>2</sub>O, 0.1 % formic acid) and B (75/25 acetonitrile:2-propanol, 0.1 % formic acid), and the flow rate was set to 0.5 mL min<sup>-1</sup>. Compounds were eluted using a linear gradient, consisting of the following steps. After % of B in the eluent increased from 0.1 - 10 % within 2 minutes, B was increased to 99 % within 5 minutes and held at 99 % for 2 minutes. Subsequently, % of B was decreased to 0.1 % for 0.3 minutes and thereafter set to 0 %. The flow rate was increased to 0.8 mL min<sup>-1</sup> for 0.5 minutes and then reduced to 0.5 mL min<sup>-1</sup> again. Finally, prior to the next injection, the eluent composition was adjusted to 0.1 % of B for 0.1 minutes. The compounds were detected with an Agilent 6550 qTOF mass spectrometer equipped with a jet stream electrospray ion source operating in positive or negative ion mode. All samples were first analyzed in positive mode. After the samples had been analyzed, the instrument was switched to negative mode and a second injection of each sample was performed. The settings were kept identical between the modes, with exception of the capillary voltage. A reference interface was connected for accurate mass measurements; the reference ions purine (4 µM) and HP-0921 (Hexakis (1H, 1H, 3H-tetrafluoropropoxy)phosphazine) (1 µM) were infused directly into the MS at a flow rate of 0.05 mL min<sup>-1</sup> for internal calibration, and the monitored ions were purine m/z 121.05 and m/z 119.03632; HP-0921 m/z 922.0098 and m/z 966.000725 for positive and

negative mode, respectively. The gas temperature was set to 150°C, the drying gas flow to 16 L min<sup>-1</sup> and the nebulizer pressure to 35 psig. The sheath gas temperature was set to 350°C and the sheath gas flow to 11 L min<sup>-1</sup>. The capillary voltage was set to 4000 V in positive ion mode, and to 4000 V in negative ion mode. The nozzle voltage was 300 V. The fragmentor voltage was 380 V, the skimmer 45 V and the OCT 1 RF Vpp 750 V. The collision energy was set to 0 V. The m/z range was 70 - 1700, and data was collected in centroid mode with an acquisition rate of 4 scans s<sup>-1</sup> (1977 transients/spectrum). The diode array detector was set to scan the interval 190 - 640 nm with a step length of 2 nm and a slit width of 4 nm.

#### *Acquisition and analysis of RNAseq transcriptome data*

Raw reads were processed follow the procedure of Nookaew et al. (2012) to obtain a read count table for further statistical analysis. In brief, raw reads will be quality trimmed with Solexaqa++ software (Cox et al. 2010) with phred score cut-off > 20. Only quality reads that have length > 25 bp were kept for alignments to the *S. cerevisiae genome* version R64 (retrieved from SGD database, [www.yeastgenome.org](http://www.yeastgenome.org)) by Stampy software (Lunter and Goodson 2011) then read count of all individual gene were calculated by bedtools2 (Quinlan and Hall 2010). The statistical analysis to compare the difference between wild type and engineered strain under the same growth phase were performed in R suite software with precision weights unlock linear model analysis approach (Law et al. 2014). The functional enrichment of gene ontology (GO) and reporter metabolite based on iTO977 model (Österlund et al. 2012) were performed by the PIANO package (Väremo et al. 2013).

#### *Acquisition and analysis of LC-qTOF metabolome data*

Mass Feature Extraction (MFE) from the data acquired was performed using the MassHunter™ Qualitative Analysis software package, version B06.00 (Agilent Technologies). Extracted features were aligned and matched between samples using Mass Profiler Professional™ 12.5 (Agilent Technologies). The final output from peak picking is an excel sheet that contains intensities, molecular mass (*m/z*), retention time (RT) of each feature or internal standard. All metabolite intensities were normalized by dividing them with the intensity of the internal standard D4-cholic acid in the respective sample (Gullberg et al. 2004). Subsequently, multivariate data analysis was performed using SIMCA 14.1 (MKS Data Analytics Solutions, Umeå, Sweden). In particular, the software was used to perform principle component analysis (PCA) and to fit an orthogonal partial least-squares to latent structures model (OPLS-DA) (Wiklund et al. 2008). Additionally, the software was used to perform pairwise comparison of the strains in each condition, i.e. to calculate the average intensities of all features together, the fold change and the statistical significance of the change (*p*-value). Feature identification was performed based on the accurate mass measurement using the METLIN library (<https://metlin.scripps.edu/index.php>) with mass error of 5 ppm. In order to

identify changing metabolic processes, KEGG IDs were retrieved for the identified compounds and used to search in the MBRole library (<http://csbg.cnb.csic.es/mbrole/Controller>).

## Results and Discussion

### *Physiological response of *S. cerevisiae* to mevalonate pathway modifications*

The strain engineered for sesquiterpene production, SCIST11 (abbreviated ENG) and the reference strain, SCIST05 (abbreviated WT) were cultivated in fed-batch mode in order to activate downregulation of *ERG9* using  $P_{HXT1}$ . The hexose transporter HXT1p is utilized in *S. cerevisiae* at higher glucose concentrations (Ozcan and Johnston 1995; Reifenberger et al. 1995). Upon reduction of the glucose concentration in the medium, expression of *ERG9* is restricted (Scalcanati et al. 2012). Since the cultivation is performed as a batch before the feed is initiated, the engineered strain can be studied in three distinct metabolic conditions. In the beginning of the experiment, excess glucose is available, resulting in respiro-fermentative metabolism and the formation of ethanol. Subsequent to glucose depletion, ethanol is respired while glucose respiration is targeted during the fed-batch phase, the objective is to obtain fully respiratory growth on glucose and to avoid ethanol formation. All cultivations were performed without addition of an extractive dodecane overlay in order to avoid interference of dodecane in downstream analytical procedures, i.e. metabolite extraction/analysis and particularly RNA extraction/sequencing. For data concerning the production of farnesene by these strains, the reader is referred to a previous study (Tippmann et al. 2016). Data for biomass, glucose and ethanol as well as the CO<sub>2</sub> content measured in the exhaust gas are presented in Figure 1 for each cultivation. Overall, strain SCIST11 (ENG) displayed very similar growth kinetics compared to the reference (SCIST05). Glucose consumption in the batch phase was prolonged and the maximum CO<sub>2</sub> content measured by the exhaust gas analyzer decreased from 1.5 to 1.0 %. Likewise ethanol respiration was slightly prolonged. In both cases, downregulation of *ERG9* could presumably lead to this phenotype as  $P_{HXT1}$  is only activated at high glucose concentrations, whereas expression of *ERG9* is expected to shut off completely during the consumption of ethanol. During the fed-batch phase, both strains grew under fully oxidative conditions since ethanol concentrations remained 0 g/L throughout the entire feeding phase. Strain SCIST05 (WT) reached final biomass concentrations of almost 25 gDCW/L, while SCIST11 (ENG) grew up to approximately 20 gDCW/L. To capture the changes observed when comparing the physiology of the two strains, Table 2 presents an overview of several parameters calculated during each of the three conditions. Particularly, the specific growth rate seemed to be slightly reduced, while biomass and ethanol yield were not affected.

### *Metabolome analysis*

We chose to analyze the metabolome using LC-qTOF. As the extraction method was shown to have a strong effect to the outcome of metabolomics studies (Duportet et al. 2012), we used a methanol-water as solvent, which has been shown to extraction yield for serum samples (A et al. 2005). In total, 1911 features could be extracted in positive mode and 1975 in negative mode. The PCA plot presented in Figure 2A provides a general overview of the structure of the data.

### *Transcriptome analysis*

As indicated by the PCA plot shown in Figure 3, the two strains of *S. cerevisiae* clearly separated by sample time point, which visualizes the differences between the three distinct metabolic conditions, i.e. respiro-fermentative metabolism on glucose (B-Glu), ethanol respiration (B-Eth) and glucose respiration (FB-Glu). However, the two strains cluster together during each the three phases, which points towards a very similar transcriptome during each condition (Figure 3). Nonetheless, there was a set of 109 genes, which changed significantly between the two strains independent of the condition. Interestingly, more genes were affected during glucose consumption in the batch phase than during the fed-batch, i.e. 630 genes. This could indicate a change in genes around glucose fermentation. A comparison of the gene expression profiles of the strains in each condition was performed using PIANO (Väremo et al. 2013). While Table 3-5 summarize the most significantly up- and downregulated genes for each condition with a *p*-value < 0.01, Figure 4 summarizes the fold change in strains SCIST11 (ENG) for genes of the mevalonate pathway and several genes involved in nitrogen metabolism. As expected, transcript levels were mostly changing for genes that were modified during the strain construction process. The genes of the upper mevalonate pathway on the other hand were not significantly changing and *ERG10*, *HMG1*, *ERG12*, 8 and 19 were only slightly upregulated during the fed-batch phase. Replacing the endogenous *ERG9* promoter by the *HXT1* promoter resulted in no significant change of expression on glucose during the batch phase, while expression was substantially decreased on the ethanol and during the fed-batch phase. This could explain why strain SCIST11 (ENG) accumulated less biomass during the cultivation. Additionally, it is noteworthy, that ethanol even was most efficient in reducing the promoter activity, which highlights its potential use as carbon source in the feed medium. Apart from the mevalonate pathway, genes involved in nitrogen assimilation as well as amino acid and redox metabolism were affected by modification of the strain. Expression of several permeases and peptide transporters was significantly enhanced independent of the condition, i.e. *GAP1*, *OPT2* and *MEP1-3*. These changes arise from deletion of *GDH1* and overexpression of *GDH2*. The effect of the *GDH1* deletion on gene expression in *S. cerevisiae* has been studied previously

(Bro et al. 2004; Patil and Nielsen 2005). Moreover, Moreira Dos Santos et al. (2003) have investigated fluxes in strains with deletion of *GDH1* and overexpression of *GDH2*.

### Conflict of Interest

The author declare to have no conflict of interest.

### Acknowledgements

The authors acknowledge support from Science for Life Laboratory, the Knut and Alice Wallenberg Foundation, the National Genomics Infrastructure funded by the Swedish Research Council, and Uppsala Multidisciplinary Center for Advanced Computational Science for assistance with massively parallel sequencing and access to the UPPMAX computational infrastructure. The authors acknowledge the Dr. Jonas Gullberg and the Swedish Metabolomics Centre in Umeå for analyzing the metabolome samples using Q-TOF LC/MS. Additionally, this work was financially supported by FORMAS and the Novo Nordisk Foundation. Lastly, we would like to thank Dr. Francesco Gatto for the helpful discussions regarding transcriptome and metabolome data analysis.

## References

- AJ, Trygg J, Gullberg J, Johansson AI, Jonsson P, Antti H, Marklund SL, Moritz T (2005) Extraction and GC/MS analysis of the human blood plasma metabolome. *Analytical Chemistry* 77(24):8086-8094 doi:10.1021/ac051211v
- Brennan TCR, Krömer JO, Nielsen LK (2013) Physiological and transcriptional responses of *Saccharomyces cerevisiae* to d-limonene show changes to the cell wall but not to the plasma membrane. *Appl Environ Microbiol* 79(12):3590-3600
- Bro C, Regenberg B, Nielsen J (2004) Genome-Wide Transcriptional Response of a *Saccharomyces cerevisiae* Strain with an Altered Redox Metabolism. *Biotechnol Bioeng* 85(3):269-276 doi:10.1002/bit.10899
- Cox MP, Peterson DA, Biggs PJ (2010) SolexaQA: At-a-glance quality assessment of Illumina second-generation sequencing data. *BMC Bioinformatics* 11(1):1-6 doi:10.1186/1471-2105-11-485
- Dimster-Denk D, Rine J (1996) Transcriptional regulation of a sterol-biosynthetic enzyme by sterol levels in *Saccharomyces cerevisiae*. *Mol Cell Biol* 16(8):3981-3989
- Dimster-Denk D, Thorsness MK, Rine J (1994) Feedback regulation of 3-hydroxy-3-methylglutaryl coenzyme A reductase in *Saccharomyces cerevisiae*. *Molecular Biology of the Cell* 5(6):655-665
- Duportet X, Aggio RBM, Carneiro S, Villas-Bôas SG (2012) The biological interpretation of metabolomic data can be misled by the extraction method used. *Metabolomics* 8(3):410-421 doi:10.1007/s11306-011-0324-1
- Ellis DI, Goodacre R (2012) Metabolomics-assisted synthetic biology. *Curr Opin Biotechnol* 23(1):22-28 doi:10.1016/j.copbio.2011.10.014
- Farrés M, Piña B, Tauler R (2016) LC-MS based metabolomics and chemometrics study of the toxic effects of copper on *Saccharomyces cerevisiae*.
- Fiehn O (2002) Metabolomics - The link between genotypes and phenotypes. *Plant Mol Biol* 48(1-2):155-171 doi:10.1023/a:1013713905833
- Gullberg J, Jonsson P, Nordström A, Sjöström M, Moritz T (2004) Design of experiments: An efficient strategy to identify factors influencing extraction and derivatization of *Arabidopsis thaliana* samples in metabolomic studies with gas chromatography/mass spectrometry. *Anal Biochem* 331(2):283-295 doi:10.1016/j.ab.2004.04.037
- Hampton R, Dimster-Denk D, Rine J (1996) The biology of HMG-CoA reductase: The pros of counter-regulation. *Trends Biochem Sci* 21(4):140-145 doi:10.1016/0968-0004(96)10017-7
- Hayakawa K, Matsuda F, Shimizu H (2016) Metabolome analysis of *Saccharomyces cerevisiae* and optimization of culture medium for S-adenosyl-L-methionine production. *AMB Express* 6(1) doi:10.1186/s13568-016-0210-3
- Hu F, Liu J, Du G, Hua Z, Zhou J, Chen J (2012) Key cytomembrane ABC transporters of *Saccharomyces cerevisiae* fail to improve the tolerance to d-limonene. *Biotechnology Letters*:1-5
- Kennedy MA, Barbuch R, Bard M (1999) Transcriptional regulation of the squalene synthase gene (ERG9) in the yeast *Saccharomyces cerevisiae*. *Biochim Biophys Acta Gene Struct Expression* 1445(1):110-122 doi:10.1016/s0167-4781(99)00035-4
- Khoomrung S, Martinez JL, Tippmann S, Jansa-Ard S, Buffing MF, Nicastro R, Nielsen J (2015) Expanded metabolite coverage of *Saccharomyces cerevisiae* extract through improved chloroform/methanol extraction and tert-butyldimethylsilyl derivatization. *Analytical Chemistry Research* 6:9-16 doi:10.1016/j.ancr.2015.10.001
- Kizer L, Pitera DJ, Pfleger BF, Keasling JD (2008) Application of functional genomics to pathway optimization for increased isoprenoid production. *Appl Environ Microbiol* 74(10):3229-3241 doi:10.1128/aem.02750-07

- Law CW, Chen Y, Shi W, Smyth GK (2014) Voom: Precision weights unlock linear model analysis tools for RNA-seq read counts. *Genome Biology* 15(2) doi:10.1186/gb-2014-15-2-r29
- Liu J, Zhu Y, Du G, Zhou J, Chen J (2013) Exogenous ergosterol protects *Saccharomyces cerevisiae* from d-limonene stress. *J Appl Microbiol* 114(2):482-491 doi:10.1111/jam.12046
- Lunter G, Goodson M (2011) Stampy: A statistical algorithm for sensitive and fast mapping of Illumina sequence reads. *Genome Res* 21(6):936-939 doi:10.1101/gr.111120.110
- Martin VJJ, Piteral DJ, Withers ST, Newman JD, Keasling JD (2003) Engineering a mevalonate pathway in *Escherichia coli* for production of terpenoids. *Nat Biotechnol* 21(7):796-802 doi:10.1038/nbt833
- Merlo M, Jankevics A, Takano E, Breitling R (2011) Exploring the metabolic state of microorganisms using metabolomics. *Bioanalysis* 3(21):2443-2458 doi:10.4155/bio.11.248
- Moreira Dos Santos M, Thygesen G, Kötter P, Olsson L, Nielsen J (2003) Aerobic physiology of redox-engineered *Saccharomyces cerevisiae* strains modified in the ammonium assimilation for increased NADPH availability. *FEMS Yeast Res* 4(1):59-68 doi:10.1016/s1567-1356(03)00155-7
- Nguyen QT, Merlo ME, Medema MH, Jankevics A, Breitling R, Takano E (2012) Metabolomics methods for the synthetic biology of secondary metabolism. *FEBS Lett* 586(15):2177-2183 doi:10.1016/j.febslet.2012.02.008
- Nielsen J (2015) Yeast cell factories on the horizon: Metabolic engineering in yeast gets increasingly more versatile. *Science* 349(6252):1050-1051 doi:10.1126/science.aad2081
- Nookaew I, Papini M, Pornputtapong N, Scalcinati G, Fagerberg L, Uhlén M, Nielsen J (2012) A comprehensive comparison of RNA-Seq-based transcriptome analysis from reads to differential gene expression and cross-comparison with microarrays: a case study in *Saccharomyces cerevisiae*. *Nucleic Acids Res* 40(20):10084-10097
- Österlund T, Nookaew I, Nielsen J (2012) Fifteen years of large scale metabolic modeling of yeast: Developments and impacts. *Biotechnology Advances* 30(5):979-988
- Ozcan S, Johnston M (1995) Three different regulatory mechanisms enable yeast hexose transporter (HXT) genes to be induced by different levels of glucose. *Mol Cell Biol* 15(3):1564-1572
- Patil KR, Nielsen J (2005) Uncovering transcriptional regulation of metabolism by using metabolic network topology. *Proc Natl Acad Sci USA* 102(8):2685-2689 doi:10.1073/pnas.0406811102
- Quinlan AR, Hall IM (2010) BEDTools: A flexible suite of utilities for comparing genomic features. *Bioinformatics* 26(6):841-842 doi:10.1093/bioinformatics/btq033
- Reifenberger E, Freidel K, Ciriacy M (1995) Identification of novel HXT genes in *Saccharomyces cerevisiae* reveals the impact of individual hexose transporters on glycolytic flux. *Mol Microbiol* 16(1):157-167
- Scalcinati G, Knuf C, Partow S, Chen Y, Maury J, Schalk M, Daviet L, Nielsen J, Siewers V (2012) Dynamic control of gene expression in *Saccharomyces cerevisiae* engineered for the production of plant sesquiterpene α-santalene in a fed-batch mode. *Metab Eng* 14(2):91-103
- Sun Z, Meng H, Li J, Wang J, Li Q, Wang Y, Zhang Y (2014) Identification of novel knockout targets for improving terpenoids biosynthesis in *Saccharomyces cerevisiae*. *PLoS ONE* 9(11) doi:10.1371/journal.pone.0112615
- Tippmann S, Scalcinati G, Siewers V, Nielsen J (2016) Production of farnesene and santalene by *Saccharomyces cerevisiae* using fed-batch cultivations with RQ-controlled feed. *Biotechnol Bioeng* 113(1):72-81 doi:10.1002/bit.25683
- Väremo L, Nielsen J, Nookaew I (2013) Enriching the gene set analysis of genome-wide data by incorporating directionality of gene expression and combining statistical hypotheses and methods. *Nucleic Acids Res* 41(8):4378-4391 doi:10.1093/nar/gkt111
- Verduyn C, Postma E, Scheffers WA, Van Dijken JP (1992) Effect of benzoic acid on metabolic fluxes in yeasts: A continuous-culture study on the regulation of respiration and alcoholic fermentation. *Yeast* 8(7):501-517

- Wiklund S, Johansson E, Sjöström L, Mellerowicz EJ, Edlund U, Shockcor JP, Gottfries J, Moritz T, Trygg J (2008) Visualization of GC/TOF-MS-based metabolomics data for identification of biochemically interesting compounds using OPLS class models. *Analytical Chemistry* 80(1):115-122 doi:10.1021/ac0713510
- Withers ST, Gottlieb SS, Lieu B, Newman JD, Keasling JD (2007) Identification of isopentenol biosynthetic genes from *Bacillus subtilis* by a screening method based on isoprenoid precursor toxicity. *Appl Environ Microbiol* 73(19):6277-6283 doi:10.1128/aem.00861-07
- Yuan J, Ching CB (2015) Dynamic control of *ERG9* expression for improved amorpho-4,11-diene production in *Saccharomyces cerevisiae*. *Microb Cell Fact* 14(1) doi:10.1186/s12934-015-0220-x
- Zhou K, Zou R, Stephanopoulos G, Too HP (2012) Metabolite Profiling Identified Methylerythritol Cyclodiphosphate Efflux as a Limiting Step in Microbial Isoprenoid Production. *PLoS ONE* 7(11)

## List of Figures

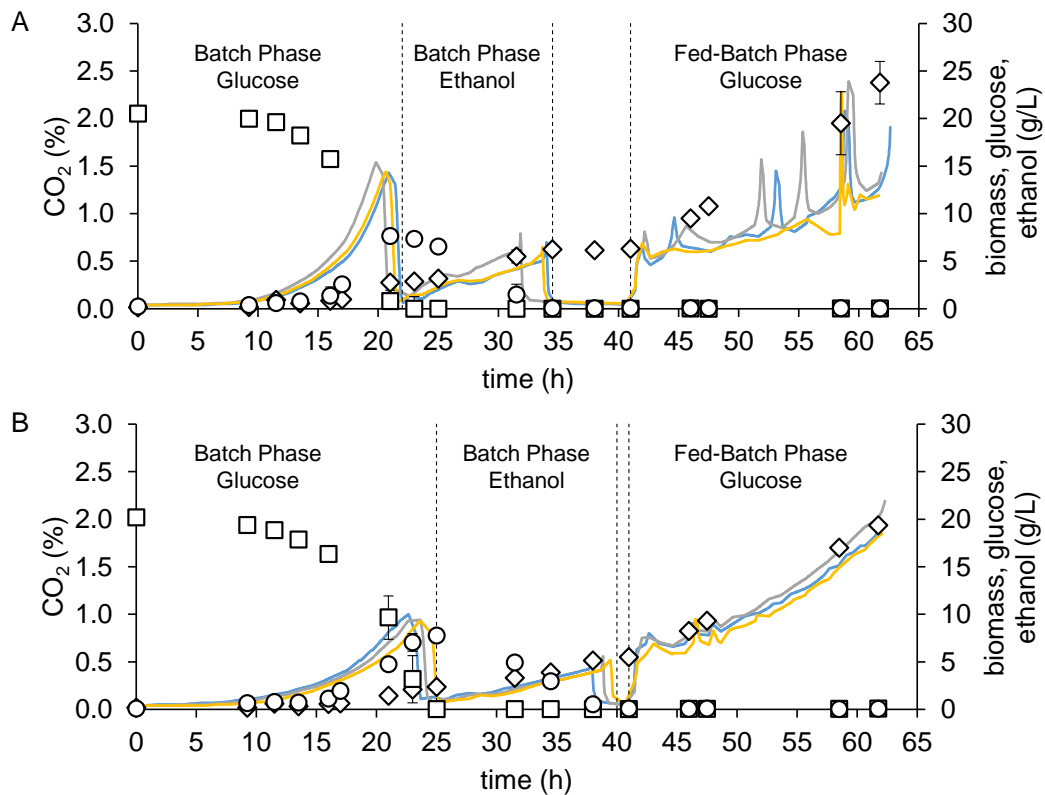


Figure 1: Physiological comparison of strains SCIST05 (WT, panel A) and SCIST11 (ENG, panel B) engineered for production of farnesene in three different conditions, i.e. glucose fermentation (batch phase), ethanol respiration (batch phase) and glucose respiration (fed-batch phase). Solid lines show CO<sub>2</sub> content of the exhaust gas. Squares-glucose, circles-ethanol, diamonds-biomass. Data represents results of three biological replicates with standard deviation. For transcriptome and metabolome analysis, samples for RNA and metabolite extraction were taken during each of the three phases according the CO<sub>2</sub> profile.

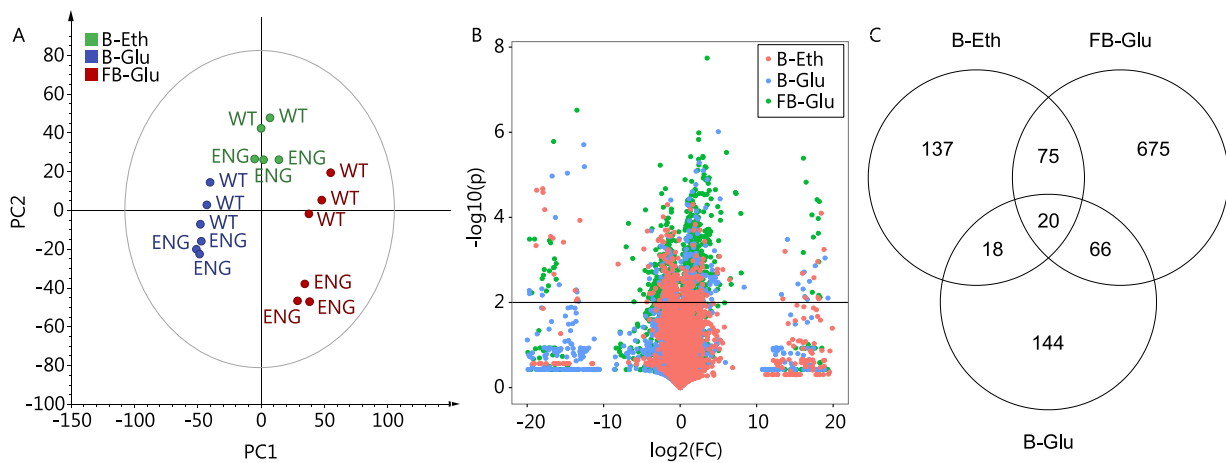


Figure 2: Metabolome analysis of *S. cerevisiae* strains SCIST05 (WT) and SCIST11 (ENG) using LC-qTOF. (A) Principle component analysis (PCA) of the complete data set. One sample was removed as an outlier. (B) Volcano plot including all metabolic features of each condition. (C) Venn diagram to identify similar and unique metabolic features of each strain and as response to each condition ( $P$ -value $<0.01$ ). B-Glu/B-Eth – sample obtained during the glucose/ethanol consumption phase of the batch, FB-Glu - sample obtained during the fed-batch phase with glucose feed.

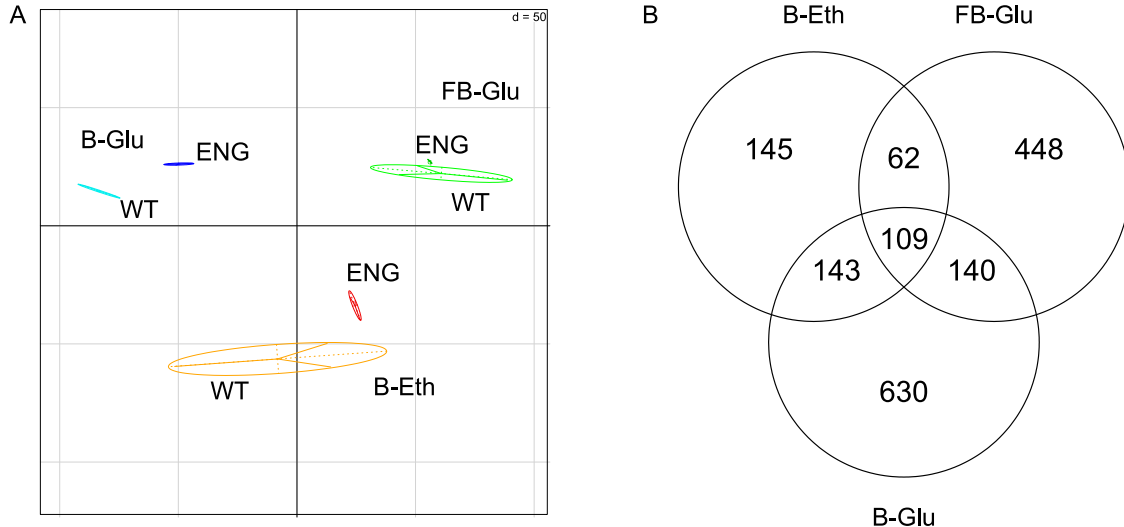


Figure 3: Transcriptome analysis of *S. cerevisiae* strains SCIST05 (WT) and SCIST11 (ENG) using RNAseq. (A) Principle component analysis (PCA) of all samples from each condition. (B) Venn diagram quantifying in which condition most genes are significantly changing ( $P$ -value $<0.01$ ) and which genes are changing independent of the three conditions. B-Glu/B-Eth – sample obtained during the glucose/ethanol consumption phase of the batch, FB-Glu - sample obtained during the fed-batch phase with glucose feed.

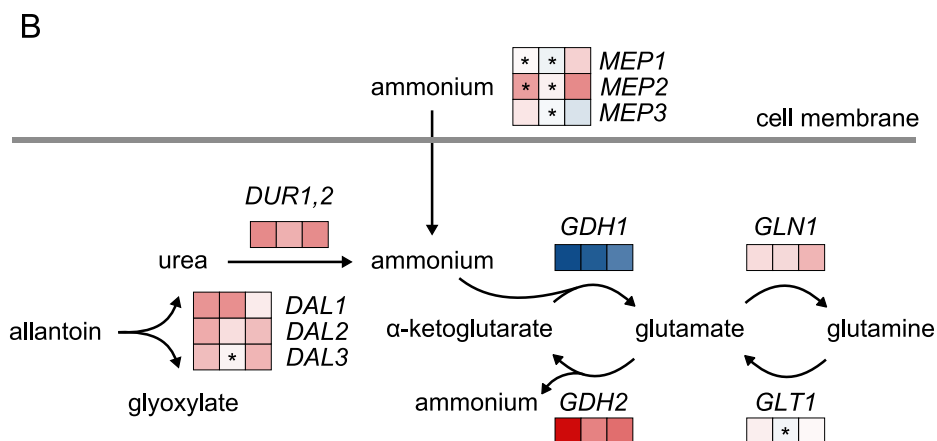
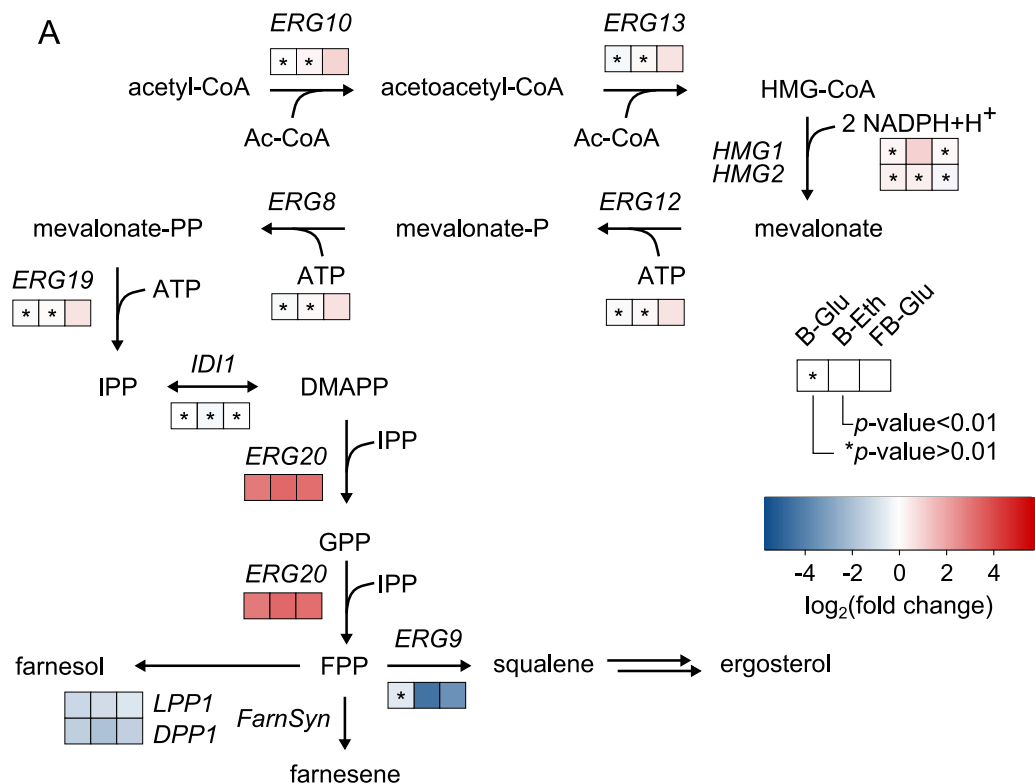


Figure 4: Transcriptomic response of strain SCIST11 (ENG) in comparison to SCIST05 (WT) in different environmental conditions (B-Glu, B-Eth, FB-Glu). Color code indicates the fold change in log<sub>2</sub> scale. Particular focus was pointed towards mevalonate pathway genes and genes targeted for engineering.

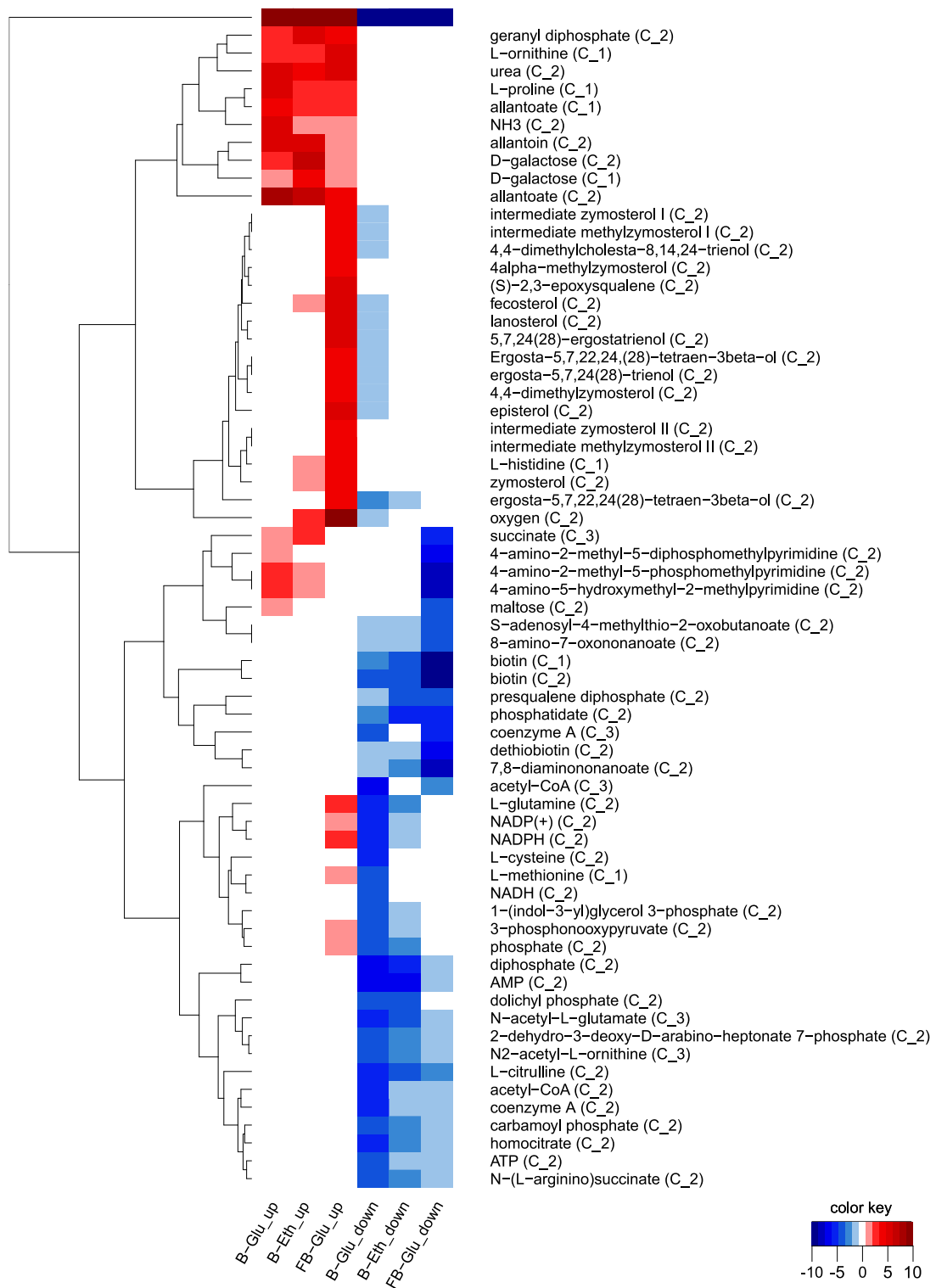


Figure 5: Reporter metabolites to highlight differences in the expression profiles between strain SCIST05 (WT) and SCIST11 (ENG) during the production of farnesene. Reporter metabolites were determined using the *S. cerevisiae* genome-scale metabolic model iTO977 (Österlund et al. 2012) with *p*-value < 0.0001.

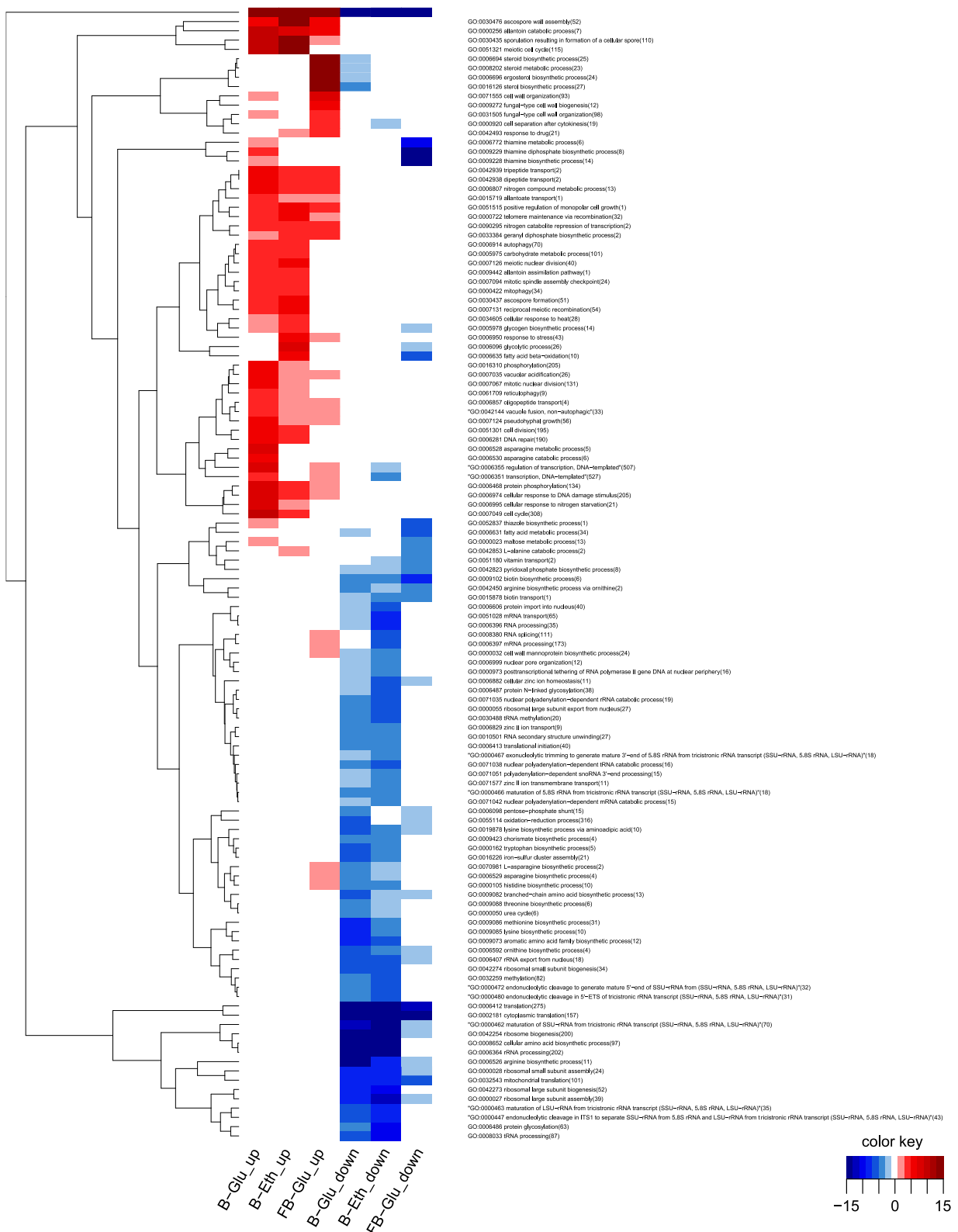


Figure 6: Gene Set Analysis to highlight enriched pathways in SCIST11 (ENG) in comparison to SCIST05 (WT) during the production of farnesene ( $p<0.0001$ ).

## List of Tables

Table 1: List of strains used in this study.

Strain	ID	Relevant genotype	Plasmid	Reference
SCIST05	WT	<i>MATa MAL2-8<sup>c</sup> SUC2</i>	$P_{TEF1}\text{-}FarnSyn$ , $P_{PGK1}\text{-}tHMG1$	(Tippmann et al. 2016)
SCIST11	ENG	<i>MATa MAL2-8<sup>c</sup> SUC2</i>  $lpp1\Delta::loxP$ $dpp1\Delta::loxP$  $P_{ERG9\Delta}\text{-}loxP\text{-}P_{HXT1}$ $gdh1\Delta::loxP$  $P_{TEF1}\text{-}ERG20$ $P_{PGK1}\text{-}GDH2$  $P_{TEF1}\text{-}FarnSyn$ $P_{PGK1}\text{-}tHMG1$	$P_{TEF1}\text{-}FarnSyn$ , $P_{PGK1}\text{-}tHMG1$	(Tippmann et al. 2016)

Table 2: Physiological parameters for strains SCIST05 and 11 obtained during the fed-batch cultivation.

Data represents average values of three biological replicates  $\pm$  standard deviation.

		Batch		Fed-Batch
		Glucose	Ethanol	Glucose
$\mu$ (h <sup>-1</sup> )	SCIST05	0.220 $\pm$ 0.005	0.074 $\pm$ 0.003	0.073 $\pm$ 0.005
	SCIST11	0.189 $\pm$ 0.020	0.058 $\pm$ 0.004	0.069 $\pm$ 0.002
$Y_{SX}$ (gDCW·g <sup>-1</sup> )	SCIST05	0.131 $\pm$ 0.002	0.457 $\pm$ 0.026	0.651 $\pm$ 0.076
	SCIST11	0.118 $\pm$ 0.009	0.375 $\pm$ 0.038	0.516 $\pm$ 0.021
$Y_{SE}$ (g·g <sup>-1</sup> )	SCIST05	0.378 $\pm$ 0.014	-	-
	SCIST11	0.397 $\pm$ 0.004	-	-
$r_s$ (g·gDCW <sup>-1</sup> ·h <sup>-1</sup> )	SCIST05	1.673 $\pm$ 0.015	0.163 $\pm$ 0.006	0.103 $\pm$ 0.007
	SCIST11	1.604 $\pm$ 0.221	0.156 $\pm$ 0.005	0.134 $\pm$ 0.003

Table 3: Overview of the 20 most down- and upregulated genes of strain SCIST11 (ENG) in comparison to strain SCIST05 (WT) identified in the batch phase during glucose consumption (B-Glu) with a *P*-value <0.01. Descriptive information on the function of these genes was retrieved from the Saccharomyces Genome Database ([www.yeastgenome.org](http://www.yeastgenome.org))

<b>Gene Name</b>	<b>Description</b>	<b>logFC</b>	<b>P-value</b>
<b>Downregulated</b>			
GDH1	glutamate dehydrogenase	-5.71	1.10E-14
GNP1	glutamine permease	-3.36	1.42E-11
BAP3	branched-chain amino acid permease	-3.29	1.93E-13
LYS20	homocitrate synthase / lysine biosynthesis	-2.10	6.26E-09
SER3	3-phosphoglycerate dehydrogenase and $\alpha$ -ketoglutarate reductase	-1.82	2.76E-07
AGP1	high-affinity glutamine permease	-1.75	3.78E-06
TIR3	cell wall mannoprotein	-1.70	1.91E-06
PDH1	putative 2-methylcitrate dehydratase	-1.49	6.07E-05
DPP1	diacylglycerol pyrophosphate phosphatase	-1.47	9.55E-07
ATR1	aminotriazole resistance / multidrug efflux pump	-1.47	1.05E-06
NAT4	n-acetyltransferase	-1.36	2.27E-03
ARG1	arginosuccinate synthetase	-1.34	3.17E-07
DLD3	D-lactate dehydrogenase	-1.31	4.69E-06
ASN1	asparagine synthetase	-1.22	4.82E-06
LPP1	lipid phosphate phosphatase	-1.21	3.22E-07
ATG41	autophagy related / unknown protein	-1.18	1.63E-06
MPC2	mitochondrial pyruvate carrier	-1.15	3.54E-07
VHT1	vitamin H symporter	-1.15	1.67E-07
CIT3	citrate synthase	-1.08	5.36E-03
RPL41A	ribosomal 60S subunit L41A	-1.03	1.50E-04
<b>Upregulated</b>			
OPT2	oligopeptide transporter	7.13	4.59E-17
GDH2	glutamate dehydrogenase	5.41	3.66E-14
DAL80	negative regulator in nitrogen degradation pathways	5.14	3.94E-13
DAL5	allantoate permease / degradation of allantoin	5.11	3.63E-17
PUT1	proline oxidase	4.82	1.19E-13
PDC5	pyruvate decarboxylase	3.64	4.17E-11
MF(ALPHA)1	mating pheromone alpha-factor	3.50	3.75E-06
CHA1	catabolic serine, threonine deaminase	3.48	4.26E-09
PUT4	proline permease	3.47	2.39E-10
GAP1	general amino acid permease	3.46	1.51E-12
ASP3-3	asparaginase / asparagine catabolism	3.34	1.08E-12
ASP3-2	asparaginase / asparagine catabolism	3.34	5.25E-13

ASP3-1	asparaginase / asparagine catabolism	3.31	7.39E-13
ASP3-4	asparaginase / asparagine catabolism	3.30	2.26E-12
PRR2	pheromone response regulator	3.09	7.31E-10
ERG20	farnesyl pyrophosphate synthetase	2.96	2.05E-12
DAL7	malate synthase / degradation of allantoin	2.92	7.41E-11
VBA1	vacuolar basic amino acid transporter	2.81	1.20E-13
CPS1	carboxypeptidase	2.77	7.74E-11
DUR1,2	urea amidolyase/ degradation of urea	2.56	1.24E-09

Table 4: Overview of the 20 most down- and upregulated genes of strain SCIST11 (ENG) in comparison to strain SCIST05 (WT) identified in the batch phase during ethanol consumption (B-Eth) with a *P*-value <0.01. Descriptive information on the function of these genes was retrieved from the Saccharomyces Genome Database ([www.yeastgenome.org](http://www.yeastgenome.org))

Gene Name	Description	logFC	P-value
<b>Downregulated</b>			
GDH1	NADP(+)-dependent glutamate dehydrogenase	-5.22	3.91E-14
ERG9	squalene synthase	-4.41	1.26E-09
COX2	subunit II of cytochrome c oxidase (complex iv)	-2.47	1.49E-03
DPP1	diacylglycerol pyrophosphate phosphatase	-1.91	3.99E-08
HXT2	high-affinity glucose transporter	-1.60	5.90E-04
COS12	endosomal protein involved in turnover of plasma membrane proteins	-1.39	1.43E-05
MAN2	mannitol dehydrogenase	-1.38	6.88E-05
DSF1	mannitol dehydrogenase	-1.36	3.56E-05
COB	cytochrome b	-1.12	7.74E-04
IZH3	membrane protein involved in zinc ion homeostasis	-1.11	2.84E-08
VHT1	plasma membrane H+-biotin (vitamin H) symporter	-1.10	3.05E-07
COX1	subunit I of cytochrome c oxidase (complex IV)	-1.06	6.80E-05
LPP1	lipid phosphate phosphatase	-1.06	1.63E-06
AQY2	water channel that mediates water transport across cell membranes	-1.05	1.28E-09
HXT13	hexose transporter	-0.94	1.26E-04
IMA2	isomaltase ( $\alpha$ -1,6-glucosidase/alpha-methylglucosidase)	-0.93	1.34E-04
ARG5,6	acetylglutamate kinase and n-acetyl-gamma-glutamyl-phosphate reductase	-0.90	1.18E-04
PHO3	acid phosphatase similar to pho5p	-0.83	8.19E-03
ATR1	multidrug efflux pump of the major facilitator superfamily	-0.79	6.63E-04
SAM3	high-affinity s-adenosylmethionine permease	-0.76	5.19E-04
<b>Upregulated</b>			
OPT2	oligopeptide transporter	4.11	1.06E-13
DAL80	negative regulator of genes in multiple nitrogen degradation pathways	3.86	2.01E-11

ERG20	farnesyl pyrophosphate synthetase	3.30	4.45E-13
GDH2	NAD(+-)dependent glutamate dehydrogenase	2.74	4.36E-10
HXT10	putative hexose transporter	2.55	1.39E-08
DAL1	allantoinase	2.47	2.50E-12
GAP1	general amino acid permease	2.30	3.94E-10
SSA3	ATPase involved in protein folding and the response to stress	2.28	2.76E-09
PUT1	proline oxidase	2.22	4.51E-09
LDS1	protein involved in spore wall assembly	2.17	9.65E-07
FIG1	integral membrane protein required for efficient mating	2.14	9.93E-07
HXT14	protein with similarity to hexose transporter family members	2.11	9.23E-09
PRM6	potassium transporter that mediates K+ influx	2.05	2.20E-03
MF(ALPHA)1	mating pheromone alpha-factor	2.01	9.05E-04
GRE1	hydrophilin essential in desiccation-rehydration process	1.99	1.14E-05
SPO19	meiosis-specific prospore protein	1.94	3.99E-05
SPR2	putative spore wall protein	1.91	1.98E-07
HSP26	small heat shock protein with chaperone activity	1.86	1.42E-05
SHH3	putative mitochondrial inner membrane protein of unknown function	1.81	7.45E-12
PDC6	pyruvate decarboxylase	1.79	3.63E-04

Table 5: Overview of the 20 most down- and upregulated genes of strain SCIST11 (ENG) in comparison to strain SCIST05 (WT) identified in the fed-batch phase (FB-Glu) with a *P*-value <0.01. Descriptive information on the function of these genes was retrieved from the *Saccharomyces* Genome Database ([www.yeastgenome.org](http://www.yeastgenome.org))

Gene Name	Description	logFC	P-value
<b>Downregulated</b>			
THI4	thiazole synthase	-6.16	3.28E-16
THI13	protein involved in synthesis of the thiamine precursor hmp	-4.12	1.40E-12
THI5	protein involved in synthesis of the thiamine precursor hmp	-4.11	2.19E-11
GDH1	NADP(+-)dependent glutamate dehydrogenase	-4.10	1.11E-12
FDH1	NAD(+-)dependent formate dehydrogenase	-3.96	6.31E-05
ADY2	acetate transporter required for normal sporulation	-3.90	8.89E-10
BIO5	putative transmembrane protein involved in the biotin biosynthesis	-3.83	4.28E-14
THI12	protein involved in synthesis of the thiamine precursor hmp	-3.78	2.64E-09
THI11	protein involved in synthesis of the thiamine precursor hmp	-3.58	1.07E-12
ERG9	squalene synthase	-3.49	2.74E-08
THI73	putative plasma membrane permease	-3.25	5.14E-08
PHO3	acid phosphatase similar to pho5p	-2.86	4.14E-08
THI2	transcriptional activator of thiamine biosynthetic genes	-2.85	7.47E-09
FAT3	protein required for fatty acid uptake	-2.57	3.63E-08
BIO3	7,8-diamino-pelargonic acid aminotransferase	-2.52	4.42E-10

THI7	plasma membrane transporter for the uptake of thiamine	-2.45	4.10E-07
ADH2	alcohol dehydrogenase II	-2.40	4.82E-08
THI20	trifunctional enzyme of thiamine biosynthesis, degradation and salvage	-2.28	5.10E-08
AAD14	putative aryl-alcohol dehydrogenase	-2.16	7.10E-12
BIO2	biotin synthase	-2.10	3.30E-08
<hr/>			
Upregulated			
GDH2	NAD(+-)dependent glutamate dehydrogenase	3.22	4.76E-11
ERG20	farnesyl pyrophosphate synthetase	3.17	7.96E-13
HES1	protein implicated in the regulation of ergosterol biosynthesis	3.10	5.61E-11
GAP1	general amino acid permease	3.07	7.99E-12
TIR1	cell wall mannoprotein	2.82	1.64E-09
TIR3	cell wall mannoprotein	2.78	4.28E-09
ATP6	subunit a of the F0 sector of mitochondrial F1F0 ATP synthase	2.70	4.64E-03
OPT2	oligopeptide transporter	2.68	3.97E-11
NCW2	structural constituent of the cell wall	2.62	4.18E-10
HXT3	low affinity glucose transporter	2.59	1.77E-13
PCK1	phosphoenolpyruvate carboxykinase	2.56	1.67E-10
DUR1,2	urea amidolyase	2.53	1.49E-09
DAL80	negative regulator of genes in multiple nitrogen degradation pathways	2.26	2.46E-08
ARI1	NADPH-dependent aldehyde reductase	2.20	9.43E-09
ERG3	C-5 sterol desaturase	2.14	2.80E-12
PUT1	proline oxidase	2.10	9.66E-09
YSR3	dihydrosphingosine 1-phosphate phosphatase	2.09	1.44E-11
AGP1	low-affinity amino acid permease with broad substrate range	2.08	5.07E-07
ATF2	alcohol acetyltransferase	2.04	7.41E-11
HXT4	high-affinity glucose transporter	2.04	8.97E-06



# **Affibody scaffolds improve production of sesquiterpenes in *Saccharomyces cerevisiae***

Stefan Tippmann, Josefina Anfelt, Florian David, Jacqueline Rand, Verena Siewers, Mathias Uhlén, Jens Nielsen and Paul Hudson

*ACS Synthetic Biology*, doi:10.1021/acssynbio.6b00109



## Affibody Scaffolds Improve Sesquiterpene Production in *Saccharomyces cerevisiae*

Stefan Tippmann,<sup>†,‡,§</sup> Josefina Anfelt,<sup>§,#</sup> Florian David,<sup>†,‡</sup> Jacqueline M. Rand,<sup>†,||</sup> Verena Siewers,<sup>†,‡</sup> Mathias Uhlén,<sup>§,⊥</sup> Jens Nielsen,<sup>†,‡,⊥</sup> and Elton P. Hudson<sup>\*,§</sup>

<sup>†</sup>Department of Biology and Biological Engineering, Chalmers University of Technology, SE412 96 Gothenburg, Sweden

<sup>‡</sup>Novo Nordisk Foundation Center for Biosustainability, Chalmers University of Technology, SE412 96 Gothenburg, Sweden

<sup>§</sup>Division of Proteomics and Nanobiotechnology, School of Biotechnology, Royal Institute of Technology (KTH), Science for Life Laboratory, SE171 21 Stockholm, Sweden

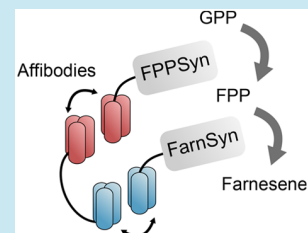
<sup>||</sup>Department of Chemical and Biological Engineering, University of Wisconsin–Madison, Madison, Wisconsin 53706, United States

<sup>⊥</sup>Novo Nordisk Foundation Center for Biosustainability, Technical University of Denmark, DK2970 Hørsholm, Denmark

### Supporting Information

**ABSTRACT:** Enzyme fusions have been widely used as a tool in metabolic engineering to increase pathway efficiency by reducing substrate loss and accumulation of toxic intermediates. Alternatively, enzymes can be colocalized through attachment to a synthetic scaffold *via* noncovalent interactions. Here we describe the use of affibodies for enzyme tagging and scaffolding. The scaffolding is based on the recognition of affibodies to their anti-idiotypic partners *in vivo*, and was first employed for colocalization of farnesyl diphosphate synthase and farnesene synthase in *S. cerevisiae*. Different parameters were modulated to improve the system, and the enzyme:scaffold ratio was most critical for its functionality. Ultimately, the yield of farnesene on glucose  $Y_{S\text{Far}}$  could be improved by 135% in fed-batch cultivations using a 2-site affibody scaffold. The scaffolding strategy was then extended to a three-enzyme polyhydroxybutyrate (PHB) pathway, heterologously expressed in *E. coli*. Within a narrow range of enzyme and scaffold induction, the affibody tagging and scaffolding increased PHB production 7-fold. This work demonstrates how the versatile affibody can be used for metabolic engineering purposes.

**KEYWORDS:** affibodies, isoprenoids, biofuels, PHB, yeast, metabolic engineering



In recent years enzyme scaffolds have arisen as an alternative to enzyme fusions to create custom enzyme complexes. To create a synthetic enzyme scaffold, protein–protein binding pairs are leveraged. The first members of the binding pairs are fused to enzymes of interest. The other members are linked together to form a protein array, so that the tagged enzymes are colocalized.<sup>1,2</sup> Such synthetic enzyme scaffolding could assist in channeling metabolic pathway intermediates from one enzyme to the other. Most binding pairs for scaffolding systems have been sourced from nature.<sup>3–5</sup> For example, cohesion-dockerin pairs ( $K_D < 1 \text{ nM}$ ) from divergent cellulolytic microorganisms have been used to construct “designer cellulosomes,” where cellulose binding domains, xylanases, and cellulases are colocalized and displayed on the surface of yeast, *E. coli*, or artificial vesicles.<sup>6</sup> These synthetic scaffolds are thought to facilitate successive metabolite channeling. In a successful example of an intracellular scaffold, various protein–protein interaction domains ( $K_D 0.1\text{--}8 \mu\text{M}$ ) from metazoans were used to tag and scaffold enzymes for the first three reactions of the mevalonate pathway; optimization resulted in a 77-fold increased titer of mevalonate in *E. coli* relative to a nonscaffolded construct.<sup>1</sup> Theoretical treatments have predicted that the scaffold effect is sensitive to several properties, including enzyme:scaffold loading<sup>1,7</sup> enzyme orientation,<sup>2</sup> and

active-site distances.<sup>8</sup> Some practical heuristics for scaffold design and implementation should also be considered, for example tagging an enzyme for scaffolding should not negatively affect its function, the protein–protein interactions on the scaffold should be of suitable affinity to localize all enzymes simultaneously,<sup>9</sup> and the synthetic scaffold should be stable against degradation.

Here we develop affibodies as a tool for both tagging and scaffolding enzymes. Affibodies (Z domains) are 58-residue, nonimmunoglobulin affinity proteins derived from the Fc-binding domain of *Staphylococcus aureus* protein A.<sup>10</sup> Previous works have generated randomized phage-display libraries of affibodies and selected affibodies for versatile diagnostic and biotechnological applications against various target proteins including insulin, HER2 (Z<sub>HER2</sub>), Taq polymerase (Z<sub>Taq</sub>), and IgA (Z<sub>IgA</sub>).<sup>11,12</sup> Additionally, anti-idiotypic affibodies have been selected as binders for several affibodies, so that Z:anti-Z binding pairs with a range of affinities are known and characterized:<sup>13</sup> Z<sub>Taq</sub>:anti-Z<sub>Taq</sub> ( $K_D 0.7 \mu\text{M}$ ); Z<sub>IgA</sub>:anti-Z<sub>IgA</sub> ( $K_D 0.9 \mu\text{M}$ ); Z<sub>HER2</sub>:anti-Z<sub>HER2</sub> ( $K_D 0.3 \mu\text{M}$ ); Z<sub>WT</sub>:anti-Z<sub>WT</sub> ( $K_D 0.05 \mu\text{M}$ ). Due to their small size, fast folding kinetics and

**Received:** April 8, 2016

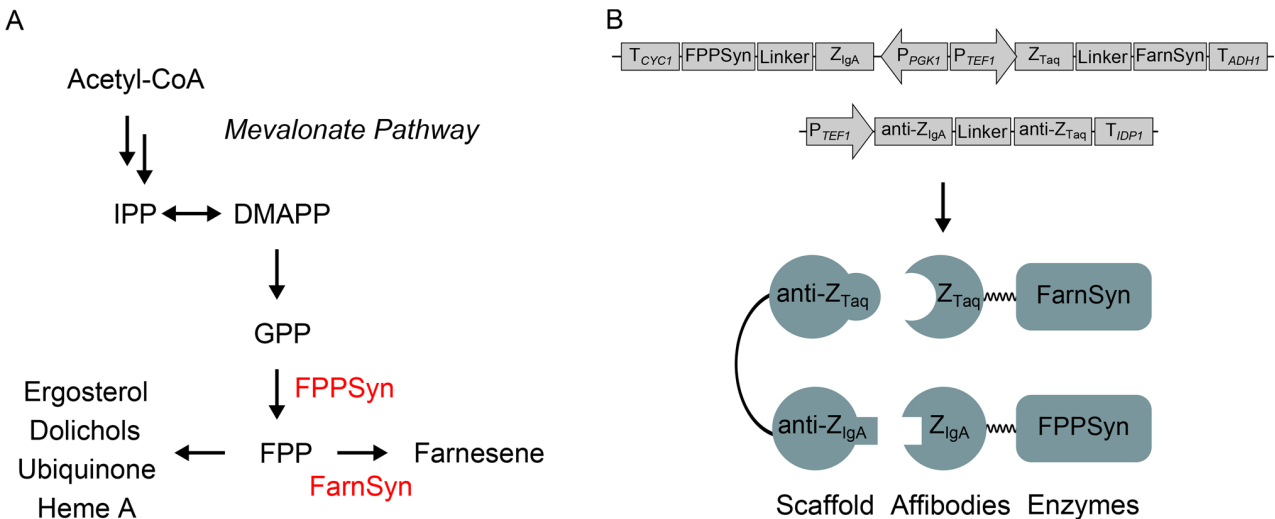


**Figure 1.** Affibody mediated enzyme fusion for production of farnesene in *S. cerevisiae*. (A) Farnesyl diphosphate (FPP) is produced from acetyl-CoA in the mevalonate pathway and represents an essential intermediate for sterol synthesis and other metabolites. In the final step, FPP is converted to farnesene by farnesene synthase. (B) To reduce side product formation from FPP and redirect flux toward farnesene, two pairs of anti-idiotypic affibodies were used to attach FPP synthase (FPPSyn) and farnesene synthase (FarnSyn) to a scaffold. Affibodies  $Z_{\text{Taq}}$  and  $Z_{\text{IgA}}$  represent target proteins, which were fused to the enzymes while the affibody scaffold consisting of anti- $Z_{\text{Taq}}$  and anti- $Z_{\text{IgA}}$  was expressed separately.

stability, affibodies could be suitable fusion tags for enzymes, and anti-idiotypic affibodies could be linked together to form a binding scaffold that is both small and stable. In a previous work, the Z-domain and dockerin were used as a yeast surface-display scaffold with the goal of creating a small artificial cellulosome. Fc-tagged endoglucanase and cohesin-tagged  $\beta$ -glucosidase were successfully colocalized on the surface-displayed scaffold. However, the scaffolding did not improve  $\beta$ -glucan degradation compared to secretion of the enzymes. The authors suggested that the ratio of enzyme:scaffold could be a point for optimization.<sup>14</sup> In this work, we sought to leverage the set of available anti-idiotypic affibody pairs to create a more versatile, intracellular scaffolding system that could be used for metabolic engineering. We first used farnesene production in *S. cerevisiae* as a case study for testing enzyme:scaffolding ratio, carbon source, and enzyme-affibody linker length. To demonstrate the generality of the affibody scaffold approach, we also constructed and applied an affibody scaffold to a three-enzyme pathway, polyhydroxybutyrate (PHB) production in *E. coli*.

Farnesene is produced from the mevalonate pathway in *S. cerevisiae*, which supplies farnesyl diphosphate (FPP) also as a precursor for sterol synthesis, dolichols, ubiquinone, heme A and as substrate for protein farnesylation (Figure 1). Metabolic engineering strategies for increasing production of farnesene have included increasing flux through the mevalonate pathway, improving cofactor balance, and redirecting flux at the FPP branch point to reduce byproduct formation. Since FPP is utilized by several competing reactions, an *in vivo* scaffold of the upstream FPP synthase (FPPSyn) and downstream farnesene synthase (FarnSyn) could keep the enzymes in close proximity and thereby enhance the effective concentrations of FPP precursor for FarnSyn. As support for this hypothesis, enzyme fusions of FPP synthase and terpene synthase were previously reported to increase titers of downstream terpenes. A fusion of FPPSyn and terpene synthase increased final concentrations of patchoulol 2-fold in *S. cerevisiae*.<sup>15</sup> In *E. coli*, a fusion of GPP/FPP synthase and terpene synthase increased production of pinene and farnesene from the heterologously expressed

mevalonate pathway by 52 and 51%, respectively, and it was found that linker length was a key determinant.<sup>16,17</sup> We thus reasoned that farnesene production was a suitable system to test the affibody scaffold.

We first tested the ability of Z-tagged proteins to be colocalized by an affibody scaffold *in vivo*. Interactions between the selected idiotypic Z-variants and their corresponding anti-idiotypic partners have previously been studied *in vitro* through nuclear magnetic resonance,<sup>18</sup> surface plasmon resonance<sup>13</sup> and Förster resonance energy transfer (FRET) measurements.<sup>19</sup> FRET-based analysis is commonly used also for the identification of intracellular protein–protein interactions within distances of 100 Å<sup>20</sup> and was therefore implemented for the verification of simultaneous binding of  $Z_{\text{Taq}}$  and  $Z_{\text{IgA}}$  to the scaffold *in vivo*. The linker length between the anti-idiotypic affibodies in a scaffold with a 20-amino acid linker can be approximated to 70–80 Å in its fully extended configuration.<sup>21</sup>  $Z_{\text{Taq}}$  and  $Z_{\text{IgA}}$  were fused to variants of CFP and YFP, respectively, and coexpressed with scaffold (BW scaffold). As positive controls we prepared an *E. coli* strain with a YFP-CFP fusion (BWpos1) and a strain with coexpression of  $Z_{\text{Taq}}$ -CFP and anti- $Z_{\text{Taq}}$ -YFP (BWpos2). Coexpression of  $Z_{\text{Taq}}$ -CFP and  $Z_{\text{IgA}}$ -YFP without scaffold (BWneg) was used as negative control. The occurrence of FRET decreases the CFP/YFP emission ratio as a result of the energy transfer from CFP to YFP.<sup>22</sup> The CFP/YFP emission ratio from  $Z_{\text{Taq}}$ -CFP and  $Z_{\text{IgA}}$ -YFP decreased from 1.9 to 1.4 when scaffold was present (Figure 2), indicating simultaneous binding of Z-fused fluorophores to the scaffold. The FRET effect however was not as strong as when the enzymes were directly fused, or when they were paired without scaffold *via*  $Z_{\text{Taq}}$  and anti- $Z_{\text{Taq}}$ . In the scaffold system, the lower FRET effect could reflect that the  $Z_{\text{Taq}}$ -CFP and  $Z_{\text{IgA}}$ -YFP are not in as close proximity as the direct fusion or direct binding, or that only a portion of the available  $Z_{\text{Taq}}$ -CFP and  $Z_{\text{IgA}}$ -YFP are in the scaffold. The latter is most likely, given the relatively modest ( $K_D$  700–900 nM) binding affinities of  $Z_{\text{Taq}}$  and  $Z_{\text{IgA}}$  to their anti-idiotypic affibodies. No FRET was detected at the lowest scaffold

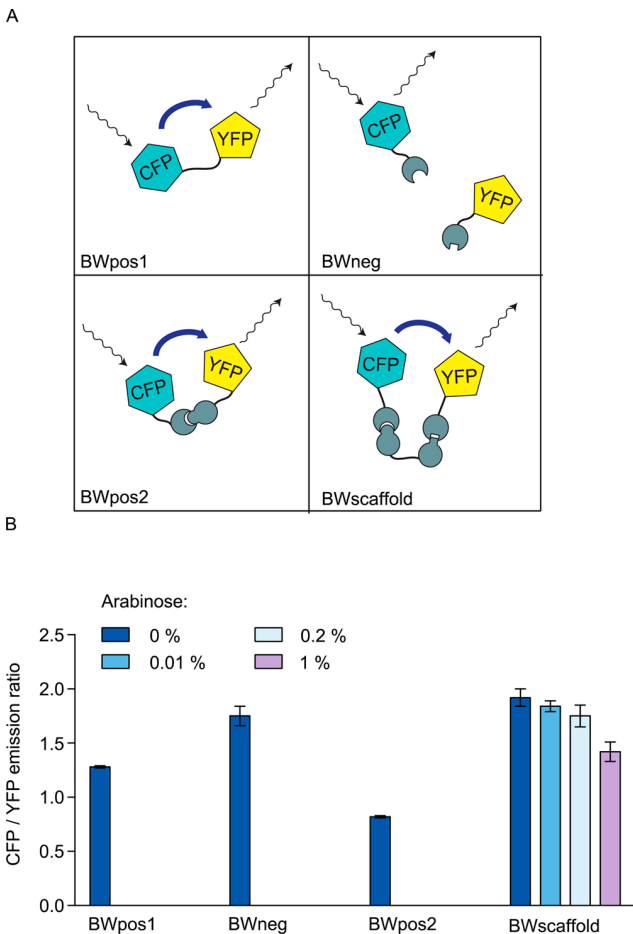


**Figure 2.** FRET analysis for detection of intracellular interaction between Z-tagged proteins and scaffold. (A) Schematic representation of constructs used in the FRET assay. Blue arrows indicate energy transfer. (B) FRET analysis of control samples (no arabinose added) and Z-tagged fluorophores coexpressed with different levels of scaffold. CFP was excited at 415 nm and emission was detected at 475 and 530 nm for CFP and YFP, respectively. A reduced 475 nm/530 nm signal ratio indicates FRET. Error bars are standard deviations of biological duplicates.

expression levels tested, illustrating the need for careful optimization of enzyme-to-scaffold ratios.

In order to evaluate the system for production of farnesene in yeast, affibodies  $Z_{Taq}$  and  $Z_{IgA}$  were fused to farnesene synthase (FarnSyn) and FPP synthase (FPPSyn, encoded by *ERG20*) and expressed from a multicopy  $2\ \mu\text{m}$  plasmid together with the scaffold, consisting of the linked anti-idiotypic partners (ScAffi15). Both enzymes and scaffold were expressed from strong constitutive promoters,  $P_{TEF1}$  and  $P_{PGK1}$ . In control strains, FarnSyn and FPPSyn were expressed without Z-fusion or scaffold (ScAffi13) and with Z-fusion but without scaffold (ScAffi14). In shake flask cultivations, neither Z-fusion nor Z-fusion with expression of scaffold had an effect on farnesene production and all three strains produced farnesene at approximately  $8\ \text{mg/L}_{\text{aq}}$  after 72 h (Figure S1A). One possible explanation for the lack of effect is an incorrect stoichiometry of the enzyme and scaffold proteins. Expressing the enzymes and scaffold from  $P_{PGK1}$  and  $P_{TEF1}$  on a single plasmid will provide high amounts of both scaffold and enzymes inside the cell. Previous reports have shown that the enzyme:scaffold ratio is essential for the functionality of protein scaffolds.<sup>1,7</sup> Levchenko

et al. used a model to investigate the action of a scaffold for the MAP-kinase signaling pathway, and found a strong dependency of the response to the scaffold concentration.<sup>7</sup> The authors hypothesized that when exceeding an optimal concentration, the scaffold confers less effect as additional scaffolds may bind none or only one of the enzymes. To reduce the scaffold abundance, we took promoters from the genes encoding alcohol dehydrogenase 1 (*ADH1*) and serine protease kexin (*KEX2*);  $P_{ADH1}$  and  $P_{KEX2}$  are weaker than  $P_{TEF1}$ , with <20% and 0.02% of  $P_{TEF1}$  activity, respectively.<sup>23,24</sup> When the scaffold was produced from  $P_{ADH1}$  (ScAffi21), we observed a small increase in farnesene titers (Figure S1B). However, due to this strain's reduced growth, the specific titer of farnesene increased by 73% relative to ScAffi14, from  $15.2$  to  $26.4\ \mu\text{g/OD}600$ . When the scaffold was under the weakest promoter,  $P_{KEX2}$ , farnesene titers were equal to ScAffi14, which indicates that scaffold expression was too low to have an effect.

To further vary the enzyme:scaffold ratio, we integrated  $Z_{Taq}$ -FarnSyn and  $Z_{IgA}$ -FPPSyn into the genome and put the scaffold on a centromeric, low copy plasmid (2–8 copies per cell<sup>25</sup>) with various promoters. Thereby, copy numbers for both enzymes and scaffold were reduced and the scaffold concentration could be varied. In this configuration, strain ScAffi04 is a reference where the Z-tagged enzymes and the low copy plasmid are present, but the plasmid is empty and does not contain scaffold. We note that here, simply fusing the Z domains to FarnSyn and FPPSyn increased farnesene titers relative to untagged enzymes (compare ScAffi02 to ScAffi04 in Figure 3). This could indicate a positive effect on the protein

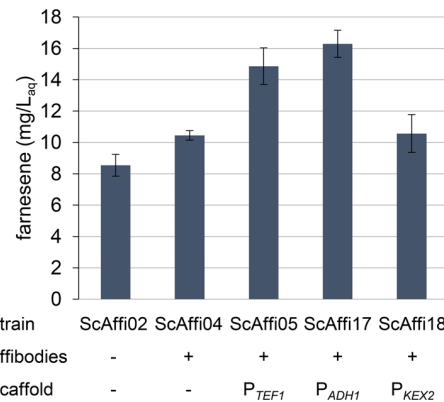


**Figure 3.** Affibody scaffold effects on farnesene production in *S. cerevisiae*. Farnesene synthase and FPP synthase were fused with the affibodies  $Z_{IgA}$  and  $Z_{Taq}$ , respectively, and integrated into the chromosome (in ScAffi02 the enzymes did not have affibody fusions). A scaffold consisting of linked anti-idiotypic affibodies, anti- $Z_{Taq}$  and anti- $Z_{IgA}$ , were on a low copy number plasmid under promoters  $P_{TEF1}$ ,  $P_{ADH1}$  or  $P_{KEX2}$ . Bars represent average farnesene concentrations per volume of aqueous medium of three biological replicates with standard deviations after 72 h of cultivation in shake flasks.

folding or stability of the enzymes, as previously seen *in vitro* for affibody-fused proteins.<sup>26</sup> In ScAffi05, the scaffold was under the  $P_{TEF1}$  promoter and this strain produced 74% more farnesene than ScAffi02, and 42% more than ScAffi04 (Figure 3). Strain ScAffi17 had a reduced scaffold production from  $P_{ADH1}$ ; this increased farnesene by 91% over ScAffi02 and by 56% over ScAffi04 and gave the highest farnesene titers ( $16\ \text{mg/L}_{\text{aq}}$ ). ScAffi18 had scaffold production from  $P_{KEX2}$  and did not produce more than the reference strain ScAffi04. The

scaffold effect was only observed if FarnSyn and FPPSyn had affibody tags (Figure S2). Furthermore, reducing the 20-residue ( $\text{SSSG}_4$ ) linker between the scaffold sites anti- $Z_{\text{Taq}}$  and anti- $Z_{\text{IgA}}$  to either 10 or 5 residues did not reduce the scaffold effect on farnesene production (Figure S3A). This suggests that direct proximity between FPPSyn and FarnSyn is not the main factor in the scaffold activation.

We next tested if the scaffold effect on farnesene production was consistent using different carbon sources. Growth on glucose, galactose, and ethanol could all affect the abundance of mevalonate pathway intermediates since acetyl-CoA is produced from different routes. To facilitate growth on ethanol, all cultivations were performed using 1% w/v of carbon source. As expected, this led to reduced concentrations of farnesene on glucose for strains ScAffi04 and ScAffi05 compared to previous data (Figure S3B). On the other hand, the relative difference in production of farnesene between these strains was found to be the same as when a higher glucose concentration (2%) was used, with a scaffold-mediated titer increase of approximately 39%. When using galactose and ethanol as carbon and energy source, the overall farnesene concentrations were slightly lower on average while the relative increase from ScAffi04 to ScAffi05 was about the same, a 41% and 42% increase compared with the reference, respectively. Hence the scaffold effect was unchanged by modification of the environmental conditions.

Lastly, we tested the effect of the affibody scaffold when it is expressed in a strain further engineered to increase availability of FPP. For this purpose, fusions  $Z_{\text{Taq}}$ -FarnSyn and  $Z_{\text{IgA}}$ -FPPSyn were integrated into strain SCICK16a which has deletions of phosphatases *DPP1* and *LPP1*, downregulation of *ERG9* to reduce loss of FPP to side reactions,<sup>27</sup> and additionally overexpresses *tHMG1* to increase the overall flux through the mevalonate pathway. The resulting strain ScAffi09 was transformed with plasmid p416TEF, pAffi5 or pAffi7 to allow for comparison between no scaffold expression (ScAffi10) to scaffold expression from  $P_{\text{TEFI}}$  (ScAffi11) and  $P_{\text{ADHI}}$  (ScAffi19). Strains were cultivated in fed-batch mode as low glucose concentrations are necessary to activate downregulation of *ERG9* using  $P_{\text{HXT1}}$ .<sup>27</sup> The results depicted in Figure 4 show that titers were increased 120% when  $P_{\text{ADHI}}$  was used for scaffold expression. This scaffold-mediated effect on farnesene titer is higher than those reported previously for FPPSyn and FarnSyn fusion.<sup>17</sup> When  $P_{\text{TEFI}}$  was used for the scaffold expression, titers increased 40%, which is identical to the improvements observed

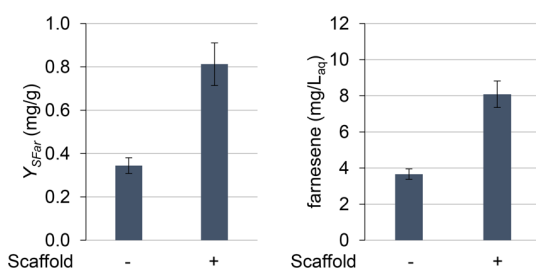


**Figure 4.** Expression of the affibody-scaffold complex for production of farnesene in fed-batch cultivations. All strains express the fusion constructs of affibodies  $Z_{\text{Taq}}$  and  $Z_{\text{IgA}}$  to the FPP and farnesene synthase from the chromosome. The anti- $Z_{\text{Taq}}$ -anti- $Z_{\text{IgA}}$  scaffold was expressed from a low copy number plasmid. No scaffold: ScAffi10; scaffold: ScAffi19 (scaffold expression under  $P_{\text{ADHI}}$ ). Data represent average values of two or three biological replicates with standard deviation 6 h after initiation of the feed phase.

in shake flasks (Figure S4). As described in the **Materials and Methods** section, an extractive dodecane overlay was added prior to initiation of the feeding. Since more time had elapsed between depletion of ethanol and addition of dodecane, farnesene concentrations were generally reduced due to product loss caused by gas stripping effects.<sup>28</sup> Considering utilization of glucose for production of farnesene from the FPP branch point, scaffold expression using  $P_{\text{TEFI}}$  improved the specific product yield  $Y_{\text{SFar}}$  by 65% from 0.458 to 0.760 mg/g, and by 135% from 0.345 to 0.813 mg/g using  $P_{\text{ADHI}}$ .

Because the optimal scaffold induction was from a low-copy plasmid with the relatively weak  $P_{\text{ADHI}}$  promoter, it is likely that most of the tagged FarnSyn and FPPSyn enzymes are not scaffolded, so that the real scaffold benefit is underestimated by these measurements. Scaffold aggregates are also possible, and here the structure of the two enzymes may play a role. While there is no general conclusion on the structure of the farnesene synthase, which has been described as monomeric and as oligomeric,<sup>29,30</sup> FPP synthase was reported to be a homodimer in its active conformation.<sup>31</sup> The FPP synthase homodimer could therefore have two  $Z_{\text{Taq}}$  fusions and possibly bind two scaffolds simultaneously. Likewise, an oligomeric farnesene synthase could bind to multiple scaffolds, leading to the formation of larger enzyme agglomerates. The scaffold effect could therefore arise from clustering of the enzymes and not necessarily substrate channeling.<sup>32,33</sup>

To extend the applicability of the affibody scaffold approach, we attempted to scaffold the three enzymes of the polyhydroxybutyrate (PHB) pathway from the cyanobacterium *Synechocystis* sp. PCC 6803, produced heterologously in *E. coli* (Figure 5A and 5B). PHB accumulates as a carbon and redox sink in various microorganisms upon nutrient limitation, and has industrial applications as a Bioplastic.<sup>34</sup> The PHB pathway is three-step linear conversion from acetyl-CoA. The first step, reversible condensation of two acetyl-CoA to acetoacetyl-CoA, catalyzed by  $\beta$ -ketothiolase (PhaA), is thermodynamically unfavorable at standard conditions and requires either a high acetyl-CoA or a low acetoacetyl-CoA concentration to have net forward flux. This unfavorable condensation step is also thought to limit *n*-butanol production when the pathway is ported to non-native hosts.<sup>35–37</sup> Efficient channeling of acetoacetyl-CoA from PhaA to PhaB, which reversibly reduces it to 3-hydroxybutyryl-CoA, could thus potentially increase the acetyl-CoA:acetoacetyl-CoA ratio and thermodynamic driving force of the condensation reaction. The PHB synthesis step catalyzed by PhaEC is thought to be irreversible. Recent efforts to increase PHB productivity in transgenic plants by fusing the three pathway enzymes instead resulted in reduced PHB production, presumably due to protein misfolding and aggregation.<sup>38</sup> The PhaA and PhaB enzymes from *Synechocystis* sp. PCC 6803 are likely homotetrameric, based on homology to the known homotetramers PhaA<sup>39</sup> and PhaB<sup>40</sup> from *Ralstonia eutropha*, which could result in formation of enzyme-scaffold aggregates. We thus hypothesized that the PHB pathway could benefit from scaffolding.

The three PHB enzymes were tagged N-terminally with affibodies to generate  $Z_{\text{WT}}$ -PhaA,  $Z_{\text{HER2}}$ -PhaB and  $Z_{\text{IgA}}$ -PhaEC. The 3-site anti-idiotypic scaffold consisted of anti- $Z_{\text{WT}}$ , anti- $Z_{\text{HER2}}$ , and anti- $Z_{\text{IgA}}$  separated by ( $\text{SSSG}_4$ ) linkers. The PHB or Z-PHB operon was placed on a plasmid (pBR322 origin) under an IPTG-inducible promoter and induced at either low (0.05 mM IPTG) or high levels (0.5 mM IPTG). The scaffold was on a separate plasmid (p15A origin) under the arabinose-

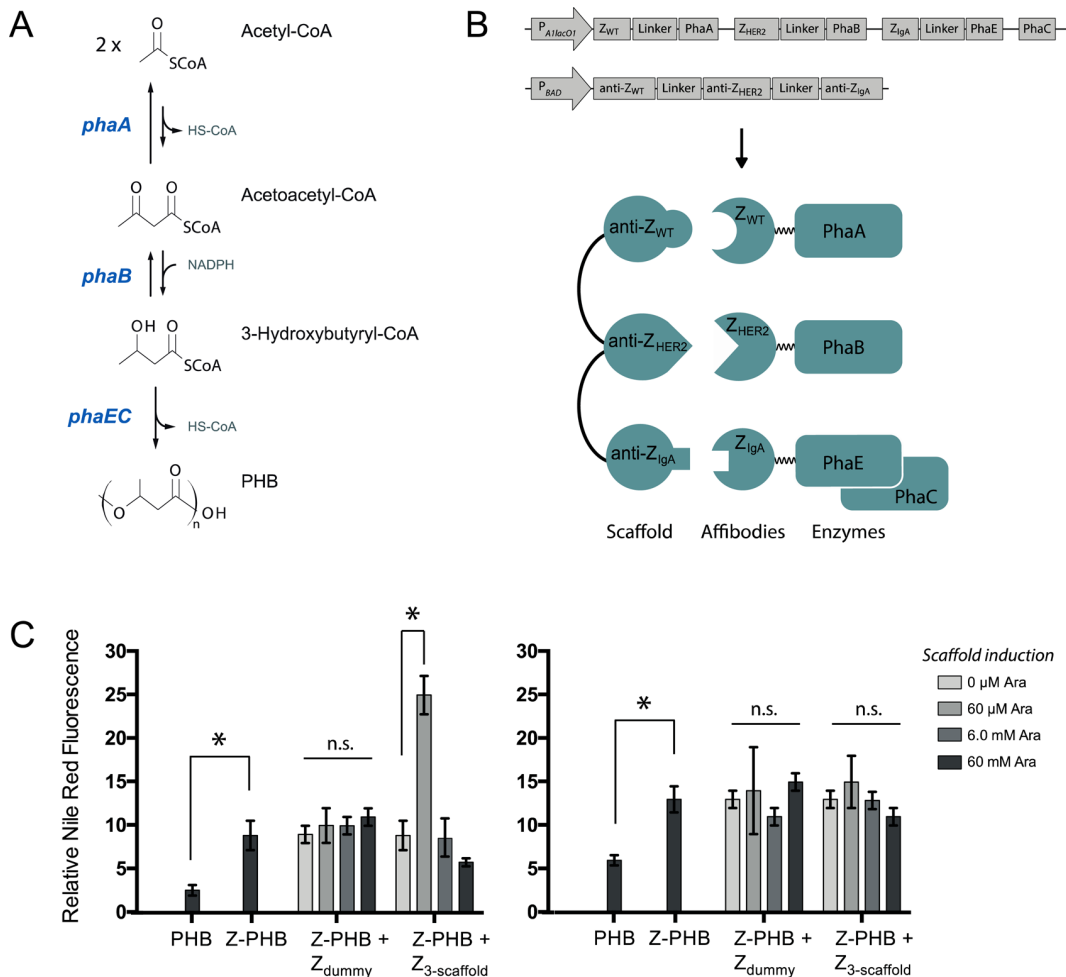


**Figure 5.** A 3-site affibody scaffold improves PHB production from *E. coli*. (A) The heterologous PHB pathway consists of three enzymes and was cloned into *E. coli*. (B) The PhaA, PhaB, and PhaEC enzymes were tagged N-terminally with Z<sub>WT</sub>, Z<sub>HER2</sub>, and Z<sub>IgA</sub>, respectively. Genes encoding the enzymes were expressed from IPTG-inducible promoter P<sub>AllacO1</sub> and the 3-site affibody scaffold (anti-Z<sub>WT</sub>-anti-Z<sub>HER2</sub>-anti-Z<sub>IgA</sub>) from arabinose-inducible promoter P<sub>BAD</sub>. (C) PHB levels 24 h after enzyme and scaffold induction in M9 media supplemented with glycerol to 2%. PHB quantification was done using Nile Red staining and fluorescence and was normalized by cell density. Left: PHB enzymes were induced at low IPTG concentrations (0.05 mM). Fusion of affibody tags increases PHB levels significantly (\*P < 0.05, n.s. not significant, P > 0.05, Student's *t* test). Induction of the Z<sub>3</sub>-scaffold also increased PHB levels, but only at low scaffold induction (60 μM arabinose). The presence of a nonbinding antibody (Z<sub>dummy</sub>) did not affect PHB levels. Right: PHB levels when PHB enzymes were induced at high IPTG concentrations (0.5 mM).

inducible P<sub>BAD</sub> promoter and induction ranged from 0 to 60 mM Arabinose, according to the published induction range of the promoter.<sup>41</sup> Affibody tagging of each enzyme as well as coexpression of the scaffold were confirmed by Western blotting with a Z-domain specific antibody (Figure S5). PHB accumulation was measured via Nile Red fluorescence.

The *E. coli* strains were grown in M9 minimal media with 2% glycerol. First, we observed that fusion of the PHB enzymes with affibody tags increased PHB production approximately 3-fold, even in the absence of scaffold (Figure 5C). This effect is similar to that observed with the farnesene pathway and thus appears to be a general benefit of affibody tagging. Induction of the scaffold increased PHB production a further 2.5-fold, but the effect was only observed at low enzyme levels and the lowest scaffold induction level (Figure 5C, left). Induction of the scaffold to higher amounts erased the boosting effect. Induction of a “dummy” scaffold that does not bind the tagged enzymes did not have an effect on PHB accumulation. At higher enzyme levels (IPTG 0.5 mM), the scaffold did not have an effect. Similar to the farnesene pathway, the scaffold effect

was only present when the enzymes and scaffold were in the proper ratios. We observed a similar, though much less pronounced trend when the cells were grown and induced for PHB production in LB media (Figure S6).

The dominant factor in the efficacy of the affibody scaffold in both systems is the ratio between enzyme and scaffold. Although linker length was not a key parameter in our experiments, we assume that other aspects regarding the construction of the complex may also have an impact. For example, C-terminal fusion of affibodies might display different properties and a different effect on production. Finally, affibodies with even higher affinity to their targets could improve the scaffold effect, by increasing the probability that a full scaffold is present. For example, the affibody pairs used here have dissociation constants ( $K_D$ ) ranging from 900 nM to 50 nM, corresponding to complex half-lives between 3 and 50 s. Median enzyme turnover numbers for central and secondary metabolism (20 s<sup>-1</sup> and 2.5 s<sup>-1</sup>, respectively)<sup>42</sup> correspond to enzyme–substrate complex lifetimes of 35–270 ms. Therefore, it is possible that the lifetime of “full” scaffold, where all three

**Table 1.** List of Plasmids Used in This Study

plasmid	description	reference
pIRP01	$P_{TEF1-tHMG1}$	48
pCfb0390	XI-3- <i>LoxP-KIURA3</i>	49
p416TEF	URA3 based expression vector with <i>TEF1</i> promoter	55
pIST02	$P_{TEF1-FarnSyn\_Cj}$	56
pFRET01	$P_{trc}$ -YFP-CFP with (SSSSG) <sub>2</sub> linker	This study
pFRET02	$P_{trc}$ - <i>Z<sub>IgA</sub></i> -YFP $Z_{Taq}$ -CFP with SGSSSG linkers	This study
pFRET03	$P_{trc}$ -anti- <i>Z<sub>Taq</sub></i> -YFP $Z_{Taq}$ -CFP with SGSSSG linkers	This study
pFRETscaffold	$P_{BAD}$ -anti- <i>Z<sub>Taq</sub></i> -anti- <i>Z<sub>IgA</sub></i> with (SSSSG) <sub>4</sub> linker	This study
pPHB	$P_{AlacO1}$ - <i>phaA<sub>6803</sub></i> <i>phaB<sub>6803</sub></i> <i>phaE<sub>6803</sub></i> <i>phaC<sub>6803</sub></i>	This study
pZPHB	$P_{AlacO1}$ - <i>Z<sub>WT</sub></i> - <i>phaA<sub>6803</sub></i> <i>Z<sub>HER2</sub></i> - <i>phaB<sub>6803</sub></i> <i>Z<sub>IgA</sub></i> - <i>phaE<sub>6803</sub></i> <i>phaC<sub>6803</sub></i>	This study
pZ <sub>3</sub> Scaff	$P_{BAD}$ -anti- <i>Z<sub>WT</sub></i> -anti- <i>Z<sub>HER2</sub></i> -anti- <i>Z<sub>IgA</sub></i> with (SSSSG) <sub>4</sub> linkers	This study
pZ <sub>dummy</sub>	$P_{BAD}$ - <i>Z<sub>WT</sub></i>	This study
pAffiRef	$P_{PGK1-ERG20}$ , $P_{TEF1-FarnSyn\_Cj}$	This study
pAffi1	$P_{PGK1-Z_{IgA}-ERG20}$ , $P_{TEF1-Z_{Taq}-FarnSyn\_Cj}$	This study
pAffi3	$P_{PGK1-Z_{IgA}-ERG20}$ , $P_{TEF1-Z_{Taq}-FarnSyn\_Cj}$ , $P_{TEF1}$ -anti- <i>Z<sub>Taq</sub></i> -anti- <i>Z<sub>IgA</sub></i> with (SSSSG) <sub>4</sub> linker	This study
pAffi5	$P_{TEF1}$ -anti- <i>Z<sub>Taq</sub></i> -anti- <i>Z<sub>IgA</sub></i> with (SSSSG) <sub>4</sub> linker	This study
pAffi7	$P_{ADH1}$ anti- <i>Z<sub>Taq</sub></i> -anti- <i>Z<sub>IgA</sub></i> with (SSSSG) <sub>4</sub> linker	This study
pAffi8	$P_{KEX2}$ anti- <i>Z<sub>Taq</sub></i> -anti- <i>Z<sub>IgA</sub></i> with (SSSSG) <sub>4</sub> linker	This study
pAffi9	$P_{PGK1-Z_{IgA}-ERG20}$ , $P_{TEF1-Z_{Taq}-FarnSyn\_Cj}$ , $P_{ADH1}$ anti- <i>Z<sub>Taq</sub></i> -anti- <i>Z<sub>IgA</sub></i> with (SSSSG) <sub>4</sub> linker	This study
pAffi10	$P_{PGK1-Z_{IgA}-ERG20}$ , $P_{TEF1-Z_{Taq}-FarnSyn\_Cj}$ , $P_{KEX2}$ anti- <i>Z<sub>Taq</sub></i> -anti- <i>Z<sub>IgA</sub></i> with (SSSSG) <sub>4</sub> linker	This study
pAffi11	$P_{TEF1}$ -anti- <i>Z<sub>Taq</sub></i> -anti- <i>Z<sub>IgA</sub></i> with (SSSSG) <sub>2</sub> linker	This study
pAffi12	$P_{TEF1}$ -anti- <i>Z<sub>Taq</sub></i> -anti- <i>Z<sub>IgA</sub></i> with SSSSG linker	This study

enzymes are colocalized simultaneously, is short relative to the enzyme–substrate cascade. It is thus important to consider that scaffold aggregates, facilitated by dimeric or multimeric enzymes, could increase the probability of an intermediate encountering the correct pathway enzyme.

In conclusion, affibody scaffolds for metabolic engineering were demonstrated in *S. cerevisiae* and *E. coli*. A two-component scaffold improved flux through the mevalonate pathway toward farnesene, and titers increased up to 56% in shake flask and 120% in fed-batch cultivations. A three-component scaffold increased productivity of the polymer PHB in *E. coli* approximately 7-fold compared to the untagged PHB operon. In comparison to conventional enzyme fusion, affibodies and their anti-idiotypic partners allow for a flexible way to colocalize enzymes, which can be tuned by manipulating the scaffold concentration. There are numerous well-characterized affibodies and several anti-idiotypic pairs available, as well as heuristics for improving the affinity of these pairs.<sup>43</sup> Affibody scaffolds could thus be used to construct scaffold aggregates, or applied to pathways involving more enzymatic reactions.

## MATERIALS AND METHODS

**Plasmid and Strain Construction.** A complete list of plasmids and strains used for this study is shown in Table 1 and 2. Plasmids for the FRET assay and PHB assays were cloned in *E. coli* XL1-Blue and expressed in *E. coli* BW25993.<sup>44</sup> Anti-*Z<sub>Taq</sub>* and anti-*Z<sub>IgA</sub>* were PCR amplified from plasmids constructed by Eklund *et al.*<sup>13</sup> The (SSSSG)<sub>4</sub> linker was introduced in primer overhangs and PCR fragments were assembled under the arabinose-inducible  $P_{BAD}$  promoter in pBAD33 using Gibson assembly,<sup>45</sup> resulting in plasmid pFRETscaffold. pFRET01–03 are all derivatives of plasmid pUCIDT (Kan) (Integrated DNA Technologies, Coralville, IA, USA), with a lacI cassette and IPTG-inducible  $P_{trc}$  promoter introduced. *Z<sub>Taq</sub>* and *Z<sub>IgA</sub>* fused with fluorophores mTurquoise<sup>46</sup> and eYFP (hereafter CFP and YFP) were ordered as gBlocks gene fragments (Integrated

DNA Technologies) and assembled under  $P_{trc}$  using traditional restriction enzyme digestion and ligation.

For construction of plasmid pAffiRef, *ERG20* encoding FPP synthase was amplified from genomic DNA of *S. cerevisiae* strain CEN.PK113–SD and ligated into plasmid pIST02 using restriction enzymes *Xba*I and *Bam*H I (Thermo Fisher Scientific, Waltham, MA, USA). All other plasmids were constructed using CPEC<sup>47</sup> with primers listed in Table S1. Sequences for promoters *ADH1*, *KEX2* and terminator *IDP1* were also amplified from *S. cerevisiae* strain CEN.PK113–SD. SCICK16a was constructed by integration of truncated *HMG1* (*tHMG1*) using cassette pIRP01.<sup>48</sup> Strains ScAffi01, 03, 07, and 09 were constructed by amplification of *ERG20* and *FarnSyn* as well as their fusions to affibody *Z<sub>IgA</sub>* and *Z<sub>Taq</sub>* in a single PCR from plasmids pAffiRef and pAffi1, respectively. To enable chromosomal integration using homologous recombination, recognition sites for integration site XI-3 were amplified from plasmid pCfb0390.<sup>49</sup> Affibody sequences are provided in the Supporting Information. A list of primers used for strain construction is presented in Table S2.

For construction of the PHB operon, the genes *phaA*, *phaB*, and *phaEC* were PCR-amplified from *Synechocystis* sp. PCC 6803 as two operons, *phaAB* and *phaEC*. Sequences for *Z<sub>WT</sub>*, *Z<sub>HER2</sub>* and anti-*Z<sub>HER2</sub>* were taken from Wällberg *et al.*<sup>50</sup> and the sequence of anti-*Z<sub>WT</sub>* was the same as *Z<sub>pA963</sub>* from Lindborg *et al.*<sup>51</sup> The affibodies were synthesized commercially (IDT gBlocks) and fused via (SSSSG)<sub>4</sub>-encoding linkers to the *phaA*, *phaB*, or *phaEC* genes using Gibson assembly. Care was taken not to alter the native ribosome binding sites upstream of *phaB* and *phaC*. The resulting PHB and Z-PHB operons were then cloned under the  $P_{AlacO1}$  promoter.<sup>52</sup> The 3-piece affibody scaffold with (SSSSG)<sub>4</sub> linkers was synthesized commercially (Integrated DNA Technologies) and cloned downstream of the  $P_{BAD}$  promoter in the commercial vector pBAD33 (ATCC).

**Growth Media.** Strains of *S. cerevisiae* with auxotrophy for uracil were grown on YPD plates containing 20 g/L glucose, 10 g/L yeast extract, 20 g/L peptone from casein and 20 g/L agar.

**Table 2.** List of Strains Used in This Study

strain	relevant genotype	plasmid	reference
<i>E. coli</i>			
<i>E. coli</i> XL1-Blue	endA1 gyrA96(nal <sup>R</sup> ) thi-1 recA1 relA1 lac gln V44 F'[:Tn10 proAB <sup>+</sup> lacI <sup>q</sup> Δ(lacZ) M15] hsdR17(r <sub>K</sub> <sup>-</sup> m <sub>K</sub> <sup>+</sup> )	—	
<i>E. coli</i> BW25993	Δ(arad-araB)S67, λ, rph-1, Δ(rhaD-rhaB)S68, hsdRS14	—	<sup>44</sup>
BW <sub>pos1</sub>	<i>E. coli</i> BW25993	pFRET01	This study
BW <sub>neg</sub>	<i>E. coli</i> BW25993	pFRET02	This study
BW <sub>pos2</sub>	<i>E. coli</i> BW25993	pFRET03	This study
BW <sub>scaffold</sub>	<i>E. coli</i> BW25993	pFRET02, pFRETscaffold	This study
PHB	<i>E. coli</i> BW25993	pPHB	This study
Z-PHB	<i>E. coli</i> BW25993	pZPHB	This study
Z-PHB + Z <sub>dummy</sub>	<i>E. coli</i> BW25993	pZPHB, pZ <sub>dummy</sub>	This study
Z-PHB + Z <sub>3-scaffold</sub>	<i>E. coli</i> BW25993	pZPHB, pZ <sub>3Scaff</sub>	This study
<i>S. cerevisiae</i>			
CEN.PK113–SD	MATA MAL2–8 <sup>c</sup> SUC2 ura3–52	—	P. Kötter, University of Frankfurt, Germany
SCICK 16a	MATA MAL2–8 <sup>c</sup> SUC2 ura3–52 lpp1Δ::loxP dpp1Δ::loxP P <sub>ERG9</sub> Δ::loxP-P <sub>HXT1</sub> P <sub>TEFI</sub> -tHMG1	—	This study
ScAffi01	CEN.PK113–SD P <sub>PGK1</sub> -ERG20 P <sub>TEFI</sub> -FarnSyn_Cj	—	This study
ScAffi02	ScAffi01	p416TEF	This study
ScAffi03	CEN.PK113–SD P <sub>PGK1</sub> -Z <sub>IgA</sub> -ERG20 P <sub>TEFI</sub> -Z <sub>Taq</sub> -FarnSyn_Cj	—	This study
ScAffi04	ScAffi03	p416TEF	This study
ScAffi05	ScAffi03	pAffi5	This study
ScAffi09	SCICK16a P <sub>PGK1</sub> -Z <sub>IgA</sub> -ERG20 P <sub>TEFI</sub> -Z <sub>Taq</sub> -FarnSyn_Cj	—	This study
ScAffi10	ScAffi09	p416TEF	
ScAffi11	ScAffi09	pAffi5	This study
ScAffi13	CEN.PK113–SD	pAffiRef	This study
ScAffi14	CEN.PK113–SD	pAffi1	This study
ScAffi15	CEN.PK113–SD	pAffi3	This study
ScAffi16	CEN.PK113–SD	pAffi4	This study
ScAffi17	ScAffi03	pAffi7	This study
ScAffi18	ScAffi03	pAffi8	This study
ScAffi19	ScAffi09	pAffi7	This study
ScAffi21	CEN.PK113–SD	pAffi9	This study
ScAffi22	CEN.PK113–SD	pAffi10	This study
ScAffi23	ScAffi03	pAffi11	This study
ScAffi24	ScAffi03	pAffi12	This study

Plasmid carrying strains were grown on selective growth medium containing 6.9 g/L yeast nitrogen base w/o amino acids (Formedium, Hunstanton, UK), 0.77 g/L complete supplement mixture w/o uracil (Formedium), 20 g/L glucose and 20 g/L agar. Shake flask cultivations were performed using minimal medium containing 30 g/L glucose, 7.5 g/L (NH<sub>4</sub>)<sub>2</sub>SO<sub>4</sub>, 14.4 g/L KH<sub>2</sub>PO<sub>4</sub>, 0.5 g/L MgSO<sub>4</sub>·7H<sub>2</sub>O, 1 mL/L trace element solution and 50 μL/L antifoam (Sigma-Aldrich, St. Louis, MO, USA). After sterilization, vitamin solution was added to a concentration of 1 mL/L. For shake flask cultivations with different carbon sources at 1% w/v, 10 g/L glucose, 10 g/L galactose or 12.7 mL/L ethanol were used instead of 30 g/L glucose. Minimal medium containing 20 g/L glucose, 5 g/L (NH<sub>4</sub>)<sub>2</sub>SO<sub>4</sub>, 3 g/L KH<sub>2</sub>PO<sub>4</sub>, 0.5 g/L MgSO<sub>4</sub>·7H<sub>2</sub>O, 1 mL/L trace element solution, 1 mL/L vitamin solution and 50 μL/L antifoam was used during the batch phase of aerated bioreactor cultivations.<sup>53</sup> The feed medium during the fed-batch phase was ten times concentrated with 200 g/L glucose. The pH was adjusted to 5 using 2 M KOH.

**Shake Flask Cultivations.** Strains of *S. cerevisiae* were grown and maintained on plates with selective medium at 30

°C. Five mL of minimal medium containing 30 g/L glucose were inoculated with a single colony and cultivated overnight at 30 °C and 200 rpm. For shake flask cultivations in different carbon sources, 5 mL minimal medium containing 0.5% w/v glucose and 0.5% w/v galactose or ethanol were inoculated with a single colony. The culture was used to inoculate 18 mL of minimal medium to an OD<sub>600</sub> of 0.1. To sequester farnesene, 2 mL of dodecane (Reagent Plus, ≥99%, Sigma-Aldrich) were added to reach a final concentration of 10% v/v. Shake flasks were cultivated at 180 rpm and 30 °C for 72 h.

**Fed-Batch Cultivations.** For preparation of the preculture, 5 mL of minimal medium were inoculated with a single colony and incubated overnight at 200 rpm and 30 °C. Subsequently, the culture was transferred to a shake flask containing 50 mL of minimal medium. After incubation at 180 rpm and 30 °C for 24 h, the OD<sub>600</sub> was measured using a Genesis20 spectrophotometer (Thermo Fisher Scientific) and the culture was used to inoculate 1 L of batch phase medium at an OD<sub>600</sub> 0.1. Cultivations in bioreactors were carried out using DasGip Parallel Bioreactor Systems (Eppendorf, Hamburg, Germany) together with 2.5 L vessels (Applikon, Delft, The Netherlands).

The vessels were aerated at a rate of 1 vvm and homogeneous mixing was enabled by two six-blade Rushton turbines at a stirring speed of 600 rpm. The temperature was maintained at 30 °C and pH was controlled at 5 using 2 M KOH and 2 M HCl. Composition of the exhaust gas was monitored online using gas analyzer GA4 (DasGip). All cultivations were started in batch. After consumption of glucose and ethanol, 200 mL of dodecane were added under aseptical conditions and the feed was initiated. The feed profile was calculated as  $\nu(t) = 0.007 \cdot \exp(0.1 \cdot t)$  to allow for exponential growth at  $\mu = 0.1 \text{ h}^{-1}$ , whereas  $\nu$  represents the feed rate in L/h and  $t$  the feed time in h.

**Measurement of Cell Growth.** Cell growth was measured in shake flasks using a Genesis20 spectrophotometer (Thermo Fisher Scientific). During cultivations in bioreactors, biomass concentration was determined by pipetting a 5 mL sample on a preweighted filter with a pore size of 0.45 µm (Sartorius, Göttingen, Germany). The filter was washed with 5 mL of water, dried in the microwave at 150 W for 15 min and weighted again.

**Quantification of Farnesene.** For quantification of farnesene, the dodecane overlay was harvested by centrifugation at 4000 rpm for 5 min at the end of the shake flask cultivation. Similarly, dodecane was collected from 10 mL samples taken during cultivation in bioreactors. Analysis was performed using a Focus GC-FID (Thermo Fisher Scientific, Waltham, MA, USA) equipped with a ZB-50 column (Phenomenex, Torrance, CA, USA) as described previously with minor modifications.<sup>28</sup> The initial temperature was held at 50 °C for 1.5 min and then increased to 170 °C at a rate of 15 °C/min. After keeping the temperature constant for another 1.5 min, it was raised at the same rate to 300 °C and held for 3.0 min. The inlet temperature was set to 250 °C and 2 µL sample were injected in splitless mode. The base temperature of the flame was set to 300 °C. Farnesene was quantified using external calibration with trans-β-farnesene as analytical standard ( $\geq 90\%$ , Sigma-Aldrich). All shake flask samples were analyzed directly in dodecane. Fermentation samples were diluted in hexane and patchoulol ( $\geq 99\%$ , a kind gift from Firmenich, Geneva, Switzerland) was added as internal standard. Concentrations of farnesene are stated based on volume of aqueous medium (mg/L<sub>aq</sub>).

**FRET Analysis.** Overnight cultures of *E. coli* BW25993 strains grown in LB medium were inoculated in a 1:100 ratio into fresh LB and cultivated at 37 °C, 200 rpm until OD<sub>600</sub> reached 0.5–0.6. Cultures were then induced with 0.5 mM IPTG and, where specified, 0.01, 0.2 or 1% arabinose and cultivated for 4 h at 30 °C, 200 rpm before sampling. Cells were centrifuged and resuspended in PBS to an OD<sub>600</sub> of 0.4 before fluorescence measurements with a SpectraMax M5 microplate reader (Molecular Devices, Sunnyvale, CA, USA). CFP was excited at 415 nm and emission was detected at 475 nm (CFP maxima) and 530 nm (YFP maxima).

**Production and Quantification of PHB.** *E. coli* strains harboring pPHB, pZ-PHB, and pZ3-scaffold plasmids were inoculated into LB media and grown overnight at 37 °C. Cultures were then either washed and resuspended at OD<sub>600</sub> 0.1 in M9 media containing 2% glycerol, or diluted 1:100 into fresh LB, and grown at 37 °C until OD<sub>600</sub> 0.4–0.5. At that time PHB and scaffold were induced by addition of IPTG to 0.05 mM or 0.5 mM and addition of arabinose to 0–60 mM. Induced cells were incubated for 24 h at 30 °C before PHB measurement. Relative quantification of PHB was done using

Nile Red staining and fluorescence assay following the method of Tyo *et al.*<sup>54</sup> who showed a linear correlation between normalized Nile Red PHB content as measured via HPLC. The Nile Red fluorescence was measured in a SpectraMax i5 plate reader (ex 500 nm, em 630 nm) and normalized by OD<sub>600</sub>.

## ■ ASSOCIATED CONTENT

### § Supporting Information

The Supporting Information is available free of charge on the ACS Publications website at DOI: [10.1021/acssynbio.6b00109](https://doi.org/10.1021/acssynbio.6b00109).

Oligonucleotide primers used for chromosomal integration in *S. cerevisiae* and plasmid construction (Table S1 and S2), nucleotide sequences of all affibodies, scaffold effect on farnesene production using single plasmid expression (Figure S1), negative control experiment (Figure S2), effect of linker length and carbon source on affibody scaffolding (Figure S3), farnesene yield on glucose and final farnesene titers obtained in fed-batch cultivations when scaffold is expressed from P<sub>TEF1</sub>, Western Blot detection of Z-fused enzymes and affibody scaffold (Figure S5), Effect of scaffold expression of PHB production in LB media (Figure S6), schematic representation of putative colocalization mediated by affibodies (Figure S7) ([PDF](#))

## ■ AUTHOR INFORMATION

### Corresponding Author

\*E-mail: [paul.hudson@biotech.kth.se](mailto:paul.hudson@biotech.kth.se). Tel: +46 8 553 783 17.

### Author Contributions

<sup>#</sup>ST and JA contributed equally.

### Notes

The authors declare no competing financial interest.

## ■ ACKNOWLEDGMENTS

This work was funded by Knut and Alice Wallenberg Foundation, the Swedish Research Council Formas, and the Novo Nordisk Foundation. The authors wish to thank John Löfblom and Ken Andersson at KTH Royal Institute of Technology for fruitful discussions and experimental assistance.

## ■ REFERENCES

- (1) Dueber, J. E., Wu, G. C., Malmirchegini, G. R., Moon, T. S., Petzold, C. J., Ullal, A. V., Prather, K. L. J., and Keasling, J. D. (2009) Synthetic protein scaffolds provide modular control over metabolic flux. *Nat. Biotechnol.* 27, 753–759.
- (2) Sachdeva, G., Garg, A., Godding, D., Way, J. C., and Silver, P. A. (2014) *In vivo* co-localization of enzymes on RNA scaffolds increases metabolic production in a geometrically dependent manner. *Nucleic Acids Res.* 42, 9493–9503.
- (3) Conrado, R. J., Varner, J. D., and DeLisa, M. P. (2008) Engineering the spatial organization of metabolic enzymes: mimicking nature's synergy. *Curr. Opin. Biotechnol.* 19, 492–499.
- (4) Kerfeld, C. A., and Erbilgin, O. (2015) Bacterial microcompartments and the modular construction of microbial metabolism. *Trends Microbiol.* 23, 22–34.
- (5) Lee, H., DeLoache, W. C., and Dueber, J. E. (2012) Spatial organization of enzymes for metabolic engineering. *Metab. Eng.* 14, 242–251.
- (6) Park, M., Sun, Q., Liu, F., DeLisa, M. P., and Chen, W. (2014) Positional assembly of enzymes on bacterial outer membrane vesicles for cascade reactions. *PLoS One* 9, e97103.
- (7) Levchenko, A., Bruck, J., and Sternberg, P. W. (2000) Scaffold proteins may biphasically affect the levels of mitogen-activated protein

- kinase signaling and reduce its threshold properties. *Proc. Natl. Acad. Sci. U. S. A.* 97, 5818–5823.
- (8) Fu, J., Liu, M., Liu, Y., Woodbury, N. W., and Yan, H. (2012) Interenzyme substrate diffusion for an enzyme cascade organized on spatially addressable DNA nanostructures. *J. Am. Chem. Soc.* 134, 5516–5519.
- (9) Sun, Q., Madan, B., Tsai, S.-L., DeLisa, M. P., and Chen, W. (2014) Creation of artificial cellulosomes on DNA scaffolds by zinc finger protein-guided assembly for efficient cellulose hydrolysis. *Chem. Commun.* 50, 1423–1425.
- (10) Nilsson, B., Moks, T., Jansson, B., Abrahmsén, L., Elmblad, A., Holmgren, E., Henrichson, C., Jones, T. A., and Uhlén, M. (1987) A synthetic IgG-binding domain based on staphylococcal protein a. *Protein Eng. Des. Sel.* 1, 107–113.
- (11) Löfblom, J., Feldwisch, J., Tolmachev, V., Carlsson, J., Ståhl, S., and Frejd, F. Y. (2010) Affibody molecules: Engineered proteins for therapeutic, diagnostic and biotechnological applications. *FEBS Lett.* 584, 2670–2680.
- (12) Nygren, P. Å. (2008) Alternative binding proteins: Affibody binding proteins developed from a small three-helix bundle scaffold. *FEBS J.* 275, 2668–2676.
- (13) Eklund, M., Axelsson, L., Uhlén, M., and Nygren, P. Å. (2002) Anti-idiotypic protein domains selected from protein A-based affibody libraries. *Proteins: Struct., Funct., Genet.* 48, 454–462.
- (14) Ito, J., Kosugi, A., Tanaka, T., Kuroda, K., Shibasaki, S., Ogino, C., Ueda, M., Fukuda, H., Doi, R. H., and Kondo, A. (2009) Regulation of the display ratio of enzymes on the *Saccharomyces cerevisiae* cell surface by the immunoglobulin G and cellulosomal enzyme binding domains. *Appl. Environ. Microbiol.* 75, 4149–4154.
- (15) Albertsen, L., Chen, Y., Bach, L. S., Rattleff, S., Maury, J., Brix, S., Nielsen, J., and Mortensen, U. H. (2011) Diversion of flux toward sesquiterpene production in *Saccharomyces cerevisiae* by fusion of host and heterologous enzymes. *Appl. Environ. Microbiol.* 77, 1033–1040.
- (16) Sarria, S., Wong, B., Martín, H. G., Keasling, J. D., and Peralta-Yahya, P. (2014) Microbial synthesis of pinene. *ACS Synth. Biol.* 3, 466–475.
- (17) Wang, C., Yoon, S. H., Jang, H. J., Chung, Y. R., Kim, J. Y., Choi, E. S., and Kim, S. W. (2011) Metabolic engineering of *Escherichia coli* for α-farnesene production. *Metab. Eng.* 13, 648–655.
- (18) Lendel, C., Dogan, J., and Härd, T. (2006) Structural basis for molecular recognition in an affibody:affibody complex. *J. Mol. Biol.* 359, 1293–1304.
- (19) Renberg, B., Nygren, P. Å., Eklund, M., and Karlström, A. E. (2004) Fluorescence resonance energy transfer-based detection of analytes using antiidiotypic affinity protein pairs. *Anal. Biochem.* 334, 72–80.
- (20) Rowland, C. E., Brown, C. W., Medintz, I. L., and Delehanty, J. B. (2015) Intracellular FRET-based probes: a review. *Methods Appl. Fluoresc.* 3, 042006.
- (21) Ainavarapu, S. R. K., Brujić, J., Huang, H. H., Wiita, A. P., Lu, H., Li, L., Walther, K. A., Carrion-Vazquez, M., Li, H., and Fernandez, J. M. (2007) Contour length and refolding rate of a small protein controlled by engineered disulfide bonds. *Biophys. J.* 92, 225–233.
- (22) Shimozono, S., and Miyawaki, A. (2008) Engineering FRET constructs using CFP and YFP. *Methods Cell Biol.* 85, 381–393.
- (23) Nacken, V., Achstetter, T., and Degryse, E. (1996) Probing the limits of expression levels by varying promoter strength and plasmid copy number in *Saccharomyces cerevisiae*. *Gene* 175, 253–260.
- (24) Partow, S., Siewers, V., Bjørn, S., Nielsen, J., and Maury, J. (2010) Characterization of different promoters for designing a new expression vector in *Saccharomyces cerevisiae*. *Yeast* 27, 955–964.
- (25) Karim, A. S., Curran, K. A., and Alper, H. S. (2013) Characterization of plasmid burden and copy number in *Saccharomyces cerevisiae* for optimization of metabolic engineering applications. *FEMS Yeast Res.* 13, 107–116.
- (26) Samuelsson, E., Moks, T., Uhlen, M., and Nilsson, B. (1994) Enhanced *in vitro* refolding of insulin-like growth factor I using a solubilizing fusion partner. *Biochemistry* 33, 4207–4211.
- (27) Scalcinati, G., Knuf, C., Partow, S., Chen, Y., Maury, J., Schalk, M., Daviet, L., Nielsen, J., and Siewers, V. (2012) Dynamic control of gene expression in *Saccharomyces cerevisiae* engineered for the production of plant sesquiterpene α-santalene in a fed-batch mode. *Metab. Eng.* 14, 91–103.
- (28) Tippmann, S., Nielsen, J., and Khoomrung, S. (2016) Improved quantification of farnesene during microbial production from *Saccharomyces cerevisiae* in two-liquid-phase fermentations. *Talanta* 146, 100–106.
- (29) Green, S., Friel, E. N., Matich, A., Beuning, L. L., Cooney, J. M., Rowan, D. D., and MacRae, E. (2007) Unusual features of a recombinant apple α-farnesene synthase. *Phytochemistry* 68, 176–188.
- (30) Rupasinghe, H. P. V., Paliyath, G., and Murr, D. P. (2000) Sesquiterpene α-farnesene synthase: Partial purification, characterization, and activity in relation to superficial scald development in apples. *J. Am. Soc. Hortic. Sci.* 125, 111–119.
- (31) Eberhardt, N. L., and Rilling, H. C. (1975) Prenyltransferase from *Saccharomyces cerevisiae*. Purification to homogeneity and molecular properties. *J. Biol. Chem.* 250, 863–866.
- (32) Castellana, M., Wilson, M. Z., Xu, Y., Joshi, P., Cristea, I. M., Rabinowitz, J. D., Gitai, Z., and Wingreen, N. S. (2014) Enzyme clustering accelerates processing of intermediates through metabolic channeling. *Nat. Biotechnol.* 32, 1011–1018.
- (33) Idan, O., and Hess, H. (2013) Origins of activity enhancement in enzyme cascades on scaffolds. *ACS Nano* 7, 8658–8665.
- (34) Gao, X., Chen, J.-C., Wu, Q., and Chen, G.-Q. (2011) Polyhydroxylkanoates as a source of chemicals, polymers, and biofuels. *Curr. Opin. Biotechnol.* 22, 768–774.
- (35) Anfelt, J., Kaczmarzyk, D., Shabestary, K., Renberg, B., Rockberg, J., Nielsen, J., Uhlén, M., and Hudson, E. P. (2015) Genetic and nutrient modulation of acetyl-CoA levels in *Synechocystis* for n-butanol production. *Microb. Cell Fact.* 14, 1–12.
- (36) Bond-Watts, B. B., Bellerose, R. J., and Chang, M. C. Y. (2011) Enzyme mechanism as a kinetic control element for designing synthetic biofuel pathways. *Nat. Chem. Biol.* 7, 222–227.
- (37) Shen, C. R., Lan, E. I., Dekishima, Y., Baez, A., Cho, K. M., and Liao, J. C. (2011) Driving Forces Enable High-Titer Anaerobic 1-Butanol Synthesis in *Escherichia coli*. *Appl. Environ. Microbiol.* 77, 2905–2915.
- (38) Mullaney, J. A., and Rehm, B. H. A. (2010) Design of a single-chain multi-enzyme fusion protein establishing the polyhydroxybutyrate biosynthesis pathway. *J. Biotechnol.* 147, 31–36.
- (39) Kim, E.-J., and Kim, K.-J. (2014) Crystal structure and biochemical characterization of PhaA from *Ralstonia eutropha*, a polyhydroxylkanoate-producing bacterium. *Biochem. Biophys. Res. Commun.* 452, 124–129.
- (40) Matsumoto, K. i., Tanaka, Y., Watanabe, T., Motohashi, R., Ikeda, K., Tobitani, K., Yao, M., Tanaka, I., and Taguchi, S. (2013) Directed evolution and structural analysis of NADPH-dependent acetoacetyl acoenzyme A (Acetoacetyl-CoA) reductase from *Ralstonia eutropha* reveals two mutations responsible for enhanced kinetics. *Appl. Environ. Microbiol.* 79, 6134–6139.
- (41) Siegele, D. A., and Hu, J. C. (1997) Gene expression from plasmids containing the araBAD promoter at subsaturating inducer concentrations represents mixed populations. *Proc. Natl. Acad. Sci. U. S. A.* 94, 8168–8172.
- (42) Bar-Even, A., Noor, E., Savir, Y., Lieberman, W., Davidi, D., Tawfik, D. S., and Milo, R. (2011) The moderately efficient enzyme: Evolutionary and physicochemical trends shaping enzyme parameters. *Biochemistry* 50, 4402–4410.
- (43) Wahlberg, E., and Härd, T. (2006) Conformational stabilization of an engineered binding protein. *J. Am. Chem. Soc.* 128, 7651–7660.
- (44) Datsenko, K. A., and Wanner, B. L. (2000) One-step inactivation of chromosomal genes in *Escherichia coli* K-12 using PCR products. *Proc. Natl. Acad. Sci. U. S. A.* 97, 6640–6645.
- (45) Gibson, D. G., Young, L., Chuang, R. Y., Venter, J. C., Hutchison, C. A., and Smith, H. O. (2009) Enzymatic assembly of DNA molecules up to several hundred kilobases. *Nat. Methods* 6, 343–345.

- (46) Goedhart, J., Van Weeren, L., Hink, M. A., Vischer, N. O. E., Jalink, K., and Gadella, T. W. J. (2010) Bright cyan fluorescent protein variants identified by fluorescence lifetime screening. *Nat. Methods* 7, 137–139.
- (47) Quan, J., and Tian, J. (2011) Circular polymerase extension cloning for high-throughput cloning of complex and combinatorial DNA libraries. *Nat. Protoc.* 6, 242–251.
- (48) López, J., Essus, K., Kim, I., Pereira, R., Herzog, J., Siewers, V., Nielsen, J., and Agosin, E. (2015) Production of  $\beta$ -ionone by combined expression of carotenogenic and plant CCD1 genes in *Saccharomyces cerevisiae*. *Microb. Cell Fact.*, DOI: 10.1186/s12934-015-0273-x.
- (49) Jensen, N. B., Strucko, T., Kildegaard, K. R., David, F., Maury, J., Mortensen, U. H., Forster, J., Nielsen, J., and Borodina, I. (2014) EasyClone: Method for iterative chromosomal integration of multiple genes in *Saccharomyces cerevisiae*. *FEMS Yeast Res.* 14, 238.
- (50) Wållberg, H., Löfdahl, P.-Å., Tschapalda, K., Uhlén, M., Tolmachev, V., Nygren, P.-Å., and Ståhl, S. (2011) Affinity recovery of eight HER2-binding affibody variants using an anti-idiotypic affibody molecule as capture ligand. *Protein Expression Purif.* 76, 127–135.
- (51) Lindborg, M., Dubnovitsky, A., Olesen, K., Björkman, T., Abrahmsén, L., Feldwisch, J., and Härd, T. (2013) High-affinity binding to staphylococcal protein A by an engineered dimeric Affibody molecule. *Protein Eng., Des. Sel.* 26, 635–644.
- (52) Lutz, R., and Bujard, H. (1997) Independent and tight regulation of transcriptional units in *Escherichia coli* via the LacR/O, the TetR/O and AraC/I1-I2 regulatory elements. *Nucleic Acids Res.* 25, 1203–1210.
- (53) Verduyn, C., Postma, E., Scheffers, W. A., and van Dijken, J. P. (1992) Effect of benzoic acid on metabolic fluxes in yeasts: A continuous-culture study on the regulation of respiration and alcoholic fermentation. *Yeast* 8, 501–517.
- (54) Tyo, K. E., Zhou, H., and Stephanopoulos, G. N. (2006) High-throughput screen for poly-3-hydroxybutyrate in *Escherichia coli* and *Synechocystis* sp. Strain PCC6803. *Appl. Environ. Microbiol.* 72, 3412–3417.
- (55) Mumberg, D., Müller, R., and Funk, M. (1995) Yeast vectors for the controlled expression of heterologous proteins in different genetic backgrounds. *Gene* 156, 119–122.
- (56) Tippmann, S., Scalcinati, G., Siewers, V., and Nielsen, J. (2016) Production of farnesene and santalene by *Saccharomyces cerevisiae* using fed-batch cultivations with RQ-controlled feed. *Biotechnol. Bioeng.* 113, 72–81.

## Supplementary Material

Affibody scaffolds improve sesquiterpene production in

*Saccharomyces cerevisiae*

Stefan Tippmann<sup>1,2\*</sup>, Josefina Anfelt<sup>3\*</sup>, Florian David<sup>1,2</sup>, Jacqueline M. Rand<sup>1,4</sup>, Verena Siewers<sup>1,2</sup>, Mathias Uhlén<sup>3,5</sup>, Jens Nielsen<sup>1,2,5</sup>, and Elton P. Hudson<sup>3\*\*</sup>

<sup>1</sup>Department of Biology and Biological Engineering,

Chalmers University of Technology, SE412 96 Gothenburg, Sweden

<sup>2</sup>Novo Nordisk Foundation Center for Biosustainability, Chalmers University of Technology, SE412 96 Gothenburg, Sweden

<sup>3</sup>Division of Proteomics and Nanobiotechnology, School of Biotechnology, Royal Institute of Technology (KTH), Science for Life Laboratory, SE171 21 Stockholm, Sweden

<sup>4</sup>Department of Chemical and Biological Engineering, University of Wisconsin-Madison, Madison, WI 53706, USA

<sup>5</sup>Novo Nordisk Foundation Center for Biosustainability, Technical University of Denmark, DK2970 Hørsholm, Denmark

\*Equal contribution

\*\*Corresponding Author: Elton P. Hudson

Division of Proteomics and Nanobiotechnology, School of Biotechnology, Royal Institute of Technology (KTH), Science for Life Laboratory, SE171 21 Stockholm, Sweden

E-mail: paul.hudson@scilifelab.se

Tel: +46 8 553 783 17

Keywords: affibodies, isoprenoids, biofuels, PHB, yeast, metabolic engineering

Supplementary Table 1: List of primers used for plasmid construction. Bold letters indicate restriction sites, italics indicate overhangs.

Plasmid	Primer	Sequence (5' → 3')	Template
pAffiRef	Erg20-5D-fwd	<b>GTTGTTGGATCCAAAACAATGGCTTCAGAAAAAGAAATT</b> A	CEN.PK
	Erg20-5D-rev	<b>GTTGTTCTCGAGCTATTGCTCTTGTAACTTT</b> T	113-5D
pAffi1	pSPGM1-fwd	AGGAGTTAGACAACCTGAAGTC	pAffiRef
	pSPGM1-rev	GCCTTATTATTGACAGAACCT	
	FarnSyn-fwd	TATTAGATAGCCAATGGTTCTG	pAffiRef
	FarnSyn-rev	<i>TCTCCGGTTCCAGTCCAGCGCAAAGATA</i> TGTCCATCCCATTATTA	
	ZTaq-fwd	GCCGCTGGAACCTGGAAACC	pAff8c_PHB_Z
	ZTaq-rev	ATCTAATCTAAGTTTAATTACAAAAAAACATGGTAGACAACAAATTCAACAAA	
	Pro-fwd	TTGTAATTAAAACCTAGATTAGATT	
	Pro-rev	<i>TGTTTCTTGTGAATTGTTGTCTACCATTGTTTTGTTTATATTGTTGTA</i> A	
	ZlgA-fwd	ATGGTAGACAACAAATTCAACA	pAff8c_PHB_Z
	ZlgA-rev	<i>TCTCTCTCTTAATTCTTTCTGAAGCACCAGAACTACTGGAGCCG</i> C	
pAffi5	Erg20-fwd	GCTTCAGAAAAGAAATTAGGAGAG	pAffiRef
	Erg20-rev	CTAGACTTCAGGTTGCTAACTCCT	
pAffi3	Affi5-1-fwd	ACAGCCAAGCTTTATTCGGC	pAffi2
	Affi5-1-rev	<i>CTAAAGGGAAACAAAGCTGGAGCTCGCACACACCATA</i> GCTTCAAATG	
	Affi5-2-fwd	<i>CGCCGAAATAAAAGCTTGGCTTGAATTACGTAGCC</i> AAAT	CEN.PK
	Affi5-2-rev	<i>GGCGAATTGGGTACCGGCCGATG</i> GTAAATGATCCGAACCTTG	113-5D
	p416TEF4-fwd	GAGCTCCAGTTGTTCCCTT	p416TEF
	p416TEF4-rev	GGCCGGTACCCAATTG	
	Affi3-1-rev	<i>GCGTTATCCAGCTGCATTAATGAGCACACACCATA</i> GCTTCAAATG	pAffi5
	Affi3-1-fwd	<i>CCTGATTCTGTGGATAACCGTATTACCGATGG</i> TAATGATCCGAACCTTG	
	Affi3-2-fwd	GGTAATACGGTTATCCACAGAAC	pAffi1
	Affi3-2-rev	TTCTCAGGTATAGCATGAGGTC	
	Affi3-3-fwd	GAGCGACCTCATGCTATAACCT	pAffi1
	Affi3-3-rev	TCATTAATGCAGCTGGATAAAC	

	Affi5-1-rev2	ATGGTAGACAACAAATTCAACAAAGAAAGAG	pAffi5
	Affi5-2-rev	GGCGAATTGGGTACCGGCCGATGGAATGATCCGAACCTG	
pAffi7	PAdh1-fwd	CTAAAGGGAACAAAAGCTGGAGCTCAGGGGATCGAAGAAATGAT	CEN.PK
	PAdh1-rev	TTTGTGAATTGTTGCTACCATTGTTTGATATGAGATAGTTGATTGCTT	113-5D
	p416TEF4-fwd	GAGCTCCAGCTTTGTTCCCTT	p416TEF
	p416TEF4-rev	GGCCGGTACCCAATTG	
	Affi5-1-rev2	ATGGTAGACAACAAATTCAACAAAGAAAGAG	pAffi5
	Affi5-2-rev	GGCGAATTGGGTACCGGCCGATGGAATGATCCGAACCTG	
pAffi8	PKex2-fwd	CTAAAGGGAACAAAAGCTGGAGCTGAGATACACGTATCTGACATG	CEN.PK
	PKex2-rev	TTTGTGAATTGTTGCTACCATTGTTTATCTGATAATGGGTTAGTAGTTATAAT	113-5D
	p416TEF4-fwd	GAGCTCCAGCTTTGTTCCCTT	p416TEF
	p416TEF4-rev	GGCCGGTACCCAATTG	
	Affi9-1-rev	GCGTTATCCAGCTGCATTAATGAAGGGGATCGAAGAAATGAT	pAffi7
	Affi3-1-fwd	CCTGATTCTGTGGATAACCGTATTACCGATGGAATGATCCGAACCTG	
pAffi9	Affi3-2-fwd	GGTAATACGGTTATCCACAGAAC	pAffi1
	Affi3-2-rev	TTCTCAGGTATAGCATGAGGTC	
	Affi3-3-fwd	GAGCGACCTCATGCTATAACCT	pAffi1
	Affi3-3-rev	TCATTAATGCAGCTGGATAAAC	
	Affi10-1-rev	GCGTTATCCAGCTGCATTAATGAGTAGATACACGTATCTGACATG	pAffi8
	Affi3-1-fwd	CCTGATTCTGTGGATAACCGTATTACCGATGGAATGATCCGAACCTG	
pAffi10	Affi3-2-fwd	GGTAATACGGTTATCCACAGAAC	pAffi1
	Affi3-2-rev	TTCTCAGGTATAGCATGAGGTC	
	Affi3-3-fwd	GAGCGACCTCATGCTATAACCT	pAffi1
	Affi3-3-rev	TCATTAATGCAGCTGGATAAAC	

	Affi11-1-fwd	GCCGCTAGACGAGCTGCC	pAffi5
	Affi11-1-rev	TGCGTTATCCCCCTGATTCTGT	
pAffi11	Affi11-2-fwd	GAGATAGGGTTGAGTGTGTTTC	
	Affi11-2-rev	CAGCTCCGGCAGCTCGTAGCGCGTAGACAACAAATTCAACAAAGAAGC	pAffi5
	Affi11-3-fwd	CTCAAAGGCGGTAAATACGGT	
	Affi11-3-rev	TTCTTAATAGTGGACTCTGTTCC	pAffi5
pAffi12	Affi12-1-fwd	GCCGGAGCTGGACGATT	pAffi5
	Affi11-1-rev	TGCGTTATCCCCCTGATTCTGT	
	Affi12-2-fwd	GAGATAGGGTTGAGTGTGTTTC	
	Affi12-2-rev	CGAAATCGTCCAGCTCCGGCGTAGACAACAAATTCAACAAAGAAGC	pAffi5
	Affi11-3-fwd	CTCAAAGGCGGTAAATACGGT	
	Affi11-3-rev	TTCTTAATAGTGGACTCTGTTCC	pAffi5

pAffi2 expresses fusion of anti-Z<sub>Fab</sub> and anti-Z<sub>IgA</sub> from P<sub>TEF1</sub> in plasmid pIYC04.<sup>1</sup>

Supplementary Table 2: Primers used for integration of farnesene synthase and FPP synthase as well as their fusions to affibodies Z<sub>Taq</sub> and Z<sub>IgA</sub>, respectively for construction of strains ScAffi01, 03, 07 and 09.

Primer	Sequence (5' → 3')	Template
FS_tHMG1-fwd	GAGCGACCTCATGCTATACCTG	pAffiRef
FS_tHMG1-rev	CTTCGAGCGTCCCAAAAC	
FS_tHMG1-fwd	GAGCGACCTCATGCTATACCTG	pAffi1
FS_tHMG1-rev	CTTCGAGCGTCCCAAAAC	
p0390_up-fwd	AGTTACTTGCTCTATGCGTTGC	
p0390_up-rev	GTAGATACTTGTGACACTTCTAA	pCfb0390 <sup>2</sup>
p0390_down-fwd	ATCCGCTCTAACCGAAAAGG	
p0390_down-rev	TGAGAACATCCGGACCAGCA	

DNA sequences (5' → 3') of anti-idiotypic affibody pairs used in this study. Start and stop codons are underlined, (SSSSG)<sub>4</sub> linker is highlighted in grey.

**Z<sub>Taq</sub>:**

ATGGTAGACAACAAATTCAACAAAGAACTGGGTTGGGCGACCTGGGAGATCTCAACTTACCTAACCTAAACGGTGTGCAAGTGAAGGCCTTCATCGATAGTTA  
CGGGATGACCCAAGCCAAAGCGCTAACCTGCTAGCAGAACGCTAAATGATGCTCAGGCGCCGAAATAA

**Z<sub>IgA</sub>:**

ATGGTAGACAACAAATTCAACAAAGAAACAATACAAGCGAGTCAAGAGATCAGACTATTACCTAACCTAAACGGTAGACAAAGCTTGCCTCATCCACAGTTAC  
TTGATGACCCAAGCCAAAGCGCTAACCTGCTAGCAGAACGCTAAATGATGCTCAGGCGCCGAAATAA

**Anti-Z<sub>Taq</sub>-anti-Z<sub>IgA</sub> scaffold with (SSSSG)<sub>4</sub> linker:**

ATGGTAGACAACAAATTCAACAAAGAAAGAGTGATTGCGATAGGTGAGATCATGCGGTTACCTAACCTAAACAGTCTCCAAGTGGTGGCCTTCATCAATAGTTA  
CGGGATGACCCAAGCCAAAGCGCTAACCTGCTAGCAGAACGCTAAATGATGCTCAGGCGCCGAAATCGTCCAGCTCGGAGCTCGTCTAGCGGCAG  
CAGCTCTCCGGTCCAGTCCAGCGCGTAGACAAACAAATTCAACAAAGAACGACAAACGGCGGGGGTGGAGATCATGGAGTTACCTAACCTAACACCCGGC  
AACTGCTGGCCTTCATCCAGAGTTACGAGATGACCCAAGCGCTAACCTGCTAGCAGAACGCTAAATGATGCTCAGGCGCCGAAATAA

**Z<sub>WT</sub>:**

ATGGTAGACAACAAATTCAACAAAGAACAAACAAAACGCGTTCTATGAGATCTTACACTTAACCTAAACGAAGAACGAAACGCCCTCATCCAAAGTTAA  
AAGATGACCAAGCCAAGCGCTAATTGCTAGCAGAAGCTAAATGATGCTCAGGCAGCAAATAA

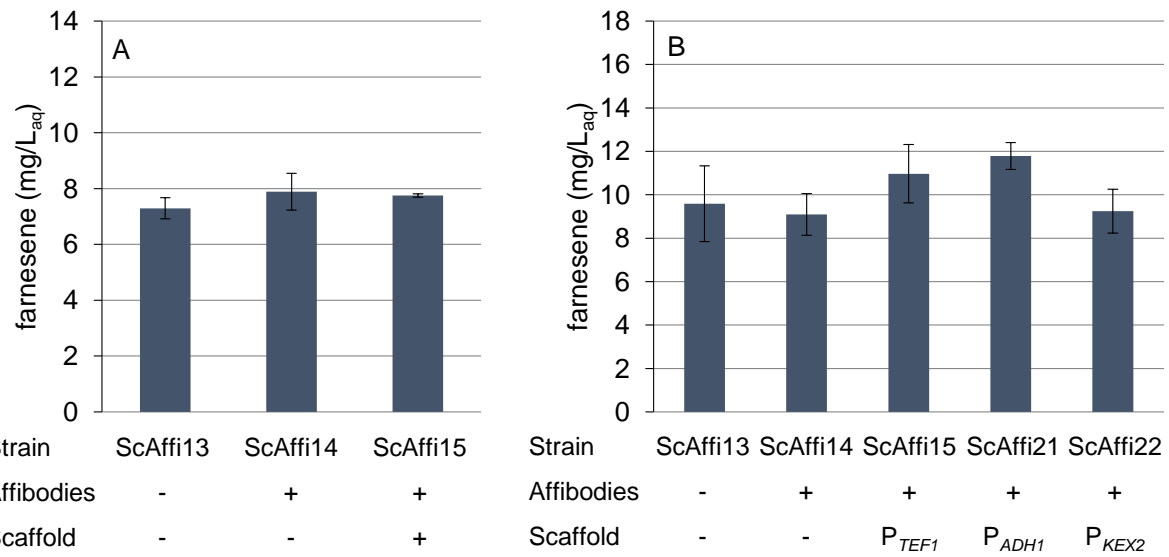
**Z<sub>HER2</sub>:**

ATGGTAGACAACAAATTCAACAAAGAACGAAACCGTATTGGGAGATCGCTCTGTTACCTAAACATCAGCAAAGCGCCCTCATCCGAGTTAT  
ATGATGACCAAGCCAAGCGCTAATTGCTAGCAGAAGCTAAATGATGCTCAGGCAGCAAATAA

**Anti-Z<sub>WT</sub>-anti-Z<sub>HER2</sub>-anti-Z<sub>IgA</sub> scaffold with (SSSG)<sub>4</sub> linkers:**

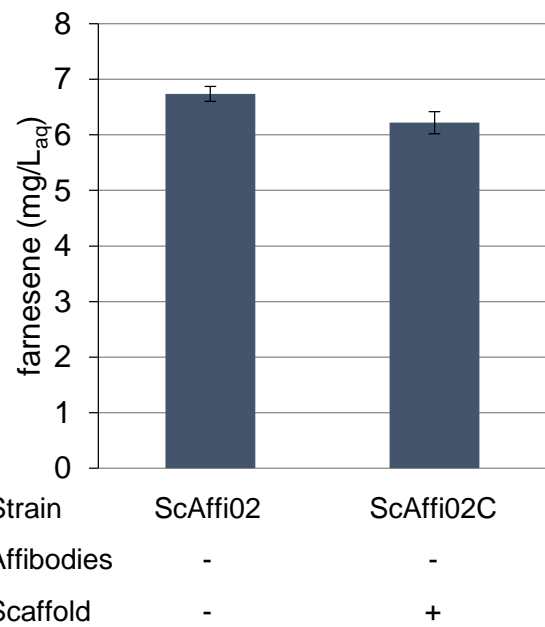
ATGCATCATCACACCACATCACTCACTGTAGATAACAAATTAAACAAAGAGACTCAGGAAGCCCTTGGGAGATCTTCACACTGCCAACCTGAACGGGCGCCAGG  
TCGCTGCATTATTAGCAGCCTGCTGGATGATCCGCTCAGAGTCAGAAACCTGTTAGCAGAGGCCAAGAACGATGCAACGATGACAAGCACCAGAAAGCTCCAGTT  
CGGGTAGCAGTCCAGTGGTTCAAGCAGCTCAGGTCGAGCTTCCGGCCTCGATAATAAGTTCAACAAAGAACGCCATGGCTGCGTACGAAATTATTGATC  
TTCCGAACTTAAACTGTTTCACTCGAGGCCCTTATTACACAGCTGAGTGATGATCCTCTCAGTCTGCGAACCTGTTAGCGGAAGCCAAGAAATTGAACGATGC  
GCAAGCGCCAAATCTTCAAGCTGGTAGCTCGTCTGGGCTTCAAGTCCGGCAGTCAGCTCCGGAGTTGACAACAAATTAAACAGGAAGCGCAAAC  
TGCGGGTGTGAAATCATGGAACTGCCAACCTGAATACACGGCAGCTCCGGTTCATCCAGTCATTACGTGATGATCCGTCAGTCAGCGAATTGCTGGCG  
GAGGCTAAAGCTCAACGATGCGCAAGCTCTAAACTAGTAA

Italics: 6His tag, Orange: Anti-Z<sub>WT</sub>, Blue: anti-Z<sub>HER2</sub>, Green: Anti-Z<sub>IgA</sub>. Gray: Linkers (SSSG)<sub>4</sub>



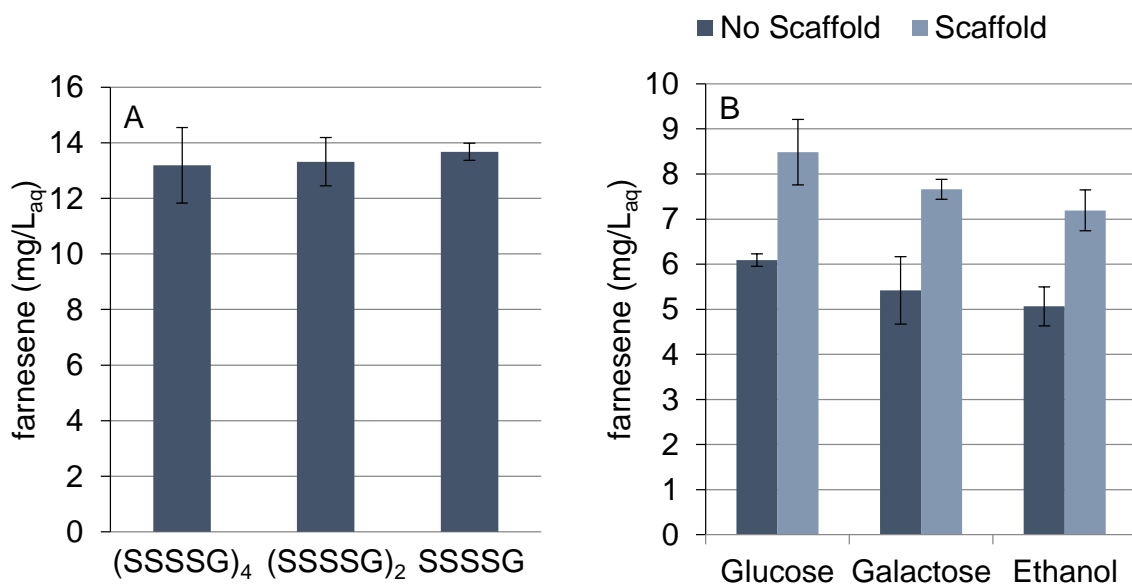
Supplementary Figure 1: Affibody scaffold expression for fusion of FPP and farnesene synthase.

Expression of farnesene and FPP synthase, fused to affibodies Z<sub>Taq</sub> and Z<sub>IgA</sub>, and the anti-Z<sub>Taq</sub>-anti-Z<sub>IgA</sub> scaffold from a single multi-copy plasmid. Scaffold was expressed under promoters (A) P<sub>TEF1</sub> and (B) P<sub>ADH1</sub> and P<sub>KEX2</sub>. Bars represent average farnesene concentrations per volume of aqueous medium of three biological replicates with standard deviations after 72 h of cultivation in shake flasks.

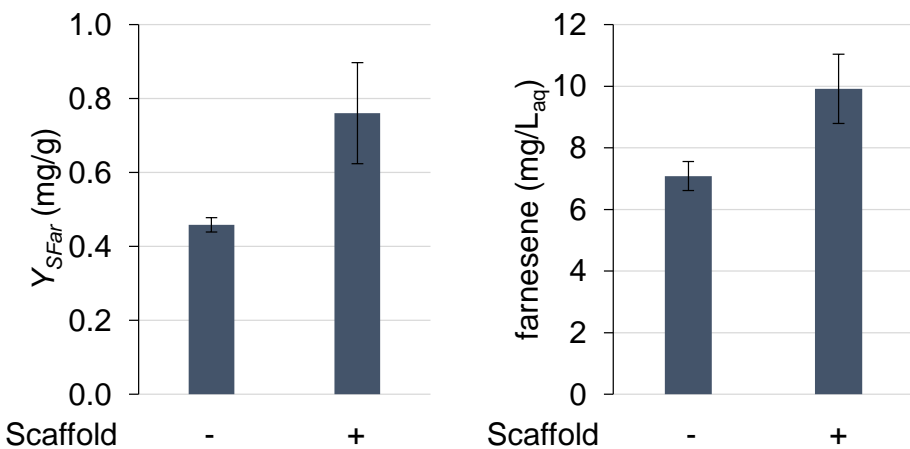


Supplementary Figure 2: Negative control experiment. Effect of scaffold expression (anti-Z<sub>IgA</sub>, anti-Z<sub>Taq</sub>) on the production of farnesene without expression of their targets (Z<sub>IgA</sub>, Z<sub>Taq</sub>). ScAffi02C expresses scaffold

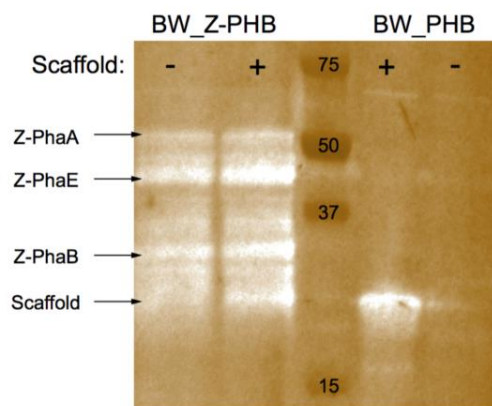
from plasmid pAffi5. Bars represent average farnesene concentrations per volume of aqueous medium of three biological replicates with standard deviations after 72 h of cultivation time in shake flasks.



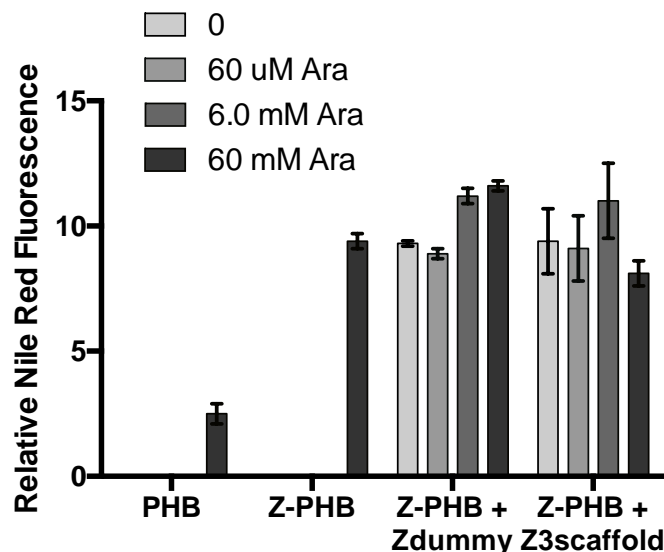
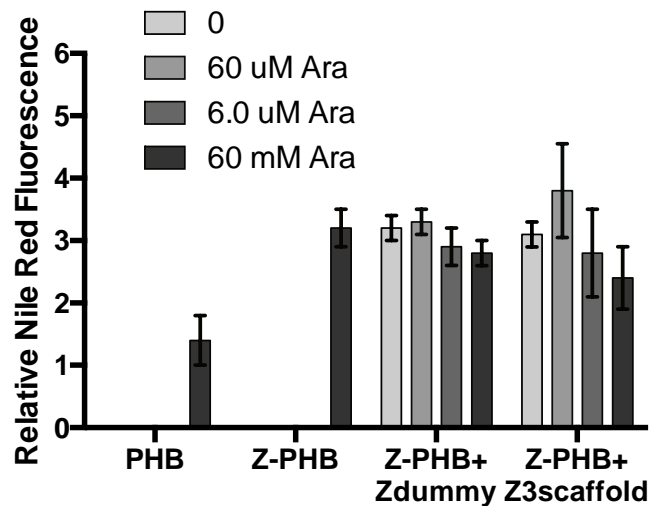
Supplementary Figure 3: Effect of different linker lengths and carbon sources on affibody mediated enzyme fusion for production of farnesene. (A) Linker length between the scaffold affibodies was reduced from 20 to 10 and 5 amino acids. All strains express affibody-enzyme fusions from the chromosome and the scaffold consisting of anti-Z<sub>Taq</sub> and anti-Z<sub>IgA</sub> from a low copy number plasmid. (SSSG)<sub>4</sub> - ScAffi05, (SSSG)<sub>2</sub> - ScAffi23 and (SSSG)<sub>2</sub> - ScAffi24. (B) Effect of scaffold expression with respect to different carbon sources. Cultivations were performed using 1 % w/v glucose, galactose and ethanol. No scaffold - ScAffi04, Scaffold - ScAffi05. Bars represent average farnesene concentrations per volume of aqueous medium of three biological replicates with standard deviations after 72 h of cultivation in shake flasks.



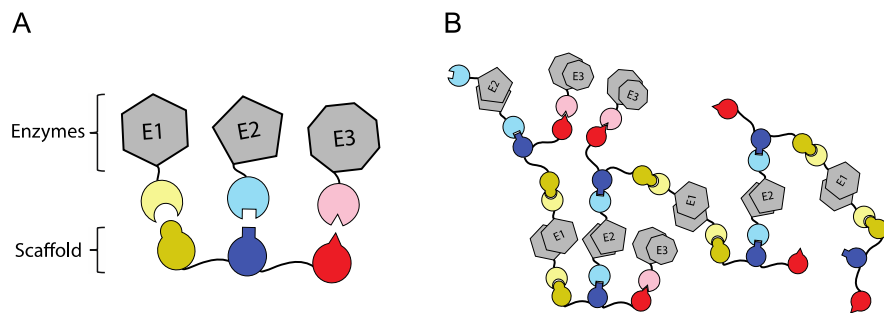
Supplementary Figure 4: Expression of the affibody-scaffold complex for production of farnesene in fed-batch cultivations. All strains express the fusion constructs of affibodies Z<sub>Taq</sub> and Z<sub>IgA</sub> to the FPP and farnesene synthase from the chromosome. The anti-Z<sub>Taq</sub>-anti-Z<sub>IgA</sub> scaffold was expressed from a low copy number plasmid. No scaffold – ScAffi10, scaffold – ScAffi11 (scaffold expression under P<sub>TEF1</sub>). Data represent average values of two or three biological replicates with standard deviation 6 h after initiation of the feed phase.



Supplementary Figure 5: Western blot detection of Z-fused enzymes and affibody scaffold in *E. coli* cell lysates. BW\_Z-PHB – strain expressing Z-tagged PHB pathway enzymes, BW\_PHB – expression of untagged enzymes.



Supplementary Figure 6: Affibody tagging and affibody scaffold effect on PHB production from *E. coli* in LB media 24 hr after induction. Top: Z-PHB induced at 0.05 mM IPTG (low induction). Bottom: Z-PHB induced at 0.5 mM IPTG (high induction).



Supplementary Figure 7: (A) Representation of three monomeric enzymes colocalized by a scaffold. (B) An example of how homodimeric enzymes, where there are two tags per enzymes, can coordinate multiple scaffolds, leading to scaffold aggregates.

## Supplemental References

- (1) Chen, Y., Daviet, L., Schalk, M., Siewers, V., and Nielsen, J. (2013) Establishing a platform cell factory through engineering of yeast acetyl-CoA metabolism, *Metab Eng* 15, 48-54.
- (2) Jensen, N. B., Strucko, T., Kildegaard, K. R., David, F., Maury, J., Mortensen, U. H., Forster, J., Nielsen, J., and Borodina, I. (2013) EasyClone: Method for iterative chromosomal integration of multiple genes in *Saccharomyces cerevisiae*, *FEMS Yeast Research*.



# **Effects of acetoacetyl-CoA synthase expression on production of sesquiterpenes in *Saccharomyces cerevisiae***

Stefan Tippmann, Raphael Ferreira, Verena Siewers, Jens Nielsen and Yun Chen

*Under Review*



# Effects of acetoacetyl-CoA synthase expression on production of sesquiterpenes in *Saccharomyces cerevisiae*

Stefan Tippmann<sup>1,2</sup>, Raphael Ferreira<sup>1,2</sup>, Verena Siewers<sup>1,2</sup>, Jens Nielsen<sup>1,2,3</sup> and Yun Chen<sup>1,2,\*</sup>

<sup>1</sup>Department of Biology and Biological Engineering,

Chalmers University of Technology, SE412 96 Gothenburg, Sweden

<sup>2</sup>Novo Nordisk Foundation Center for Biosustainability, Chalmers University of Technology, SE412 96 Gothenburg, Sweden

<sup>3</sup>Novo Nordisk Foundation Center for Biosustainability, Technical University of Denmark, DK2970 Hørsholm, Denmark

\*Corresponding Author: Yun Chen

Department of Biology and Biological Engineering,

Chalmers University of Technology, Kemivägen 10, SE412 96, Gothenburg, Sweden.

E-mail: [yunc@chalmers.se](mailto:yunc@chalmers.se)

Tel: +46 31772 38 04

Fax: +46 31 772 38 01

Keywords: isoprenoids, mevalonate pathway, biofuels, yeast, metabolic engineering

## Abstract

Efficient production of sesquiterpenes in *Saccharomyces cerevisiae* requires a high flux through the mevalonate pathway. To achieve this, supply of acetyl-CoA plays a crucial role, partially because three moles of acetyl-CoA are necessary to produce one mole of farnesyl diphosphate, but also to overcome the thermodynamic constraint imposed on the first reaction, in which acetoacetyl-CoA is produced from two moles of acetyl-CoA by acetoacetyl-CoA thiolase. Recently, a novel acetoacetyl-CoA synthase (*nphT7*) has been identified from *Streptomyces* sp. strain CL190, which catalyzes the irreversible condensation of malonyl-CoA and acetyl-CoA to acetoacetyl-CoA and therefore represents a potential target to increase the flux through the mevalonate pathway. The present study investigates the effect of acetoacetyl-CoA synthase on growth as well as the production of farnesene and compares different homologs regarding their efficiency. Plasmid-based expression of *nphT7* as well as construction of an alternative pathway, which exclusively relies on the malonyl-CoA bypass, significantly reduced final farnesene titers. However, *nphT7* from *Streptomyces glaucescens*, which clearly showed higher efficiency compared to *Streptomyces* sp. strain CL190 and modulation of the expression level could improve production by 4 fold.

## Introduction

The mevalonate pathway is of crucial importance for *Saccharomyces cerevisiae* as it is used for synthesis of sterols, ubiquinone and dolichols. Besides, the pathway has been exploited for production of sesquiterpenes, which have different applications within the chemical industry and can be provided from microbial fermentation using renewable carbon sources [21]. In the first reaction of the pathway, acetoacetyl-CoA thiolase (encoded by *ERG10*) catalyzes the reversible non-decarboxylative Claisen condensation of two acetyl-CoA molecules to produce acetoacetyl-CoA (Fig. 1). Activity of this enzyme was shown to be regulated by intracellular sterol levels [6,7], whereas loss of *ERG10* was reported to result in mevalonate auxotrophy [9]. However, acetoacetyl-CoA thiolytic is thermodynamically favorable ( $\Delta G^{\circ}\approx 7$  kcal/mol [13,32]), imposing constraints on the concentrations of acetyl-CoA to enable acetoacetyl-CoA synthesis. Recently, *nphT7* present in the mevalonate pathway gene cluster in *Streptomyces* sp. strain CL190 was identified to encode a novel acetoacetyl-CoA synthase [19], which catalyzes the energetically more favorable (estimated  $\Delta G^{\circ}=-0.9$  kcal/mol [32]) decarboxylative condensation of malonyl-CoA and acetyl-CoA to acetoacetyl-CoA. The enzyme was reported to produce acetoacetyl-CoA also from malonyl-CoA as sole substrate, but most importantly, it did not display thiolytic activity *in vitro* [19]. For this reason, it was suggested to be ideal for production of butanol, polyhydroxyalkanoates and isoprenoids. In *S. cerevisiae*, the enzyme successfully supported butanol production and also displayed similar enzymatic activity *in vitro* in comparison to the endogenous acetoacetyl-CoA thiolase [27]. In contrast, Menon et al. reported 6.2-fold higher titers of butanol produced from *Escherichia coli* using the endogenous acetoacetyl-CoA thiolase (*atoB*) over *nphT7* for supply of acetoacetyl-CoA [17]. Furthermore, acetoacetyl-CoA synthase has also been used for production of butanol in *Synechococcus elongatus* [13], for production of propane in *E. coli* [17] and for poly-3-hydroxybutyrate production in mesophylllic cells of sugarcane [16]. The objective of this study was to investigate the effect of the acetoacetyl-CoA synthase on the production of sesquiterpenes in *S. cerevisiae* using farnesene as an example. Farnesene is directly produced from farnesyl diphosphate (FPP) using farnesene synthase and as its production requires 9 mol ·mol<sup>-1</sup> of acetyl-CoA, efficient conversion to acetoacetyl-CoA using *nphT7* for increased flux through the pathway represents a potential target to improve production of these compounds. Since the enzyme requires malonyl-CoA as extender substrate, overexpression of the modified acetyl-CoA carboxylase (*ACC1\*\**), which displayed enhanced activity, was used additionally to promote the influx from malonyl-CoA into the pathway [28]. As increased levels of acetoacetyl-CoA could potentially stimulate acetoacetyl-CoA thiolytic and result in a futile cycle, the endogenous *ERG10* was replaced by *nphT7* as an alternative approach to produce

acetoacetyl-CoA exclusively from malonyl-CoA and to compare both pathways regarding growth and product formation. Since carboxylation of acetyl-CoA to malonyl-CoA requires additional ATP, which could reduce the product yield, this route becomes less efficient with respect to free energy conservation (Fig. 1). However, energy released from ATP hydrolysis ( $\Delta G^0 < -7$  kcal/mol) could be utilized successfully to drive biochemical reactions for butanol production, by compensating for the required energy for acetoacetyl-CoA synthesis via condensation of two molecules of acetyl-CoA [13].

## Materials and Methods

### Plasmid and strain construction

The *nphT7* gene from *Streptomyces* sp. strain CL190 (*nphT7<sub>SCL</sub>*) as well as the homologous genes from *Streptomyces glaucescens*, *Streptomyces afghaniensis*, *Streptomyces lactacystinaeus* and *Nocardia brasiliensis* were codon optimized and synthesized from GenScript (Piscataway, NJ, USA). *nphT7<sub>SCL</sub>* was amplified by PCR and cloned into pSP-GM1 using restriction enzymes *NotI* and *PacI*, resulting in plasmid pIST07. For construction of plasmids pIST12-16, the truncated *HXT7* promoter  $P_{HXT7}$  and *HIS5* terminator  $T_{HIS5}$  were amplified from *S. cerevisiae* CEN.PK113-5D and fused to each of the genes by PCR. The constructed cassettes were amplified by PCR to generate the complementary overhangs for insertion into plasmid pIST05 using CPEC [23]. A list of primers used for plasmid construction is shown in Table S1. Chromosomal integration of *ACC1\*\** [28] into site X-2 was achieved using plasmid pMG96, a derivative of vector pCfB353 [10]. Substitution of *ERG10* by *nphT7* from *Streptomyces* sp. strain CL190 were constructed in strains RF14 and IMX581 using CRISPR/Cas9. [14]. IMX581 and the CRISPR plasmid backbone (pMEL10) were obtained from EUROSCARF (Frankfurt, Germany). The guide RNA targeting the *ERG10* locus was designed using the Yeastriction webtool (<http://yeastriction.tnw.tudelft.nl/>). The *nphT7<sub>SCL</sub>* gene was amplified from pIST07 by PCR and used as repair fragment. Simultaneous transformation with pMEL10, the *ERG10* specific guide RNA and the *nphT7<sub>SCL</sub>* repair fragment resulted in the *in vivo* assembly of the plasmid, mediating a double strand cut in the *ERG10* gene by the Cas9 nuclease. The double-strand break allowed integration of the *nphT7<sub>SCL</sub>* cassette by homologous recombination, ultimately resulting in strain SCIST17, 19 (*nphT7* expression using endogenous promoter and terminator) and SCIST38 (*nphT7<sub>SCL</sub>* expression using  $P_{TEF1}/T_{ADH1}$ ). Replacing the endogenous *FAS1* promoter  $P_{FAS1}$  by  $P_{HXT1}$  for construction of strain SCIST41 was performed as described previously by [4]. Table S2 lists primers used for construction of these strains.

### Growth medium

*S. cerevisiae* strains with uracil auxotrophy were grown on YPD plates containing 20 g/L glucose, 10 g/L yeast extract, 20 g/L peptone from casein and 20 g/L agar. Plasmid carrying strains were grown on selective growth medium containing 6.9 g/L yeast nitrogen base w/o amino acids (Formedium, Hunstanton, UK), 0.77 g/L complete supplement mixture w/o uracil (Formedium), 20 g/L glucose and 20 g/L agar. Shake flask cultivations were performed in minimal medium containing 30 g/L glucose, 7.5 g/L  $(\text{NH}_4)_2\text{SO}_4$ , 14.4 g/L  $\text{KH}_2\text{PO}_4$ , 0.5 g/L  $\text{MgSO}_4 \cdot 7\text{H}_2\text{O}$ , 2 mL/L trace element solution and 50  $\mu\text{L}/\text{L}$  antifoam (Sigma-Aldrich, St. Louis, MO, USA). After sterilization, vitamin solution was added at a concentration of 1 mL/L. The batch phase medium during aerated bioreactor cultivations contained 10 g/L glucose, 5 g/L  $(\text{NH}_4)_2\text{SO}_4$ , 3 g/L  $\text{KH}_2\text{PO}_4$ , 0.5 g/L  $\text{MgSO}_4 \cdot 7\text{H}_2\text{O}$ , 1 mL/L trace element solution, 50  $\mu\text{L}/\text{L}$  antifoam and 1 mL/L vitamin solution. During the fed-batch phase, the feed medium was five times concentrated and contained glucose to a concentration of 100 g/L. The composition of the trace element and vitamin solution has been reported by Verduyn et al. [31].

### Shake flask cultivations

For cultivations in shake flasks, 5 mL of minimal medium were inoculated with a single colony from an agar plate with selective medium and incubated at 200 rpm and 30 °C for 48 h. Subsequently, the pre-culture was used to inoculate 18 mL of minimal medium in shake flasks without baffles and a total volume of 100 mL at an OD<sub>600</sub> of 0.1. Lastly, 2 mL of dodecane ( $\geq 99\%$ , Reagent Plus, Sigma-Aldrich) were added to a final concentration of 10 % v/v to sequester farnesene during the cultivation. Shake flasks were incubated at 180 rpm and 30 °C for 72 h.

### Bioreactor cultivations

For cultivation of *S. cerevisiae* strains in bioreactors, a single colony from a plate with selective medium was used to inoculate 5 mL of minimal medium used for shake flask cultivations. After incubation at 200 rpm and 30 °C overnight, the culture was transferred to a shake flask with 45 mL of minimal medium and incubated at 180 rpm and 30 °C for another 24 h. Subsequently, the culture was used to inoculate 400 mL of batch phase medium. Cultivations in bioreactors were performed using DasGip Parallel Bioreactor Systems for Microbiology (Eppendorf, Hamburg, Germany). The vessels were aerated at 30 L/h and homogeneous mixing was accomplished using a six-blade Rushton turbine at a stirring speed of 600 rpm. The temperature was adjusted to 30 °C and the pH was controlled at 5 using 2 M HCl and 2 M KOH. Composition of the exhaust gas was monitored on-line using the DasGip GA4 gas analyzer (Eppendorf). Bioreactor cultivations were started in batch mode. After glucose and ethanol depletion, 80 mL of dodecane were added under aseptic conditions and the feed was initiated. To allow for exponential

growth at  $\mu=0.08 \text{ h}^{-1}$ , the feed rate was set to  $v(t)=0.003 \cdot \exp(0.08 \cdot t)$ , with  $v$  as the feed rate in L/h and  $t$  as feed time in h. In addition, the feed was stopped at values of the respiratory quotient ( $RQ$ ) above one to avoid overflow metabolism [30].

#### BioLector cultivations

Growth curves were recorded using the BioLector (m2p-labs, Baesweiler, Germany). For this purpose, a single colony was picked from an agar plate with selective medium and used to inoculate 3 mL of minimal medium. After 48 h of incubation at 30 °C and 200 rpm, the culture was used to inoculate 1 mL of minimal medium at an OD<sub>600</sub> of 0.1. Subsequently, the culture was transferred into a 48-well microtiter plate (MTP-48-B FlowerPlate, m2p-labs) and incubated at 30 °C and 1200 rpm using the BioLector. The optical density was measured on-line in 30 min intervals at a filter gain of 30.

#### Measurement of cell growth

A spectrophotometer (Genesis20, Thermo Fisher Scientific, Waltham, MA, USA) was used to measure cell growth at the end of the shake flask cultivations. For cultivations in bioreactors, the biomass was measured by pipetting a 5 mL sample onto a pre-weighted filter with a pore size of 0.45 µm (Sartorius, Göttingen, Germany). The filter was rinsed with water, dried at 150 W for 15 min and kept in a desiccator until it was weighted again. Biomass concentrations are expressed as gram dry cell weight per volume (gDCW/L).

#### Quantification of extracellular metabolites

For quantification of glucose and ethanol, samples were taken at the end of the shake flask cultivation and during the bioreactor cultivations. For this purpose, the biomass was removed by centrifugation at 4000 rpm for 3 min or by filtration using a 0.45 µm nylon filter (VWR International AB, Stockholm, Sweden). Sample analysis was performed by HPLC using a Dionex Ultimate 3000 (Dionex, Sunnyvale, CA, USA) together with an Aminex HPX-87H column (300 x 7.8 mm, Bio-Rad Laboratories, Hercules, CA, USA) and a refractive index detector (512 µRIU). The column temperature was kept constant at 45 °C and 15 µL were injected into the mobile phase consisting of 5 mM H<sub>2</sub>SO<sub>4</sub>. The flow rate was set to 0.6 mL/min.

#### Quantification of farnesene

At the end of the cultivation, the dodecane overlay was harvested by centrifugation at 4000 rpm for 3 min. Similarly, samples were collected during cultivations in bioreactors. Analysis was performed using a Focus GC-FID (Thermo Fisher Scientific) equipped with a ZB-50 column (Phenomenex, Torrance, CA, USA) as described previously with minor modifications [29]. The initial temperature was held at 50 °C for 1.5 min and then increased to 170 °C at a rate of 15 °C/min. After keeping the temperature constant for

another 1.5 min, it was raised at the same rate to 300 °C and held for 3.0 min. The inlet temperature was set to 250 °C and 2 µL sample were injected in splitless mode. The base temperature of the flame was set to 300 °C. Farnesene was quantified using external calibration with trans-β-farnesene as analytical standard ( $\geq 90\%$ , Sigma Aldrich). Samples were diluted in hexane and patchoulool ( $\geq 99\%$ , a kind gift from Firmenich, Geneva, Switzerland) was added as internal standard. Concentrations of farnesene are stated based on the volume of the aqueous phase of the medium (mg/L<sub>aq</sub>).

#### Quantification of lipids

Samples for lipid analysis were taken at the end of the fed-batch cultivations, after 15 h of feeding. For this purpose, 5 mL of the cultivation broth were added to 20 mL of methanol (Sigma-Aldrich), which was kept at -40 °C using a Huber CC-410 thermostat (Huber, Offenburg, Germany). Subsequently, the samples were centrifuged at 4000 rpm and -20 °C for 5 min. The supernatant was discarded and the cells were washed using 5 mL of methanol. After centrifugation at 4000 rpm and -20 °C for 5 min, the biomass was freeze-dried using an Christ alpha 2-4 LSC (Christ Gefriertrocknungsanlagen, Osterode, Germany) and analyzed as described by Khoomrung et al. [12].

## Results

### Heterologous expression of different *nphT7* homologs for farnesene production

Acetoacetyl-CoA synthase from *Streptomyces* sp. strain CL190 was identified to catalyze the irreversible decarboxylative condensation of malonyl-CoA and acetyl-CoA to acetoacetyl-CoA and could hence improve production of isoprenoids. In order to determine the effect of the enzyme on the production of sesquiterpenes, *nphT7<sub>SCL</sub>* was expressed from a multi-copy plasmid together with a farnesene synthase from *Citrus junos* (*FarnSyn*), which converts FPP to farnesene [15] and a truncated version of the HMG-CoA reductase (*tHMG1*), which reduces HMG-CoA to mevalonate, but lacks the NH<sub>2</sub>-terminal transmembrane domain [8]. The structure of plasmid pIST12 is presented in Fig. S7 of the supplementary material. In addition, four homologous genes from other bacterial species, i.e. *S. glaucescens*, *S. afghaniensis*, *S. lactacystinaeus* and *N. brasiliensis*, were selected to identify differences regarding the efficiency of the enzymes. The first two genes encode for putative acetoacetyl-CoA synthases, while the latter two belong to the class of β-ketoacyl-ACP synthase (KAS) III enzymes, which convert malonyl-ACP and acetyl-CoA to acetoacetyl-ACP. Although *nphT7<sub>SCL</sub>* is homologous to *fabH* (KASIII) from *E. coli*, also containing the highly conserved catalytic triad at Cys115, His256 and Asn286, the enzyme did not show KASIII activity, presumably because it lacks an important arginine residue required for ACP binding [19].

On the contrary, KASIII enzymes from *S. lactacystinaeus* and *N. brasiliensis* share an AGGSR motif with the amino acid sequence of NphT7, which is not present in FabH from *E. coli*, but was suggested to be involved in recognition of the CoA moiety [19]. Hence, these enzymes could potentially be able to accept malonyl-CoA as substrate. Multiple sequence alignment of the homologs showing the putative CoA binding motif and results of a BLAST of these homologs to NphT7 from *Streptomyces* sp. strain CL190 are presented in Fig. S1 and Table S3 of the supplementary material. When *S. cerevisiae* strain CEN.PK113-5D was transformed with plasmids pIST12-16 and cultivated in shake flasks, expression of *nphT7<sub>SCL</sub>* from *Streptomyces* sp. strain CL190 did not improve production of farnesene in comparison to strain SCIST05, which does not express an acetoacetyl-CoA synthase (Fig. 2A). In fact, final farnesene titers slightly decreased on average from 9.3 to 7.6 mg/L<sub>aq</sub>. Furthermore, no difference between the strains expressing the different homologs was observed as farnesene concentrations were almost equal with approximately 8 mg/L<sub>aq</sub>. Since the effect of the enzymes could be restricted by the supply of malonyl-CoA, which is a crucial intermediate in fatty acid synthesis, we aimed at increasing the availability of malonyl-CoA as extender substrate for the acetoacetyl-CoA synthase. For this reason, plasmids pIST12-16 were also introduced into strain SCIST26, which carries a chromosomal integration of the mutated acetyl-CoA carboxylase (*ACC1\*\**) (Fig. 2B). Site mutations at Ser1157 and Ser659 had been shown to reduce sensitivity to Snf1 mediated phosphorylation, which led to a substantial increase in Acc1p activity [28]. However, even with expression of *ACC1\*\** there was no improvement of farnesene production and no difference between the different homologs. Surprisingly, final farnesene titers were reduced overall to approximately 6 mg/L<sub>aq</sub>.

#### Evaluation of an alternative pathway for sesquiterpene production

Overexpression of *nphT7<sub>SCL</sub>* did not result in improved production of farnesene. Promoted thiolysis of acetoacetyl-CoA to acetyl-CoA due to increased levels of acetoacetyl-CoA could explain these results. In order to confirm this observation, we aimed at providing acetoacetyl-CoA exclusively via the malonyl-CoA route, allowing for a comparison of the native and the modified pathway. Therefore, endogenous *ERG10* was replaced in frame by *nphT7<sub>SCL</sub>*, leaving the *ERG10* promoter and terminator. While the endogenous pathway is limited by thermodynamic constraints, the bypass via malonyl-CoA requires an additional reaction and increases the ATP demand of the pathway. Although ATP conservation plays a crucial role in metabolic engineering and an increased ATP demand is preferably avoided [5], ATP has recently been used as a driving force for the production of butanol in *S. elongatus* PCC 7942 [13].

Substitution of *ERG10* by *nphT7<sub>SCL</sub>* was performed in strains with and without *ACC1\*\** integration.

Although the increased conversion of acetyl-CoA to malonyl-CoA using *ACC1\*\** by itself had a negative effect on production of farnesene, i.e. the final titers decreased by 30 % (Fig. 2B), more flux towards malonyl-CoA might be beneficial to support the pathway when *ERG10* is removed. However, in both strains, the loss of *ERG10* resulted in a substantial decrease of final farnesene titers by more than 90 %, whereas titers were slightly higher without overexpression of *ACC1\*\**. Since both strains utilize the endogenous *ERG10* promoter and terminator, these results indicate that the expression of *nphT7<sub>SCL</sub>* is not sufficient to compensate for the loss of *ERG10*. Variation of the promoter strength is commonly used to improve expression [1]. Likewise, the terminator sequence has been shown to alter expression by changing mRNA stability [3]. Hence, integration of the gene was also performed using  $P_{TEF1}$  and  $T_{ADH1}$  to enhance the transcript level. Although farnesene concentrations remained significantly lower compared to the reference (SCIST05), manipulation of the *nphT7<sub>SCL</sub>* expression level resulted in an almost 4-fold increase of farnesene production compared to SCIST20 (*ACC1\*\**, *erg10Δ::nphT7<sub>SCL</sub>* with pIST05) (Fig. 3A). In order to evaluate the selected homologs when acetoacetyl-CoA cannot be degraded by acetoacetyl-CoA thiolase, plasmids pIST12-16 carrying the different *nphT7<sub>SCL</sub>* homologous genes, were introduced into strain SCIST19 (*ACC1\*\**, *erg10Δ::nphT7<sub>SCL</sub>*). Similar to varying the promoter strength of the chromosomally integrated *nphT7* from *Streptomyces* sp. strain CL190, a higher copy number (using a strong promoter) also led to higher final farnesene titers (SCIST33, Fig. 3B). Furthermore, a clear variation between the different homologs was observed, where expression of acetoacetyl-CoA synthase from *S. glaucescens* improved production 4-fold compared to SCIST20. Surprisingly, a decrease in production was observed for acetoacetyl-CoA synthase from *S. afghaniensis*. Overexpression of KASIII enzymes from *S. lactacystinaeus* and *N. brasiliensis* did not have a significant effect on production of farnesene.

Considering the final optical density, the growth of the strains expressing *nphT7<sub>SCL</sub>* instead of *ERG10* was clearly affected (Fig. S2). While SCIST15 (control, CEN.PK113-5D background) and SCIST16 (*ACC1\*\**) reached an equal final OD<sub>600</sub> of 12.4 after 72 h of cultivation, strains SCIST18 (*erg10Δ::nphT7<sub>SCL</sub>*) and SCIST20 (*ACC1\*\**, *erg10Δ::nphT7<sub>SCL</sub>*) reached a final OD<sub>600</sub> of 5.5 and 7.2 on average, respectively. In accordance with this, the cultivation broth of strain SCIST18 and 20 still contained 5.0 and 3.6 g/L of ethanol. On the other hand, final OD and ethanol concentration were almost identical when expression of *nphT7<sub>SCL</sub>* was enhanced using  $P_{TEF1}$  (SCIST39). This observation prompted us to investigate the growth kinetics in more detail. For this purpose, strains SCIST15, 16, 18, 20 and 39 were cultivated using the BioLector to monitor growth continuously. From the recorded growth curves shown in Fig. 4 it can be seen that strains SCIST15 and 16 entered diauxic shift after approximately 20 h of cultivation and

reached stationary phase after approximately 35 h. In contrast, for strains SCIST18 and 20 the diauxic shift occurred after approximately 30 h and consumptions of all carbon sources from the medium required up to 90 h. Especially during the second half of the cultivation, while the control (SCIST15) was still growing exponentially, these strains displayed significantly impaired growth, which could point towards transcriptional regulation of *ERG10* during the ethanol consumption phase. Strain SCIST39 (*ACC1\*\**, *erg10Δ::P<sub>TEF1</sub>-nphT7<sub>SCL</sub>*) with enhanced expression of *nphT7<sub>SCL</sub>* using *P<sub>TEF1</sub>* displayed a longer lag phase, but otherwise similar growth in comparison to the reference. In order to quantify the effect of the *ERG10* substitution by *nphT7<sub>SCL</sub>* the specific growth rates were calculated for exponential growth during each phase (Fig. S3), which demonstrates a clear reduction that can be assigned to this modification. Lastly, the identical experiment was also performed with strains SCIST33-37 (*ACC1\*\**, *erg10Δ::nphT7<sub>SCL</sub>*), which express the different homologs in addition to the integrated *nphT7* from *Streptomyces* sp. strain CL190 (Fig. S4) to examine their effect on growth. In accordance with the results for final farnesene titers (Fig. 3B), *nphT7* from *S. glaucescens* showed the most significant effect on growth, particularly during the ethanol consumption phase in comparison to the reference SCIST20 (*ACC1\*\**, *erg10Δ::nphT7<sub>SCL</sub>*) as stationary phase was reached after 60 h instead of over 100 h of cultivation.

Manipulating the pool of malonyl-CoA by downregulation of fatty acid synthesis Farnesene concentrations decreased substantially after replacing acetoacetyl-CoA thiolase by the respective acetoacetyl-CoA synthase from *Streptomyces* sp. strain CL190. Malonyl-CoA represents an important precursor for this pathway as well as for fatty acid synthesis and therefore its availability for the mevalonate pathway might be insufficient. Since overexpression of *ACC1\*\** alone did not improve pathway efficiency, downregulation of fatty acid synthase could serve as a potential strategy to redirect more flux towards the mevalonate pathway. For this purpose, *P<sub>HXT1</sub>* was used to downregulate *FAS1*, encoding the beta subunit of the fatty acid synthase in yeast, which utilizes acetyl-CoA and malonyl-CoA to synthesize fatty acyl-CoA. The hexose transporter Hxt1p was shown to be active in *S. cerevisiae* at higher glucose concentrations ( $\geq 1\%$  [24], full induction at 4 % [20]) and its promoter has previously been used to increase production of sesquiterpenes by diverting flux from the FPP branch point [26]. For this reason, strains were cultivated in fed-batch mode to obtain low glucose concentrations and to activate downregulation of *FAS1*. The feeding profile was designed to allow for exponential growth and to keep the glucose concentration close to zero. With the objective to reduce overflow metabolism and to maintain fully respiratory conditions, the respiratory quotient (*RQ*) was additionally used as a control parameter to indirectly control the concentration of glucose in the medium [30]. In order to utilize the

available pool of malonyl-CoA more efficiently as a substrate for the mevalonate pathway, strain SCIST41 (*ACC1\*\**, *erg10Δ::P<sub>TEF1</sub>-nphT7<sub>SCL</sub>*, *P<sub>FAS1</sub>Δ::P<sub>HXT1</sub>*) was transformed with plasmid pIST13 carrying *nphT7* from *S. glaucescens*, which showed higher efficiency compared to the one from *Streptomyces* sp. strain CL190 (Fig. 3B). Strain SCIST40 (*ACC1\*\**, *erg10Δ::P<sub>TEF1</sub>-nphT7<sub>SCL</sub>*) did not contain the modification of *FAS1* and was used as a reference. The two strains showed significantly different growth profiles during the batch phase as indicated by their CO<sub>2</sub> profiles, showing that downregulation of *FAS1* resulted in reduced CO<sub>2</sub> formation during the glucose and ethanol phase (Fig. S5). During the fed-batch phase the medium was fed exponentially to theoretically support a specific growth rate of  $\mu=0.08\text{ h}^{-1}$ . However, both strains did not maintain growth at 0.08 h<sup>-1</sup> with strain SCIST40 reaching a growth rate of  $0.068 \pm 0.003\text{ h}^{-1}$ . Ethanol reached 2.3 g/L on average and glucose remained close to zero over 18 h. After approximately 12 h, the RQ control was activated, which was used as feedback control to avoid overflow metabolism, resulting in slightly oscillating RQ values (Fig. S6). Farnesene was produced at a yield of  $0.57 \pm 0.19\text{ mg/g glucose}$  with final titers of  $13.8 \pm 4.1\text{ mg/L}_{\text{aq}}$ . On the contrary, the percentage of CO<sub>2</sub> in the exhaust gas slightly decreased over time for strain SCIST43 (Fig. S6) and biomass concentrations stayed almost constant at approximately 2.2 gDCW/L. Farnesene and ethanol could only be detected in minor quantities. Consistent with these data, the glucose concentration increased, reaching up to  $16.4 \pm 0.7\text{ g/L}$ . In order to identify changes in fatty acid metabolism due to downregulation of *FAS1*, the lipid content of the cell was analyzed at the end of the fed-batch (Table 3). The most significant differences were observed considering the content of storage lipids as triacylglycerides dropped by 88 % from  $31.6 \pm 8.5$  to  $3.9 \pm 0.4\text{ mg/gDCW}$ . Besides, a clear effect was observed regarding the membrane composition as phosphatidylcholine, phosphatidylinositol as well as ergosterol decreased substantially.

## Discussion

A recently identified acetoacetyl-CoA synthase from *Streptomyces* sp. strain CL190, which catalyzes the condensation of malonyl-CoA and acetyl-CoA to generate acetoacetyl-CoA, has been proposed as a potential target for acetoacetyl-CoA derived product formation. In the present study the encoding gene, *nphT7*, was expressed in *S. cerevisiae* and its effect on cell growth and production of farnesene was investigated. Besides, different homologs were compared with the objective to identify an acetoacetyl-CoA synthase with superior efficiency. For this purpose, *nphT7<sub>SCL</sub>* and the respective homologs from *S. glaucescens*, *S. afghaniensis*, *S. lactacystinaeus* and *N. brasiliensis* were expressed from plasmid together with genes encoding farnesene synthase (*FarnSyn*) and a truncated version of the HMG-CoA reductase (*tHMG1*), which has been identified as a flux controlling enzyme of the mevalonate pathway [18]. Most

importantly, expression of acetoacetyl-CoA synthase did not result in increased production of farnesene in our experiments. Also, no difference was observed between yeast strains expressing the selected homologs from other bacterial species considering the final titers of farnesene. In fact, final titers appeared to be slightly decreased in comparison to the reference (no expression of *nphT7<sub>SCL</sub>*, SCIST05). Two aspects were taken into consideration to explain these results. First, the levels of malonyl-CoA could play a crucial role for this route and the overall effect of the enzyme. However, increasing the pool of malonyl-CoA by overexpression of *ACC1\*\** did not confirm this hypothesis and revealed to have a negative effect on the production of farnesene. Secondly, higher concentrations of acetoacetyl-CoA may promote the thiolysis activity of endogenous acetoacetyl-CoA thiolase (*ERG10*), ultimately generating a futile cycle between acetyl-, malonyl- and acetoacetyl-CoA. Therefore, we aimed at blocking thiolysis activity of acetoacetyl-CoA thiolase by replacing *ERG10* by *nphT7* from *Streptomyces* sp. strain CL190. This step is critical as deletion of *ERG10* was shown to result in mevalonate auxotrophy [9]. Although *nphT7<sub>SCL</sub>* was able to compensate for the loss of *ERG10*, significant changes were observed considering growth and product formation. Strains with *nphT7<sub>SCL</sub>* integrations displayed slower growth, particularly during the ethanol consumption phase (Fig. 4). Similarly, production of farnesene was strongly impaired as final titers decreased by almost 93 % (SCIST15 vs. SCIST18, Fig. 3A). To enhance the flux via the malonyl-CoA bypass, this strategy was combined with overexpression of *ACC1\*\**. However, consistent with previous results, increasing the level of malonyl-CoA did not improve farnesene production. Altogether, these results illustrate that the bypass via malonyl-CoA is significantly less efficient compared to the endogenous pathway. Clearly, production of FPP is not only extended by an additional reaction in the altered pathway, the demand of ATP also increases from 9 to 12 moles of ATP per mole of FPP due to the conversion of acetyl-CoA to malonyl-CoA, which makes the pathway disadvantageous from an energetic perspective. However, sufficient flux towards malonyl-CoA is essential to maintain growth as it represents an essential building block in lipid metabolism. Instead of the greater ATP cost of the pathway, insufficient efficiency of the acetoacetyl-CoA synthase could cause these detrimental effects. To further investigate this hypothesis, two approaches were pursued to enhance expression of *nphT7<sub>SCL</sub>*. First, a different promoter ( $P_{TEF1}$ ) was used for expression instead of the *ERG10* promoter, which resulted in an almost 4-fold increase (Fig. 3A, SCIST39 vs. SCIST20). Although data on the activity of the promoters in these conditions is not available, transcriptional regulation of *ERG10* could be impaired when  $P_{TEF1}$  is used for expression [6]. Secondly, the copy number was increased by expressing the gene from a multi-copy plasmid in addition to the integrated copy (also using a strong promoter). In this case, a more than 2-fold increase in final farnesene titers was detected (Fig. 3B, SCIST05 vs. SCIST33). Surprisingly, a

difference between the selected homologs became apparent, clearly indicating superior efficiency of *nphT7* from *S. glaucescens*, showing a 4-fold increase. Similarly, Lan and Liao [13] tested *in vitro* activity of different NphT7 homologs, e.g. *Streptomyces coelicolor*, *Streptomyces avermitilis* and *Pseudomonas aeruginosa*, but found NphT7 from *Streptomyces* sp. strain CL190 to be the most active. Besides farnesene production, also the growth kinetics could be improved by enhancing the expression or increasing the copy number. Except for the extended lag phase, SCIST39 ( $P_{TEF1-}ACC1^{**}$ , *erg10Δ::P<sub>TEF1-</sub>nphT7<sub>SCL</sub>*) almost showed the same growth profile as SCIST15 (control) (Fig. 4). Similarly, SCIST34, which expresses *nphT7* from *S. glaucescens* from plasmid showed the most significant improvement in growth compared with SCIST20 (Fig. S4). Based on these results, we conclude that acetoacetyl-CoA synthase activity is not sufficient to enable high fluxes through the mevalonate pathway. This could also partially explain why no improvement was attained when levels of malonyl-CoA were elevated by *ACC1\*\** overexpression. Besides, lipid synthesis, which is strongly dependent on malonyl-CoA as substrate, may divert the flux away from the mevalonate pathway. Therefore, downregulation of *FAS1* aimed at increasing the availability of this substrate, which might otherwise be lost to this competing reaction. Previous studies have shown that the activity of the *HXT1* promoter amounts to less than half of the *FAS1* promoter at 2 % of glucose [11], which was clearly visible during batch phase (Fig. S5) and as anticipated, even more pronounced during the fed-batch phase (Fig. 5B, Fig. S6). This observation was also confirmed by quantification of storage lipids (TAGs) and phospholipids, which were significantly reduced when *FAS1* was downregulated (Table 3). However, instead of using the pool of malonyl-CoA for the mevalonate pathway to a greater extend, the metabolic activity of the strain was significantly reduced as seen by the CO<sub>2</sub> profile as well as the production of farnesene and ethanol (Fig. S6 and Fig. 5B). This phenotype could potentially arise from a build-up of malonyl-CoA to toxic levels, a mechanism, which has previously been studied in human cancer cells [22].

In conclusion, the present study investigated utilization of *nphT7* from *Streptomyces* sp. strain CL190 as a target to improve production of farnesene. Similar studies have been performed for example for the production of butanol with diverse outcomes. In *E. coli*, overexpression of the *nphT7* route was significantly less efficient for acetoacetyl-CoA supply compared with the *atoB* route [17]. Schadeweg et al. on the other hand could show that NphT7 supports production of butanol [27]. In our experiments, expression of *nphT7<sub>SCL</sub>* did not improve production. We could show that the efficiency of the enzyme represents a central aspect that affects the functionality of the overall pathway. Additionally, by replacing *ERG10* with *nphT7<sub>SCL</sub>*, which eliminates the degradation reaction of acetoacetyl-CoA to acetyl-CoA, showed a severe effect on the growth profile. Laboratory evolution could be used in the future as a

strategy to improve growth of the strain. Nonetheless, *nphT7<sub>SCL</sub>* was able to compensate for the loss of *ERG10*, which otherwise would result in an auxotrophy for mevalonate. Furthermore, expressing different homologs of *nphT7<sub>SCL</sub>* in this background allowed for identification of a superior candidate from *S. glaucescens*. Lastly, in order to overcome disadvantageous properties of acetoacetyl-CoA synthase, other enzymes may serve as targets to improve flux through the first part of the pathway. Alternatively, acetoacetyl-CoA thiolase from *Clostridium acetobutylicum* showed significantly higher activity *in vitro* compared with *S. cerevisiae* [27], which has also been utilized for production of farnesene [25]. Besides, further genetic modification might be required to pull more flux through the mevalonate pathway, particularly to re-direct flux from the FPP branch point to farnesene.

### Competing Interests

The authors declare to have no competing interests.

### Acknowledgements

This work was funded by the Knut and Alice Wallenberg Foundation, the Swedish Research Council, FORMAS and the Novo Nordisk Foundation.

## References

1. Blazeck J, Alper HS (2013) Promoter engineering: Recent advances in controlling transcription at the most fundamental level. *Biotechnol J* 8:46-58. doi:10.1002/biot.201200120
2. Chen Y, Partow S, Scalcinati G, Siewers V, Nielsen J (2012) Enhancing the copy number of episomal plasmids in *Saccharomyces cerevisiae* for improved protein production. *FEMS Yeast Res* 12:598-607. doi:10.1111/j.1567-1364.2012.00809.x
3. Curran KA, Karim AS, Gupta A, Alper HS (2013) Use of expression-enhancing terminators in *Saccharomyces cerevisiae* to increase mRNA half-life and improve gene expression control for metabolic engineering applications. *Metab Eng* 19:88-97
4. David F, Nielsen J, Siewers V (2016) Flux Control at the Malonyl-CoA Node through Hierarchical Dynamic Pathway Regulation in *Saccharomyces cerevisiae*. *ACS Synth Biol* 5:224-233. doi:10.1021/acssynbio.5b00161
5. De Kok S, Kozak BU, Pronk JT, Van Maris AJA (2012) Energy coupling in *Saccharomyces cerevisiae*: Selected opportunities for metabolic engineering. *FEMS Yeast Res* 12:387-397. doi:10.1111/j.1567-1364.2012.00799.x
6. Dimster-Denk D, Rine J (1996) Transcriptional regulation of a sterol-biosynthetic enzyme by sterol levels in *Saccharomyces cerevisiae*. *Mol Cell Biol* 16:3981-3989
7. Goldstein JL, Brown MS (1990) Regulation of the mevalonate pathway. *Nature* 343:425-430
8. Hampton RY, Rine J (1994) Regulated degradation of HMG-CoA reductase, an integral membrane protein of the endoplasmic reticulum, in yeast. *J Cell Biol* 125:299-312
9. Hiser L, Basson ME, Rine J (1994) *ERG10* from *Saccharomyces cerevisiae* encodes acetoacetyl-CoA thiolase. *J Biol Chem* 269:31383-31389
10. Jensen NB, Strucko T, Kildegaard KR, David F, Maury J, Mortensen UH, Forster J, Nielsen J, Borodina I (2013) EasyClone: Method for iterative chromosomal integration of multiple genes in *Saccharomyces cerevisiae*. *FEMS Yeast Res*
11. Keren L, Zackay O, Lotan-Pompan M, Barenholz U, Dekel E, Sasson V, Aidelberg G, Bren A, Zeevi D, Weinberger A, Alon U, Milo R, Segal E (2013) Promoters maintain their relative activity levels under different growth conditions. *Molecular Systems Biology* 9. doi:10.1038/msb.2013.59
12. Khoomrung S, Chumnanpuen P, Jansa-Ard S, Staišhlman M, Nookae W, Borén J, Nielsen J (2013) Rapid quantification of yeast lipid using microwave-assisted total lipid extraction and HPLC-CAD. *Analytical Chemistry* 85:4912-4919. doi:10.1021/ac3032405
13. Lan EI, Liao JC (2012) ATP drives direct photosynthetic production of 1-butanol in cyanobacteria. *Proc Natl Acad Sci USA* 109:6018-6023. doi:10.1073/pnas.1200074109
14. Mans R, van Rossum HM, Wijsman M, Backx A, Kuijpers NGA, van den Broek M, Daran-Lapujade P, Pronk JT, van Maris AJA, Daran JMG (2015) CRISPR/Cas9: A molecular Swiss army knife for simultaneous introduction of multiple genetic modifications in *Saccharomyces cerevisiae*. *FEMS Yeast Res* 15:1-15. doi:10.1093/femsyr/fov004
15. Maruyama T, Ito M, Honda G (2001) Molecular cloning, functional expression and characterization of (E)- $\beta$ -farnesene synthase from *Citrus junos*. *Biol Pharm Bull* 24:1171-1175
16. McQualter RB, Petrasovits LA, Gebbie LK, Schweitzer D, Blackman DM, Chrysanthopoulos P, Hodson MP, Plan MR, Riches JD, Snell KD, Brumbley SM, Nielsen LK (2015) The use of an acetoacetyl-CoA synthase in place of a  $\beta$ -ketothiolase enhances poly-3-hydroxybutyrate production in sugarcane mesophyll cells. *Plant Biotechnol J* 13:700-707. doi:10.1111/pbi.12298
17. Menon N, Pásztor A, Menon BRK, Kallio P, Fisher K, Akhtar MK, Leys D, Jones PR, Scrutton NS (2015) A microbial platform for renewable propane synthesis based on a fermentative butanol pathway. *Biotechnology for Biofuels* 8. doi:10.1186/s13068-015-0231-1

18. Ohto C, Muramatsu M, Obata S, Sakuradani E, Shimizu S (2009) Overexpression of the gene encoding HMG-CoA reductase in *Saccharomyces cerevisiae* for production of prenyl alcohols. *Appl Microbiol Biotechnol* 82:837-845
19. Okamura E, Tomita T, Sawa R, Nishiyama M, Kuzuyama T (2010) Unprecedented acetoacetyl-coenzyme A synthesizing enzyme of the thiolase superfamily involved in the mevalonate pathway. *Proc Natl Acad Sci USA* 107:11265-11270. doi:10.1073/pnas.1000532107
20. Ozcan S, Johnston M (1995) Three different regulatory mechanisms enable yeast hexose transporter (HXT) genes to be induced by different levels of glucose. *Mol Cell Biol* 15:1564-1572
21. Padden CJ, Westfall PJ, Pitera DJ, Benjamin K, Fisher K, McPhee D, Leavell MD, Tai A, Main A, Eng D, Polichuk DR, Teoh KH, Reed DW, Treynor T, Lenihan J, Jiang H, Fleck M, Bajad S, Dang G, Dengrove D, Diola D, Dorin G, Ellens KW, Fickes S, Galazzo J, Gaucher SP, Geistlinger T, Henry R, Hepp M, Horning T, Iqbal T, Kizer L, Lieu B, Melis D, Moss N, Regentin R, Secret S, Tsuruta H, Vazquez R, Westblade LF, Xu L, Yu M, Zhang Y, Zhao L, Lievense J, Covello PS, Keasling JD, Reiling KK, Renninger NS, Newman JD (2013) High-level semi-synthetic production of the potent antimalarial artemisinin. *Nature* 496:528-532
22. Pizer ES, Thupari J, Han WF, Pinn ML, Chrest FJ, Frehywot GL, Townsend CA, Kuhajda FP (2000) Malonyl-coenzyme-A is a potential mediator of cytotoxicity induced by fatty-acid synthase inhibition in human breast cancer cells and xenografts. *Cancer Res* 60:213-218
23. Quan J, Tian J (2011) Circular polymerase extension cloning for high-throughput cloning of complex and combinatorial DNA libraries. *Nat Protoc* 6:242-251
24. Reifenberger E, Freidel K, Ciriacy M (1995) Identification of novel HXT genes in *Saccharomyces cerevisiae* reveals the impact of individual hexose transporters on glycolytic flux. *Mol Microbiol* 16:157-167
25. Sandoval CM, Ayson M, Moss N, Lieu B, Jackson P, Gaucher SP, Horning T, Dahl RH, Denery JR, Abbott DA, Meadows AL (2014) Use of pantothenate as a metabolic switch increases the genetic stability of farnesene producing *Saccharomyces cerevisiae*. *Metab Eng* 25:215-226
26. Scalcinati G, Knuf C, Partow S, Chen Y, Maury J, Schalk M, Daviet L, Nielsen J, Siewers V (2012) Dynamic control of gene expression in *Saccharomyces cerevisiae* engineered for the production of plant sesquiterpene α-santalene in a fed-batch mode. *Metab Eng* 14:91-103
27. Schadeweg V, Boles E (2016) N-Butanol production in *Saccharomyces cerevisiae* is limited by the availability of coenzyme A and cytosolic acetyl-CoA. *Biotechnology for Biofuels* 9. doi:10.1186/s13068-016-0456-7
28. Shi S, Chen Y, Siewers V, Nielsen J (2014) Improving production of malonyl coenzyme A-derived metabolites by abolishing Snf1-dependent regulation of Acc1. *mBio* 5. doi:10.1128/mBio.01130-14
29. Tippmann S, Nielsen J, Khoomrung S (2016) Improved quantification of farnesene during microbial production from *Saccharomyces cerevisiae* in two-liquid-phase fermentations. *Talanta* 146:100-106. doi:10.1016/j.talanta.2015.08.031
30. Tippmann S, Scalcinati G, Siewers V, Nielsen J (2016) Production of farnesene and santalene by *Saccharomyces cerevisiae* using fed-batch cultivations with RQ-controlled feed. *Biotechnol Bioeng* 113:72-81. doi:10.1002/bit.25683
31. Verduyn C, Postma E, Scheffers WA, Van Dijken JP (1992) Effect of benzoic acid on metabolic fluxes in yeasts: A continuous-culture study on the regulation of respiration and alcoholic fermentation. *Yeast* 8:501-517
32. Weber AL (1991) Origin of fatty acid synthesis: Thermodynamics and kinetics of reaction pathways. *J Mol Evol* 32:93-100

## List of Figures

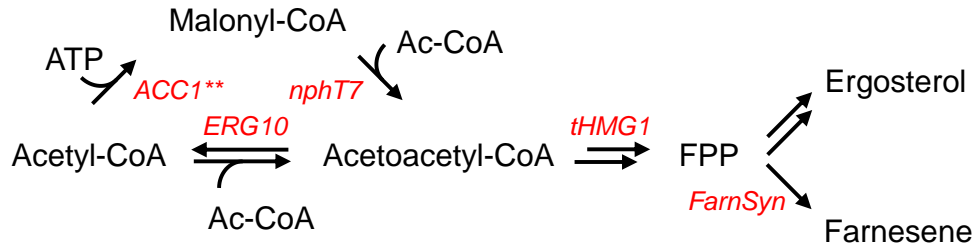


Fig. 1 Simplified illustration of the mevalonate pathway in *S. cerevisiae*, which is utilized for sterol synthesis. Besides, farnesyl diphosphate (FPP) can be converted to farnesene. In the first reaction of the pathway, acetoacetyl-CoA thiolase (*ERG10*) produces acetoacetyl-CoA from two molecules of acetyl-CoA. Alternatively, acetoacetyl-CoA can be produced from malonyl-CoA using acetoacetyl-CoA synthase (*nphT7*) identified from *Streptomyces* sp. strain CL190, which was investigated in this study.

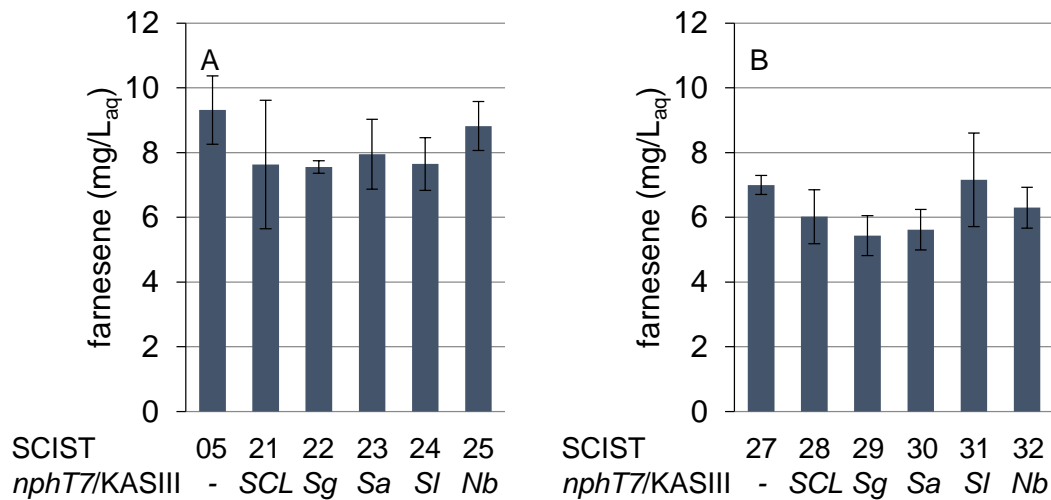


Fig. 2 Effect of the heterologous acetoacetyl-CoA synthase on production of farnesene in *S. cerevisiae*. Strains carry plasmids for expression of farnesene synthase, truncated HMG-CoA reductase and acetoacetyl-CoA synthase (*nphT7*) from different bacterial strains, without (A) and with (B) chromosomal integration of double mutant acetyl-CoA carboxylase (*ACC1\*\**). *SCL*-*Streptomyces* sp. strain CL190, *Sg*-*S. glaucescens*, *Sa*-*S. afghaniensis*, *SI*-*S. lactacystinaeus* and *Nb*-*N. brasiliensis*. Bars represent average

concentrations of farnesene with respect to the volume of aqueous medium of three biological replicates with standard deviations.

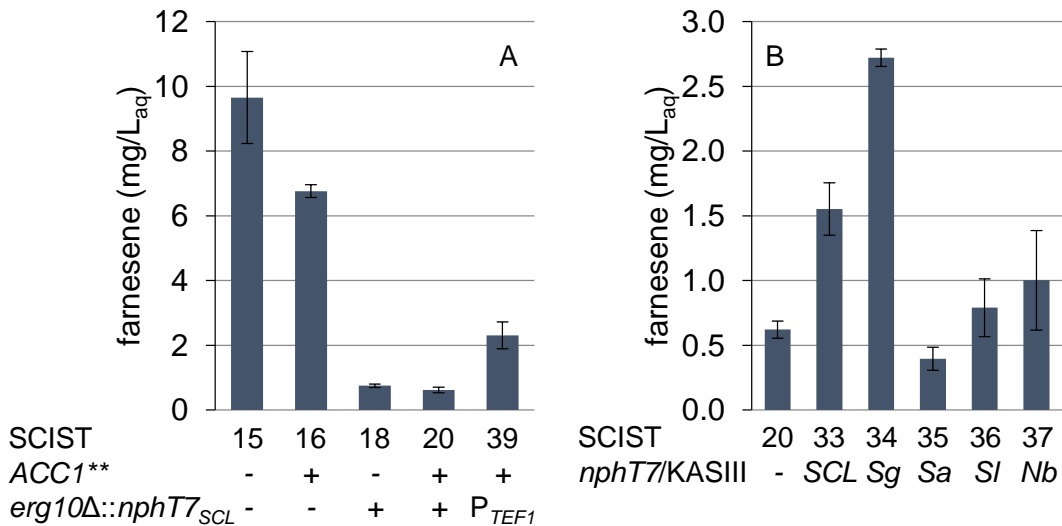


Fig. 3 (A) Replacing endogenous *ERG10* in *S. cerevisiae* by *nphT7* from *Streptomyces* sp. strain CL190 in combination with *ACC1\*\** overexpression for production of farnesene. All strains carry plasmid pIST05 for expression of farnesene synthase and truncated HMG-CoA reductase. (B) Comparison of different *nphT7* homologs in strain SCIST19 (*ACC1\*\**, *erg10Δ::nphT7<sub>SCL</sub>*). The homologs were expressed from plasmid together with farnesene synthase and truncated HMG-CoA reductase. *SCL*-*Streptomyces* sp. strain CL190, *Sg*-*S. glaucescens*, *Sa*-*S. afghaniensis*, *Sl*-*S. lactacystinaeus* and *Nb*-*N. brasiliensis*. Bars represent average concentrations of farnesene with respect to the volume of aqueous medium of at least three biological replicates with standard deviation.

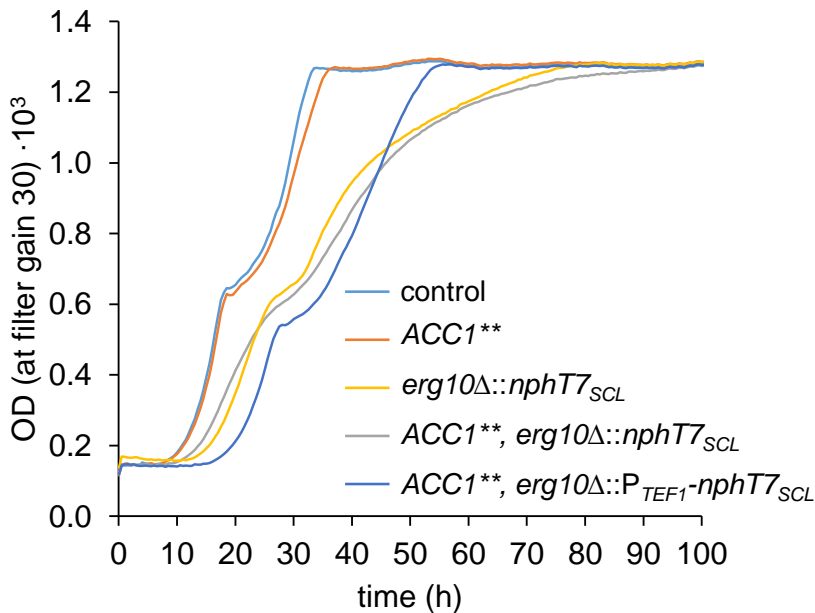


Fig. 4 Effect on replacing endogenous *ERG10* by bacterial *nphT7<sub>SCL</sub>* on growth of *S. cerevisiae*. Average optical density of four biological replicates measured online using BioLector. Indicated relevant genotypes refer to strains: SCIST15, 16, 18, 20, 39 (from top to bottom).

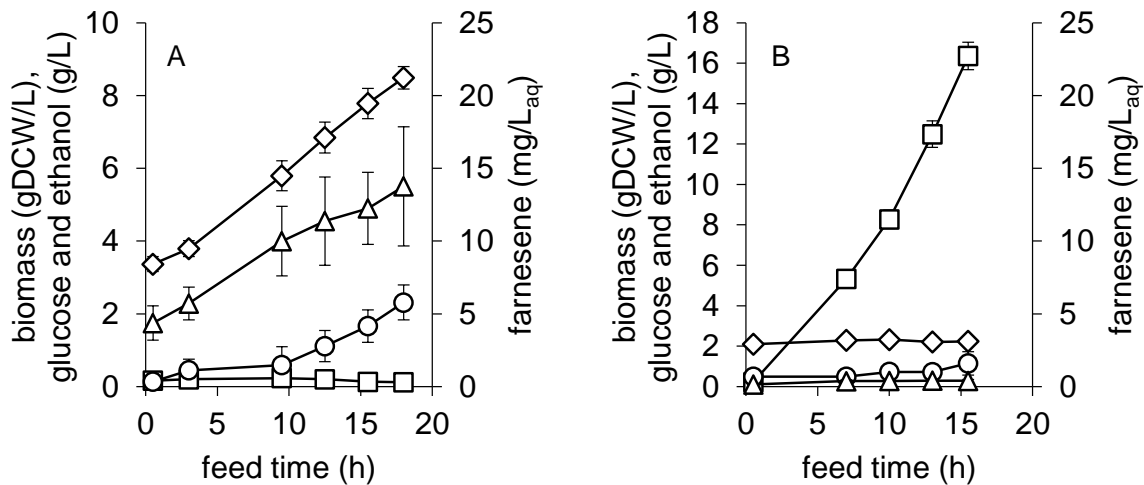


Fig. 5 Downregulation of *FAS1* using  $P_{HXT1}$  in *S. cerevisiae* with *ACC1\*\** overexpression and *erg10Δ::P<sub>TEF1</sub>-nphT7<sub>SCL</sub>* substitution from *Streptomyces* sp. strain CL190 for improved utilization of malonyl-CoA as substrate for the mevalonate pathway. (A) Strain SCIST40 without *FAS1* downregulation and (B) strain SCIST43 with *FAS1* downregulation. In addition to the integrated copy, both strains express *nphT7* from *S. glaucescens* from plasmid pIST13. Data represents average values of four biological replicates with

standard deviation obtained during the fed-batch phase. Diamonds – biomass, squares – glucose, circles – ethanol and triangles – farnesene.

## List of Tables

Table 1 List of plasmids used in this study.

Plasmid	Description	Reference
pSP-GM1	$P_{TEF1}\text{-}P_{PGK1}$ bidirectional promoter (2 $\mu\text{m}$ , <i>URA3</i> )	[2]
pMEL10	gRNA- <i>CAN1.Y</i> (2 $\mu\text{m}$ , <i>URA3</i> )	[14]
piST05	$P_{PGK1}\text{-}tHMG1$ , $P_{TEF1}\text{-}FarnSyn\_Cj$	[30]
pMG96	$P_{TEF1}\text{-}ACC1^{**}$	This study
piST07	$P_{TEF1}\text{-}nphT7_{SCL}$	This study
piST12	piST05, $P_{tHXT7}\text{-}nphT7_{SCL}$	This study
piST13	piST05, $P_{tHXT7}\text{-}nphT7_{Sg}$	This study
piST14	piST05, $P_{tHXT7}\text{-}nphT7_{Sa}$	This study
piST15	piST05, $P_{tHXT7}\text{-}nphT7_{SI}$	This study
piST16	piST05, $P_{tHXT7}\text{-}nphT7_{Nb}$	This study

Table 2 List of strains used in this study.

Name	Relevant Genotype	Plasmid	Reference
CEN.PK113-	<i>MATa MAL2-8<sup>c</sup> SUC2 ura3-52</i>	-	P. Kötter, University of Frankfurt, Germany
5D			
SCIST05	<i>MATa MAL2-8<sup>c</sup> SUC2 ura3-52</i>	piST05	[30]
IMX581	<i>MATa MAL2-8<sup>c</sup> SUC2 ura3-52 can1Δ::cas9-natNT2</i>	-	[14]
SCIST15	<i>MATa MAL2-8<sup>c</sup> SUC2 ura3-52 can1Δ::cas9-natNT2</i>	piST05	This study
RF14	<i>MATa MAL2-8<sup>c</sup> SUC2 ura3-52 P<sub>TEF1</sub>-ACC1&lt;**&gt; P<sub>TEF1</sub>-kanMX can1Δ::cas9-natNT2</i>	-	This study
SCIST16	<i>MATa MAL2-8<sup>c</sup> SUC2 ura3-52 P<sub>TEF1</sub>-ACC1&lt;**&gt; P<sub>TEF1</sub>-kanMX can1Δ::cas9-natNT2</i>	piST05	This study
SCIST17	<i>MATa MAL2-8<sup>c</sup> SUC2 ura3-52 can1Δ::cas9-natNT2 erg10Δ::nphT7<sub>SCL</sub></i>	-	This study
SCIST18	<i>MATa MAL2-8<sup>c</sup> SUC2 ura3-52 can1Δ::cas9-natNT2 erg10Δ::nphT7<sub>SCL</sub></i>	piST05	This study
SCIST19	<i>MATa MAL2-8<sup>c</sup> SUC2 ura3-52 P<sub>TEF1</sub>-ACC1&lt;**&gt; can1Δ::cas9-natNT2 erg10Δ::nphT7<sub>SCL</sub></i>	-	This study

SCIST20	MATa <i>MAL2-8<sup>c</sup> SUC2 ura3-52 P<sub>TEF1-ACC1** can1Δ::cas9-</sub></i>	pIST05	This study
	<i>natNT2 erg10Δ:: nphT7<sub>SCL</sub></i>		
SCIST21	MATa <i>MAL2-8<sup>c</sup> SUC2 ura3-52</i>	pIST12	This study
SCIST22	MATa <i>MAL2-8<sup>c</sup> SUC2 ura3-52</i>	pIST13	This study
SCIST23	MATa <i>MAL2-8<sup>c</sup> SUC2 ura3-52</i>	pIST14	This study
SCIST24	MATa <i>MAL2-8<sup>c</sup> SUC2 ura3-52</i>	pIST15	This study
SCIST25	MATa <i>MAL2-8<sup>c</sup> SUC2 ura3-52</i>	pIST16	This study
SCIST26	MATa <i>MAL2-8<sup>c</sup> SUC2 ura3-52 P<sub>TEF1-ACC1** P<sub>TEF1-kanMX</sub></sub></i>	-	This study
SCIST27	MATa <i>MAL2-8<sup>c</sup> SUC2 ura3-52 P<sub>TEF1-ACC1** P<sub>TEF1-kanMX</sub></sub></i>	pIST05	This study
SCIST28	MATa <i>MAL2-8<sup>c</sup> SUC2 ura3-52 P<sub>TEF1-ACC1** P<sub>TEF1-kanMX</sub></sub></i>	pIST12	This study
SCIST29	MATa <i>MAL2-8<sup>c</sup> SUC2 ura3-52 P<sub>TEF1-ACC1** P<sub>TEF1-kanMX</sub></sub></i>	pIST13	This study
SCIST30	MATa <i>MAL2-8<sup>c</sup> SUC2 ura3-52 P<sub>TEF1-ACC1** P<sub>TEF1-kanMX</sub></sub></i>	pIST14	This study
SCIST31	MATa <i>MAL2-8<sup>c</sup> SUC2 ura3-52 P<sub>TEF1-ACC1** P<sub>TEF1-kanMX</sub></sub></i>	pIST15	This study
SCIST32	MATa <i>MAL2-8<sup>c</sup> SUC2 ura3-52 P<sub>TEF1-ACC1** P<sub>TEF1-kanMX</sub></sub></i>	pIST16	This study
SCIST33	MATa <i>MAL2-8<sup>c</sup> SUC2 ura3-52 P<sub>TEF1-ACC1** can1Δ::cas9-</sub></i>	pIST12	This study
	<i>natNT2 erg10Δ:: nphT7<sub>SCL</sub></i>		
SCIST34	MATa <i>MAL2-8<sup>c</sup> SUC2 ura3-52 P<sub>TEF1-ACC1** can1Δ::cas9-</sub></i>	pIST13	This study
	<i>natNT2 erg10Δ:: nphT7<sub>SCL</sub></i>		
SCIST35	MATa <i>MAL2-8<sup>c</sup> SUC2 ura3-52 P<sub>TEF1-ACC1** can1Δ::cas9-</sub></i>	pIST14	This study
	<i>natNT2 erg10Δ:: nphT7<sub>SCL</sub></i>		
SCIST36	MATa <i>MAL2-8<sup>c</sup> SUC2 ura3-52 P<sub>TEF1-ACC1** can1Δ::cas9-</sub></i>	pIST15	This study
	<i>natNT2 erg10Δ:: nphT7<sub>SCL</sub></i>		
SCIST37	MATa <i>MAL2-8<sup>c</sup> SUC2 ura3-52 P<sub>TEF1-ACC1** can1Δ::cas9-</sub></i>	pIST16	This study
	<i>natNT2 erg10Δ:: nphT7<sub>SCL</sub></i>		
SCIST38	MATa <i>MAL2-8<sup>c</sup> SUC2 ura3-52 P<sub>TEF1-ACC1** can1Δ::cas9-</sub></i>	-	This study
	<i>natNT2 erg10Δ::P<sub>TEF1-</sub> nphT7<sub>SCL</sub></i>		
SCIST39	MATa <i>MAL2-8<sup>c</sup> SUC2 ura3-52 P<sub>TEF1-ACC1** can1Δ::cas9-</sub></i>	pIST05	This study
	<i>natNT2 erg10Δ::P<sub>TEF1-</sub> nphT7<sub>SCL</sub></i>		
SCIST40	MATa <i>MAL2-8<sup>c</sup> SUC2 ura3-52 P<sub>TEF1-ACC1** can1Δ::cas9-</sub></i>	pIST13	This study
	<i>natNT2 erg10Δ::P<sub>TEF1-</sub> nphT7<sub>SCL</sub></i>		
SCIST41	MATa <i>MAL2-8<sup>c</sup> SUC2 ura3-52 P<sub>TEF1-ACC1** can1Δ::cas9-</sub></i>	-	This study
	<i>natNT2 erg10Δ::P<sub>TEF1-</sub> nphT7<sub>SCL</sub> P<sub>TEF1-kanMX</sub> P<sub>FAS1Δ::P<sub>HXT1</sub></sub></i>		
SCIST42	MATa <i>MAL2-8<sup>c</sup> SUC2 ura3-52 P<sub>TEF1-ACC1** can1Δ::cas9-</sub></i>	pIST05	This study
	<i>natNT2 erg10Δ::P<sub>TEF1-</sub> nphT7<sub>SCL</sub> P<sub>TEF1-kanMX</sub> P<sub>FAS1Δ::P<sub>HXT1</sub></sub></i>		

SCIST43	<i>MATa MAL2-8<sup>c</sup> SUC2 ura3-52 P<sub>TEF1</sub>-ACC1** can1Δ::cas9-</i> <i>natNT2 erg10Δ::P<sub>TEF1</sub>- nphT7<sub>SCL</sub> P<sub>TEF1</sub>-kanMX P<sub>FAS1</sub>Δ::P<sub>HXT1</sub></i>	pIST13	This study
---------	--	--------	------------

Table 3 Lipid quantification in strains SCIST40 and 43 after 15 h of exponential feeding. Data represent average values in mg/gDCW of four biological replicates ± standard deviation.

	- <i>FAS1</i> downregulation (SCIST42)	+ <i>FAS1</i> downregulation (SCIST43)
Triacylglycerol	31.56 ± 8.49	3.89 ± 0.41
Phosphatidylinositol	2.47 ± 0.50	0.46 ± 0.07
Phosphatidylcholine	2.33 ± 0.45	0.80 ± 0.10
Ergosterol	3.43 ± 0.60	1.72 ± 0.21

## Supplementary Material

### Effects of acetoacetyl-CoA synthase expression on production of sesquiterpenes in *Saccharomyces cerevisiae*

Stefan Tippmann<sup>1,2</sup>, Raphael Ferreira<sup>1,2</sup>, Verena Siewers<sup>1,2</sup>, Jens Nielsen<sup>1,2,3</sup> and Yun Chen<sup>1,2,\*</sup>

<sup>1</sup>Department of Biology and Biological Engineering,  
Chalmers University of Technology, SE412 96 Gothenburg, Sweden

<sup>2</sup>Novo Nordisk Foundation Center for Biosustainability, Chalmers University of Technology, SE412 96  
Gothenburg, Sweden

<sup>3</sup>Novo Nordisk Foundation Center for Biosustainability, Technical University of Denmark, DK2970  
Hørsholm, Denmark

\*Corresponding Author: Yun Chen

Department of Biology and Biological Engineering,

Chalmers University of Technology, Kemivägen 10, SE412 96, Gothenburg, Sweden.

E-mail: [yunc@chalmers.se](mailto:yunc@chalmers.se)

Tel: +46 31772 38 04

Fax: +46 31 772 38 01

Keywords: isoprenoids, mevalonate pathway, biofuels, yeast, metabolic engineering

Table S1 List of primers used for plasmid construction. Italics indicate overhangs, bold letters indicate restriction sites.

Plasmid	Primer Name	Sequence (5' → 3')
pIST07	SCL190-fwd	<i>GTTGTTGC</i> GGCCGC <del>AAAACAATGACCGATGTTAGATT</del>
	SCL190-rev	<i>GTTGTTTAA</i> TTAATTACCATTCAATCAAGGCAA
pIST12/13/ 14/15/16	PHXT7-fwd	<i>GGAATTGCC</i> ATGAAGCCGAATCGTAGGAACAATT <del>T</del> CGGG
	PHXT7-rev	TTTTGATTAAAATTAATTTAAAAACTTTTG
	THIS5-fwd	ATAGATTAATTTAACAGTATATGTACAG
	THIS5-rev	GTAACAATATCATGAGACCTTTATA
pIST12	nphT7-fwd	<i>TTTTAATTTAATC</i> AAAAAAAACAATGACCGATGTTAGATT <del>CAGA</del>
	nphT7-rev	<i>TACTGTTAAATTAATCT</i> ATTACCAATTCAATCAAGGCA
pIST13	Sgl-fwd	<i>TTTTAATTTAATC</i> AAAAAAAACAATGATTACTACAGGTACTC
	Sgl-rev	<i>TACTGTTAAATTAATCT</i> ATTATCTTGTAAACAATGCCA
pIST14	Saf-fwd	<i>TTTTAATTTAATC</i> AAAAAAAACAATGGCTGCATCTAC
	Saf-rev	<i>TACTGTTAAATTAATCT</i> ATTATCTATTACCCAACTAATTAA
pIST15	Sla-fwd	<i>TTTTAATTTAATC</i> AAAAAAAACAATGACCGATGTTAG
	Sla-rev	<i>TACTGTTAAATTAATCT</i> ATTACCAACTAAAGCGA
pIST16	Nbr-fwd	<i>TTTTAATTTAATC</i> AAAAAAAACAATGAATAACATTGCTG
	Nbr-rev	<i>TACTGTTAAATTAATCT</i> ATTACCACTCGACTAAAGTC <del>AAA</del>
pIST12/13/ 14/15/16	T7Cassette-fwd	<i>GGCGTTATCCAGCTGC</i> ATTAATGATCGTAGGAACAATT <del>T</del> CGGG
	T7Cassette-rev	<i>CTGATTCTGTGGATAACCGT</i> ATTACCGTAACAATATCATGAGACCTTTATA
	Affi3-2-fwd	GGTAATACGGTTATCCACAGAATC
	Affi3-2-rev	TTCTCAGGTATAGCATGAGGTC
	Affi3-3-fwd	GAGCGACCTCATGCTATAACCT
	Affi3-3-rev	TCATTAATGCAGCTGGATAAAC

Table S2 Primers for replacing *Erg10* by *nphT7<sub>SCL</sub>* using CRISPR/Cas9.

Repair fragment	Primer Name	Sequence (5' → 3')
<i>nphT7<sub>SCL</sub></i>	NphRF-fwd	AAAGGTAGCCTAAAACAAGGCCATATCATATATTTATACAGATTAGACGTACTCAA AAAACAATGACCGATGTTAGATT
	NphRF-rev	AAGCCATTATATATTTATGTATTTATGAAAAAGATCATGAGAAAATCGCAGAACGTA TTACCATTCAATCAAGGCA
P <sub>TEF1</sub> - <i>nphT7<sub>SCL</sub></i> - T <sub>ADH1</sub>	NphRF2-fwd	AAAGGTAGCCTAAAACAAGGCCATATCATATATTTATACAGATTAGACGTACTCAA GCACACACCATACTGCTTCAA
	NphRF2-rev	AAGCCATTATATATTTATGTATTTATGAAAAAGATCATGAGAAAATCGCAGAACGTA GAGCGACCTCATGCTATAAC

Table S3 BLAST results to compare amino acid sequence of the NphT7 homologs to NphT7 from *Streptomyces* sp. strain CL190.

Origin	Accession number	E-value	Identity (%)
<i>Streptomyces glaucescens</i>	AIR99429.1	2e-120	60
<i>Streptomyces afghaniensis</i>	WP_020277513.1	4e-103	56
<i>Streptomyces lactacystinaeus</i>	BAP82212.1	7e-175	75
<i>Nocardia brasiliensis</i>	GAJ84426.1	4e-142	66

sp|D7URV0|NPHT7\_STRC1  
gi|701462379|dbj|BAP82212.1|  
gi|635329189|dbj|GAJ84426.1|  
gi|692323226|gb|AIR99429.1|  
gi|519357735|ref|WP\_020277513.

-----MTDVRFRIIGTGYAVPERIVSNDEVGAPAGVDDDWIRKT  
-----MTDVRILGTGYAVPERIVSNDEAAAAAGVDDAWITDRT  
-----MNNIAVLGTSYLPDRIVSNSEVGSGADVDSEWIIRKT  
MITTGTHHDGHPTASVGILGTGSCLPSQVTNDEAGLPAGVDDAIIHSRT  
-----MAASTGVTPEWIERKT

sp|D7URV0|NPHT7\_STRC1  
gi|701462379|dbj|BAP82212.1|  
gi|635329189|dbj|GAJ84426.1|  
gi|692323226|gb|AIR99429.1|  
gi|519357735|ref|WP\_020277513.

GIRQRRAAADDQATSDLATAAGRAALKAAGITPEQLTVIAVATSTPDRPQ  
GIRERRWAADGQATSDLATAAGRAALRSAGISAEELSVIVATSTPDRPQ  
AIRERRWALPDQATSDLATRAARAALDAAGIGADEVSALVVATSTPDPHQ  
GIRTRRWAKPDEATSDLAVAAGRAALENAGIRAAELSIVVATSTPDAPO  
GILERRYAEDDQAASDLAAEAGRRLAQNAGVGPAELSIIVATSTPDPQO  
\* \* \*; \* \* \*; \* \* \*; \* \* \*; \* \* \*; \* \* \*; \* \* \*; \* \* \*; \* \* \*

sp|D7URV0|NPHT7\_STRC1  
gi|701462379|dbj|BAP82212.1|  
gi|635329189|dbj|GAJ84426.1|  
gi|692323226|gb|AIR99429.1|  
gi|519357735|ref|WP\_020277513.

```

PPTAAYVQHHLGAT-GTAAFDVNACSGTVFALSSVAGTLVYRGG--YA
PPTAAYVQQRLGAS-GAAA FDVNACSGTVFALSAAEGVLARTGG--HA
PPTAAFVQHNLGAR-GASA FDVNACSGFVFALSAVEAAIARAGGG--YG
PPTASAVADGLGAGPGTAAFDVNAVCSCGFVFALTAERMLRGTGG--YA
PPTAAVVQRLLGAD-RAAA FDVNACVGFFVALRAGASMTLEDGRHGGR
*****: *   ***   :*****: * * ** : * .
```

sp|D7URV0|NPHT7\_STRC1  
gi|701462379|dbj|BAP82212.1|  
gi|635329189|dbj|GAJ84426.1|  
gi|692323226|gb|AIR99429.1|  
gi|519357735|ref|WP\_020277513.

LVIGADLYSRLNPAADRKTIVLFGDAGAMVLGPTSTGTGPIVRRVALHT  
LVIGADLYSRLNRADRTTIVLFGDAGAVVLG-APVDHGPVRVRLSLSH  
LVVGADVYSRLNPAADRRTVVLFGDAGAVVLPSSASGG--LRRFGLHT  
VVVGADIYSRILDRAADRRTAILFGDAGAVVLPAAAGGRAGITARLAG--  
LVIGSDVYSSRIVDPSSRRTAPLFGDAGAVVLPVAEAGG--LLGGSVAT  
\*:\*\*\*\*\*:\*\*\*\*\*: : \*:\*\*\*\*\*:\*\*\*\*\*:\*\*\*\*\*:\*\*\*\*\*:

sp|D7URV0|NPHT7\_STRC1  
gi|701462379|dbj|BAP82212.1|  
gi|635329189|dbj|GAJ84426.1|  
gi|692323226|gb|AIR99429.1|  
gi|519357735|ref|WP\_020277513.

FGGLTDLIRVPAGGSRQPLTDGLDAGLQYFAMDGREGVRRFTTEHLPQLI  
FGELSGLIEVPAGGSRMPVDQTVLDAGLQYFAMDGRGVRFVGDHLPQLV  
FGDLTSLIRVPAGGSRQPYDPAAHELGAQYFTMDGRGVRAFVNGLPVLV  
FGAERDLIQVPAGGSRLPASADTLREGLHYFKMNGRAVREFVADQVAPAI  
DSRLLDLIGITAGGSRQPSSTDITLEHYFRMRGREGVRDYVTRELPRAV  
.....\*\*\*.....\*\*\*\*\* \* .. \* ; \*\*\* \* \* \* \* \* ; \* .. ; ..

sp|D7URV0|NPHT7\_STRC1  
gi|701462379|dbj|BAP82212.1|  
gi|635329189|dbj|GAJ84426.1|  
gi|692323226|gb|AIR99429.1|  
gi|519357735|ref|WP\_020277513.

KGFLHEAGVDAADISHFVPHQANGVMILDEVFGELHLPRATMVRTVETYGN  
KGFLHECGVAPGDIDHFVPHQANGTMILDSVFADIALPRATMVRTLTHYAN  
KQFLHDSGVAPDDITHLIPHQANGVMIAELAEEGLGVNATMHTTVRYYGN  
TRFLADQGVDPDRDIDHFVPHQANGRMQLQDLAERVGIPAGRMRRTTVESYGN  
HDLLTDLSVPPEEIRHFIIPHQANGAMRLDIWGHGLPHAHHLMPVARHGN  
\*: \* : \* : \* : \* : \* : \* : \* : \* : \* : \* : \* : \* : \* : \* : \*

sp|D7URV0|NPHT7\_STRC1  
gi|701462379|dbj|BAP82212.1|  
gi|635329189|dbj|GAJ84426.1|  
gi|692323226|gb|AIR99429.1|  
gi|519357735|ref|WP\_020277513.

TGAASIPITMDAAVRAGSFRPGEVLVLLAGFGGGMAASFALIEW---  
MGAASIPITLDAARAGAFTPGDLILLAGFGGGMSAGFALVEW---  
TGAASIPITLDNAARTGGIRPGDKVLLVGFGGGMAVGTLVEW---  
TGSASIPVTLDAAARRGGIRPGDRVLLAGFGGGMAMGLALLTR---  
TGAASIPIALDHAAHRSGRLAAGELVLLAGFGGGMTGTSLISWGNR  
\* : \* \* \* ; : \* \* \* ; : \* ; : \* \* \* ; \* \* \* ; : \* ; : \*

Fig. S1 Sequence alignment of amino acid sequences for *nphT7* and four different homologs using CLUSTALW 2.1 on (<http://www.genome.jp/tools/clustalw/>). Region highlighted in grey indicates the motif potentially involved in CoA recognition.

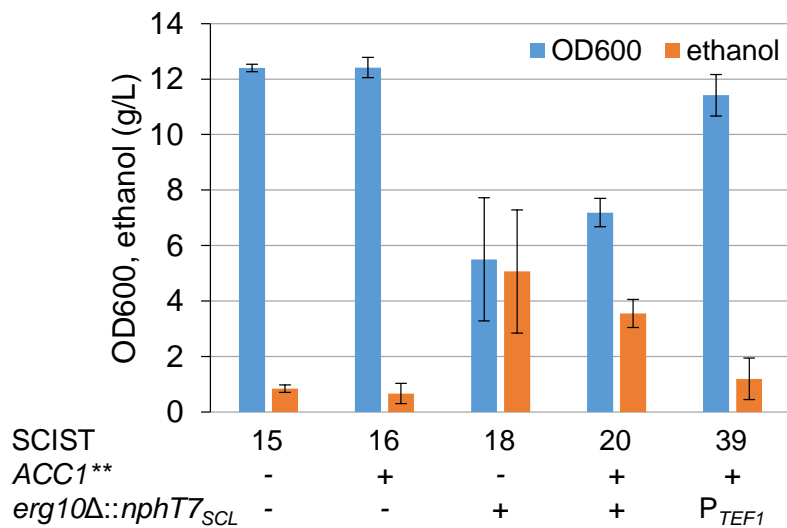


Fig. S2 Ethanol concentration and final OD600 values after 72 h of cultivation after replacing endogenous *ERG10* in *S. cerevisiae* by *nphT7* from *Streptomyces* sp. CL190 in combination with *ACC1\*\** overexpression. Bars represent average values of at least three biological replicates with standard deviation. The corresponding final titers of farnesene are shown Fig. 3A.

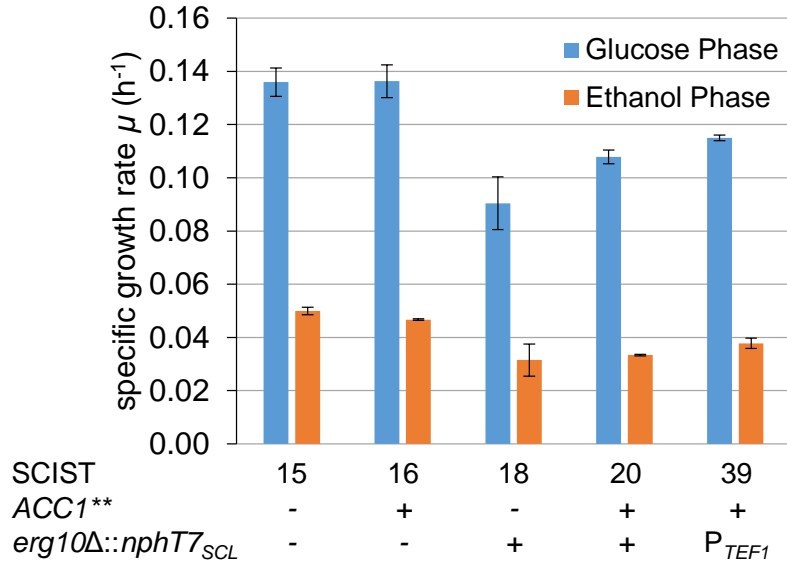


Fig. S3 Specific growth rates calculated during the glucose and ethanol phase using the OD measurements from the BioLector cultivation presented in Fig. 4.

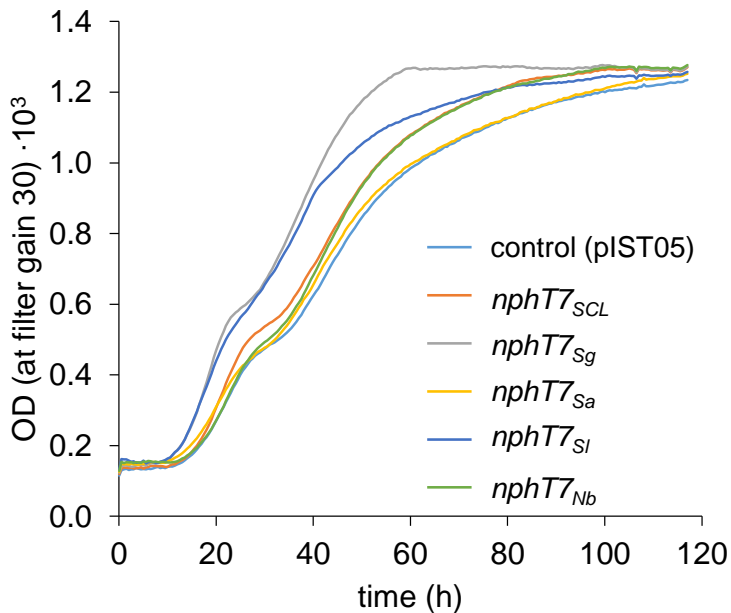


Fig. S4 Effect of different *nphT7* from various bacterial species on growth of *S. cerevisiae*. Average optical density of three biological replicates measured online using BioLector. All genes were expressed from plasmid in strain SCIST19 (*ACC1\*\**, *erg10Δ::nphT7<sub>SCL</sub>*).

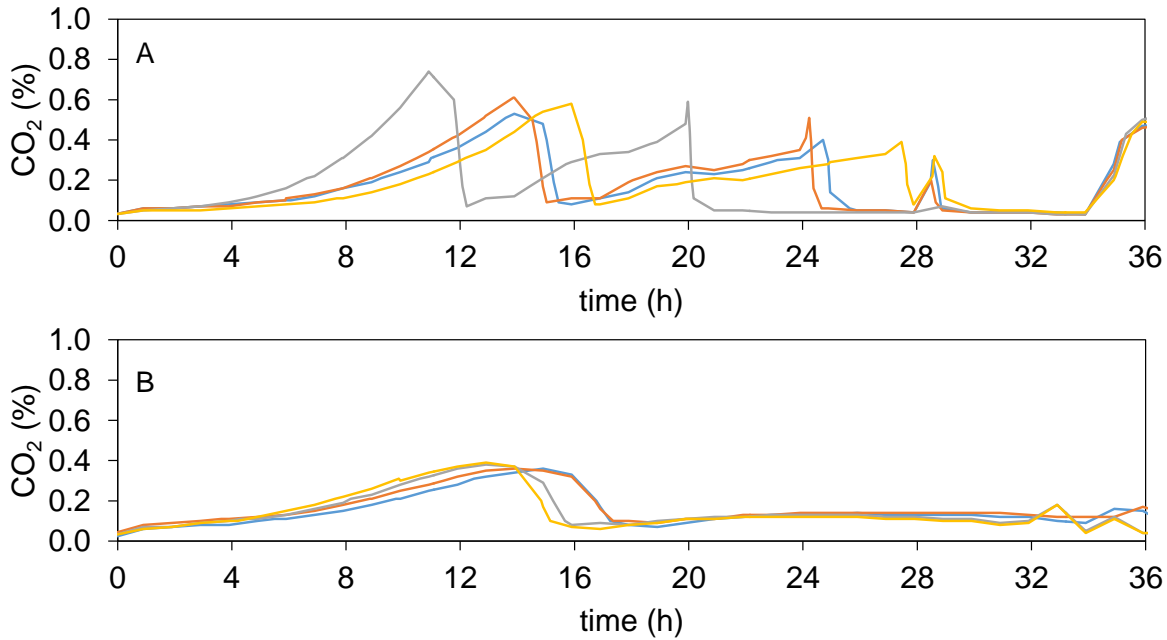


Fig. S5 CO<sub>2</sub> profile for four biological replicates of strain SCIST40 (A) and SCIST43 (B) during aerobic batch cultivation using 10 g/L glucose. SCIST42 - P<sub>TEF1</sub>-ACC1\*\*, erg10Δ::P<sub>TEF1</sub>- nphT7<sub>SCL</sub> and SCIST43 - P<sub>TEF1</sub>- ACC1\*\*, erg10Δ::P<sub>TEF1</sub>- nphT7<sub>SCL</sub>, P<sub>FAS1Δ</sub>::P<sub>HXT1</sub>.

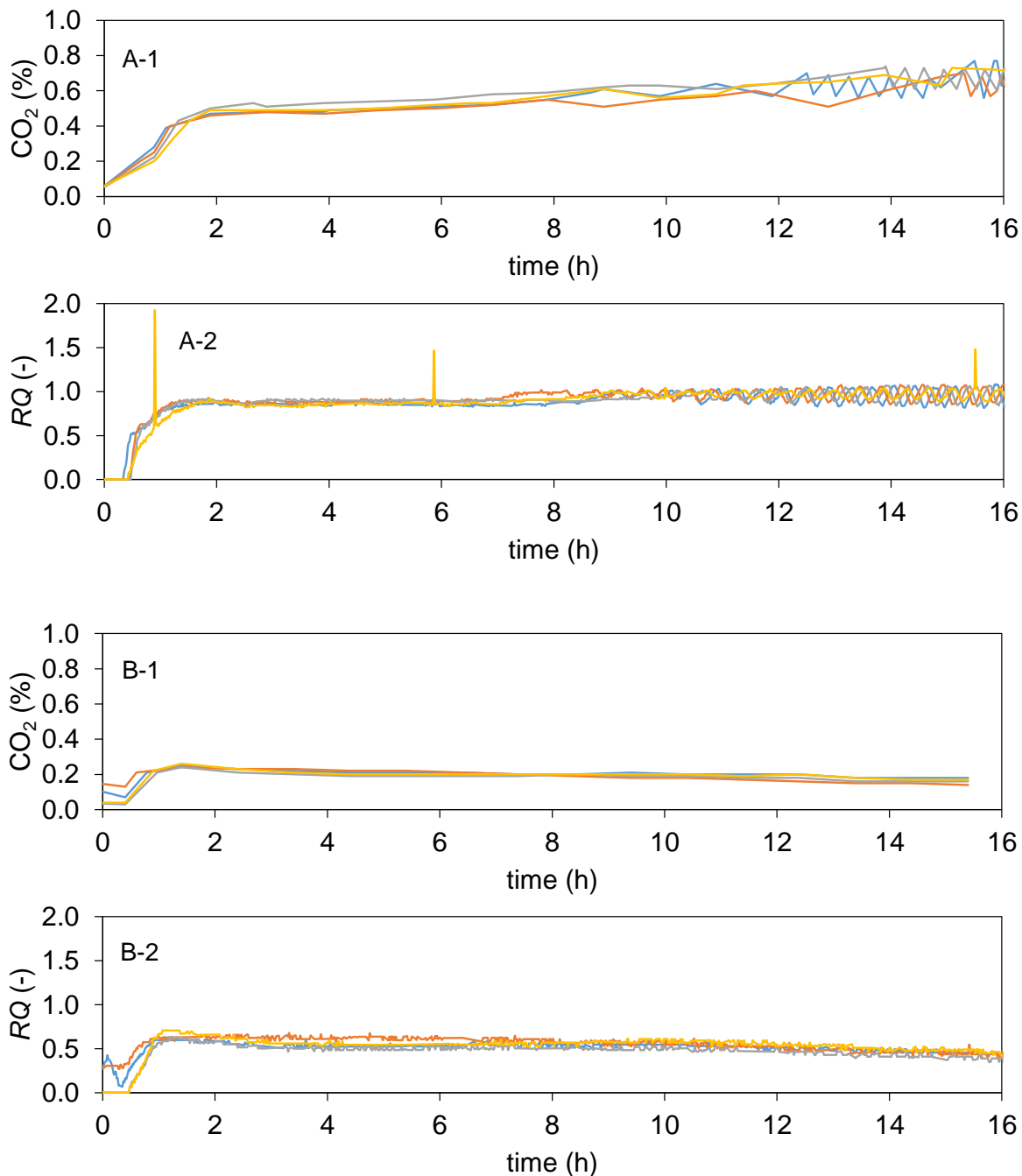


Fig. S6  $\text{CO}_2$  and respiratory quotient (RQ) profiles for four biological replicates of strain SCIST40 (A-1, A-2) and SCIST43 (B-1, B-2) during the fed-batch phase of aerobic cultivations in bioreactors using exponential feeding. SCIST42 -  $P_{TEF1}\text{-}ACC1^{**}$ ,  $erg10\Delta::P_{TEF1-}nphT7$  and SCIST43 -  $P_{TEF1}\text{-}ACC1^{**}$ ,  $erg10\Delta::P_{TEF1-}nphT7$ ,  $P_{FAS1}\Delta::P_{HXT1}$ .

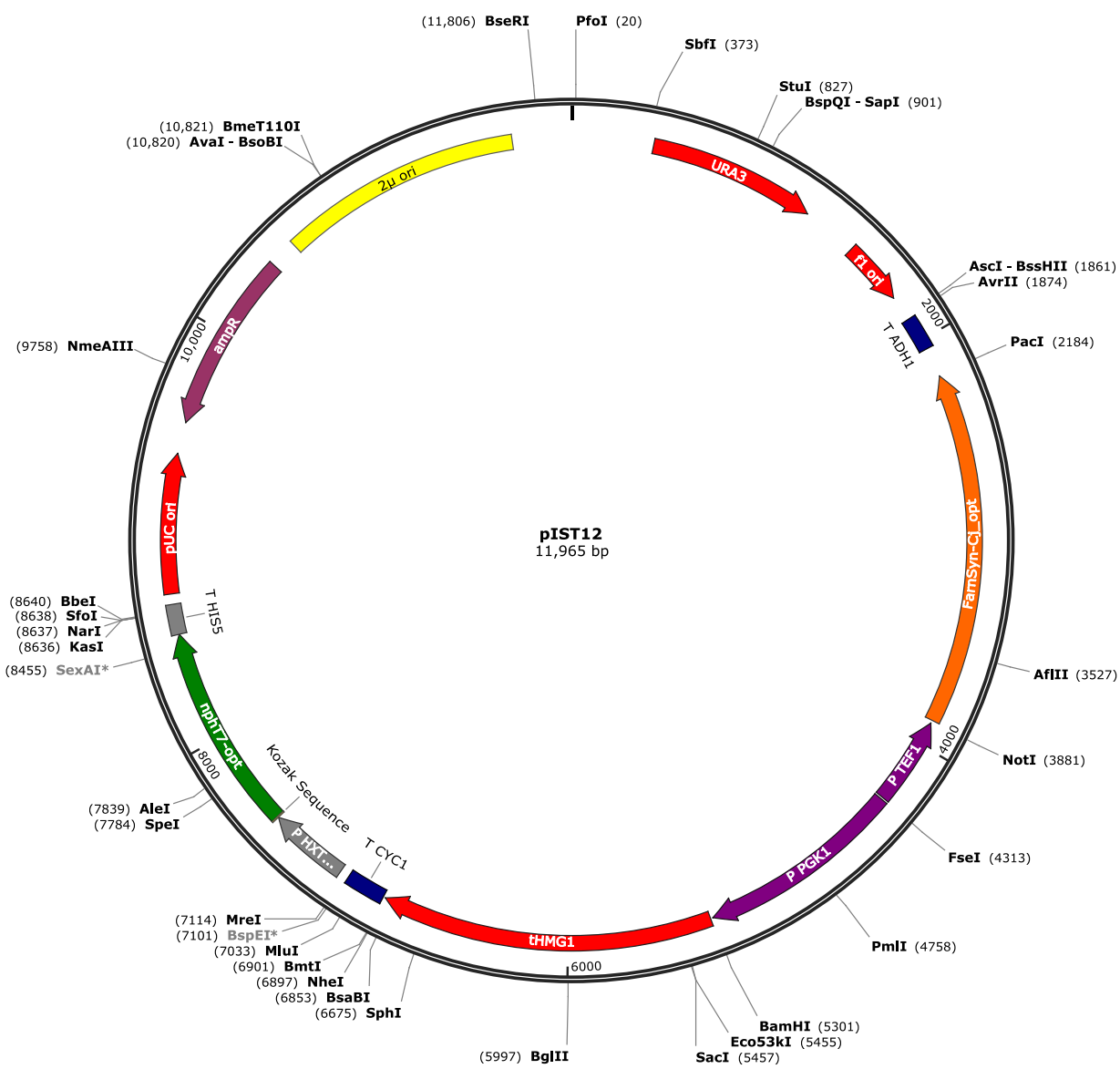


Fig. S7 Plasmid map of pIST12 for expression of farnesene synthase from *Citrus junos* (*FarnSyn\_Cj*), truncated HMG-CoA reductase (*tHMG1*) and acetoacetyl-CoA synthase (*nphT7*) from *Streptomyces* sp. strain CL190. Plasmid pIST13-16 are identical, but express *nphT7* homologs from other bacterial strains.

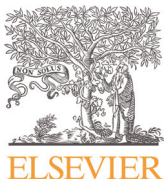


# **Improved quantification of farnesene during microbial production from *Saccharomyces cerevisiae* in two-liquid-phase fermentations**

Stefan Tippmann, Jens Nielsen and Sakda Khoomrung

*Talanta* 146:100-106, 2016





# Improved quantification of farnesene during microbial production from *Saccharomyces cerevisiae* in two-liquid-phase fermentations

Stefan Tippmann <sup>a,b,c</sup>, Jens Nielsen <sup>a,b,c,d</sup>, Sakda Khoomrung <sup>a,b,\*</sup>

<sup>a</sup> Department of Biology and Biological Engineering, Chalmers University of Technology, SE41296 Gothenburg, Sweden

<sup>b</sup> Chalmers Metabolomics Centre, Chalmers University of Technology, Gothenburg, Sweden

<sup>c</sup> Novo Nordisk Foundation Center for Biosustainability, Chalmers University of Technology, SE41296 Gothenburg, Sweden

<sup>d</sup> Novo Nordisk Foundation Center for Biosustainability, Technical University of Denmark, DK2970 Hørsholm, Denmark

## ARTICLE INFO

### Article history:

Received 31 March 2015

Received in revised form

12 August 2015

Accepted 15 August 2015

Available online 17 August 2015

### Keywords:

Isoprenoids

Biofuels

GC-MS

GC-FID

Metabolic engineering

## ABSTRACT

Organic solvents are widely used in microbial fermentations to reduce gas stripping effects and capture hydrophobic or toxic compounds. Reliable quantification of biochemical products in these overlays is highly challenging and practically difficult. Here, we present a significant improvement of identification and quantification methods for farnesene produced by *Saccharomyces cerevisiae* in two-liquid-phase fermentations using GC-MS and GC-FID. By increasing the polarity of the stationary phase introducing a ZB-50 column (50%-phenyl-50%-dimethylsiloxane) peak intensity could be increased and solvent carryover could be minimized. Direct quantification of farnesene in dodecane was achieved by GC-FID whereas GC-MS demonstrated to be an excellent technique for identification of known and unknown metabolites. The GC-FID is a suitable technique for direct quantification of farnesene in complex matrices as shown by the good calibration curve ( $R^2 > 0.998$ ,  $N=5$ ) within the tested concentration range of 1–50 µg/mL and the reproducibility of the intensity (intraday; < 10% RSD at each concentration;  $N=5$ ). The limit of detection (LOD) and limit of quantification (LOQ) of the method were 0.24 and 0.80 µg/mL, respectively. Furthermore, the FID method proved to be highly stable with regard to the intensity of the calibration ( $N=6$ ) when the measurements were performed across 250 samples that were derived from a dodecane overlay.

© 2015 Elsevier B.V. All rights reserved.

## 1. Introduction

Isoprenoids are of great commercial interest due to numerous applications in the food, pharmaceutical and fuel industry. In recent years, metabolic engineering has acted as enabling technology to allow for their efficient production in microorganisms from renewable carbon sources, which represents a promising alternative to plant extraction and chemical synthesis [1,2].

Analytical methods for identification and quantification of target products as well as other by-products play an important role during strain development. However, development of analytical methods in yeast research, including sampling, sample preparation, separation, detection or data analysis is mostly done for intracellular metabolites [3–8]. On the other hand, analysis of extracellular metabolites is a highly challenging task as seen by the example of isoprenoids. Isoprenoids are hydrophobic molecules and dissolve poorly in the aqueous medium, which complicates

sampling and analysis. In combination with their ability to form aerosols, which applies mostly to short chain isoprenoids e.g., mono-, sesqui- and diterpenes, they are stripped from the medium in aerated bioreactor cultivations [9]. Therefore production of isoprenoids by microbes often applies an organic overlay on top of the cultivation medium to capture the product (*in situ* extraction), which is subsequently analyzed by GC-MS [10]. The addition of an organic overlay during the cultivation process is intended to prevent product loss and to reduce toxicity effects that arise from the product [10]. Although this approach is adding only a little experimental complexity, several requirements are imposed on the solvents used, which make the selection of an appropriate organic overlay tedious. Some of the main criteria include the compatibility with the host organisms, high product capacity, immiscibility with the medium, easy phase separation, suitability for sample analysis, waste treatment and cost effectiveness [11,12]. Since long chain hydrocarbons are generally not affecting growth and sufficiently capture the product, solvents such as decane [13], dodecane [9,14,15], isopropyl myristate (IPM) [16,17] or methyl oleate [17] are commonly utilized as organic overlays.

Quantification of products derived from organic overlays is highly challenging due to the large diversity of chemical

\* Corresponding author at: Department of Biology and Biological Engineering, Chalmers University of Technology, Kemivägen 10, SE-41296 Gothenburg, Sweden

E-mail addresses: [sakda@chalmers.se](mailto:sakda@chalmers.se),

[\(S. Khoomrung\).](mailto:Skhoomrung@gmail.com)

substances that originate from the microbial host, the aqueous media and the organic solvent used. Traditionally, the organic overlay is harvested from the cultivation broth by centrifugation and subsequently analyzed by GC-MS [13,14]. This way of analysis is fast, simple, convenient and widely accepted in the community. However, we observed that this approach leads to instability of the instrument and low reproducibility of the method with increasing number of measurements. Additionally, using a recommended siloxane based stationary phase (normally 95%-dimethylsiloxane) for the analysis of dodecane often resulted in solvent carryover.

In this study, we have systematically investigated step-by-step problems regarding reproducibility and sensitivity of the analysis of farnesene in two-liquid-phase fermentation. Finally, we have established a platform for identification and quantification of farnesene in organic overlay based on GC-MS and GC-FID. Our results provide a simple, reliable and accurate quantification method, which can be applied either in research or industrial applications.

## 2. Materials and methods

### 2.1. Reagents and standards

All reagents and standards used in this study were analytical grade, dodecane ( $\geq 99\%$ ), trans- $\beta$ -farnesene ( $\geq 90\%$ ) and farnesene (mixture of isomers) were purchased from Sigma-Aldrich, St. Louis, MO, USA. Patchoulol ( $\geq 99\%$ ) was a kind gift from Firmech, Geneva, Switzerland.

### 2.2. Yeast strains and cultivation media

A farnesene producing strain was constructed by transforming CEN.PK 113-5D with plasmid pIST05 carrying a  $\beta$ -farnesene synthase gene from *Citrus junos* [28]. The strain was maintained on agar plates containing 6.9 g/L yeast nitrogen base w/o amino acids (Formedium, Hunstanton, UK), 0.77 g/L complete supplement mixture w/o uracil (Formedium), 20 g/L glucose and 20 g/L agar. All liquid cultivations were carried out using minimal medium as described by Verduyn et al. [18], containing 20 g/L glucose, 5 g/L  $(\text{NH}_4)_2\text{SO}_4$ , 3 g/L  $\text{KH}_2\text{PO}_4$ , 0.5 g/L  $\text{MgSO}_4 \cdot 7\text{H}_2\text{O}$ , 1 mL trace element solution and 50  $\mu\text{L}/\text{L}$  antifoam. The pH was adjusted to 5, the medium was autoclaved and 1 mL/L of filter sterilized vitamin solution was added subsequently.

### 2.3. Preparation of preculture and shake flask cultivations

A visible colony of the farnesene producing strain was picked from a freshly streaked agar plate and transferred into 5 mL minimal medium as described above. After cultivation overnight at 200 rpm and 30 °C, 3 mL of the suspension were used to inoculate 50 mL of the same medium in baffled shake flasks. After approximately 24 h of cultivation time, the cells were harvested by centrifugation at 2500 rpm for 5 min. and re-suspended in fresh medium. At last, the bioreactors were inoculated with the preculture at OD 0.05. Subsequent to inoculation, dodecane was added under aseptic conditions to a final concentration of 10% v/v.

### 2.4. Bioreactor cultivations

Cultivation of the farnesene producing strain was carried out using the Microbiology PD system from DasGip (DasGip Information and Process Technology, Jülich, Germany), with a reaction volume of 500 mL. To assure homogeneous mixing, the medium was stirred at 400 rpm with a six blade Rushton turbine. The temperature was set to 30 °C and pH was controlled at 5 using 2 M

KOH and 2 M HCl. Aeration of the vessels was adjusted to 1 vvm. The off-gas was cooled to maintain the reaction volume constant. Analysis of the exhaust gas was used to monitor growth.

### 2.5. Measurement of cell growth

For the determination of biomass concentration a 5 mL sample was pipetted on pre-weighted 0.45  $\mu\text{m}$  filter (Sartorius Stedim Biotech GmbH, Göttingen, Germany). The filter was rinsed with 10 mL Milli-Q water and dried in a microwave oven at 120 W for 15 min. Previous to weighing, the filter was left to cool down in a desiccator. Subsequently, the biomass concentration was calculated as grams of dry cell weight per liter of cultivation medium (gDCW/L).

### 2.6. Extraction of farnesene from aqueous medium

For the extraction of farnesene, a 18 mL sample was taken from the cultivation broth. Subsequently, 2 mL of dodecane containing 100  $\mu\text{g}/\text{mL}$  patchoulol (used as internal standard) were added to obtain a final dodecane concentration of 10% (v/v). The mixture was shaken at 2000 rpm for 3 min for extraction and centrifuged at 5000 rpm for 5 min for complete separation of the two phases. At last, a sample was taken from the top phase, which was analyzed by GC-MS.

### 2.7. Quantification of farnesene by GC-MS and GC-FID

Detection and quantification of farnesene were performed on a Focus GC ISQ single quadrupole GC-MS and a Focus GC-FID (Thermo Fisher Scientific, Waltham, MA, USA). The measurement conditions on both GCs were identical if not stated otherwise. Zebron capillary GC columns, ZB-5MS and ZB-50 (30 m  $\times$  0.25 mm I.D., 0.25  $\mu\text{m}$  film thickness; Phenomenex, Torrance, CA, USA), were used with helium as carrier gas at a flow rate of 1 mL/min. The inlet temperature was set to 200 °C and the sample volume of 1  $\mu\text{L}$  for GC-MS and 2  $\mu\text{L}$  for GC-FID were injected in splitless mode. Initial oven temperature was set at 50 °C (1.5 min), increased up to 170 °C (30 °C/min) and was held for 1.5 min. The temperature was then increased to 300 °C (15 °C/min) and maintained for 3 min. For MS detection, the mass transfer line and the ion source were set to 250 and 200 °C, respectively. Electron ionization at 70 eV was used to detect farnesene and the internal standard patchoulol in full scan at  $m/z$  50–650 and selected ion monitoring mode was performed at  $m/z$  of 93, 204 for farnesene and  $m/z$  of 93, 138, 204 for patchoulol. The GC-MS was used for identification of farnesene from *S. cerevisiae* by comparing the mass spectrum profile and retention time with the synthetic standard. A five point external calibration in the range of 1–50  $\mu\text{g}/\text{mL}$  was used for quantitative analysis.

## 3. Results and discussion

### 3.1. Product loss in aerated bioreactor cultivations without dodecane overlay

In order to quantitatively determine the loss of farnesene during fermentation, we first tested the effect of using a dodecane overlay to capture farnesene during the cultivation process. For this purpose, our farnesene producing strain was cultivated with overlay (*in situ* extraction) and without overlay (*ex situ* extraction). For the *in situ* experiment, dodecane containing 10  $\mu\text{g}/\text{mL}$  of patchoulol (internal standard) was added directly to the aqueous medium at 10% v/v at the beginning of the cultivation. After 48 h, the dodecane phase (top phase) was collected by centrifugation

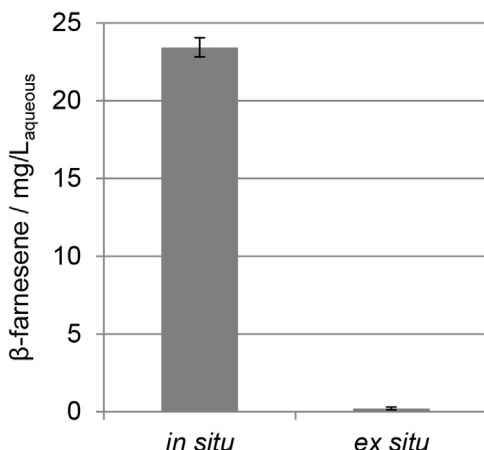


**Fig. 1.** Comparison of  $\beta$ -farnesene production by *S. cerevisiae* in aerated batch cultivations with (*in situ*) and without (*ex situ*) dodecane to quantify product loss by gas stripping. Bars represent average concentration with respect to cultivation medium  $\pm$  standard variation of three biological replicates.

and subsequently analyzed by GC-MS. The *ex situ* experiment was performed under identical conditions, but without addition of dodecane. Instead, a sample was collected from the aqueous medium after 48 h and farnesene was extracted using 10% v/v dodecane containing 10  $\mu$ g/mL of patchoulool. All cultivations were performed with three biological replicates, whereas the same preculture was used to inoculate two bioreactors, *i.e.* one with dodecane and one without dodecane, in order to avoid fluctuations caused by the variability between biological replicates. Both, the farnesene concentration as well as the recovery of patchoulool were much higher in the *in situ* experiment (Fig. 1), confirming that dodecane can be used as overlay to efficiently capture hydrophobic compounds. As significantly lower farnesene concentrations were obtained in the *ex situ* experiment, we presumed product loss due to gas stripping during the cultivation process. The low recovery of patchoulool (38%) found in the *ex situ* experiment was likely caused by insufficient extraction, which could be improved by further optimization of the method. However, improved recovery by extending the extraction time is unlikely to prevent loss of farnesene from the cultivation. Interestingly, using dodecane as overlay led to higher biomass compared to having no dodecane in the system ( $7.75 \pm 0.56$  vs.  $5.78 \pm 0.25$  gDCW/L). Similarly, isopropyl myristate was observed to increase viability of cells during the production of artemisinin [16]. We speculate that higher biomass yield from *in situ* experiment could be due to the fact that having dodecane overlay minimizes the contact of the cells to toxic products or other by-products from the cultivation medium. Since exposure of *S. cerevisiae* to different concentrations of farnesene, however, revealed no apparent effect on growth, we concluded farnesene at these concentrations not to be toxic (Fig. S1). Yet, the use of dodecane as an organic overlay could promote secretion and thereby prevent intracellular accumulation of farnesene, which may become a metabolic burden to the host organism.

#### 4. Analysis of farnesene in dodecane

##### 4.1. Minimizing solvent carryover by increasing polarity of stationary phase

As seen by the result presented in Fig. 1, utilization of an organic overlay was essential to reduce loss of farnesene due to gas stripping. Dodecane is widely used for this purpose due to its excellent ability of capturing hydrophobic or toxic products

[15,19,20]. However, dodecane is not a common solvent used in GC-MS analysis, especially when the analysis is performed on non-polar stationary phases. In connection to this, solvent carry-over is a common problem, which is observed by elution of dodecane from the column in runs even when dodecane is not injected. To obtain a carryover-free system, we first tested several methods for solvent removal with the objective to replace the final solvent with hexane, ethyl acetate or other common solvents used in GC-MS analysis. Evaporation of dodecane at small volumes (1 mL) under vacuum conditions failed or was successful only after 60 min or more (Table S1). Organic phases can be subjected to purification process *e.g.* liquid–liquid extraction or solid phase extraction. These, however, increase the length of sample preparation and the possibility of product loss. We therefore did not pursue this approach. Secondly, we looked for an alternative solution by increasing the polarity of the stationary phase of the GC columns. Analysis of terpenes from different samples by GC-MS is often performed on ZB-5MS (5% phenyl-arylene, 95% dimethylsiloxane) or similar phases *e.g.*, SLB-5MS [14], VF-5MS [19], HP-5MS [21,22], DB-5MS [23,24], TR-5MS [15] and Rxi-5MS [25]. These types of columns are extremely non-polar with high thermal stability (up to 350 °C), high reproducibility and low bleeding. Additionally, these columns work well in combination with solvents that are commonly used in GC-MS analysis such as hexane, ethyl acetate or acetonitrile. However, in our experiments problems regarding solvent carryover occurred when solvent was dodecane. It was not possible to remove dodecane from the column even if the final temperature was set to 350 °C and kept for additional 30 min or running a bake out program several times. Trimming of 2–3 feet in the beginning of the column was the only way to clean it. This is because dodecane is highly non-polar and interacts strongly with non-polar stationary phase. After exploring several possibilities of column choices, we introduced a ZB-50 column (50%-phenyl-50%-dimethylsiloxane) which has a significantly higher polarity than ZB-5MS (approximately 3 times). Farnesene could be successfully separated with a shorter retention time (7.3 min) in comparison to ZB-5MS (Fig. 2). The mass spectrum of farnesene separated on the ZB-50 column was remarkably clean; no trace spectra interferences from other compounds were observed similar to the ZB-5MS column. Furthermore, the results in Fig. 3 clearly show that there was no solvent carryover when injecting dodecane on this type of column. We demonstrated a carryover-free system by performing sequential analysis of hexane, dodecane and hexane on ZB-50 column on a GC-FID system. First, we injected hexane into the system (Fig. 3-A), followed by injection of dodecane (Fig. 3-B). Finally we re-injected hexane solvent (Fig. 3-C). As it can be seen there was no trace of dodecane peak left in the third injection (Fig. 3-C), indicating no solvent carryover. These results can be assigned to the increased polarity of the column, which reduces the interaction between dodecane and the stationary phase. Although the ZB-50 column is significantly more polar compared to the ZB-5MS, it has similar properties to the ZB-5 MS column as very high thermal stability (up to 340 °C), which allows for other applications that runs at high temperatures.

##### 4.2. Identification and quantification by GC-MS

Direct analysis of sesquiterpenes such as farnesene in organic overlays by GC-MS is convenient and widely used [13–15]. However, the organic overlay is not only containing the product but most likely other volatile, semi-volatile or non-volatile substances either from cultivation medium or from host producer. These compounds can be identified by mass spectrum, which makes GC-MS an indispensable tool during strain construction as it allows for profound comparison of different metabolic engineering strategies

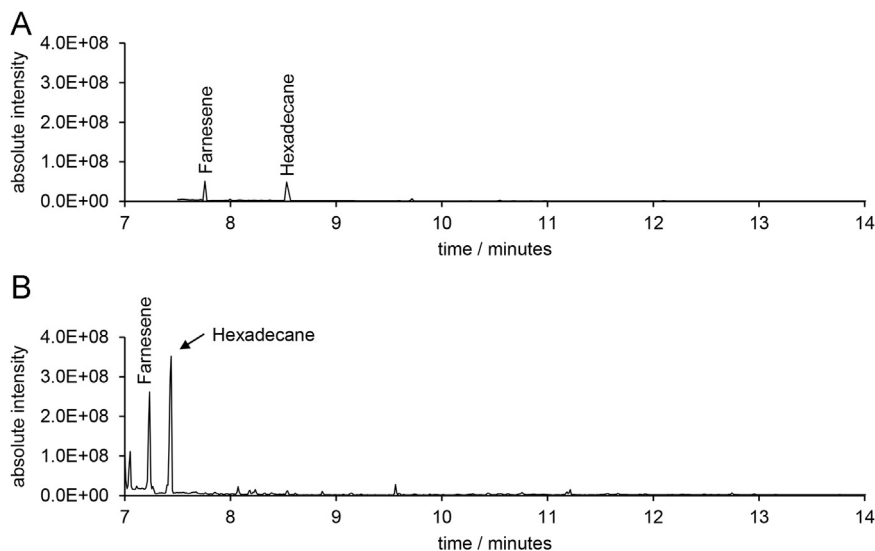


**Fig. 2.** Separation of  $\beta$ -farnesene in dodecane by GC-MS on ZB-5MS column (A) and ZB-50 column (B).

and for identification of by-products. As shown by the chromatogram in Fig. 4, other metabolites such as farnesol and sesquiphellandrene, which originate from the same pathway as farnesene, could be identified. However, analysis of these samples in a large number of measurements could influence the reproducibility and stability of the instrument. To address this question, we constructed a five-point calibration curve (1–50  $\mu\text{g}/\text{mL}$ ) for farnesene, dissolved in dodecane on GC-MS. The result presented in Fig. 5-A shows a calibration curve, which was sufficient for quantitative analysis within the provided concentration range between 1–50  $\mu\text{g}/\text{mL}$  ( $R^2=0.987$ , intraday; <3% RSD in every concentration;  $N=5$ ). This indicates that the GC-MS method is suitable for

quantification of farnesene when using dodecane as solvent. We further explored stability and reproducibility of the instrument by analyzing 50 samples derived from dodecane overlay in between two sets of standard solutions. A substantial drop in sensitivity of the instrument was clearly observed in Fig. 5-B. The drop in sensitivity accounted for approximately 54% on average, which made accurate quantification in the real samples impossible. In further experiments, we attempted to confirm these results and found that the drop in sensitivity was different from 54%. This indicated that inconsistency in sensitivity or stability of the instrument resulted from the contaminants present in the dodecane overlay, which were visible on the surface of the ion source (Fig. S2). In

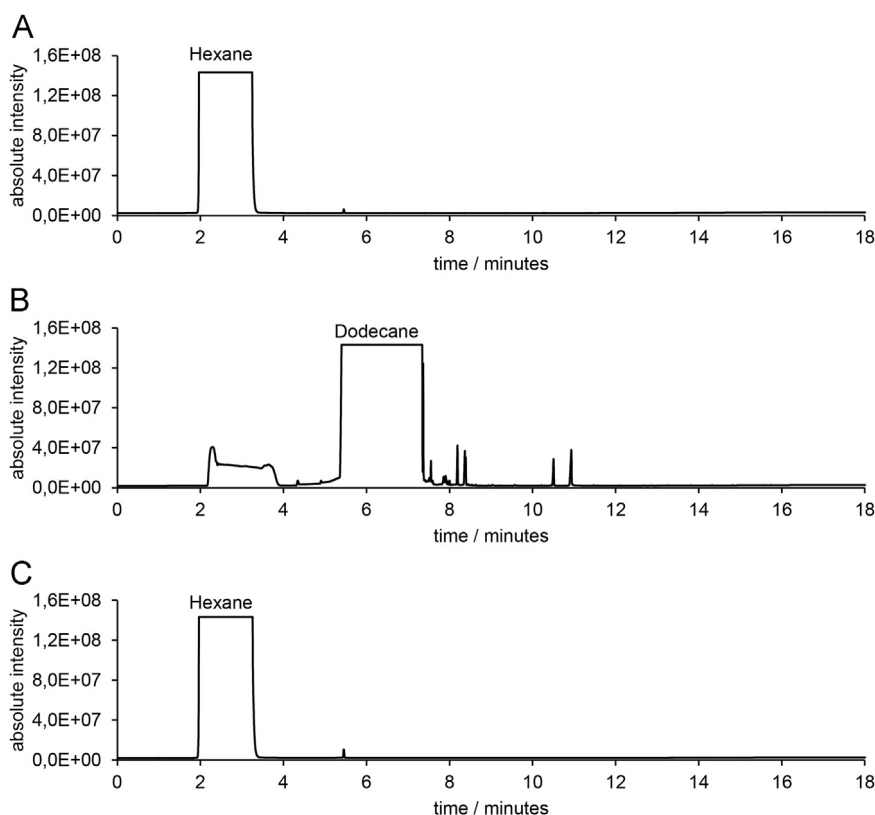


**Fig. 3.** Solvent carryover on ZB-50 column. A: injection of hexane on a newly installed ZB-50. B: injection of farnesene dissolved in dodecane on the same ZB-50 column. C: injection of hexane on the same ZB-50.

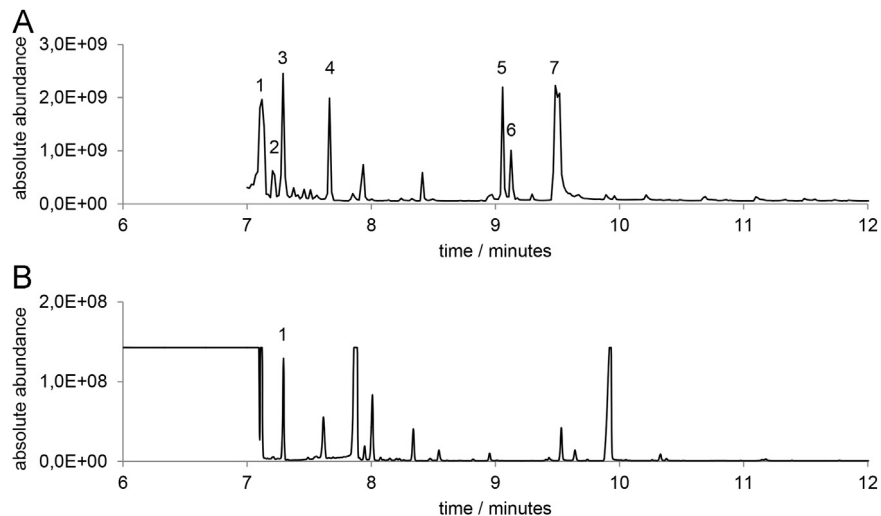


**Fig. 4.** Analysis of dodecane overlay obtained from two-liquid-phase fermentation of *S. cerevisiae* expressing  $\beta$ -farnesene synthase from *C. juncos*. A: identification of farnesene and other metabolites by mass spectrum using NIST library; 1-  $\beta$ -farnesene, 2-sesquiphellandrene, 3-cyclododecane, 4-sesquiphellandrene, 5-farnesol, 6-patchoulool (internal standard), 7-hexadecanol. B: Identification and quantification of  $\beta$ -farnesene (1) by GC-FID under identical conditions using analytical standard.

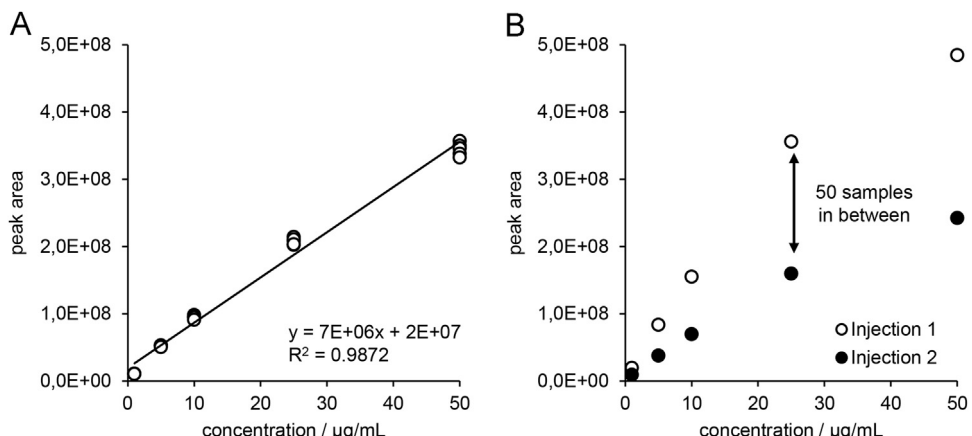


**Fig. 5.** Quantification of  $\beta$ -farnesene in dodecane by GC-MS. A: calibration curve for farnesene in dodecane from five measurements ( $N=5$ ). B: calibration curve for farnesene from two set of standards (injection 1 and 2) with the measurement of 50 dodecane samples in between. White circles indicate first set of injections; black circles indicate second set of injections.

order to eliminate those contaminations, the ion source temperature could be set higher than 200 °C (current setting). However, a higher ion source temperature often results in a lower relative abundance of the molecular ion and increases the possibility of ion degradation [26]. An ion source temperature above 200 °C reduces the probability of NIST library identification as 200 °C is set as the reference point for tuning the mass spectrometer (manufacturer's recommendations). We therefore explored other possibilities for direct quantification of farnesene while maintaining stability and sensitivity of the instrument during the measurement with other methods.

#### 4.3. Reduction of MS instability by utilization of a co-solvent

As direct analysis of isoprenoids in dodecane by GC-MS is convenient, we investigated the possibilities to maintain the sensitivity of GC-MS for detection of farnesene and other related metabolites by using hexane as co-solvent. Hexane is frequently used as solvent for GC-MS analysis as it combines several advantages, e.g. it has a low boiling point, it does not interact with the column and mobile phase, it elutes at the void volume, is able

to dissolve farnesene and provides good quality MS spectra. We therefore prepared 10 times dilutions of dodecane samples in hexane to assess the impact on the detector when hexane is used as co-solvent. As shown in Fig. 6, the sensitivity of the GC-MS could be maintained by the addition of hexane to the samples as no change of the signal intensity was observed between 2 sets of standards. However, a dilution of the organic layer by hexane is simply a dilution of its contaminants. While this step increases the stability of the instrument, it reduces the sensitivity of the method. Additionally, high dilutions were required in our experiments to minimize the effects of the dodecane samples (Fig. S3).

#### 4.4. Identification and quantification by GC-FID

The Flame Ionization Detector (FID) is widely used due to its predictable response, robustness, high sensitivity towards hydrocarbons, linearity over a wide measurement range and its low costs [27]. The FID is a destructive, mass flow dependent detector, which uses a hydrogen flame for ionization of the compounds. Interestingly, all compounds are burned when entering the flame, whereas only hydrocarbons give response to the recorder. Other

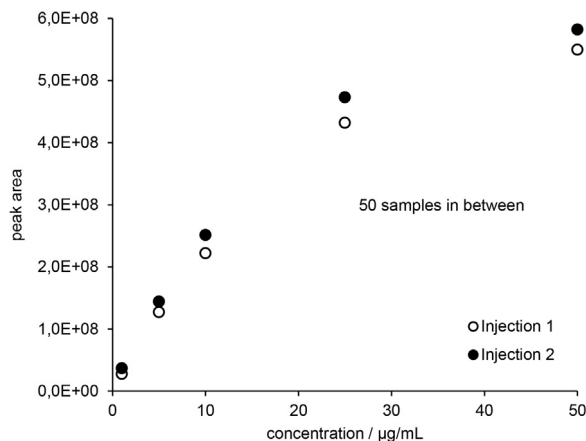


**Fig. 6.** Measurement of  $\beta$ -farnesene by GC-MS using hexane as co-solvent ( $N=2$ ). Injection of 50 dodecane samples in between each set of external standards, whereas all samples were diluted 10 times in hexane. White circles indicate first set of injections; black circles indicate second set of injections.

substances or impurities, e.g., inorganic compounds,  $\text{CO}_2$ , CO or non-hydrocarbons generally do not give a recordable signal and are decomposed by the flame. This prevents an accumulation of contaminants or substances at the detector and maintains the stability of the instrument. We therefore investigated utilization of the FID detector for direct quantification of farnesene derived from dodecane overlay. The calibration (Fig. 7-A) of farnesene obtained from the FID detector proved to be reliable for quantification as indicated by the calibration curve ( $R^2 > 0.998$ , intraday;  $< 10\%$  RSD;  $N=5$ ). We further generated a second calibration curve with 6 sets of farnesene standards, whereas 50 samples derived from dodecane overlay were run in between each set of standards. Overall, the total length of the sequence amounted to 286 injections. Results in Fig. 7-B show insignificant differences in comparison with the calibration obtained in Fig. 7-A regarding sensitivity (slope) and  $R^2$  of the calibration. This indicates that using FID for direct analysis of farnesene in the dodecane overlay did not result in a sensitivity drop of the instrument. Moreover, we observed that the reproducibility of the method during the analysis of over 286 measurements could be assured. Additionally, the limit of detection (LOD) and limit of quantification (LOQ) were determined by analyzing the lowest concentration of the farnesene standard ( $N=10$ ) [4]. The calculation was based on  $3 \times \text{SD}/m$  (LOD) and  $10 \times \text{SD}/m$  (LOQ), where SD = standard deviation of 10 times measurements of 1  $\mu\text{g}/\text{mL}$  and  $m$  = slope of the calibration curve. The estimated LOD and LOQ for the GC-FID method were 0.24 and

0.80  $\mu\text{g}/\text{mL}$ .

The measuring principle of the FID, which comprises the decomposition of all compounds, allows the detector to stay clean and maintain its sensitivity at all times. On the other hand, the MS detector (electron ionization) works by ionizing most of the molecules that enter the ionization chamber. The ionized molecules and their fragments then travel towards the detector, whereas non-ionized molecules tend to accumulate on the surface of the ion source, which results in a drop of sensitivity in subsequent runs.

Although the GC-FID has been used to assay of amorphadiene production in two-liquid-phase fermentations, the analysis was performed after several steps of sample purification [17]. Here in this study we demonstrated the use of GC-FID for direct quantification of farnesene product in two-liquid-phase fermentations without sample purification. This approach is not only reducing of sample handling processes but also minimizing sample lost from multi-steps of sample preparation processes.

The main disadvantage of FID is that detector does not provide structure information compared to MS detection. For these reasons, we set GC-MS to reveal the identity of metabolites when sample is derived two-liquid phase fermentation (Fig. 4), whereas the GC-FID is set for the purpose of quantification.

## 5. Conclusions

The application of organic solvents as overlays to the aqueous medium is widely used for microbial fermentations in order to sequester the product and thereby reduce toxicity or gas stripping effects. However, complications that occur during analytical procedures arising from organic overlays are rarely discussed. Dodecane, a very non-polar hydrocarbon proved to be suitable for this purpose and was essential to avoid significant product loss. However, sample analysis using dodecane as the solvent revealed to be a challenging task owing to solvent carryover and instability of the GC-MS. The presented results show that solvent carryover can be overcome by increasing polarity of the stationary phase, whereas the use of FID provides a very stable, reliable quantification method to quantify farnesene in an organic overlay.

Since the chemical properties are similar among many isoprenoids, this study sets the general frame for the analytical part of isoprenoid production in microbial hosts.

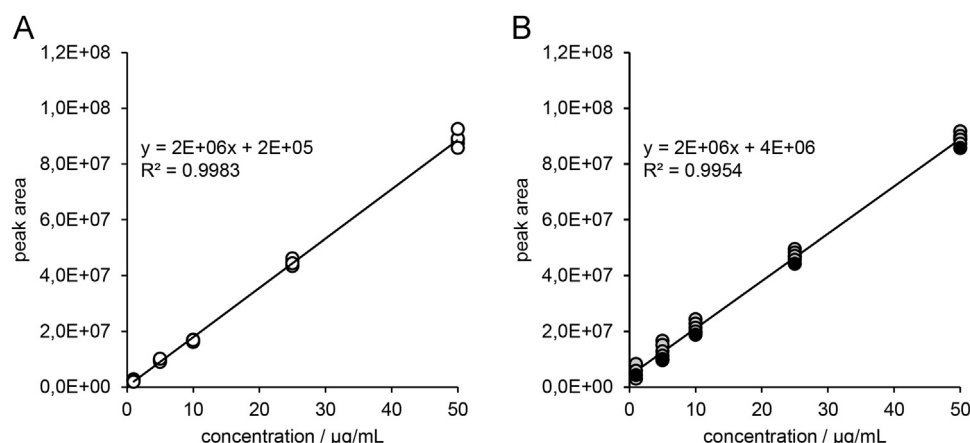


**Fig. 7.** A: calibration curve for quantification of  $\beta$ -farnesene in dodecane by GC-FID. A: calibration curve for farnesene in dodecane from five measurements ( $N=5$ ). B: calibration curve for farnesene standards were injected repetitively 6 times, with 50 injections of undiluted dodecane samples in between.

## Competing interests

The authors declare to have no competing interests.

## Authors' contributions

ST, SK and JN designed the study. ST performed the experiments and wrote the manuscript. SK and JN edited the manuscript.

## Acknowledgments

The authors wish to thank the Knut and Alice Wallenberg Foundation, FORMAS, the Swedish Research Council and the Novo Nordisk Foundation. We thank Nils-Gunnar Carlsson and Suwanee Jansa-Ard for technical assistance and Dr. Rahul Kumar for constructive comments.

## Appendix A. Supplementary material

Supplementary data associated with this article can be found in the online version at

<http://dx.doi.org/10.1016/j.talanta.2015.08.031>.

## References

- [1] J.D. Keasling, ACS Chem. Biol. 3 (2008) 64–76.
- [2] S. Tippmann, Y. Chen, V. Siewers, J. Nielsen, Biotechnol. J. 8 (2013) 1435–1444.
- [3] S. Khoomrung, P. Chumnanpuen, S. Jansa-Ard, I. Nookaew, J. Nielsen, Appl. Microbiol. Biotechnol. 94 (2012) 1637–1646.
- [4] S. Khoomrung, P. Chumnanpuen, S. Jansa-Ard, M. Stahlman, I. Nookaew, J. Boren, J. Nielsen, Anal. Chem. 85 (2013) 4912–4919.
- [5] A.B. Canelas, A. ten Pierick, C. Ras, R.M. Seifar, J.C. van Dam, W.M. van Gulik, J. Heijnen, Anal. Chem. 81 (2009) 7379–7389.
- [6] S. Kim, Y. Lee do, G. Wohlgemuth, H.S. Park, O. Fiehn, K.H. Kim, Anal. Chem. 85 (2013) 2169–2176.
- [7] J.D. Rabinowitz, E. Kimball, Anal. Chem. 79 (2007) 6167–6173.
- [8] M. Zimmermann, U. Sauer, N. Zamboni, Anal. Chem. 86 (2014) 3232–3237.
- [9] P.K. Ajikumar, W.H. Xiao, K.E.J. Tyo, Y. Wang, F. Simeon, E. Leonard, O. Mucha, T.H. Phon, B. Pfeifer, G. Stephanopoulos, Science 330 (2010) 70–74.
- [10] A.J. Daugulis, Curr. Opin. Biotechnol. 8 (1997) 169–174.
- [11] J.J. Malinowski, Biotechnol. Adv. 19 (2001) 525–538.
- [12] R. Muñoz, M. Chambaud, S. Bordel, S. Villaverde, Appl. Microbiol. Biotechnol. 79 (2008) 33–41.
- [13] C. Wang, S.H. Yoon, H.J. Jang, Y.R. Chung, J.Y. Kim, E.S. Choi, S.W. Kim, Metab. Eng. 13 (2011) 648–655.
- [14] M.A. Asadollahi, J. Maury, K. Möller, K.F. Nielsen, M. Schalk, A. Clark, J. Nielsen, Biotechnol. Bioeng. 99 (2008) 666–677.
- [15] P.P. Peralta-Yahya, M. Ouellet, R. Chan, A. Mukhopadhyay, J.D. Keasling, T.S. Lee, Nat. Commun. 2 (2011) 483.
- [16] C.J. Paddon, P.J. Westfall, D.J. Pitera, K. Benjamin, K. Fisher, D. McPhee, M. D. Leavell, A. Tai, A. Main, D. Eng, D.R. Polichuk, K.H. Teoh, D.W. Reed, T. Treynor, J. Lenihan, M. Fleck, S. Bajad, G. Dang, D. Dengrove, D. Diola, G. Dorin, K.W. Ellens, S. Fickes, J. Galazzo, S.P. Gaucher, T. Geistlinger, R. Henry, M. Hepp, T. Horning, T. Iqbal, H. Jiang, L. Kizer, B. Lieu, D. Melis, N. Moss, R. Regentin, S. Secret, H. Tsuruta, R. Vazquez, L.F. Westblade, L. Xu, M. Yu, Y. Zhang, L. Zhao, J. Lievense, P.S. Covello, J.D. Keasling, K.K. Reiling, N. S. Renninger, J.D. Newman, Nature 496 (2013) 528–532.
- [17] P.J. Westfall, D.J. Pitera, J.R. Lenihan, D. Eng, F.X. Woolard, R. Regentin, T. Horning, H. Tsuruta, D.J. Melis, A. Owens, S. Fickes, D. Diola, K.R. Benjamin, J. D. Keasling, M.D. Leavell, D.J. McPhee, N.S. Renninger, J.D. Newman, C. J. Paddon, Proc. Natl. Acad. Sci. USA 109 (2012) E111–E118.
- [18] C. Verduyn, E. Postma, W.A. Scheffers, J.P. van Dijken, Yeast 8 (1992) 501–517.
- [19] T.C. Brennan, C.D. Turner, J.O. Krömer, L.K. Nielsen, Biotechnol. Bioeng. 109 (2012) 2513–2522.
- [20] D.K. Ro, E.M. Paradise, M. Quellet, K.J. Fisher, K.L. Newman, J.M. Ndungu, K. A. Ho, R.A. Eachus, T.S. Ham, J. Kirby, M.C.Y. Chang, S.T. Withers, Y. Shiba, R. Sarpong, J.D. Keasling, Nature 440 (2006) 940–943.
- [21] C. Wang, S.H. Yoon, A.A. Shah, Y.R. Chung, J.Y. Kim, E.S. Choi, J.D. Keasling, S. W. Kim, Biotechnol. Bioeng. 107 (2010) 421–429.
- [22] K. Zhou, K. Qiao, S. Edgar, G. Stephanopoulos, Nat. Biotech. 33 (2015) 377–383.
- [23] S. Khoomrung, G. Raber, K. Laoteng, K.A. Francesconi, Eur. J. Lipid Sci. Technol. 116 (2014) 795–804.
- [24] G. Raber, S. Khoomrung, M.S. Taleshi, J.S. Edmonds, K.A. Francesconi, Talanta 78 (2009) 1215–1218.
- [25] B. Engels, P. Dahm, S. Jennewein, Metab. Eng. 10 (2008) 201–206.
- [26] A.B. Fialkov, U. Steiner, S.J. Lehota, A. Amirav, Int. J. Mass Spectrom. 260 (2007) 31–48.
- [27] T. Holm, J. Chromatogr. A 842 (1999) 221–227.
- [28] S. Tippmann, G. Scalcinati, V. Siewers and J. Nielsen. Production of farnesene and santalene by *Saccharomyces cerevisiae* using fed-batch cultivations with RQ-controlled feed. Biotechnology and Bioengineering. <http://dx.doi.org/10.1002/bit.25683>.

## Supplementary Material

### Improved quantification of farnesene during microbial production from *Saccharomyces cerevisiae* in two-liquid-phase fermentations

Stefan Tippmann<sup>1, 2, 3</sup>, Jens Nielsen<sup>1, 2, 3, 4</sup>, Sakda Khoomrung<sup>1, 2,\*</sup>

<sup>1</sup>Department of Biology and Biological Engineering,

Chalmers University of Technology, SE41296 Gothenburg, Sweden

<sup>2</sup>Chalmers Metabolomics Centre, Chalmers University of Technology, Gothenburg, Sweden

<sup>3</sup>Novo Nordisk Foundation Center for Biosustainability, Chalmers University of Technology, SE41296

Gothenburg, Sweden

<sup>4</sup>Novo Nordisk Foundation Center for Biosustainability, Technical University of Denmark, DK2970

Hørsholm, Denmark

\*Corresponding Author:

Email: [sakda@chalmers.se](mailto:sakda@chalmers.se) or [Skhoomrung@gmail.com](mailto:Skhoomrung@gmail.com)

Department of Biology and Biological Engineering,

Chalmers University of Technology,

Kemivägen 10, SE-412 96,

Gothenburg, Sweden.

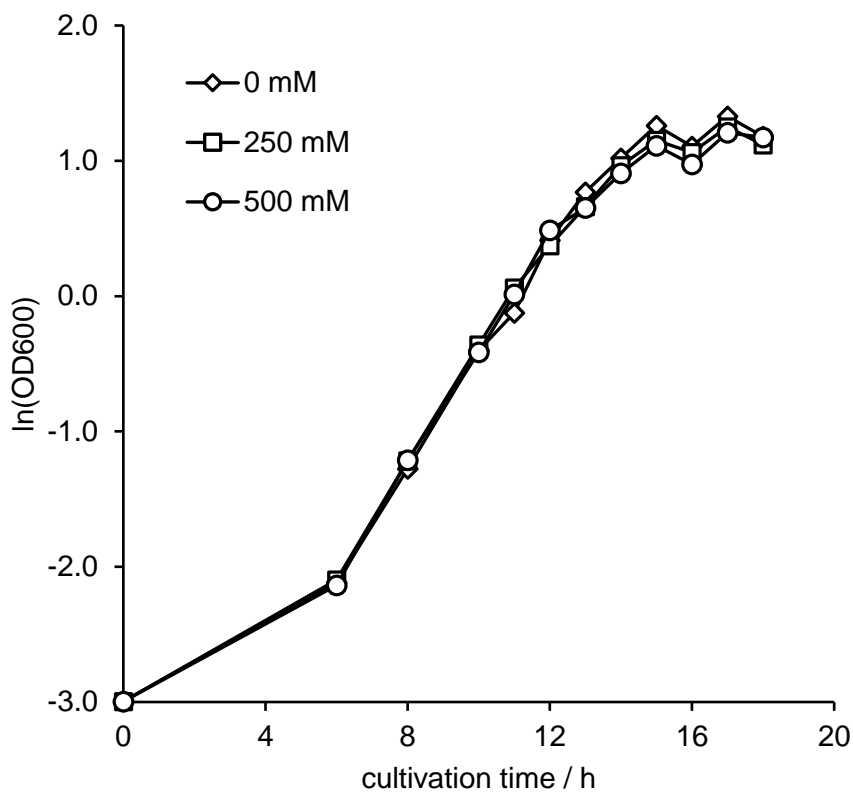


Figure S1: Growth comparison of *S. cerevisiae* strain CEN.PK 113-7D under different concentrations of farnesene. Data represents average values of three biological replicates.

Table S1: Evaporation of organic solvents in a centrifugal evaporator under different conditions.

Dilutions were prepared in ethyl acetate on 1 mL final volume. Red – not evaporated, yellow – partly evaporated, green – completely evaporated.

		65 °C		80 °C	
		45 min	60 min	45 min	60 min
Dodecane	100%	●	●	●	●
	75%	●	○	○	○
	50%	○	○	○	○
	25%	○	○	○	●

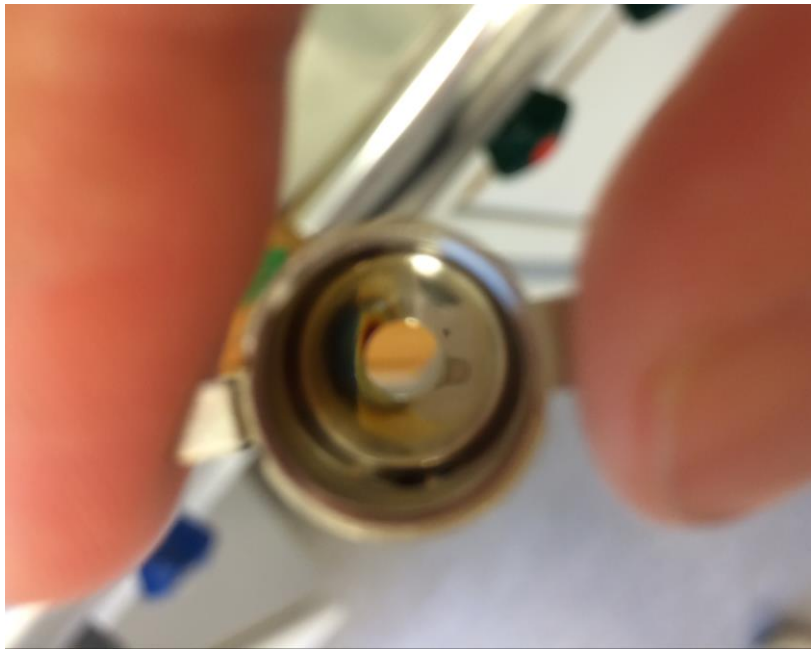


Figure S2: Visible contaminations on the ion source after several injections of dodecane.

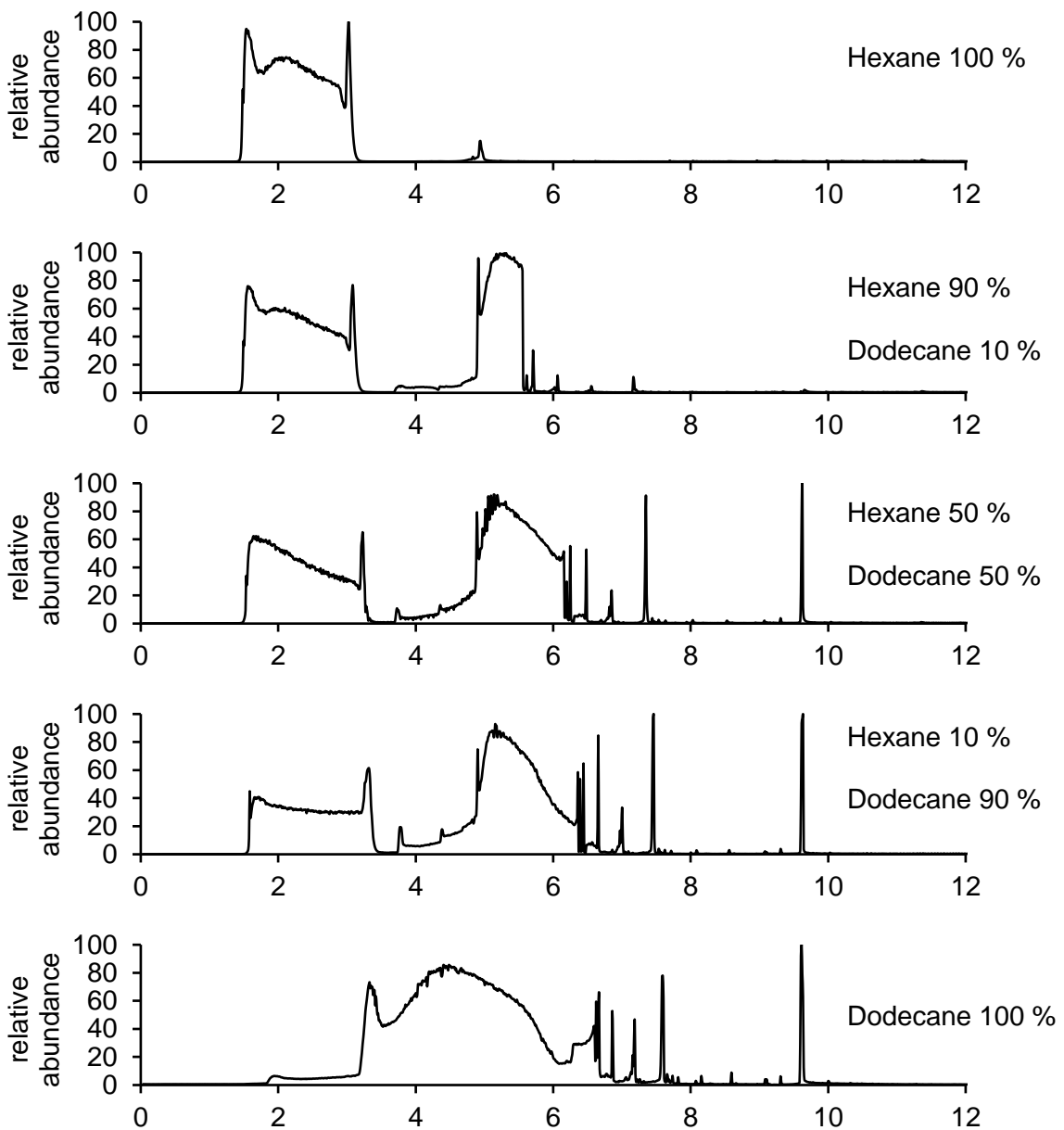


Figure S3: Chromatograms showing solvent fronts on GC-MS for pure dodecane and different

dilutions with hexane.